Technical Report

TR-06-32

Determination and assessment of the concentration limits to be used in SR-Can

Duro L, Grivé M, Cera E, Gaona X, Domènech C, Bruno J
Enviros Spain S.L.

December 2006

Svensk Kärnbränslehantering AB
Swedish Nuclear Fuel
and Waste Management Co
Box 5864
SE-102 40 Stockholm Sweden
Tel 08-459 84 00
+46 8 459 84 00
Fax 08-661 57 19
+46 8 661 57 19

Determination and assessment of the concentration limits to be used in SR-Can

Duro L, Grivé M, Cera E, Gaona X, Domènech C, Bruno J
Enviros Spain S.L.

December 2006

Keywords: Solubilities, Radionuclides, Asssessment, Concentration limits.

Abstract

This report presents the results for solubility limit calculations for the SR-Can assessment. It has been organized into five chapters that constitute the core of the report, supported by several appendices containing additional and supporting information. The updated thermodynamic database used to conduct the solubility calculations has been issued as a separate report /Duro et al. 2005/.

The near field system for which the concentration limits of the radionuclides are assessed and the scenarios selected by SKB to calculate the solubility limits are thoroughly described.

Several sources of information have been used to support the calculated solubility limits. In particular results from selected spent fuel dissolution experiments and natural analogue data are discussed to introduce the proper perspective to the results from the thermodynamic calculations.

In addition, the main conceptual and numerical uncertainties associated to the assessment of the concentration limits of each element are numerically evaluated and discussed.

Equilibrium calculations have been conducted to select the solubility limiting solid phase for each element. Furthermore a sensitivity analysis of parameters of interest for each element is presented and the impact of the uncertainties identified on the solubility of each element quantified.

The results are presented in a series of tables containing the calculated solubility for each radionuclide under the reference conditions.

Finally concentration limits that are recommended result from the expert judgement built-up around the various sources of information together with the quantification of radionuclide solubility data and their associated uncertainties. The results are compared to previous solubility limits determination performed by SKB in SR 97, as well as the recommended values from other HLNW management organisations.

Sammanfattning

Den här rapporten presenterar resultaten från beräkningarna av löslighetsbegränsningar för säkerhetsanalysen SR-Can. Den har organiserats i fem kapitel, vilka utgör kärnan av rapporten. Dessa stöds av ett antal appendix, vilka Innhåller stödjande information. Den uppdaterade termodynamiska databas som ligger till grund för beräkningarna har publicerats som ett separat dokument /Duro et al. 2005/.

Närområdet, där löslighetsbegränsningarna för radionuklider är bestämda och de scenarier som valts av SKB för att utgöra grunden till beräkningarna är utförligt beskrivna.

Ett flertal informationskällor har används för att stödja de beräknade löslighetsvärdena. I synnerhet har resultat från bränslelakningsförsök och data från naturliga analogier använts för att få det rätta perspektivet på resultaten från de termodynamiska beräkningarna.

De huvudsakliga konceptuella och numeriska osäkerheterna kopplade till löslighetskoncentration för varje element har utvärderats kvantitativt och diskuterats.

Jämviktsberäkningar har genomförts för att välja den löslighetsbegränsande fasen för varje element. Dessutom har en sensitivitetsanalys för de intressanta parametrarna för samtliga element genomförts och betydelsen av de identifierade osäkerheterna har kvantifierats.

Resultaten presenteras i en serie av tabeller som innehåller de beräknade lösligheterna för en uppsättning referensförhållanden.

Slutligen rekommenderas löslighetsvärden som är ett resultat av ”expert judgement” uppbyggt runt de tillgängliga informationskällorna tillsammans med de kvantifierade lösligheterna och deras associerade osäkerheter. Resultaten jämförs med de värden som bestämdes för den förra säkerhetsanalysen som genomfördes av SKB i SR 97, tillsammans med utvalda värden från andra internationella avfallsorganisationer.

Contents

1 Background and objectives

The establishment of concentration limits for radionuclides in the near and far-field of a HLNW repository is an issue of the utmost relevance for the safety assessment of the repository.

In this context, during the SR 97 exercise a large effort was devoted to determine and assess proper solubility limits. The result of the study was published as a SKB Technical Report /Bruno et al. 1997/ and was later presented as a scientific publication in Radiochimica Acta /Bruno et al. 2000/.

The SKI review of the aforementioned SR 97 exercise resulted in the identification of several deficiencies in the assessment of the solubility limits. This, besides the last development of thermodynamic databases motivated that, within the new SR-Can exercise, SKB settle a review and update of the assessment of concentration limits of radionuclides in the near-field. The results of this new assessment are reported in this document.

The present review of the solubility assessment for radionuclides aims at giving the adequate input for all those PA calculations that need of the use of solubility limits for radionuclides. The deficiencies identified SKI in the former SR 97 exercise have been now specifically addressed.

The main issues revealed by the SKI review of the solubility assessment in the near-field conducted within the SR 97 exercise, as well as the methodology put in place by SKB to give appropriate answers to the SKI concerns are presented below:

- The SKI report 00:47 /SKI 2000/ questioned the consistency of the thermodynamic database used to perform the calculations presented in /Bruno et al. 1997/. Given the relevance of the database in any solubility assessment, SKB wanted to ensure the consistency and completeness of the thermodynamic database used in the new assessment of concentration limits for radionuclides. Thus, a complete revision of the thermodynamic database was conducted and reported to SKB /Duro et al. 2005/ as supporting documentation to the present report.
- SKI reviewers criticised the use of a pore water composition resulting from the interaction of the MX-80 bentonite with a synthetic groundwater /Wanner et al. 1992/ instead of the results obtained in /Bruno et al. 1999/ concerning the chemical evolution of bentonite porewaters in the frame of the same SR-97 safety assessment exercise. Due to time constraints, solubility calculations were performed simultaneously with near-field modelling and, consequently, the chemical evolution of the bentonite porewater was available only after the calculation of the solubility limits had been already completed. In the present work solubility limits are calculated by considering four different groundwater types: granitic, saline, ice-melt water and bentonite groundwater composition that has resulted from the interaction of bentonite and the Forsmark reference groundwater, as it is currently being developed and reported by /Arcos et al. 2005/. This will ensure the consistency of the whole exercise.
- The last comment made by SKI regarding the solubility assessment was related to the uncertainty assessment. The reviewer considered that the approach of using only two limiting values for a given variable of influence on the solubility of a radioelement when judging its importance was not a sufficiently good approach from a perspective of quality assurance, and he suggested a probabilistic approach for the solubility calculations. The same reviewer, though, recognised the inherent difficulties of applying a probabilistic approach to this type of data analyses. Due to this complexity and to the uncertain adequacy or probabilistic analyses for solubility assessment, what has been developed here is a sensitivity analysis that yields the variability of the solubility of a given element with the main groundwater parameters.

2 Structure of this document

The present report has been organized into five chapters that form the core of the report, supported by several appendices containing supporting information. The updated thermodynamic database used to conduct the solubility calculations has been issued as a separate report /Duro et al. 2005/.

The main body of this report is conformed by the following chapters:

Chapter 3. Use in Sr-Can

This chapter defines the system for which the concentration limits of the radionuclides are assessed, and it presents documents and justifies the scenarios selected by SKB to assess solubility limits, and describes the methodology followed to conduct the solubility assessment.

Chapter 4. Sources of information

This chapter presents other sources of information, besides the solubility calculations, involved in the expert judgement conducted for the selection of the concentration limits. Results from spent fuel dissolution tests and from natural analogues are reported and discussed from the perspective useful to the present analyses.

Chapter 5. Uncertainty assessment

This chapter presents the main conceptual and numerical uncertainties associated to the assessment of the concentration limits of each element. The numerical level of uncertainty is detailed in Chapter 6 for each element.

Chapter 6. Quantification of data and uncertainties

This chapter presents the calculations conducted to select the solubility limiting solid phase for each element, a sensitivity analyses for those parameters of interest for each element and a quantification of the impact of the uncertainties identified in Chapter 5 on the solubility of each element. Tables containing the calculated solubility for each radionuclide under the reference conditions are presented.

Chapter 7. Recommended concentration limits

This chapter presents the recommended concentration limits that result from the expert judgement built-up around the sources of information detailed in Chapter 4 and the quantification of data and uncertainties presented in Chapter 6.

The Technical Annexes included in this document are:

Appendix A: summary of concentrations of radioelements measured from spent fuel dissolution experiments.

Appendix B: summary of the concentrations of elements measured in natural waters.

Appendix C: review of the concentration limits recommended by other nuclear waste management organisations.

Appendix D: comparison of the recommended concentration limits with those calculated during the SR 97 exercise, those measured from spent fuel dissolution experiments and concentration measured in natural waters.

3 Use in SR-Can

In this chapter the system under study is defined, the scenarios for release are described, and the methodology of the calculations is presented.

3.1 System definition

For the assessment of the concentration limits of radionuclides, it is mandatory to define the system under study, and the conditions under which the concentration limits are recommended.

In this work, we will assess the concentration limits of the radionuclides in the vicinity of the spent nuclear fuel. The limits provided here are not intended to be used in the far-field of the repository, that is, in a system where the radionuclides can interact with major minerals present in the crystalline host-rock, but only in the area close to the fuel. A schematisation of the system is shown in Figure 3-1, and a more detailed picture of the fuel characteristics is shown in Figure 3-2.

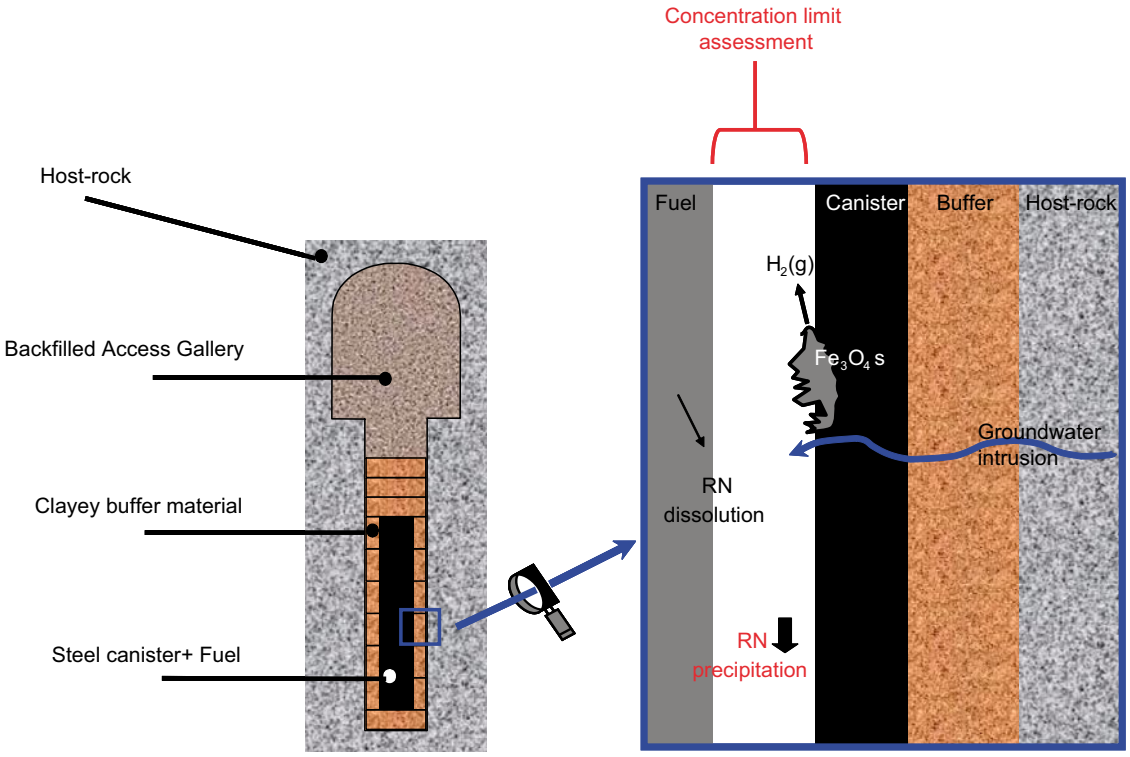

Figure 3-1. *Schematic representation of the system under study.*

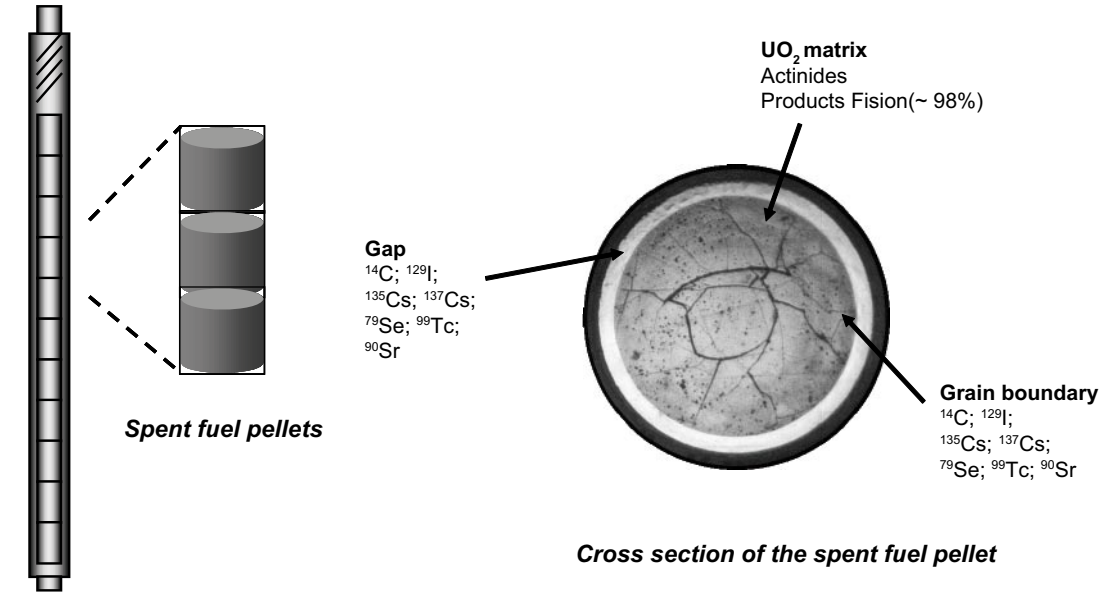

Figure 3-2. *Schematic representation of the spent fuel rods and pellets.*

It is important to keep in mind the former definition of the system when analysing the work presented in this report. The definition of the system constrains the scenarios of interest, predominantly: i) the groundwater compositions used in the solubility assessment; ii) the redox state of the system, and iii) the approaches followed to calculate the solubilities.

These three constraints are briefly described below and more extensively discussed in the forthcoming sections.

i) Groundwater composition

The groundwater interacting with the fuel can enter either

a) flowing directly along fast-paths through the buffer and canister without interacting with either the buffer or the canister, or

b) interacting with the buffer and/or the canister prior to contacting the fuel.

In the first case (a), three different groundwater compositions will be considered in the solubility assessment:

- reference deep Forsmark groundwater,
- ice-melting water intrusion after a glaciation period,
- saline water after a regional uplift.

In the second case (b), the composition of the groundwater contacting the canister will be mainly modified by its interaction with the bentonitic buffer with respect to the major cation and anion composition, and by the interaction with the canister with respect to the redox conditions.

ii) Redox state of the system

As previously analysed, the reference redox state will be that represented by the reference deep Forsmark groundwater.

Two variations of the redox state will be accounted for in this analysis:

- The event of ice-melting water intrusion will be characterised by high oxygen content.
- The event of water interacting with the canister will be characterised by the modification of the redox properties due to the presence of iron and production of magnetite in a first step and of hematite in a second step.

iii) Approaches used to calculate the radionuclide solubilities

As presented in Figure 3-1, we are focusing the solubility assessment in the gap in between the spent fuel and the steel canister. No major minerals, except those resulting from the corrosion of the steel, are expected to be present in this zone at its initial state. Thus, one of the most typical processes that may account for the solubility control of trace components in any system, such as their association with major minerals, will not be as relevant in our system as it is usually considered in the far-field of the repository.

This is the reason why coprecipitation approaches are only conceptually discussed, but the selection of the solubility limits are not centred in this type of processes, on the contrary to that case when the assessment of solubilities relates to the conditions in the far-field of the repository.

The former, as well as several other constraints imposed by the system, are described in more detail in section 3.2.

3.2 Calculation scenarios

Four different water compositions have been used as representative of the possible different scenarios resulting from some critical geochemical processes and/or climate changes. These different groundwaters are: reference groundwater, saline groundwater ice-melting groundwater and buffer equilibrated groundwater.

Those four compositions relate to the major changes that the groundwater contacting the repository may suffer as a result of hydrogeological events occurring in the surrounding host-rock.

In addition those parameters that may affect groundwater compositions at more local scale, such as temperature and redox conditions were also selected because of their relevance on the solubility calculations. In the next subsections we discuss and present in detail the different scenarios considered.

At the end of this section, Table 3.2. summarises the different scenarios considered in the calculations.

3.2.1 Selected groundwaters

Modifications of groundwater composition caused by external events, like intrusion of ice-melting water, the eventual uplift of saline waters to the repository level or interaction with the buffer material may cause an important change in the geochemical state of the system. Thus, in order to estimate radionuclide solubilities under different scenarios it is essential to assess the composition of the water that can potentially contact the spent fuel.

The different groundwater compositions selected by SKB are described below.

Reference groundwater composition

The selected reference water corresponds to the SICADA (database containing the analyses of the groundwaters of the Forsmark area) code KFM02A of the groundwater sampled in Forsmark on 2003 June the 13th packed in the interval 509–516.08 m. This composition was selected as the most representative for the reference scenario, in agreement with SKB.

The chemical composition of this groundwater is summarized in Table 3-1.The Stiff diagram of the reference groundwater is shown in Figure 3-3, from where it can be appreciated the Na^+-K^+-Cl^- character of the sample.

Table 3-1. Selected composition of the reference, saline, ice-melting and buffer equilibrated waters. Concentrations in mole·dm^{-3}.

	Forsmark reference water [1]	Saline water [2]	Ice melting water [3]	Buffer-equilibrated water [4]
pH (downhole in situ for reference water)	7	7.9	9.6	7.1
Eh (downhole in situ for reference water) (mV)	–143	–314	–200	–130
[Na^+]tot	8.88E–02	3.49E–01	6.90E–04	0.145
[K^+]tot	8.75E–04	7.41E–04	5.00E–06	0.153
[Ca^{2+}]tot	2.33E–02	4.63E–01	1.40E–04	0.0130
[Mg^{2+}]tot	9.30E–03	1.11E–04	6.20E–07	5.46E–03
[HCO_3^-]	1.77E–03	1.47E–04	4.50E–04	2.19E–03
[Cl^-]tot	1.53E–01	1.28E+00	1.60E–04	0.153
[S]tot	6.80E–03	3.56E–02	6.10E–05	2.09E–02
[Br^-]tot	2.98E–04	3.90E–03	3.80E–07	
[F^-]tot	4.42E–05	8.42E–05	3.60E–04	
[Si]tot	1.85E–04	4.99E–05	2.50E–04	6.64E–05
[Fe]tot	3.31E–05	7.66E–06	3.00E–09	3.31E–05
[Mn]tot	3.93E–05		5.00E–09	
[Li^+]tot	7.35E–06	7.74E–04		
[Sr^{2+}]tot	9.18E–05		2.00E–06	
[P]tot		3.23E–05		
Ionic strength	0.19	1.86	0.0012	0.21

[1] SKB. Pers. Comm.

[2] KLX02 in the interval 1,420–1,705 m with date of sampling 94/01/17. /Laaksoharju et al. 1995/.

[3] Grimsel groundwater composition [discharging groundwater from the Migration shear zone (AU 96)]. (Data compiled from /Bajo et al. 1989/, /Aksoyoglu et al. 1990/ and /Eikenberg et al. 1991/.)

[4] Forsmark groundwater interacted with the bentonite buffer /Arcos et al. 2006/.

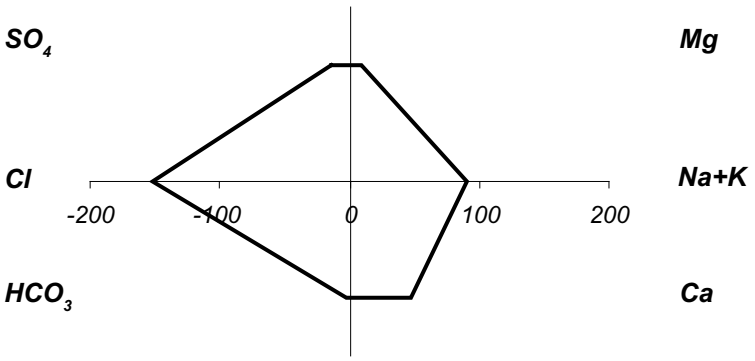

Figure 3-3. *Stiff diagram of the reference groundwater. X-Axis represents meq/l.*

Saline groundwater composition

Saline groundwater was selected in order to represent a saline uplift to the repository level. To this aim, several preliminary calculations were conducted to obtain a representative composition for the saline water to be used in the solubility calculations.

One of the calculations conducted was to take seawater (3.5% salinity) and add NaCl up to 10%. The main problem of this test was that the final Na concentration was too high when compared with saline groundwaters sampled at depth either in Olkiluoto or in Laxemar. The next step was to take seawater (3.5% salinity) and add $CaCl_2$ up to 10%. In this case calcite became oversaturated in the system and when letting it precipitate the final pH was too low in comparison with that typical of saline groundwaters.

Finally, after discussions with SKB, the groundwater composition reported in /Laaksoharju et al. 1995/ as KLX02 in the interval 1,420–1,705 m with date of sampling 94/01/17, was selected as saline water to conduct the calculations. This composition is in very good agreement with the composition of Olkiluoto brines reported in /Puigdomènech 2001/ and is selected as best representative of this sampling interval in the mentioned report.

The chemical composition of the water considered in the solubility calculations is published in /Laaksoharju et al. 1995/ and given in Table 3-1.

Ice-melting groundwater composition

Water resulting from the infiltration of melting of ice to deeper areas is expected to be rather diluted. Differently to the case of the saline or the reference groundwater, there is no a typical "ice-melting groundwater composition" selected for the scenarios of interest for SKB. For this reason, we have selected a diluted granitic groundwater, such as the one sampled in the Grimsel Test Site, as an analogue for the diluted groundwater composition expected from ice melting processes. The chemical composition is given in Table 3-1.

Buffer equilibrated groundwater composition

The composition of the groundwater once equilibrated with the bentonite of the buffer has been taken from the model reported in /Arcos et al. 2006/. It corresponds to the simulation of the interaction between the reference Forsmark groundwater and the MX-80 bentonite at 15°C after 1,000 years of interaction.

The selected compositions are shown in Table 3-1.

3.2.2 Temperature variation

The reference temperature has been fixed at 15°C, which is the average expected in groundwater at the repository depth.

Due to the presence of the waste, it is foreseen that temperature can reach up to 100°C. This thermal effect can have some effect on the solubility of the radioelements of interest. Solubility calculation at temperatures different from 25°C require of data on reaction enthalpy. This type of data is not always available for all the aqueous complexes and solids relevant in our study (for explanations see /Duro et al. 2005/). These data gaps are not very relevant to assess a change of temperatures from 25°C to 15°C, but it can importantly affect the calculations at 100°C. Given the difficulty in assessing the temperature effect at 100°C we have preferred to report only solubilities calculated at 15°C.

3.2.3 Redox state variation

The redox state of the water contacting the fuel is one of the parameters of major influence on the solubility of the radioelements, mainly the actinides U, Pu, Tc and Se.

The redox state of the water in the near field can be affected by different processes such as the corrosion of the canister or an oxic intrusion due to a fast infiltration of glacial melt water which is, normally, much more oxidising than the most common deep granitic groundwaters.

Therefore, the solubility assessment here presented has been also extended to cover the following extreme cases of variation in redox potential.

Effect of the canister corrosion

Under anoxic conditions, and when the main oxidant present in water is water itself, Fe corrodes, in a first step, to produce $Fe(OH)_2(s)$, which, in turn can experiment the Schikorr reaction to transform into magnetite, Fe_3O_4, being the overall reaction as follows:

$$Fe(s) + 4\ H_2O = Fe_3O_4(s) + 4\ H_2(g) \qquad \text{eq. 1}$$

Magnetite has been proposed as the most stable corrosion product of the canister under moderately anoxic conditions. The process causes the generation of hydrogen.

Given the large availability of iron from the canister, a hydrogen overpressure can, theoretically, build up in the system, giving rise to a decrease in the redox potential of the environment. The maximum hydrogen overpressure will be limited by the maximum lithostatic pressure at the repository depth, which has been indicated as 10 MPa (100 atm).

Consequently, the minimum redox potential that the system can reach will correspond to a pH_2 = 10 Mpa which, on a redox potential scale, implies a Eh = –476 mV at the pH of the reference groundwater (7.0).

Further corrosion of magnetite will cause the formation of Fe(III) oxides, whose most stable phase in the long term conditions of interest for PA is hematite (α-Fe_2O_3).

This means that at long-term, a dynamic equilibrium between magnetite and hematite can be established in the system, corresponding to the following reaction:

$$2Fe_3O_4 + H_2O = 3\alpha\text{-}Fe_2O_3 + H_2(g) \qquad \text{eq. 2}$$

with $\log K^0 = -6.27$ /Hummel et al. 2002/.

The boundary between the stability field of magnetite and the one of hematite will occur, thus, at a $pH_2 = 10^{-6.27}$ atm, what would give the long-term redox potential in the system when assuming steel corrosion going-on. In order to represent the range in values in the literature for this equilibrium constant (for a detailed discussion see /Hummel et al. 2002/, we selected a value of $pH_2 = 10^{-7}$ atm which, at the pH of the reference groundwater implies a value of Eh = –207 mV.

Effect of an oxic disturbance

To consider the scenario of an oxic intrusion into the system, the calculations have considered also a case with an oxygen partial pressure equal to the atmospheric value (pO_2 = 0.2 atm).

A summary of the conditions under which the solubility of the different radionuclides considered has been calculated in this report is presented in Table 3-2.

Table 3-2. Conditions assumed for solubility calculations corresponding to each groundwater considered.

Groundwater	Conditions redox	T (°C)
Reference cases	Groundwater pe (–2.42)	15
	$pH_2(g)$ (atm) = 10^{-7}	15
	$pH_2(g)$ (atm) = 10^{2}	15
	$pO_2(g)$ (atm) = 0.2	15
Ice-melting	Groundwater pe (–3.38)	15
Saline	Groundwater pe (–5.32)	15
Buffer eq.	Groundwater pe (–2.20)	15

3.3 Modelling approaches

Solubility limits have been assessed for the list of 21 radioelements given in Table 3-3.

A sensitivity analysis has been first conducted, in order to study the influence of the main groundwater composition on the geochemistry of the selected radionuclides. These calculations have been used by means of the MEDUSA software package /Puigdomènech 2002/.

From the sensitivity analyses, the main solid phases thermodynamically able to precipitate in the system can be identified. Nevertheless, an important contribution of expert judgement must be used when selecting, from all possible thermodynamically favourable phases, those kinetically more likely to form. This expert judgement has been conducted by using several of the sources of information presented in Chapter 4, such as information from laboratory experiments and natural systems.

Once the solid phase is selected, the solubility of this phase under the conditions of the groundwater has been calculated by adding the radioelement to the solution until equilibrium with the solid phase is achieved. In this way, it is ensured that the only modification of the solution with regards the composition of the groundwater of interest is related to the concentration of the metal of interest.

Individual solubility calculations have been performed by using the PHREEQC code /Parkhust and Appelo 2001/ and assuming equilibration of the corresponding metal ions with the pure solid phases considered in each case. In general, we have assumed the basic principle that the less crystalline phases are kinetically favoured and consequently they constitute the initial solubility limiting solid phases.

Special attention was focused on the ionic strength corrections and the different approaches used by the computer codes. In the next sub-section we discuss on the different approaches used and the corrections accounted for.

Table 3-3. List of radionuclides studied in this exercise.

Carbon	Palladium	Thorium
Nickel	Silver	Protactinium
Selenium	Tin	Uranium
Strontium	Caesium	Neptunium
Zirconium	Samarium	Plutonium
Niobium	Holmium	Americium
Technetium	Radium	Curium

3.3.1 Ionic strength corrections

The HYDRA-MEDUSA code uses eq. 3 to calculate the activity coefficient of a species. Eq. 3 is a variation of the Extended Debye_Hückel equation based on an approximation to the model by /Helgeson et al. 1981/ and /Oelkers and Helgeson 1990/. Z_i is the charge of the ion, I the ionic strength (m), A is a constant equal to 0.5100 $mol^{-0.5}$ $kg^{0.5}$ at 25°C, B is a parameter defined by temperature, pressure and the dielectric constant of water and b is a parameter dependent on temperature and pressure.

$$\log(\gamma_i) = -z_i^2 \left(\frac{A\sqrt{I}}{1 + B\sqrt{I}} \right) - \log(1 + 0.018I) + bI \qquad \text{eq. 3}$$

The PHREEQC code can use two different equations to calculate the activity coefficient of a species. By default, it applies the Davies equation (eq. 4). But in case that the values of a and b in eq. 3 are available, the PHREEQC code uses eq. 5 for the calculation of the activity coefficients ai and bi are ion-specific parameters fitted from mean – salt activity – coefficient data /Parkhurst and Appelo 2001/.

$$\log(\gamma_i) = -0.5102\, z_i^2 \left(\frac{\sqrt{I}}{1 + \sqrt{I}} - 0.3\, I \right) \qquad \text{eq. 4}$$

$$\log(\gamma_i) = -z_i^2 \left(\frac{A\sqrt{I}}{1 + Ba_i\sqrt{I}} \right) + b_i I \qquad \text{eq. 5}$$

All these approaches (eq. 3 to eq. 5) are commonly accepted to calculate activity coefficients for species at ionic strengths lower than 0.1 m, reaching in some cases to good extrapolations until I = 0.2 m. Nevertheless, they are not applicable to ionic strengths as high as the one of the saline groundwater we study in this work (I = 1.86 m). In this case, and in agreement with the NEA guidelines, the Specific Ion Interaction Theory (SIT) is preferred. None of the codes uses the SIT methodology to calculate the activity coefficient of a species as a function of the ionic strength; the activity coefficient is such case is defined according to eq. 6.

$$\log(\gamma_i) = -z_i^2 \left(\frac{A\sqrt{I}}{1 + Ba_i\sqrt{I}} \right) + \sum_k \varepsilon_{(i,k,I)}\, m_k \qquad \text{eq. 6}$$

where a_i is the effective diameter of the hydrated ion, $\varepsilon_{(I,k,I)}$ is the ion interaction coefficient and m_k is the molality.

Differences in ionic strengths as a function of the groundwater composition lead us to assess variations due to the different approaches used for ionic strength corrections. In general, we did not find significant variations (within ± 0.3 log units for log solubility) in our calculations due to the equation used to correct for ionic strength effects. In those cases where larger differences were detected, we selected the activity coefficient calculated by using the SIT methodology, and the solubility values in agreement with this approach. The main differences were found as expected in the saline water composition and in those cases where the aqueous speciation was dominated by highly charged species with a stability very dependant on ionic strength, i.e. silver chlorides.

3.4 Sensitivity analyses

The sensitivity analyses presented in Chapter 6 is based on the variation of the parameters that most affect each one of the elements included in this assessment. Although the results of this analyses are extensively reported in Chapter 6, we present in Table 3-4 which are the parameters of interest for each element.

Table 3-4. Main geochemical parameters affecting to the geochemical behaviour of each radionuclide under study. Shadowed cells indicate that the element in the row is sensitive to the parameter indicated in the column within the range of variability of the parameter studied.

Element	pH	pe	ligand
C	■		Ca^{2+}
Cs			Cl^-
Sr	■		CO_3^{2-}, SO_4^{2-}
Ra	■		CO_3^{2-}, SO_4^{2-}, Cl^-
Sn	■		Ca^{2+}
Se	■	■	Fe(II)
Zr			–
Nb	■		–
Tc	■	■	–
Ni	■	■	–
Pd	■		Cl^-
Ag	■		Cl^-
Sm	■		CO_3^{2-}
Ho	■		CO_3^{2-}
Th	■		CO_3^{2-}
Pa			–
U	■	■	CO_3^{2-}, Ca^{2+}, $Si(OH)_4$
Np	■	■	CO_3^{2-}
Pu	■	■	CO_3^{2-}
Am and Cm	■		CO_3^{2-}

For those elements sensitive to pH, the analyses has been extended from pH 6 to 11.

For those elements sensitive to pe, the analyses has been extended from pe –8 (constrained by the maximum pH_2 = 100 atm at pH = 7) to oxidising.

For those elements sensitive to a given ligand or major component of the water, the concentration of that component has been varied in the range typical for natural groundwaters and is indicated for each case in Chapter 6.

3.5 Thermodynamic database

The aim of this work has been to modify and/or update as well as to complete, if considered appropriate, the NAGRA-PSI TDB /Hummel et al. 2002/, which has been used as a basic thermodynamic database in the assessment of the solubility limits.

The update and check for consistency and completeness of the database to be used has been conducted in the light of the open scientific literature and the available information from the various experimental programmes undertaken by the different nuclear waste management agencies with special attention to the internal consistency of the data included in the TDB as well as on formation and reaction enthalpy data for temperature corrections.

The information regarding the thermodynamic database used in the calculations is supplied in a separate report /Duro et al. 2005/. Many of the discussions presented in this report are related to a previous database selection conducted by Enviros Spain on behalf of ANDRA /Bruno et al. 2001/ and the reader is directed to the aforementioned reference when necessary.

3.6 Geochemical codes

The solubility calculations and the sensitivity analyses have been conducted by two different geochemical codes: PHREEQC and HYDRA-MEDUSA, respectively.

The PHREEQC interactive code version 2.10.0.0 (released 2nd. November 2005) /Parkhust and Appelo 2001/ is a very powerful geochemical program that allows speciation and solubility calculations among other capabilities. The reason for selecting this code, among others, is that it is an open code developed by the USGS that has been widely used in multitude of geochemical calculation and is, therefore, extensively tested in many different type of problems. The thermodynamic database for radioelements has been changed in agreement with the supporting information reported in /Duro et al. 2005/.

The HYDRA-MEDUSA package is a combination of a thermodynamic database and a geochemical code that allows a very easy drawing of many different types of chemical diagrams: predominance, fraction, solubility, among others. The package has been developed by Puigdomènech at KTH. The version used is that released on 18th February 2004. HYDRA is a hydrochemical equilibrium-constant database that allows an easy creation of input files for MEDUSA, which is the windows interface to the MS-DOS versions of INPUT, SED and PREDOM FORTRAN programs drawing chemical equilibrium diagrams. The HYDRA databases have been updated for radioelements following the supporting information reported in /Duro et al. 2005/. The selection of this code-package is fully justified by the extensive use of the codes reported in the open literature and what permits a full reliability on its performance for the type of calculations of interest in this report.

The PHREEQC code has the capability of calculating the solubility for all radionuclides at a time, thus considering possible competitions among complexes. This is not possible to do with the HYDRA-MEDUSA package, given that their inputs are limited to a maximum of 9 basic components. Thus, we selected the PHREEQC code to report the final individual solubility results. Nevertheless, the advantage of the HYDRA-MEDUSA in front of PHREEQC is that the former allows a very fast and easy visualisation of predominance, fractional and solubility diagrams for the radioelements and thus, it has been used in the sensitivity analyses, where plots of the influence of different geochemical parameters on the solubility of the elements of interest are calculated. This justifies the use of two different codes in this work.

4 Sources of information

In this chapter we describe the different sources of information that will be used for carrying out the expert judgement analysis at the end of this report after compilation of all the relevant information.

These sources of information include:

1) Radionuclide concentrations measured in laboratory spent fuel dissolution experiments.
2) Reported radionuclide concentrations measured in natural analogue studies. This allows a comprehensive picture of the concentration limits we may expect and their affection by the main geochemical parameters.
3) Calculations of the concentration limits for those scenarios described in Chapter 3. These calculations are reported in Chapter 6 and are the core of this report and of the assessment on the concentration limits to be used in PA exercises.

This chapter presents data from the two first bullet points, while the last point is detailed in Chapter 6.

4.1 Apparent solubility limits in spent fuel dissolution experiments

Spent fuel dissolution data have been updated with spent fuel dissolution experiments performed in the recent years after the 1997 report /Bruno et al. 1997/. Although most of the experiments were not designed to obtain equilibrium radionuclide solubilities, because of the long experimental periods involved, and the changing chemical conditions, steady state concentrations were reached in most of the experiments and consequently, they may be interpreted in terms of apparent solubilities /Bruno et al. 1985/. This information provides another reference level to the present assessment.

Data reported in this section correspond to long-term spent fuel dissolution tests performed within the various national programmes. The reported results have been obtained in different laboratories: AECL in Canada /Tait et al. 1991/ and /Stroes-Gascoyne 1992/, PNL in USA /Wilson and Shaw 1987, Gray 1988, Wilson 1990ab/, Studsvik in Sweden /Forsyth 1997, Bruno et al. 1999a, 2003ab/, FZK-INE in Germany /Grambow et al. 1996, 2000/, CEA in France /Grambow et al. 2000/, and Argonne National Lab (ANL) in USA /Friese et al. 2003/.

Different experimental procedures have been used and this has an impact on the adequacy on the use of the reported data to the system under study here, although the conditions normally mimic those expected in the various HLNW repositories. Among them, different parameters such as the redox condition, the chemical composition of the leaching solutions, the surface/volume ratio and the saturation effects have been identified as the most significant. In spite of this, spent fuel dissolution data constitute an excellent test-bed to compare with the calculated solubilities, particularly for the transuranium radionuclides, where natural system data are very scarce or do not exist at all.

In Table 4-1 we present a brief description of the experimental conditions used in the different studies. For more details the reader is referred to the aforementioned references.

A table summarising the reported concentrations is given in Appendix A.

Table 4-1. Experimental conditions used by the different laboratories.

Laboratory	Fuel Type	Redox Cond.	Solution Comp.	T (°C)
AECL	CANDU	Ar/3% H_2	DI water	
		Ar	granitic gw	> 100
		Air	NaCl brine	
PNL	PWR SF:			
	– bare fuel	Air	J-13 water	25 and 85
	– fragments	Fe/no Fe	NaCl brine	30
Studsvik	SF segments:	Air	DI water	
	PWR/BWR	Ar	granitic gw	20–25
	27–49 MWd/kgU	Ar + 5%H_2		
Studsvik	SF fragments	Ar	DI water	25
			$2 \cdot 10^{-3}$M NaCl	
	PWR		Granitic gw	
	40 MWd/kgU		10^{-2}M $NaHCO_3$	
			10^{-2}M $NaHCO_3$ +$2 \cdot 10^{-3}$M NaCl	
FzK-INE	SF	Ar		
	PWR 50 MWd/kgU	Fe		
	– pellets		DI water	25
			NaCl brine	150
	– powder		NaCl brine/0.03%CO_2	25
			NaCl brine/1%CO_2	
			granite water/0.03%CO_2	
			bentonite water/0.03%CO_2	
CEA	SF	Ar+3%H_2	clay and granite water	90
			granite and granite water	
	60 MWd/kgU		clay and clayey water	
			granite and clayey water	
ANL	Commercial Spent Nuclear Fuel (CSNF): ATM-103 and ATM-106		J-13 water	

Apparent solubility limits are summarised and compared in the following sub-sections element by element by grouping the results of the different laboratories in different graphs as a function of the redox conditions:

i) oxic, in contact with air,

ii) anoxic, experiments carried out in an Ar atmosphere. Therefore the oxidants and reductants present in the system are generated by water radiolysis,

iii) reducing, including those experiments carried out in the presence of a given percentage of hydrogen and those tests were metallic iron was added to the system.

The same graphical representation is used to show the results for:

iv) deionised water (DIw),

v) groundwater (gw),

vi) NaCl brines (NaCl).

The temperature for the experiments represented in the following figures are at room temperature unless otherwise indicated. High-temperature data are indicated in grey.

4.1.1 Elements of the groups IA to VIIIA

Caesium

Caesium is a radioelement not expected to be solubility limited. The release of this element is mainly governed by an instant release fraction of the Cs located in the gaps and in the grain boundaries at short contact times, followed by its congruent release with the dissolution of the matrix at long term. Therefore, the different caesium concentrations reported under reducing and under anoxic conditions are the results of the effect of the chemical conditions on matrix dissolution. In this sense no important influence of the composition of the contacting solution on the aqueous Cs concentration is observed. The only influence is found in brines, where a higher caesium release under reducing conditions is observed.

According to these data, two ranges of caesium concentrations can be identified depending on the redox conditions of the system at low temperature, for reducing conditions concentrations are in the range of 10^{-7}–$10^{-5.5}$ mole·dm^{-3} and under oxic and anoxic conditions the measured concentrations fall between $10^{-5.5}$ and $10^{-4.5}$ mole·dm^{-3} (Figure 4-1).

Strontium

The measured strontium concentrations under reducing conditions range between 10^{-9} and 10^{-7} mole·dm^{-3} approximately (Figure 4-2). The range of concentrations in deionised water is lower than in brines and this is in turn lower than in groundwaters. Measured concentrations at high temperature are in general lower than those at room temperature.

Sr concentrations under anoxic conditions are slightly higher than under reducing conditions in all the water compositions, with values ranging between $10^{-7.5}$ and 10^{-5} mole·dm^{-3}. Given that this radionuclide is not redox sensitive, these differences indicate that its release, at least under reducing conditions, is controlled by the matrix dissolution even at the long contact times reported in most of the studies. The stability of the matrix under reducing conditions leads to a small Sr release without reaching Sr concentrations that may allow the precipitation of a secondary solid phase. The ranges of concentrations under anoxic conditions are closer to the solubilities exerted by the precipitation of celestite ($SrSO_4$) or strontianite ($SrCO_3$).

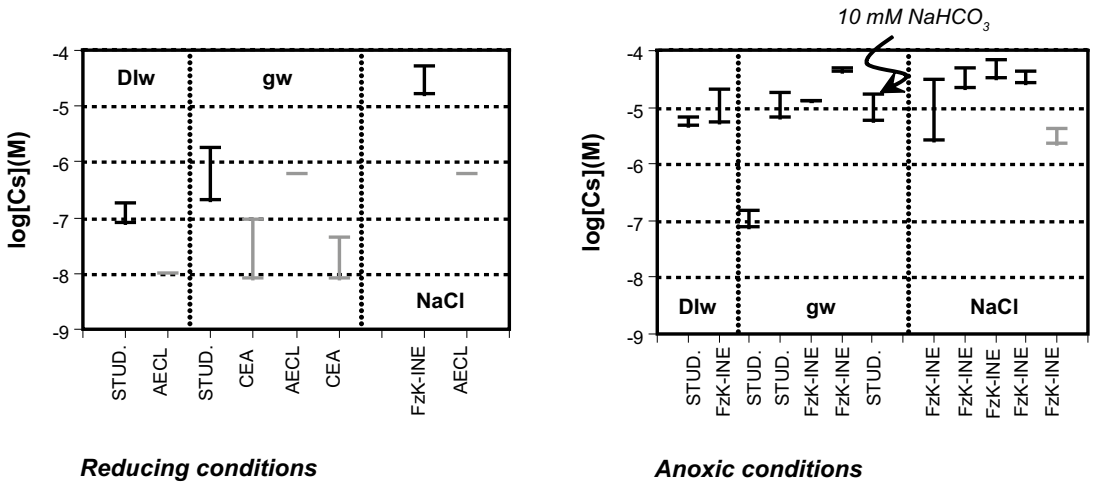

Figure 4-1. *Measured caesium concentrations reported by the different laboratories. Data in grey correspond to high temperatures (> 85°C).*

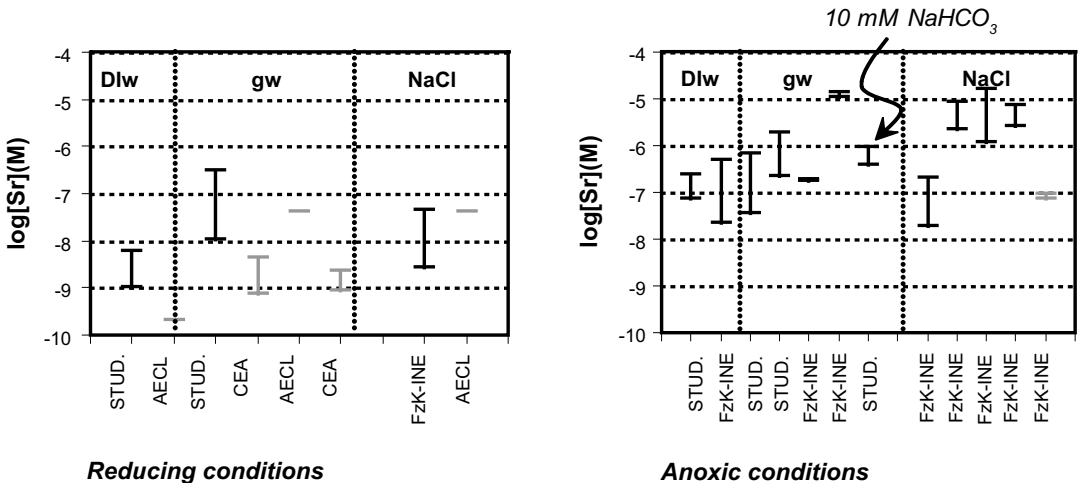

Figure 4-2. *Measured strontium concentrations reported by the different laboratories. Data in grey correspond to high temperatures (> 85°C).*

The different concentration range measured in groundwater is the result of the different carbonate contents in the solutions contacting the fuels. Two ranges of concentrations are obtained in NaCl brines, as for the other radionuclides, the different fuel samples used in the tests had an important effect on the release of Sr to solution.

Strontium concentrations measured under oxic conditions, in granitic groundwater range between $10^{-7.3}$ and $10^{-6.3}$ mole·dm^{-3}, values that are within the ranges shown in the previous figure for anoxic conditions.

4.1.2 Transition elements

Zirconium

Few Zr data are reported in the literature from long contact time spent fuel dissolution experiments. Selected values are in anoxic and oxidising conditions, at room temperature and by using granitic groundwater as leaching solution /Forsyth 1997/. Values range between $10^{-7.1}$ and $10^{-8.9}$ mole·dm^{-3}.

Technetium

Technetium concentrations under reducing conditions are about two orders of magnitude lower than under oxidising conditions, at room and high temperatures. Tc concentrations range between 10^{-9} and 10^{-7} mole·dm^{-3} under reducing conditions, and between 10^{-7} and 10^{-5} mole·dm^{-3} under oxidising conditions. No clear effect of temperature is observed.

Tc concentrations (Figure 4-3) under anoxic conditions do not show a clear dependence on the solution composition; most values reported in the literature range between $10^{-7.5}$ and $10^{-5.5}$ mole·dm^{-3} (Figure 4-3). This range agrees with the assumption of technetium concentrations controlled by the solubility of $TcO_2 \cdot xH_2O$. The highest ranges determined in FZK-INE correspond to those experiments carried out by using a sample of spent fuel powder.

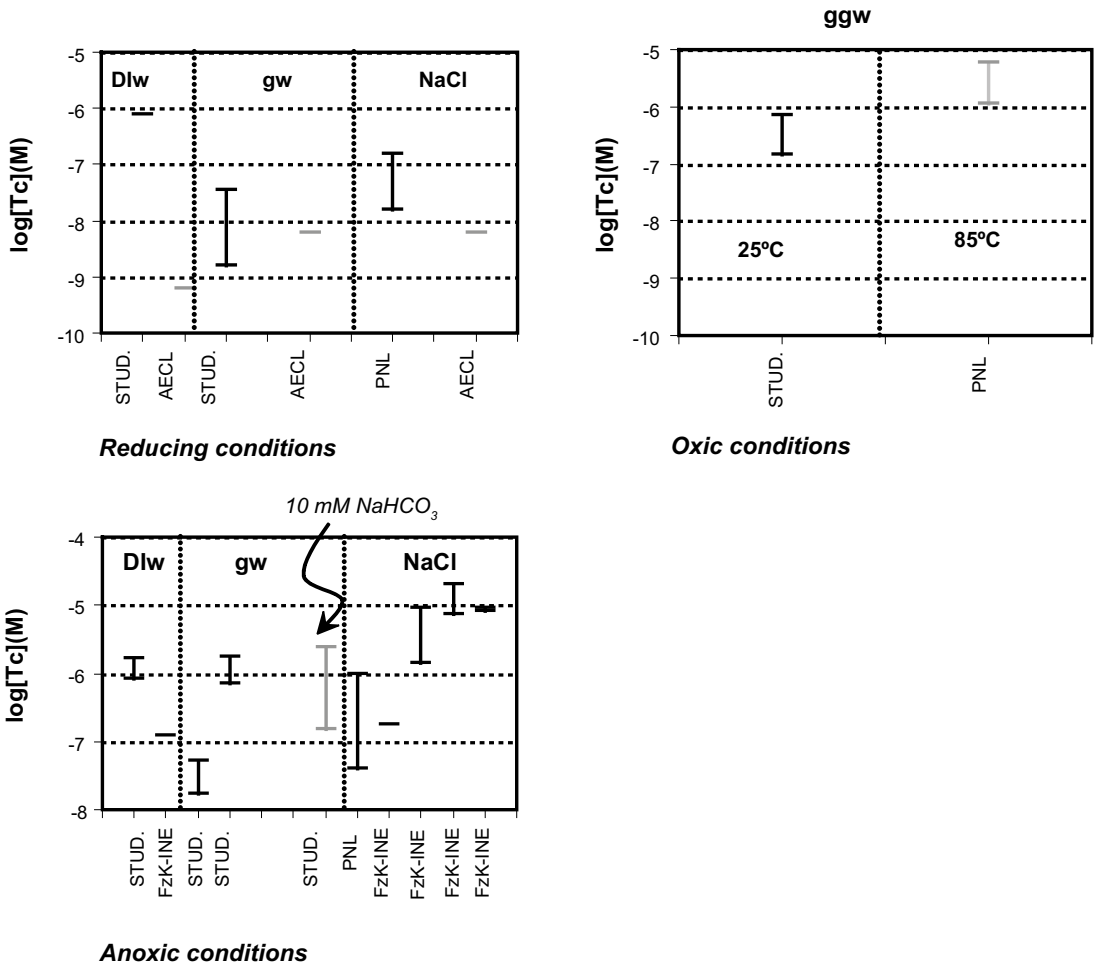

Figure 4-3. *Technetium concentrations measured by the different laboratories. References reported in the previous section. Data in grey correspond to high temperatures (> 85°C).*

4.1.3 Lanthanides

Samarium

Measured samarium concentrations from spent fuel dissolution experiments carried out in granitic groundwaters at room tempeature range between 10^{-9} and 10^{-8} mole·dm^{-3}.

4.1.4 Actinides

Uranium

Measured uranium concentrations reported in the literature at long contact times are shown in the following figures grouped by similar redox conditions.

Uranium concentrations measured under reducing conditions range between 10^{-7} and 10^{-9} mole·dm^{-3} in deionised water with no dependence on the temperature of the system, while they are up to two orders of magnitude higher in groundwater (Figure 4-4). In this medium, the concentrations measured at high temperature are clearly lower than the ones measured at room temperature, as expected from the dependence on the solubility of the UO_2(s) matrix with T in carbonate medium. Concentrations measured in brines are at the same level as those measured in groundwater.

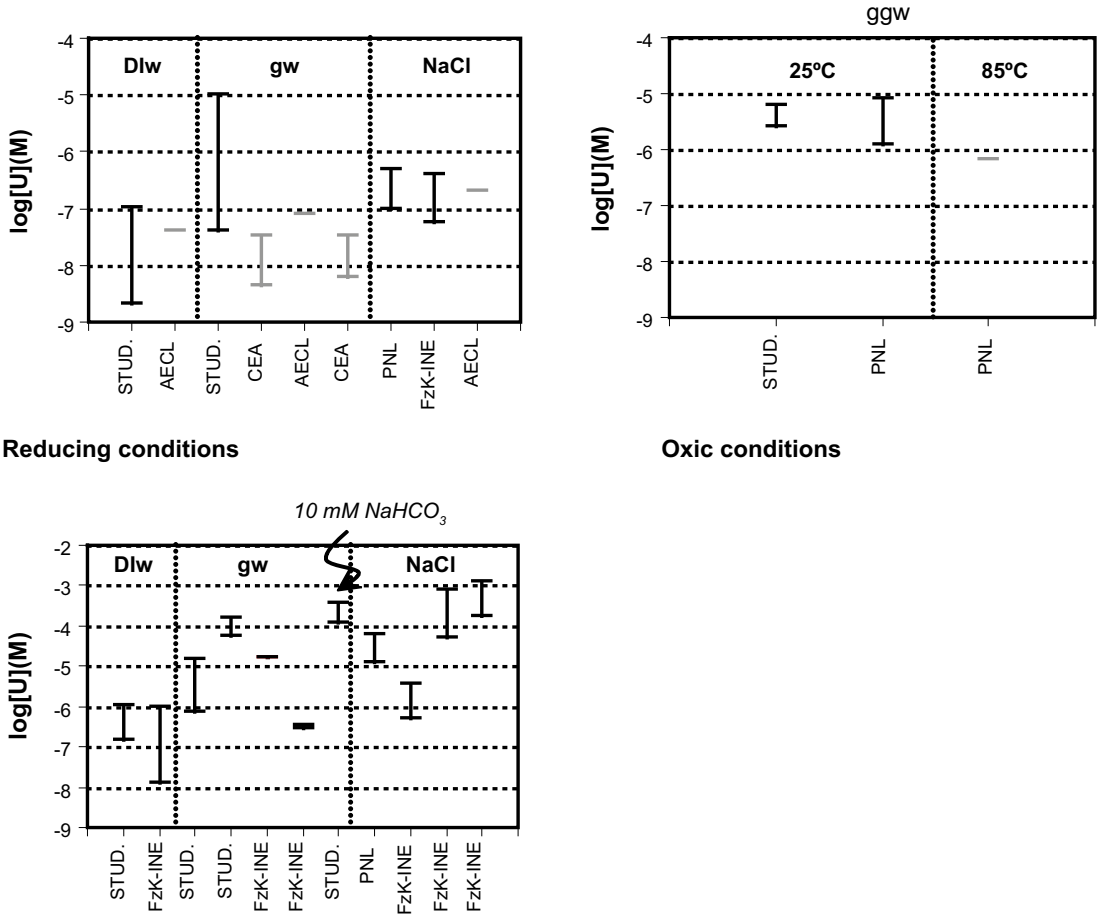

Figure 4-4. *Uranium concentrations measured by the different laboratories. Data in grey correspond to high temperatures (> 85°C). (ggw stands for granitic groundwater).*

Concentrations measured under oxic conditions are in the upper range measured under reducing conditions when comparing with the same type of solution composition, that is 10^{-6}–10^{-5} mole·dm^{-3}, and are in the range expected for the solubility of U(VI) hydroxide phases, such as schoepite (Figure 4-4). Concentrations measured at high temperatures are also lower than those obtained at room temperature.

U concentrations measured in anoxic conditions range from 10^{-8} to 10^{-6} mole·dm^{-3} in deionised water, slightly higher than under reducing conditions (Figure 4-4). The range of concentrations measured in groundwater is wider, mainly due to the different carbonate contents of the solutions used by the different laboratories. In general, we may expect higher uranium concentrations when increasing the carbonate content. The largest U concentrations are obtained in those experiments carried out in a 10 mM carbonate solution. Measured U concentrations range between $10^{-6.5}$ and 10^{-3} mole·dm^{-3}. This range is also found for those experiments carried out in brines, probably due to ionic strength effects. On the other hand, U concentrations measured in brines show at least two differentiated ranges of concentrations in anoxic conditions. These differences are attributed to the different character of the solid samples used, powder and pellets. U concentrations controlled by solubility are expected to be in the lower ranges of carbonate-free solutions, that is the case of tests performed in brines.

Summarising, concentrations measured in anoxic systems are larger than those measured under reducing conditions. Differences can be in some cases up to three orders of magnitude; reflecting the different solid phases exerting the solubility control under the various redox conditions.

Neptunium

No Np data under reducing conditions are available. Most of the neptunium concentrations selected from the literature range from 10^{-9} to 10^{-6} mole·dm^{-3} (Figure 4-5). The major differences may be related to the different carbonate content in the leaching solutions. No differences are observed in the concentrations measured under oxic or anoxic conditions, indicating that the solid phases able to precipitate and, consequently, governing the concentration of this radionuclide in the aqueous phase are the same. Np concentrations measured at high temperature are in the lower range, indicating a negative enthalpy of dissolution for the solubility controlling solid phases. Calculated entalphy of dissolution reaction for NpO_2(am) based on thermodynamic data of /Lemire 1984/ is –81.16 ± 8.79 as reported in /Duro et al. 2005/. The much wider range of concentrations observed in the case of the experiments performed by ANL (Argonne National Lab) is due to the different methodology used, drip tests. In the graph, only the concentrations of Np obtained after 1 year of the star of the test have been plotted. High concentrations, in the order of 10^{-6} moles Np/dm^3 were measured in the initial stages of the alteration of the fuel, and these concentrations evolved towards values in the range of 10^{-9}–10^{-10} mole/dm^3 with time (after approx. 1 year of the starting of the test). Although we have represented ANL data under oxic conditions, the explanation by the authors on the drip tests indicate that there is no sufficient oxygen in the system to oxidize more than 1% of the fuel.

Plutonium

The general rule is that plutonium concentrations measured at room temperature are larger than those measured at high temperatures, that, as in the case of Np, indicates negative dissolution enthalpies. Calculated entalphy of dissolution reaction for PuO_2(am) based on thermodynamic data of /Lemire 1984/ is –58.55 ± 7.76 as reported in /Duro et al. 2005/.

Pu concentrations measured in deionised water and under reducing conditions are on the order of 10^{-8} mole·dm^{-3} (Figure 4-6). These concentrations are larger than the ones measured in groundwater or NaCl brines (10^{-9}–$10^{-10.5}$ mole·dm^{-3}) under the same redox conditions. Measured concentrations in oxic conditions are, as expected, higher than those under reducing conditions.

A different trend is obtained under anoxic conditions. Measured Pu concentrations in deionised water are lower than those determined in groundwater or brines. The two ranges of concentrations measured in brines are attributed to the different type of solid material used (powder and pellets) and consequently active surface area. Pu concentrations governed by a solubility control are expected to be in the lower range (10^{-9}–10^{-7} mole·dm^{-3}).

In general the measured Pu concentrations agree with solubility control exerted by the precipitation of Pu(IV) oxides or hydroxides, as we will show in Chapter 6. The different ranges measured in groundwaters are attributed to the varying carbonate content of the solutions used in the tests.

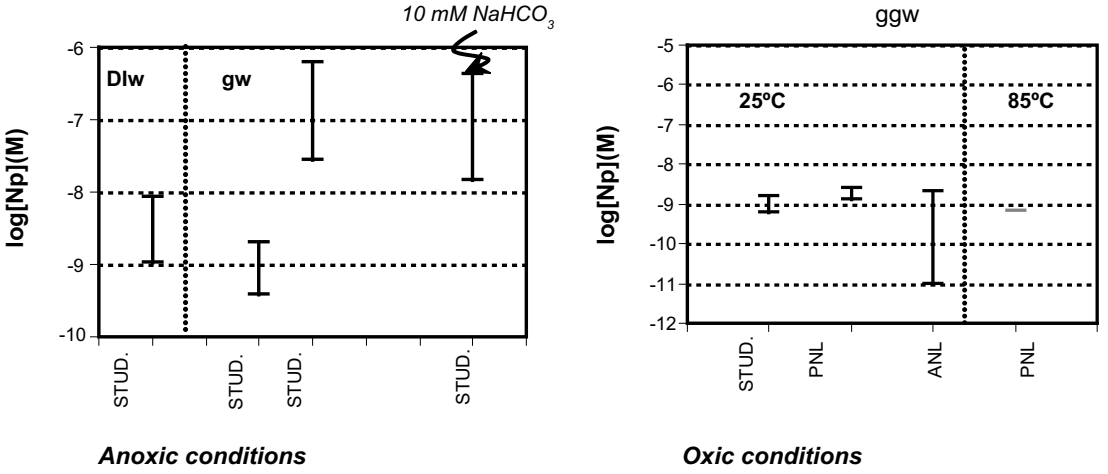

Figure 4-5. *Measured neptunium concentrations by the different laboratories. Data in grey correspond to high temperature (85°C). (ggw stands for granitic groundwater.)*

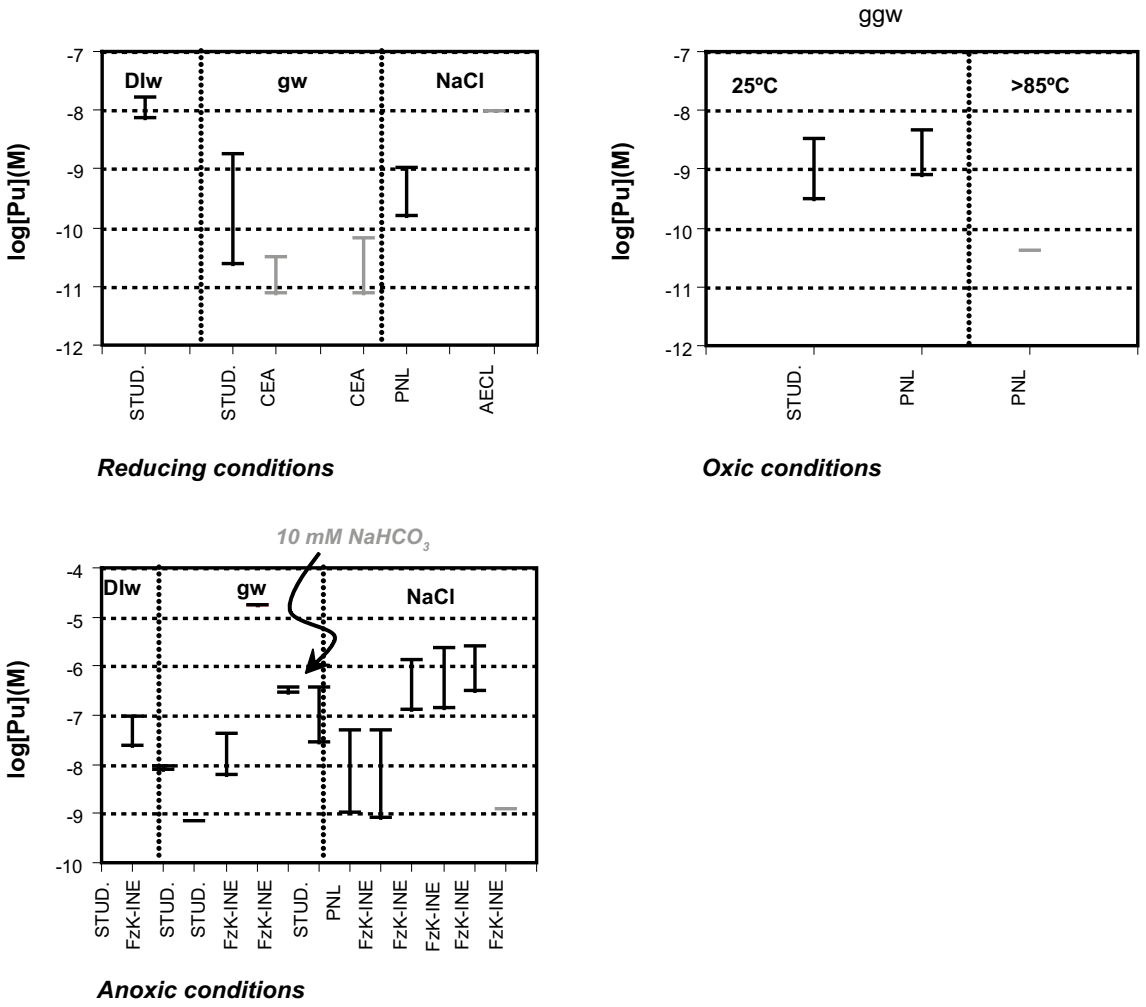

Figure 4-6. *Measured plutonium concentrations by the different laboratories. Grey symbols correspond to high temperatures (> 85°C). (ggw stands for granitic groundwater.)*

Americium and curium

Am and Cm concentrations reported at high temperature are in the same range (10^{-12}–10^{-14} mole·dm^{-3}) with no dependence on the redox conditions. Concentrations measured at room temperature are more than two orders of magnitude higher (Figure 4-7).

Am concentrations under anoxic conditions at room temperature range between 10^{-9} and 10^{-7} mole·dm^{-3}. Concentrations measured in deionised water are in the lower range while the ones measured in groundwater are around 10^{-8} mole·dm^{-3}. Cm concentrations measured in anoxic media range between $10^{-10.2}$ and $10^{-9.6}$ mole·dm^{-3} and $10^{-10.6}$ and $10^{-8.6}$ mole·dm^{-3} in deionised water and brines respectively. These ranges are around one order of magnitude lower than those obtained for Am.

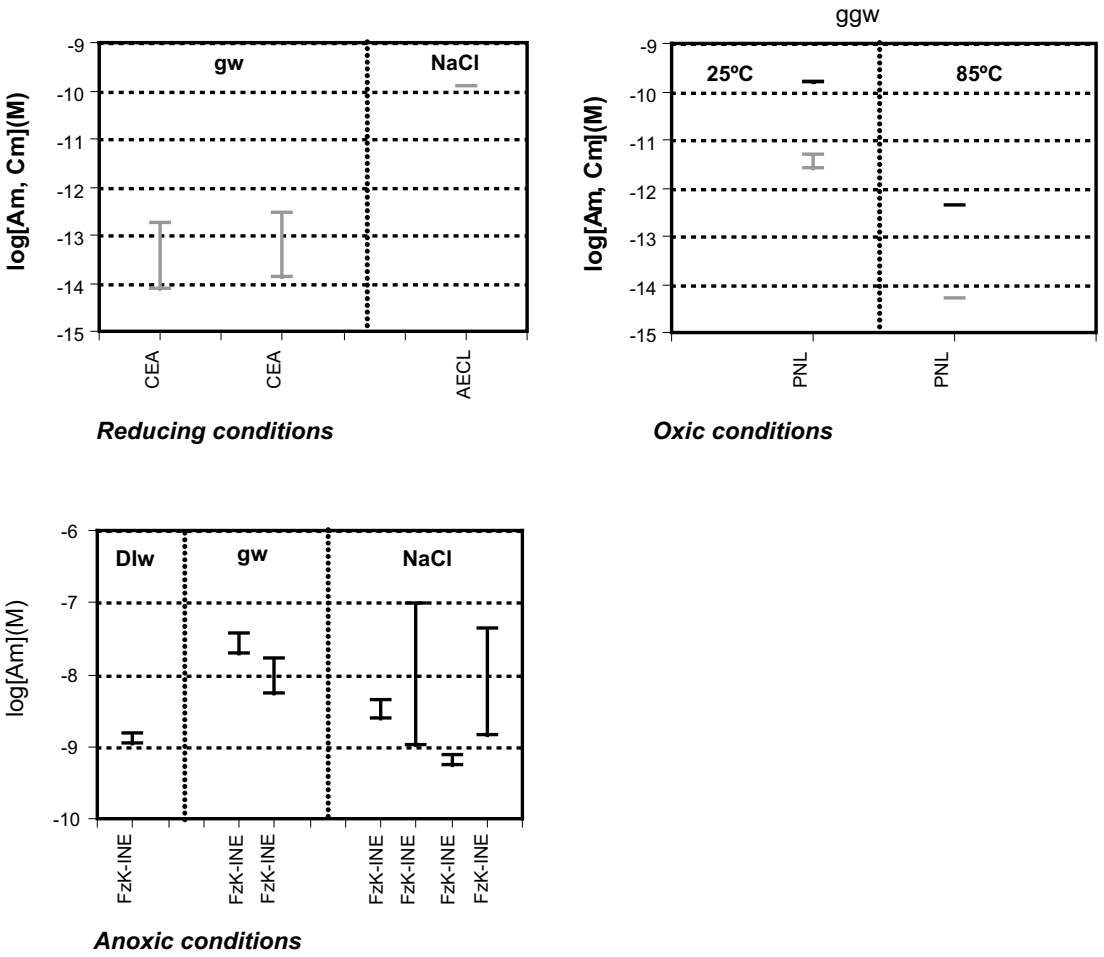

Figure 4-7. *Measured americium and curium concentrations by the different laboratories. Data reported in the previous sections. Oxic conditions: grey data for curium and black data for americium. (ggw stands for granitic groundwater.)*

4.2 Concentrations in nature

The information contained in /Bruno et al. 1997/ has been updated with those new data reported in /Bruno et al. 2002/, as a result of the summary information obtained from 7 different natural analogue projects:

- Oman, a system of hyperalkaline springs generated by low temperature serpentinisation reactions.
- Poços de Caldas (Brazil), a Mesozoic volcanic ring-structure hosting a U-Th mineralisation.
- Cigar Lake (Canada), a 1.3 billion year old U deposit located in a water saturated sandstone where the ore is surrounded by a clay-rich halo.
- Maqarin (Jordan), spontaneous combustion of bituminous-rich marl has produced natural cements which, through interaction with normal pH groundwater, has produced hyperalkaline waters similar to those expected within a cementitious radioactive waste repository.
- El Berrocal (Spain), a granitic Hercinian massif intercepted by a quartz vein with associated primary U mineralisations.
- Oklo (Gabon), a fossil natural nuclear reactor systems located in a Precambrian sedimentary basin.
- Palmottu (Finland), a U deposit located within Precambrian metamorphosed supracrustral and sedimentary rocks in SW Finland.

The elements for which data are available in each one of the natural analogue sites mentioned previously are indicated in Table 4-2.

We present the main natural sources and sinks for each element. A compilation of the measured contents in rocks, minerals and aqueous concentrations in surface and groundwaters is also presented when available.

For further information on concentrations of trace metals in groundwaters studied within the different Natural Analogue projects undertaken by various Nuclear Waste Management Agencies all over the world the reader is referred to /Bruno et al. 2002/ and references therein.

4.2.1 Elements of the groups IA to VIIIA

Caesium

Caesium content and occurrence in rocks and minerals

The average abundance of caesium in soils, earth crust, sediments and igneous rocks is 5, 1, 10 and 10 ppm respectively /Bockris 1977/.

Some studies on granite crystalline media show Cs concentration in rocks (Äspö Underground Research Laboratory) around 3 ppm.

Investigations in clayey environments show that Cs present in bentonites from Cabo de Gata (Spain) is the less mobile of all the trace elements analysed /Caballero et al. 1986/. Likewise, the Cs content in samples of the massive U-ore from Cigar Lake site can be as high as 1.3 ppm /Smellie et al. 1994/.

The normal Cs contents in the rock samples from Poços de Caldas (Brazil), an alkaline volcanic environment, is about 0.5 ppm but at the redox front it can exceed 5 ppm /MacKenzie et al. 1991/ due to accumulation processes.

Table 4-2. Elements of interest for this work studied in each of the natural analogue projects mentioned in the text.

Element	El Berrocal	Palmottu	Oklo	Cigar Lake	Poços	Oman	Maqarin
Sr	x	x		x	x		
Ra							x
Sn						x	x
Se						x	x
Zr						x	
Tc				x			
Ni	x	x	x	x	x	x	x
Pd						x	
REE		x	x				
Th	x	x		x	x	x	x
Pu				x			
U	x	x	x	x	x	x	x

Caesium content in natural waters

Cs is a cation with a low polarising ability, therefore it is weakly hydrolysed and complexed in both freshwater and seawater and its aqueous speciation is dominated by the free cation Cs^+ /Turner et al. 1981/.

Cs concentration in sea water ranges between $2.3 \cdot 10^{-9}$ mole/dm^3 /Whitfield and Turner 1987/ and $3.7 \cdot 10^{-9}$ mole/dm^3 /Lloyd and Heathcote 1985/ and the main form in which caesium occurs is Cs^+. The residence time of Cs in the ocean is $6 \cdot 10^5$ years /Whitfield and Turner 1987/.

The average contents in granitic Äspö groundwaters is $1.9 \cdot 10^{-8}$ mole/dm^3 /Miller et al. 1994/ while Cs content in groundwaters sampled in the Cigar Lake uranium deposit is found to be $5.2 \cdot 10^{-7}$ mole/dm^3 /Cramer et al. 1994/.

Strontium

Strontium content and occurrence in rocks and minerals

The average abundance of strontium in soils, earth crust, sediments and igneous rocks is 300, 385, 450 and 350 ppm respectively /Bockris 1977/.

Its valence and ionic size (1.12 Å) indicate that strontium can potentially substitute a variety of elements, such as Pb, Ca and Ba in rocks and minerals. Celestine ($SrSO_4$) is the main Sr mineral source and is found in evaporite deposits or in hydrothermal veins.

Strontianite ($SrCO_3$(s)) forms a complete and continuous solid-solution with $BaCO_3$ and is most commonly found as hydrothermal veins, often in association with lead mineralisation.

The upper Sr contents of the reference granite from El Berrocal is of 6.85 ppm /Pérez del Villar et al. 1995/.

Samples from clay media of the massive U-ore from the Cigar Lake deposit have a Sr content of 1,680 ppm /Smellie et al. 1994/.

In the alkaline volcanic media of Poços de Caldas the Sr contents in rocks range between 100 and 350 ppm /MacKenzie et al. 1991/.

Strontium content in natural waters

Strontium forms the divalent cation Sr^{2+} that is the dominant strontium aqueous species in most natural waters, together with strontium carbonate and sulphate complexes.

Sr concentrations in sea water ranges between 8.9 and $9.0 \cdot 10^{-5}$ and its average residence time is $4 \cdot 10^6$ years /Whitfield and Turner 1987/.

Similar Sr concentrations are found in all granitic groundwaters where data are available: Sr concentrations in El Berrocal groundwaters were very close to the analytical detection limit, in the order of 10^{-6} mole/dm^3, while similar or slightly higher concentrations were measured in Palmottu groundwaters. /Edmunds et al. 1989/ report Sr concentration in UK groundwaters in the range from below $2.2 \cdot 10^{-7}$ mole/dm^3 to about $8 \cdot 10^{-11}$ mole/dm^3. In the Cigar Lake groundwater samples, concentrations of Sr are in the range of 10^{-6} to 10^{-7} mole/dm^3. The measured concentrations of this element in alkaline volcanic media like Poços de Caldas present a larger scatter, from 10^{-8} to 10^{-5} mole/dm^3 reflecting the differences in the geochemistry of this site.

Radium

Radium content in rocks and minerals

Trace radium concentrations in groundwaters tend to coprecipitate with barium to form barite solid solutions, Ba-Ra-SO_4 /Doerner and Hoskins 1925/ that can behave ideally at trace Ba concentrations. In fact, this coprecipitation process is the basis for the removal of radium

from mine waters and uranium mill tailings solutions /Sebesta et al. 1981, Paige et al. 1993/. The calculated partition coefficient for Ra in alkaline-earth sulphates is larger in celestite, $SrSO_4$(280), decreasing through anglesite, $PbSO_4$(11) to barite (1.8) /Langmuir and Riese 1985/.

The behaviour of radium in sedimentary brines of the Palo Duro Basin in Texas has been investigated by /Langmuir and Melchior 1985/. All brines were undersaturated with respect to pure $RaSO_4$, but concentrations of ^{226}Ra ($0.2–5 \cdot 10^{-12}$ mole/dm^3) were probably limited by the formation of solid solutions of Ra with barite and celestite. The brines were saturated with respect to gypsum, anhydrite, celestite and barite.

Rock/brine concentration ratios for Ra in high temperature (300°C) brines from the Salton Sea geothermal field are approximately unity /Zukin et al. 1987/. The high Ra solubility in these brines is attributed to chloride complexing and reducing conditions which prevent the formation of $RaSO_4$.

Radium content in natural waters

Radium is mainly in the form of divalent cation in waters. It is mainly complexed by sulphate and carbonates in groundwaters. Chloride complexation can be important in brines.

Radium concentrations are often high in saline waters /Kraemer and Reid 1984, Dickson 1985, Laul et al. 1985/ and geothermal waters /Mazor 1962, Wollenberg 1975/, but relatively low in low-temperature, low salinity groundwaters /Michel and Moore 1980, Krishnaswami et al. 1982/.

Radium isotope activities in thermal waters of the Yellowstone National Park have been investigated by /Sturchio et al. 1993/. These authors found that radium concentrations/activities in the waters were inversely correlated with temperature and that controls on these concentrations were exerted either by the formation of a Ra-barite solid solution or by ion exchange processes of Ra in zeolites.

Radium concentrations in natural waters rarely exceed 10^{-12} mole/dm^3 /Langmuir and Melchior 1985/. In seawater Ra contents range between $1.6 \cdot 10^{-16}$ and $7 \cdot 10^{-16}$ mole/dm^3 /Whitfield and Turner 1987/.

Groundwaters from Cigar Lake have a content of Ra between 0.012 and $0.5 \cdot 10^{-12}$ mole/dm^3 /Cramer et al. 1994/, while field data on Ra concentrations measured at the hyperalkaline waters of Maqarin indicate values below 10^{-10} mole/dm^3.

Tin

Tin content and occurrence in rocks and minerals

The average abundance of tin in soils, earth crust, sediments and igneous rocks is 10, 40, 16 and 32 ppm respectively /Bockris 1977/.

The principal economic source of tin is the oxide, cassiterite (SnO_2) which is associated with granitic magmatism. Sn forms solid solutions with various ferromagnesian silicates such as pyroxenes, micas and amphiboles. This relates to the substitution of Sn (ionic radius 0.71Å) for Ti (ionic radius 0.68 Å) and Fe^{3+} (ionic radius 0.64 Å). Sn in biotite and muscovite may be as high as 1,250 ppm. Tin also occurs in sulphides such as stannite, Cu_2FeSnS_4, canfieldite, Ag_8SnS_6 and teallite, $PbSnS_2$.

About 30 ppm of Tin have been measured in the reference granite from El Berrocal /Pérez del Villar et al. 1995/. The normal Sn contents of rock samples from Poços de Caldas range between 5 and 20 ppm /MacKenzie et al. 1991/.

Tin content in natural waters

The oxidation state of tin in seawater is IV, and its content ranges between 5 and $20 \cdot 10^{-12}$ M /Whitfield and Turner 1987/.

/Byrd and Andreae 1986/ report an arithmetic mean for dissolved tin in the world's rivers of $20.5 \cdot 10^{-12}$ M and estimate a dissolved flux of tin to the oceans of $0.76 \cdot 10^{6}$ mol yr^{-1} and $300–600 \cdot 10^{6}$ mol yr^{-1} for the particulate fraction.

/Edmunds et al. 1989/ measured tin concentrations in groundwaters in various aquifers of the U.K. Values in the range $2.5–8.4 \cdot 10^{-9}$ M were found in groundwaters in the Millstone Grit and Carboniferous Limestone of Derbyshire, the Old Red Sandstone of Moray, the Trias of Shropshire, the Wealden and Lower Greensand. In only one sample was tin above $8.4 \cdot 10^{-9}$ M. 19 Bulgarian saline deep groundwaters have Sn concentrations in the range 0–5.6 µM /Pentcheva 1965/. The abundance of tin in hot springs (16–92°C) in Japan was in the range $0.84–8.4 \cdot 10^{-9}$ M /Ikeda 1955/.

Aqueous concentrations of Tin in Natural Analogues have been determined in Oklo sandstone-clayey groundwaters, in the bituminous limestone and marl site at Maqarin in Jordan and in Oman. The concentrations of this element in Oklo groundwaters are below 10^{-9} mol/dm^3. Comparable concentrations are found in the hyperalkaline waters of Oman and Maqarin.

Selenium

Selenium content and occurrence in rocks and minerals

Selenium has a crustal abundance of 0.05 ppm and is thus a comparatively rare element. Selenium concentrations in shales are normally one order of magnitude higher (0.6 ppm) than in igneous rocks such as granite or basalt /Krauskopf 1967/. Selenium is normally associated to sulphur in Nature, an estimate of the ratio of selenium to sulphur in igneous rocks is 1 to 6,000. In seleniferous soils, selenium content may be as high as 80 ppm.

The content of selenium in coal and fuel oil ranges from 1.47 to 8.1 and from 2.4 to 7.5 ppm, respectively. The combustion of fossil fuels mobilises ~ $4.5 \cdot 10^{8}$ g of selenium annually, whereas the annual flux from river discharges to the oceans is $7.2 \cdot 10^{9}$ g /Siu and Berman 1989/. Because of the similarity of ionic radius between sulphide (S^{2-} = 1.84 Å) and selenide (Se^{2-} = 1.91 Å), selenium will substitute readily for sulphur in solid sulphides and occurs in varying proportions in pyrite, chalcopyrite, pyrrhotite, galena, sphalerite, cinnababar, stibnite, molybdenite, arsenopyirte and others.

The only evidence of native Se formation is the redox front developed at the Mina Fe (Salamanca, Spain) uranium deposit, but no data on the Se concentrations in the groundwater contacting the zone are available. Native Se occurs in nature only rarely. Selenium is a major component of 40 minerals and a minor constituent of 37 others /Elkin 1982/. Some selenium-bearing minerals are: ferroselite ($FeSe_2$); clausthalite (PbSe), stilleite (ZnSe), cadmoselite (CdSe), berzelianite (Cu_2Se) and eucairite (AgCuSe). Galena (PbS) and clausthalite (the most abundant Se-mineral) form an isomorphous series. Se also occurs as selenites (cf. sulphites, which do not occur in nature). Selenates are very rare minerals, many selenates are isostructural with their corresponding sulphates (e.g. $PbSO_4$ is isostructural with $PbSeO_4$, kerstenite). Silicates of Se are not known. Typical Se contents in minerals are /Wedepohl 1978/; galena: 0–20%; molybdenite: 0–1000 ppm; pyrite: 0–3%; pyrrhotite: 1–60 ppm; pentlandite: 27–67 ppm; sphalerite: 1–120 ppm; millerite: 5–10 ppm; marcasite: 3–80 ppm. Ferroselite occurs in roll front-type uranium deposits in sandstones and occurs at the interface between oxidised sandstone (containing goethite, limonite and hematite) and reduced pyritic uranium ore /Howard 1977/. This implies that selenium and ferrous iron in aqueous solution produced by the oxidation of seleniferous pyrite have combined to form ferroselite. Therefore, ferroselite is stable under conditions more oxidising than those required for pyrite.

The normal Se contents of the alkaline volcanic rock samples from Poços de Caldas range between 0 and 10 ppm but at the redox front they can be above 120 ppm /MacKenzie et al. 1991/. According to /Linklater et al. 1994/, the mineralogical data indicate the presence of Ca-selenate and elemental selenium in the hyperalkaline waters at Maqarin.

Selenium content in natural waters

In aqueous systems, selenium may occur as one of three oxidation states (-II, IV, VI). Only two oxidation states of selenium are thought to be important in seawater: +4 and +6.

Se contents in seawater range between 0.2 and $2.4 \cdot 10^{-9}$ mole/dm^3, and the average residence time is 30,000 years /Whitfield and Turner 1987/. The total selenium content of rivers world-wide is in the range 0.2–$9 \cdot 10^{-9}$ mole/dm^3 /Cutter 1989/. Selenium concentrations in the Truckee, Walker, and Carson River systems which drain the eastern slope of the low Se content Sierra Nevada, California and Nevada, are low, ranging from less than $0.3 \cdot 10^{-9}$ mole/dm^3 to about $16 \cdot 10^{-9}$ mole/dm^3 /Doyle et al. 1995/.

The Se concentration in slightly oxidising groundwaters at pH 7 range between $1.2 \cdot 10^{-9}$ and $1.2 \cdot 10^{-8}$ mole/dm^3 /Edmunds et al. 1989/.

The concentration of Se in Cigar Lake groundwaters never reach the analytical detection limit ($0.38 \cdot 10^{-6}$ mole/dm^3) /Cramer et al. 1994/. The aqueous concentration of Se in the hyperalkaline Maqarin groundwaters is in the range 10^{-6}–10^{-5} mole/dm^3, while in Oman the reported concentrations were always below $3 \cdot 10^{-9}$ mole/dm^3.

4.2.2 Transition elements

Zirconium

Zirconium content and occurrence in rocks and minerals

Zirconium is a refractory lithophile element and occurs predominantly in the 4+ valence state with an ionic radius of 0.78 Å.

The average abundance of zirconium in soils, earth crust, sediments and igneous rocks is 300, 190, 200 and 170 ppm respectively /Bockris, 1977/.

The most abundant Zr minerals are zircon ($ZrSiO_4$) and baddeleyite (ZrO_2). Zr forms a range of oxides, silicates, halides, oxyhalides and chalcogenides. Zr will substitute for a range of elements of similar ionic radius, such as: Mg^{2+} (0.80 Å); Fe^{2+} (0.86 Å); Y^{3+} (0.98 Å); Ti^{4+} (0.69 Å); Nb^{5+} (0.72 Å); and Ta^{5+} (0.72 Å). Ilmenite, rutile and perovskite can contain up to 0.1% Zr. Varying, but significant amounts of Zr can be found in clinopyroxene, amphibole, mica and garnet. Concentrations of ~100 ppm in these minerals are frequently encountered. These substitutions may be of the type: $Zr^{4+} = Na^{+}+Fe^{3+}$. There are ~10 oxides, 2 carbonates and sulphates and ~20 silicates listed in /Wedepohl 1978/.

The Zr contents of the reference granite from El Berrocal range between 50 and 65 ppm /Pérez del Villar et al. 1995/. The samples from the U-ore from Cigar Lake site have a Zr content of about 2,700 ppm /Smellie et al. 1994/. The normal Zr contents of the rock samples from Poços de Caldas range between 100 and 2,500 ppm /MacKenzie et al. 1991/.

Zirconium content in natural waters

In seawater, Zr is rapidly removed from seawater on the surfaces of sinking particles /McKelvey and Orians 1993/. These authors measured a dissolved Zr content of seawater varying from 12–$95 \cdot 10^{-12}$ mole/dm^3 in surface waters to $300 \cdot 10^{-12}$ mole/dm^3 in deep water. This suggests that there is both a detrital and a sea-floor source of Zr in the oceans. Phosphatic fish debris can act

as a major sink for Zr and REE dissolved in seawater, suggesting strong complexation of Zr by phosphate ligands /Oudin and Cocherie 1988/.

/Salvi and Williams-Jones 1990/ inferred from fluid inclusion compositions that hydrothermal solutions (~100°C) transporting Zr in altered granite were of low-salinity and fluorine-rich.

In a survey of alkaline thermal waters in granites in southern Europe, /Alaux-Negrel et al. 1993/ concluded that zirconium (along with other tri- and tetravalent elements) was associated with a particulate fraction (< 450 mm) in groundwaters. This indicates that Zr was sorbed on the particulate fraction of the groundwaters and it was not in true solution. In a survey of over 400 groundwater compositions in a variety of rocks in the U.K. /Edmunds et al. 1989/ detected Zr in only one sample of groundwater ($34 \cdot 10^{-9}$ M). Elsewhere, Zr was below the analytical detection limits ($2.1–7.7 \cdot 10^{-9}$ mole/dm^3). Zr in oilfield waters of the U.S.A. are in the range $0.11–0.22 \cdot 10^{-9}$ M /Rittenhouse et al. 1969/.

Only in a few groundwater samples from the alkaline volcanic media of Poços de Caldas, Zr contents surpass $1.1 \cdot 10^{-6}$ mole/dm^3 /Nordstrom et al. 1991/, which was probably in colloidal form. In the hyperalkaline groundwater samples of Maqarin (Jordan) concentrations of Zr were always below 10^{-7} mole/dm^3.

Niobium

Niobium content and occurrence in rocks and minerals

Niobium is a refractory lithophilic element (like zirconium) and has an identical abundance of 20 ppm in the crust, granite, basalt and shale /Krauskopf 1967/. The greatest abundance of Nb is in syenites and alkaline rocks (~100 ppm). The lowest abundance is in peridotittes (1.5 ppm).

Niobium minerals are almost exclusively oxides. Niobite, $(F, Mn)(Nb, Ta)_2O_6$ shows continuous solid solution with tantalite, thus forming the columbite suite of minerals. The chief hosts for Nb in most rocks are ferromagnesian minerals such as pyroxene, amphibole, biotite, muscovite, sphene, ilmenite and magnetite. Nb contents in these minerals may be up to a few 1,000 ppm. Approximately 50 oxides/hydroxides, 1 borate and 10 silicates of Nb are listed in /Wedepohl, 1978/ as occurring in nature. ~30 minerals are listed as containing up to 5% Nb.

Considerable amount of Nb may be found in natural cassiterites (SnO_2) of magmatic and hydrothermal origin, suggesting possible coherence of geochemical behaviour with tin under hydrothermal conditions /Möller et al. 1988/.

The average abundance of niobium in soils is 115 ppm /Bockris 1977/. The samples of the U-ore from Cigar Lake site have a Nb content that reaches 50 ppm /Smellie et al. 1994/. The normal Nb contents of the rock samples from Poços de Caldas range between 30 and 320 ppm /MacKenzie et al. 1991/.

Niobium content in natural waters

Nb(V) is the dominant redox state under natural water conditions /Baes and Mesmer 1976/. Its abundance in seawater is 10^{-10} mole/dm^3. No data are available of niobium concentrations from natural waters.

Technetium

Technetium contents in rocks and minerals

The maximum ^{99}Tc contents of one sample from Cigar Lake ore is $0.85 \cdot 10^{-6}$ ppm /Fabryka-Martin et al. 1994/. Other technetium concentrations in natural systems are due to recent anthropogenic inputs.

Technetium content in natural waters

Tc has since then been decayed to levels below detection under natural water conditions. However, in 1994, operation of the Shellafield Enhanced Actinide Removal Plant (EARP) to treat stored wastes led to increased discharges of Tc-99 which could not be treated and the distribution of Tc-99 in the Irish Sea has been subject to a number of studies /Leonard et al. 1997, Hunt et al. 2002/.

In the Cigar Lake site, the bounding concentrations for nuclear reaction products in groundwaters were calculated. The maximum calculated ^{99}Tc concentration in those waters is 10^{-9} mole/dm^3 /Fabryka-Martin et al. 1994/.

Nickel

Nickel occurrence and contents in rocks and minerals

Ni is concentrated in ultramafic and mafic rocks in the Earth's crust, with typical abundances in these rock types of 2,000 and 200 ppm, respectively. In comparison, granite and shale contain only 0.5 and 95 ppm, respectively.

Nickel is present in sandstones on average at concentrations lower than 20 ppm but like many other metals, its content is higher in clays and shales (up to 100 ppm). Ni is strongly associated to manganese and also to iron oxides. In most aquifers nickel is present as Ni^{2+} which is stable at pH values up to 9. At higher pH values, nickel(II) solubility might be limited by the precipitation of $Ni(OH)_2$ /Edmunds et al. 1989/.

In igneous rocks, Ni partitions into ferromagnesian minerals such as olivine, pyroxene, amphibole and spinel, whereas at lower temperatures it will be incorporated into a variety of silicates and hydroxides, such as smectite clay, sepiolite, talc and brucite /Decarreau 1985, Velde 1988/. Ni does not form discrete pure carbonate minerals and is the least stable of the M^{2+} ions in $Ca^{2+}M^{2+}(CO_3)_2$ (dolomite) compounds. Ni has appreciable chalcophilic behaviour, and in the presence of HS^- forms sulphides, either substituting for Fe^{2+} in pyrite, FeS_2 (there is almost complete solid solution in the FeS_2-NiS_2 system), co-precipitating with Fe^{2+} in pentlandite (Fe, Ni_9S_8), with Fe^{2+} and Cu^{2+} in chalcopyrite ($CuFeS_2$), or as discrete Ni-sulphides, such as the pyrite-structured vaesite (NiS_2) or millerite (NiS).

Nickel is enriched up to a factor of 4 during lateritic weathering of ultramafic rocks, so that such soils may be commercially-mined deposits of Ni /Golightly 1981/ Si and Mg are preferentially removed in weathering solutions, but Ni is concentrated in solid products such as (with Ni end-member in parenthesis) sepiolite ("falcandoite", $Ni_4Si_6O_{15}(OH)_2.6H_2O$), talc ("kerolite", $Ni_3Si_4O_{10}(OH)_2$), serpentine ("nepouite", $Ni_3Si_2O_5(OH)_4$), and saponite ("pimelite", $Ni_3Si_4O_{10}(OH)_2$). The solubilities of the Ni end-member minerals are considerably less than those of other metals except Al /Golightly 1981/. Although nickel may be sorbed strongly by goethite, there is no apparent incorporation of nickel into this mineral. At higher temperatures, NiO is the least soluble of a range of divalent metal (Ca, Mg, Mn, Fe) oxides in the temperature range 400–700°C /Lin and Popp 1984/. This concurs with the low mobility of Ni relative to Ca, Mn, Fe, Zn, Cu exhibited in hydrothermal (> 300°C) water-rock systems, both experimentally /Seyfried and Dibble 1980, Seyfried and Bischoff 1981/ and in natural systems /Humphris and Thompson 1978/.

The normal Ni contents of alkaline volcanic samples from Poços de Caldas is below 10 ppm but at the redox front it can reach 60 ppm /MacKenzie et al. 1991/.

Nickel content in natural waters

Ni(II) concentrations in sea water range between $2 \cdot 10^{-9}$ mole/dm^3 and 10^{-8} mole/dm^3, and the average residence time is 80,000 years /Whitfield and Turner 1987/. The average Ni(II) concentration in stream waters is $3 \cdot 10^{-9}$ mole/dm^3 /Wedepohl 1978/.

The concentration of Ni(II) measured in the granitic groundwaters of El Berrocal is around 10^{-6} mole/dm^3, while at Palmottu it is two orders of magnitude lower, around 10^{-8} mole/dm^3. In the sandstone-clayey Oklo environment, Ni(II) concentrations are similar to those measured in El Berrocal. In Poços de Caldas, an alkaline volcanic media, the concentrations are similar to the ones found in Palmottu, around 10^{-7} mole/dm^3.

In the hyperalkaline media of Maqarin, the levels are of the same order of magnitude and in the Cigar Lake groundwaters only 2 analytical data (around 10^{-7} mole/dm^3) are available; the other samples contain Ni(II) concentrations below the analytical detection limit.

Palladium

Palladium occurrence and contents in rocks and minerals

There are 6 naturally-occurring isotopes of Pd: ^{102}Pd (0.96%), ^{104}Pd (10.97%), ^{105}Pd (22.2%), ^{106}Pd (27.3%), ^{108}Pd (26.7%), ^{110}Pd (11.8%). Palladium is a platinum group metal and its behaviour is strongly linked to other transition elements of the platinum group (platinum, ruthenium, osmium, rhodium, iridium), being thus strongly siderophilic. These metals have a crustal abundance of < 0.05 ppm /Krauskopf 1967/.

Pd may occur in olivine (50 ppb), bronzite (10 ppb), diopside (20 ppb) and serpentine (80 ppb). Zircones may contain up to 5,000 ppb Pd. The average Pd content of rock-forming minerals is < 10 ppb. Accessory minerals such as gadolinite and columbite may be enriched in Pd. Major Pd ore deposits are associated with dunitic ultrabasic rocks and gabbros containing Cu-sulphides. Ni-sulphides are much higher in Pd than non Ni-sulphides. Platinum metals are also found in dunites as discrete native metal occurrences. Platinum metals are strongly enriched in the so-called “black (bituminous) shales”, along with elements such as arsenic, silver, zinc, cadmium, lead, uranium, vanadium, molybdenum, antimony and bismuth. Although these rocks are organic-rich, the presence of high concentrations of rare metals are more likely due to deposition from oxidising chloride-rich fluids at a redox front.

The normal Pd contents of the rock samples from Poços de Caldas ranges between 0.4 and 3 ppm but at the redox front values as high as 26 ppm can be reached /MacKenzie et al. 1991/.

Palladium content in natural waters

Pd concentration in seawater ranges between 0.18 and $0.66 \cdot 10^{-12}$ M, and its residence time in the ocean is of 50,000 years /Whitfield and Turner 1987/.

Pd concentrations in the Salton Sea geothermal brines have been determined to be in the range $0.2–20 \cdot 10^{-9}$ mole/dm^3 by /McKibben et al. 1990/ at 300°C and pH = 5.4 and log f_{O2} = –30 bars (sulphate-sulphide boundary).

/McKinley et al. 1988/ determined concentrations of Pd in hyperalkaline groundwaters of Oman in the range $3–7 \cdot 10^{-9}$ mole/dm^3.

Silver

Silver contents and occurrence in rocks and minerals

The average abundance of silver in soils, earth crust, sediments and igneous rocks is 1, 0.06, 0.5 and 0.2 ppm respectively /Bockris 1977/.

The most important Ag-ore minerals are found in hydrothermal zones. Galena is one of the most abundant sources of Ag at trace amounts.

The sedimentary galena from Oklo site may contain between 6 and 40 ppm of Ag /Gauthier-Lafaye 1995/. The normal Ag contents of the rock samples from Poços de Caldas range between 0.2 and 3 ppm but at the redox front it can reach 10 ppm /MacKenzie et al. 1991/.

Silver content in natural waters

The major inorganic species in natural waters for that element are Ag^{+}, AgCl (aq), $AgCl^{2-}$, AgCl. In sea water Ag(I) forms complexes with Cl^{-} /Stumm and Morgan 1996/.

The system Ag-Cl-S-O-H in Eh-pH space /Brookins 1988/ shows the importance of dissolved chloride on Ag transport under oxidising, acidic conditions. The mobility of Ag is relatively high in acidic conditions /Bockris 1977/.

In seawater, the predominant aqueous complexes are $AgCl_2^{-}$ and $AgCl_3^{2-}$ /Bockris 1977/. The silver(I) concentration in the Pacific Ocean ranges between 10^{-12} mole/dm^3 at surface and $23 \cdot 10^{-12}$ mole/dm^3 at depht. The residence time is 5,000 years /Whitfield and Turner 1987/.

In dilute oxygenated groundwater Ag concentrations range between 9.26 and $92.6 \cdot 10^{-11}$ mole/dm^3 /Edmunds et al. 1989/. In several goundwater samples from Poços de Caldas the content of Ag can be as high as $0.5 \cdot 10^{-6}$ mole/dm^3 /Nordstrom et al. 1991/.

Lanthanides

Samarium

Samarium contents and occurrence in rocks and minerals

Natural samarium is a mixture of seven isotopes, three of which are unstable with long half-lives /Weast 1975/.

Samarium has a crustal abundance of 7.3 ppm, being concentrated in granitic rocks (9.4 ppm) /Krauskopf 1967/.

/Grauch 1989/ made a comprehensive review of the samarium contents in metamorphic rocks. /McLennan 1989/ studied the elemental contents and processes related with the LREE occurrences in sedimentary rocks.

Samarium is found along with other members of the REE in many minerals, including monazite (to the extent of 2.8%) and bastnasite /Weast 1975/. /Gimeno 1999/ determined the concentration of samarium in some lutite samples from the Val-Bádenas stream (Aragón, Spain), which ranges from 5 to 13 ppm.

Approximately 200 minerals are known to contain up to 0.01 % lanthanides. Highest concentrations are found in bastnaesite (64 wt%), monazite (60 wt%) and cerite (59 wt%). 3 fluorides, 10 oxides, 10 carbonates, 1 borate, 1 sulphate, 8 phosphates and 20 silicate minerals containing REE are listed in /Wedepohl 1978/. REE contents in basalts and gabbros are concentrated in clinopyroxene rather than plagioclase. Biotites from granites contain more REE than feldspars and quartz.

The Sm average content of the reference granite samples from El Berrocal is around 2 ppm /Pérez del Villar et al. 1995/. On the other hand, the natural Sm contents of the sandstone-clay media in the reactor zone of Oklo range between 1.7 and 24 ppm /Gauthier-Lafaye 1995/. The samples of the massive U-ore from Cigar Lake site have a Sm content which reaches 48.2 ppm /Smellie et al. 1994/. The normal Sm contents of the alkaline volcanic media samples from Poços de Caldas is lower than in the previous case and ranges between 3 and 10 ppm /MacKenzie et al. 1991/.

Samarium concentrations in natural waters

Sm(III) concentration in sea water ranges between 2.7 and $6.8 \cdot 10^{-12}$ mole/dm^3, and the average residence time is 200 years /Whitfield and Turner, 1987/.

In North Atlantic Ocean the Sm content increase slightly with depth and its around $4.5 \cdot 10^{-12}$ mole/dm^3 /Elderfield and Greaves 1989/.

/Elderfield et al. 1990/ report REE analyses of rivers and seawaters. Sm values in river waters are in the range 46–$810 \cdot 10^{-12}$ mole/dm^3.

Sm concentrations in the range 9–$239 \cdot 10^{-12}$ mole/dm^3 are reported by /Michard et al. 1987/ in CO_2-rich groundwaters in granites from Vals-les Bains, France. Their enrichment of heavy REE in these waters is ascribed to carbonate complexation. The presence of REE in alkaline groundwaters in granites in southern Europe was associated with colloids /Alaux-Negrel et al. 1993/. /Smedley 1991/ measured samarium concentrations in shallow groundwaters in the Carnmenellis granite and surrounding metasedimentary rocks in the range 0.3–$66 \cdot 10^{-9}$ mole/dm^3. /Gosselin et al. 1992/ investigated concentrations of REE in chloride-rich groundwater in the Palo Duro Basin, Texas. These authors noted Sm concentrations in the range 0.035–$48 \cdot 10^{-9}$ mole/dm^3. They concluded that chloride complexes dominated the REE speciation with only minor contributions from carbonate and sulphate species. Fresh groundwaters from wells in the schists of the Virginia Piedmont area of the U.S.A. have 60 ppb REE /Wedepohl 1978/.

/Michard 1989/ has reported REE analyses in waters from geothermal systems in Italy, Valles Caldera, Salton Sea and mid-Atlantic Ridge. Sm contents are in the range 0.0053–$107 \cdot 10^{-9}$ mole/dm^3 REE concentrations of these fluids increase as pH decreases.

/Gimeno 1999/ has reported REE concentrations in stream waters in Spain (Val-Bádenas stream). Samarium concentrations in these two systems ranged from 2–$70 \cdot 10^{-11}$ mole/dm^3. In the Garone and Dordogne rivers the Sm concentration is $0.051 \cdot 10^{-12}$ mole/dm^3 /Brookins 1989/.

In the Oklo clay groundwaters, Sm concentrations are about 10^{-12} mole/dm^3. In deep alkaline groundwater from Poços de Caldas the average Sm(III) concentration is below $6.6 \cdot 10^{-9}$ mole/dm^3 /Miekeley et al. 1991/. Finally, at the hyperalkaline groundwater samples of Maqarin the concentration of Sm is always below the detection limit ($6.6 \cdot 10^{-12}$ mole/dm^3) but in one sample, which is $1.33 \cdot 10^{-10}$ mole/dm^3.

Holmium

Holmium contents and occurrence in rocks and minerals

/Grauch 1989/ made a comprehensive review of the holmium contents in metamorphic rocks. /McLennan 1989/ studied the contents and processes related with the LREE occurrence in sedimentary rocks.

/Gimeno 1999/ studied the REE contents in some lutite formations and reported a range between 0.5–2 ppm.

Holmium occurs in gadolinite, monazite (to the extent of 0.05%) and in other rare-earth minerals /Weast 1975/.

/Gosselin et al. 1992/ investigated concentrations of REE in chloride-rich groundwater in the Palo Duro Basin, Texas. These authors noted Ho concentrations below $8.5 \cdot 10^{-9}$ mole/dm^3. They concluded that chloride complexes and the free-ion dominated the REE aqueous speciation with only minor contributions from carbonate and sulphate species.

The average Ho content of the reference granite samples from El Berrocal is about 0.3 ppm /Pérez del Villar et al. 1995/. The Ho contents in samples from Poços de Caldas are about 2 ppm /MacKenzie et al. 1991/.

Holmium concentrations in natural waters

Ho contents in seawater range between 1 and $3.6 \cdot 10^{-12}$ mole/dm^3 /Whitfield and Turner 1987/.

/Smedley 1991/ measured holmium concentrations in shallow groundwaters in the Carnmenellis granite and surrounding metasedimentary rocks in the range $5.5 \cdot 10^{-9}$ mole/dm^3 and below the detection limit ($0.3 \cdot 10^{-9}$ mole/dm^3).

/Brookins 1989/ reports Ho concentrations in the Garone and Dordogne rivers of $8.7 \cdot 10^{-15}$ mole/dm^3.

/Gimeno 1999/ in the Val-Bádenas stream system study found that holmium concentrations ranged from 0 to $1.2 \cdot 10^{-10}$ mole/dm^3 depending on the sampled point.

During the Oklo project, analyses of the aqueous REE concentrations in groundwater indicated values in the range 10^{-10}–10^{-13} mole/dm^3. In deep groundwater from Poços de Caldas the average content of Ho was below $3.7 \cdot 10^{-9}$ mole/dm^3 /Miekeley et al. 1991/.

Actinides

Thorium

Thorium contents and occurrence in rocks and minerals

Thorium and uranium are ubiquitous in nature with contents in soils, sediments and rocks as high as several tens of parts per million /Choppin and Stout 1989/.

Thorium is a lithophilic element with a crustal abundance of 9.6 ppm /Krauskopf 1967/. The average granite, basalt and shale contents are 17, 2.2 and 11 ppm, respectively. The ionic radius of Th^{4+} is 1.02 Å. Similarities in ionic size and bond character link the geochemical behaviour of thorium to cerium, zirconium and tetravalent uranium.

Th occurs as a major mineral only in rare phases such as thorianite (ThO_2) and thorite ($ThSiO_4$). The former mineral is isomorphous with uraninite, the latter with zircon. Consequently, a large part of naturally-occurring Th is in zircon. The chief source of Th is monazite (Ce, La, Y, Th)PO_4 which usually contains 3–9% and up to 20% ThO_2. There are many examples of isostructural compounds of Th, Ce, U and Zr: ThS, US, CeS and ZrS; ThO_2, CeO_2, ZrO_2; $ThSiO_4$, $USiO_4$, $ZrSiO_4$; $ThGeO_4$, $UGeO_4$, $CeGeO_4$, $ZrGeO_4$; $BaThO_3$, $BaUO_3$, $BaCeO_3$, $BaZrO_3$. However, there are only a few Th silicates known as compared with the large number of Zr-silicates. A large number of Th-sulphides, selenides and tellurides is known. Feldspars, biotites and amphiboles may contain only 0.5–50 ppm Th.

Most Th hosting minerals are refractory to weathering so that Th is considered a poorly soluble and immobile element. Th is usually fractionated from U during weathering because of the relatively higher solubility of U(VI). Th is strongly adsorbed by clays and oxyhydroxides so that relatively high concentrations of Th occur in bentonites, marine pelagic clays, manganese nodules and bauxites.

The Th content of the reference granite from El Berrocal is about 7 ppm /Pérez del Villar et al. 1995/. The samples of the U-ore from Cigar Lake site have a Th content that reached 141 ppm /Smellie et al. 1994/.

Thorium concentrations in natural waters

Th in fresh surface waters ranges from 0.043 to $4.3 \cdot 10^{-9}$ mole/dm^3. Th concentrations in natural waters are more likely to be limited by mineral dissolution kinetics and sorption than by true mineral-fluid equilibria /Langmuir and Herman 1980/.

/Copenhaver et al. 1993/ investigated retardation of ^{232}Th decay chain radionuclides in aquifers in Long Island and Connecticut. They measured retardation coefficients on the order 10^4–10^5 for Th. Rock/brine concentration ratios of ~$5 \cdot 10^5$ were observed for ^{232}Th in high temperature (300°C) brines of the Salton Sea geothermal field, indicating immobility of Th /Zukin et al. 1987/.

In oceanic water the contents of Th range between 5 and $148 \cdot 10^{-14}$ mole/dm^3 /Whitfield and Turner 1987/. The residence time is 50 years.

In natural waters, concentrations of thorium are lower than in rocks and minerals and it is often uncertain how the measured concentrations are distributed between species in true solution

and those sorbed on suspended material. Uranium is rather abundant in surface seawater, $12 \cdot 10^{-9}$ mole/dm^3, while thorium is present only at $2.5 \cdot 10^{-12}$ mole/dm^3 /Choppin and Stout 1989/.

Th concentrations of $0.06 \cdot 10^{-9}$–$0.14 \cdot 10^{-9}$ mole/dm^3 were measured in groundwaters in altered phonolites at Poços de Caldas /Bruno et al. 1992/. Th was significantly associated with colloids in groundwaters in contact with uranium ore bodies at Nabarlek and Koongarra in the Alligator Rivers region, Northern Territory, Australia /Short and Lowson 1988/. Only in two granitic groundwater samples from El Berrocal the ^{232}Th contents is over $1.75 \cdot 10^{-11}$ mole/dm^3 /Gómez et al. 1995/. Concentrations of Th measured at the clayey waters of Cigar Lake are in the range 10^{-9}–10^{-10} mole/dm^3 /Cramer et al. 1994/. The groundwater sampled in Oklo, indicated concentrations in the order of 10^{-9} mole/dm^3. Th in alkaline groundwaters in granites in southern Europe was found to be mainly associated with particulate material and not contained in true solution /Alaux-Negrel et al. 1993/. In the hyperalkaline Maqarin groundwaters, values in the order of 10^{-11} mole/dm^3 are measured, and /McKinley et al. 1988/ report concentrations below $0.2 \cdot 10^{-9}$ mole/dm^3 in Oman.

Protactinium

Protactinium contents and occurrence in rocks and minerals

The contents of Pa in marine sediments are 10^{-5} ppm and in the continental earth crust 10^{-6} ppm /Fukai and Yokoyama 1982/.

Protactinium occurs in pitchblende to the extent of about 0.1 ppm. Ores from Congo have about 3 ppm. Protactinium has thirteen isotopes, the most common of which is ^{231}Pa with a half-life of 32,500 years /Weast 1975/.

Protactinium content in natural waters

In seawater the concentration of Pa ranges between 10^{-14} mole/dm^3 /Lloyd and Heathcote 1985/ and 10^{-17} mole/dm^3 /Fukai and Yokoyama 1982/.

Uranium

Uranium contents and occurrence in rocks and minerals

Uranium is a lithophilic element whose geochemistry is intimately linked with that of thorium. Uranium has a crustal abundance of 2.7 ppm, concentrated in granite (4.8 ppm) and shale (3.2 ppm) /Krauskopf 1967/.

Naturally-occurring uranium consists of three isotopes: ^{238}U, ^{235}U, and ^{234}U. ^{238}U and ^{235}U are parent isotopes for 2 separate radioactive decay series. No natural fractionation of ^{238}U and ^{235}U has been observed and all materials have a ^{238}U/^{235}U ratio of 137.5.

Although valence states between +3 and +6 could exist in nature, only the +4 and +6 valence states are of geochemical relevance.

Uranium occurs in a variety of minerals, but is concentrated in only a few of them. The most abundant uranium mineral is uraninite with a stoichiometric formula varying from UO_2 to U_3O_8. Well-crystallised UO_2 is described as uraninite and the microcrystalline form, pitchblende. Typical uranium contents of rock-forming minerals are as follows: feldspar: 0.1–10 ppm; biotite: 1–60 ppm; muscovite: 2–8 ppm; hornblende: 0.2–60 ppm; pyroxene: 0.1–50 ppm; olivine: ~0.05 ppm; allanite: 30–1,000 ppm; apatite: 10–100 ppm. In /Wedepohl 1978/ the following uranium minerals are listed: 15 oxides, 12 carbonates, 6 sulphates, 30 phosphate-arsenates, 10 vanadates, 15 silicates, 4 niobates and 5 molybdates.

Under oxidising conditions, pitchblende and uraninite are converted to bright-coloured minerals such as carnotite, $K_2(UO_2)_2(VO_4)_2 \cdot 3H_2O$, tyuyamunite, $Ca(UO_2)_2(VO_4)_2 \cdot nH_2O$, autunite,

$Ca(UO_2)_2(PO_4)\cdot nH_2O$, and rutherfordine, UO_2CO_3. These minerals are soluble so that uranium may be transported by oxidising groundwater to be re-deposited under more reducing conditions.

The granite reference of El Berrocal has a U content of about 16.5 ppm /Pérez del Villar et al. 1995/. The samples of the U-ore from Cigar Lake site have a U content that can reach 220 ppm /Smellie et al. 1994/.

Uranium concentrations in natural waters

Seawater contains $13.5\cdot10^{-9}$ mole/dm^3 of uranium, mainly in the VI oxidation state. The ocean residence time is $3\cdot10^5$ years /Whitfield and Turner 1987/.

/Edmuns et al. 1989/ noted that most analyses of uranium in groundwaters in aquifers in the UK were below 10^{-7} mole/dm^3, although several anomalous values up to 10^{-5} mole/dm^3 were observed. Uranium concentrations in alkaline-thermal waters in granites in southern Europe were limited by uraninite solubility /Alaux-Negrel et al. 1993/. /Bruno et al. 1992/ concluded that in waters sampled at Poços de Caldas U was associated to Fe(III) oxy-hydroxides, with concentrations in the range: $1.7\cdot10^{-7}$–$1.7\cdot10^{-8}$ mole/dm^3. A similar behaviour across the redox transition was observed in waters in contact with deep seabed sediments of the North Atlantic Abyssal Plain /Santschi et al. 1988/, with concentrations ranging from 0.4 to $8\cdot10^{-9}$ mole/dm^3. In CO_2-rich waters from Val-les-Bains (France), uranium concentrations are in the range $1–3.5\cdot10^{-9}$ mole/dm^3 /Michard et al. 1987/.

At higher temperatures and under reducing conditions the concentrations of uranium appear to be controlled by the uraninite-coffinite transition. /Kraemer and Kharaka 1986/ measured uranium concentrations in saline waters in geo-pressured aquifers (T: 109–166°C), in the US Gulf Cost, in the range $0.1–2\cdot10^{-10}$ mole/dm^3.

/Edmunds et al. 1987/, measured uranium concentrations in deep groundwaters of the Carnmenllis granite in the range: $8\cdot10^{-11}$–$1.8\cdot10^{-7}$ mole/dm^3. Uranium concentrations in Stripa are in the range: $4\cdot10^{-8}$ to $3.7\cdot10^{-7}$ mole/dm^3. The concentrations measured at El Berrocal and Palmottu are rather close (between 10^{-6} and 10^{-9} mole/dm^3), as would be expected from the geochemical similarities between these two sites. In the Cigar Lake uranium deposit uranium concentrations in the reduced zone are in the range $6\cdot10^{-9}$ to 10^{-7} mole/dm^3, indicating that the waters are in equilibrium with a slightly oxidised uraninite, represented by the stoichiometry U_3O_7(s) /Bruno and Casas 1994/. Uranium concentrations range between 10^{-9} and $2\cdot10^{-6}$ mole/dm^3 in the oxidised part of Cigar Lake. This would suggest a control by the association of U(VI) to Fe(III) oxyhydroxides, present in this zone. Uranium concentrations associated with the uranium deposit at Crawford (Nebraska), have been reported by /Spalding et al. 1984/, in the range 20 to $300\cdot10^{-9}$ mole/dm^3. A wider concentration range is measured in the clayey media of Oklo (10^{-5}–10^{-10} mole·dm^3), due to the very different Eh values measured in the reaction zones of Okélobondo and Bagombé. The range of concentrations measured at Poços de Caldas is fairly narrow, in the order of 10^{-9} mole/dm^3, and the concentrations measured at Oman and Maqarin are below the ranges measured at all the other sites (of the order of 10^{-11} mole·dm^{-3}).

Neptunium

Neptunium concentration in natural waters

In the Cigar Lake site, the bounding concentrations for nuclear reaction products in ground-waters had been calculated. The maximum Np-237 concentrations in those waters are 10^{-10} M /Fabryka-Martin et al. 1994/.

Plutonium

Plutonium contents and occurrence in rocks and minerals

Plutonium exists in trace quantities in naturally-occurring uranium ores. It is formed in much the same manner as neptunium, by irradiation of natural uranium with neutrons /Weast 1975/.

Fifteen isotopes of plutonium are known. By far the most important is the isotope ^{239}Pu, with a half-life of 24,360 years, produced in extensive quantities in nuclear reactors from natural uranium /Weast 1975/.

Of the synthetic transuranium elements plutonium and, to a lesser extent, americium are detectable in ecosystems /Choppin and Stout 1989/. Plutonium is found at relatively higher concentrations in the soil and water near the nuclear test sites and reprocessing facilities, primarily associated with subsurface soils, sediments or suspended particulates in water columns. When vegetation, animals, litter, and soils are compared, more than 99% of the plutonium is found in the sediments.

The average ^{239}Pu contents of three samples from Cigar Lake ore is $1.2 \cdot 10^{-6}$ ppm /Fabryka-Martin et al. 1994/. The Pu and U release from the reaction zone of Oklo had been incorporated into the framework of the newly formed chlorite /Gauthier-Lafaye 1995/.

Plutonium concentrations in natural waters

Very little plutonium is found in natural aquatic systems ($2.89 \cdot 10^{-17}$ mole/dm^3), making it difficult to obtain reliable values for the concentration /Choppin and Stout 1989/. Moreover, the amount of plutonium associated to suspended particulates may be more than an order of magnitude larger than that in true solution. In the Mediterranean Sea, the plutonium activity in sea water was reduced 25-fold by passage of the sample though a 0.45 µm filter.

The Pu concentrations in sea water, rivers and fresh water range between $2.6 \cdot 10^{-18}$ mole/dm^3 in the Mediterranean Sea and $1.6 \cdot 10^{-14}$ mole/dm^3 in the Irish Sea, near to Windscale /Choppin and Stout 1989/.

In the laboratory, the solubility of plutonium added to filtered seawater was measured to be $1.3 \cdot 10^{-11}$ mole/dm^3 after 30 days with 40% in ionic form /Choppin and Stout 1989/. The inclusion of humic material in these seawater samples increased the solubility of Pu six-fold after one month. Humic material is believed to be responsible for the higher concentrations of plutonium in organic-rich rivers and lakes.

In marine sediments from Palomares (Spain), plutonium was found to be associated mainly with organic mater and sesquioxides /Anton et al. 1994/.

In marine natural waters, the limiting solubility of actinides is usually associated with either carbonate or hydroxide compounds. The insolubility of $Pu(OH)_4$ determines the amount of plutonium in solution, even if Pu(V) or Pu(VI) are the more stable redox states /Choppin and Stout 1989/.

In Cigar Lake site, the bounding concentrations for nuclear reaction products in groundwaters were calculated. The maximum ^{239}Pu concentration in those waters is 10^{-9} mole/dm^3 /Fabryka-Martin et al. 1994/.

Americium and curium

Americium and curium contents and occurrence in rocks and minerals

Observations of the distribution of ^{241}Am in marine environments indicate that Am has a high affinity for solid surfaces /Shanbhag and Morse 1982/.

Thirteen isotopes of curium are known. The most stable, ^{247}Cm, with a half-life of 16 millions years, is so short-lived compared to the earth's age that any primordial curium must have disappeared. Natural curium has never been detected, not even in natural deposits of uranium /Weast 1975/.

A summary of the values presented here is given in Appendix B.

5 Uncertainty assessment

The solubility limits discussed and selected in this work contain an important level of uncertainty. It is of the utmost relevance to assess which are the main uncertainties hidden below the limit selection.

The main uncertainties that will be discussed in this chapter can be classified into the following groups:

1. Conceptual uncertainties
   Most of the conceptual uncertainties are related to the choice of models selected to conduct the solubility assessment. In this section we will define "model" as the set of hypothesis enunciated to define our system. Any given model must be exclusively applied once the modeller is aware of which are these hypothesis and has assumed their validity in the system under study. That is, any model must be accompanied with the range of validity and with a list of limitations.
2. Numerical uncertainties
   Numerical uncertainties are relevant in the sense that a wrong number can be selected if the values of the parameters used to calculate it are not correct. Nevertheless, it is much easier to correct a numerical mistake than a conceptual one.

In the forthcoming subsections we will present and describe the main conceptual and numerical uncertainties of the model used to assess solubility limits. In this chapter we will identify the main sources of uncertainty, while in Chapter 6 there is a more detailed quantitative description of data and uncertainties for each element.

It is not the intention of this chapter to describe in depth the uncertainties applying to each one of the elements included in the analyses, but to set the basis for the type of uncertainties found in our work.

Below, a short description of each identified uncertainty and of consequences is presented.

5.1 Conceptual uncertainties

The system under study in this work has been previously presented in Chapter 3. We do not intend to assess solubility limits applicable to the *far-field* of the repository, not even for the *medium-field*, but to the *very-near field*, when water enters the canister gap and interacts with the waste. Therefore, it must be clearly stated that the solid phases selected as likely to precipitate apply to the conditions found in the vicinity of the fuel and the canister.

One of the most relevant uncertainties having an impact on the assessment conducted is related to the *composition of the interacting groundwater*. Although this could be seen, a priori as a numerical uncertainty, there is a non trivial conceptual component in it. In this work, we have considered that the composition of the groundwater interacting with the waste is that of the reference groundwater sampled in the Forsmark site. Although this hypothesis has been enunciated in agreement with the general agreement of the Performance Assessment exercise conducted by SKB, the fact is that is very likely that groundwater interacts with the engineering barriers before contacting the waste. The way to deal with this uncertainty has been to define, besides the central case where the reference groundwater composition has been used, a set of cases where the solubility of the radionuclides has been assessed for different groundwater compositions. These cases consider the composition of the reference groundwater after having interacted with i) the buffer, ii) after an intrusion of oxidising groundwater and iii) under the

assumption of a saline water uplift. These variations in the assessment are reported in Table 8-1, and cover the expected range of variability of the groundwater composition, thus allowing an estimation of the solubility of the radionuclides under different events.

One of the hypotheses enunciated in this work deals with assumption of the *precipitation of pure solid phases* of the elements. We have not conducted calculations implying formation of mixed solid phases. This may appear as a non-realistic approach, given the low concentrations under which the elements contained in the spent fuel matrix are expected to occur. There is a very clear statement by /Grenthe 1991/ saying that *"it is not likely that actinides (with the exception of U) and fission products will form separate mineral phases, they will rather be incorporated into minerals formed…."* This sentence contradicts the general approach followed in this report; nevertheless, we must again go back to the definition of our system and consider that:

i) we are not dealing with high water volumes,

ii) we are not dealing with dispersed elements that have been dissolved from the matrix and released to the geo-environment surrounding the deposit,

iii) we are dealing with the contact of water with the fuel and the "weathering" of the fuel, that is, the transformation of the elements present in the fuel due to the effect of water,

iv) in this system we do not expect the presence of major minerals, except those arising from the corrosion of the canister materials,

v) in this case, the local element concentrations may be higher than those found in the far-field, and in such a case, it is more likely that the solubility assessment must consider formation of individual solid phases. These will be the solid phases acting as "source-term" for the release of radionuclides to the near and the far-fields.

In any case, and in order to constrain this conceptual uncertainty, for those elements that maybe affected by, we have pointed it out in Chapter 6 and an estimation of the effect of considering association of radionuclides with major components is given.

Another conceptual uncertainty deals with the fact that we have credited the *precipitation of amorphous, or less crystalline solid phases*, over crystalline solids.This assumption is partly based on the Ostwald Step Rule. This rule postulates that the precipitate with the highest solubility, that is, the least stable solid phase will form first. This results because the nucleation of a more soluble phase is kinetically favoured over that of the less soluble phase. Small particles have a higher ratio surface area to particle mass than large particles and therefore will have high surface energy, thus dissolving preferentially. The higher solubility of small particles produces solutions which are supersaturated relative to large particles.

The kinetics of precipitation of more crystalline solid phases can be accelerated with temperature. According to the estimations made by SKB in former PA exercises, the maximum temperature developing in the vicinity of the waste canisters is of 100°C. Our reference system is at 15°C.

Many of the processes of crystallization of metallic oxides, for example, occur through a process of dehydration, which is favoured when increasing temperature. Dehydration may occur due to different causes, such as the formation of hematite (α-Fe_2O_3) from hydrous ferric oxide ("FeOOH") with time, or the dehydration of $Ni(OH)_2$ to NiO with temperature (this latter process does not occur until temperatures exceeding 285°C). Therefore, in our system, the formation of the more crystalline solid phases is not considered in front of amorphous phases.

No metallic of native phases have been in principle considered. This decision has been taken in the light of the very slow formation kinetics of this type of phases under the conditions of interest. This has, nevertheless, a certain level of uncertainty.

A third conceptual uncertainty arises with the *sulphate to sulphide reduction* process. In our reference calculations we have not considered that this system is in thermodynamic equilibrium.

Multi-electron transfers only occurs by one electron at a time and, therefore, take place in several steps which require many successive encounters between electron donor and electron acceptor, resulting in a slow global reaction. The reduction of sulphate:

$$SO_4^{2} + 9\ H^{+} + 8\ e = HS + 4\ H_2O \qquad \text{eq. 7}$$

implies the transfer of 8 electrons. This process is so slow that equilibrium between hydrogen sulphide and sulphate has never been observed in any abiotic system below 200°C [97GRE/PUI]. The former reaction is accelerated, though, in the presence of bacterial activity. In fact, inorganic sulphur species more oxidized than sulphide can act as electron acceptors in the oxidation of organic matter by bacteria. In the process the sulphur is reduced to sulphide.

In the system we deal with in this work, the presence of sulphate reducing bacteria (SRB) has not been clearly evidenced so far. Therefore, we have decoupled the +VI from the –II oxidation states of sulphur, precluding the possibility of reduction of sulphate to sulphide. Should the bacterial activity be considered, different solubilities would be suggested for some of the radionuclides studied here. This uncertainty will mainly affect to those elements whose solubility is considered to be limited by sulphate solids, such as Sr. A more detailed discussion on the consequences of this uncertainty is given in Chapter 6 for each of the radionuclides affected.

5.2 Numerical uncertainties

As introduced previously, one of the main numerical uncertainties is the composition of the groundwater contacting the fuel. Besides the values of the master parameters, Eh and pH, and the analytical error in all the reported concentrations, there are two specific uncertainties which can be specifically important in some cases i) the *concentration of phosphate* and ii) the *concentration of iron*. A more detailed discussion follows:

The lack of data on phosphate concentrations in groundwaters is an important drawback in the prediction of the solubility of some elements of PA relevance, mainly for REEs and trivalent actinides. In most of the groundwater compositions used in this work, a zero phosphate concentration in solution has been considered. The reason for this assumption is the lack of reliable data on phosphate concentrations in the analysed groundwaters. In many cases, the lack of data is a consequence of the detection limit of the analytical techniques used in the groundwater analyses. In some data from the analyses of groundwaters sampled in Simpevarp, concentrations of phosphate in the order of 10^{-8} mole/dm^3 have been analysed (data from KSH01A in the 245–261.5 m depth sampling interval). The consideration of phosphate in the groundwater composition may cause a change in the selected solubility controlling phases as well as in the solubility limits recommended for some of the radionuclides. Those cases where this can be of relevance are discussed in Chapter 6.

The concentration of iron in the groundwater composition will mainly affect to those elements that can form Fe-bearing solid phases. This is mainly relevant for Selenium, where the possibility of formation of FeSe has been considered in this analysis. The effect of a variation in the aqueous iron concentration on the solubility of this element is presented in the corresponding section of Chapter 6.

Another important numerical uncertainty is the *Thermodynamic Database (TDB)* used in the calculations. The TDB used is reported in /Duro et al. 2005/ where the procedure for data selection and uncertainty assignment is fully documented. The most relevant uncertainty associated with the TDB is the effect of temperature on the stability of aqueous species and solid compounds. In the mentioned report, a selection of reaction enthalpy is included, although in some cases no enthalpy data are available. The approach to correct the equilibrium constants for temperature effects follows the Van't Hoff equation, where $\Delta_r H^0$ is considered constant with temperature. This approach is valid under the temperature regime expected in the studied system.

The treatment of *activity corrections* also represents an uncertainty to the current solubility assessment. The range of ionic strength (I) in the groundwaters used in this work spans from 10^{-3} to 2 mole/dm^3. The most appropriated procedure to conduct activity corrections in this I range would be the Specific Interaction Theory (SIT), as recommended by the NEA guidelines, which is expressed by eq. 8.

$$\log(\gamma_i) = -z_i^2 \left(\frac{A\sqrt{I}}{1 + Ba_i\sqrt{I}} \right) + \sum_k \varepsilon_{(i,k,I)} m_k \qquad \text{eq. 8}$$

where log (γi) is the logarithm of the activity coefficient of species i, a_i is the effective diameter of the hydrated ion, $\varepsilon_{(I,k,I)}$ is the ion interaction coefficient and m_k is the molality of the background electrolyte.

Nevertheless, this approach is not still implemented in the geochemical codes that we have used in our calculations and, therefore, the extended Debye-Hückel theory (see eq. 9) has been used for activity corrections in this report.

$$\log(\gamma_i) = -z_i^2 \left(\frac{A\sqrt{I}}{1 + Ba_i\sqrt{I}} \right) + b_i I \qquad \text{eq. 9}$$

where Z_i is the charge of the ion, I the ionic strength (m), A is a constant equal to 0.5100 mol$^{-0.5}$ kg$^{0.5}$ at 25°C, B is a parameter defined by temperature, pressure and the dielectric constant of water and b is a parameter dependent on temperature and pressure.

The results obtained by using the extended Debye-Hückel approach are comparable with the ones obtained by the SIT for those cases where the comparison is possible. The main differences were found as expected in the saline water composition and in those cases where the aqueous speciation was dominated by highly charged species with a stability very dependant on ionic strength, i.e. silver chlorides.

The last numerical uncertainty we have to deal with is the *geochemical code* used in the calculations. This is very much related to the previous uncertainty, as shown by the use of the activity corrections approach. We have used two different geochemical codes, as presented in Chapter 3.6: HYDRA-MEDUSA and PHREEQC. The HYDRA-MEDUSA pack has been used in the sensitivity analyses, while the punctual solubility given in the tables has been calculated by using the PHREEQC code. The reason for using two different codes is twofold: i) the HYDRA-MEDUSA code has a very easy graphical interface that allow to draw the output plots in a very straightforward manner as well as drawing the predominance Pourbaix diagram that are used for the preliminary assessment of the solubility limiting solid phase and the predominant aqueous species but ii) with the HYDRA-MEDUSA code we cannot calculate the solubilities of all elements at a time, which is possible when using the PHREEQC code. The differences between the calculations with both codes are minimal and in all cases the results obtained with one of the codes have been tested in front of those obtained with the other, thus ensuring that the sensitivity analyses and the punctual solubility calculations are in agreement.

The major sources of uncertainty for each of the radionuclides of interest is given in Table 5-1.

Table 5-1. Main type of uncertainty affecting to each one of the radionuclides under study.

Element	Associated uncertainty
C	Reduction to $CH_4(g)$
Cs	
Sr	SO_4^{2-} to HS^- reduction possibility of coprecipitation with other elements' carbonates
Ra	SO_4^{2-} to HS^- reduction possibility of coprecipitation with other elements' carbonates
Sn	SO_4^{2-} to HS^- reduction
Se	Formation of native Se^0 SO_4^{2-} to HS^- reduction
Zr	Crystallinity of the solid phase
Nb	Scarcity of TDB
Tc	Formation of metallic Tc^0
Ni	SO_4^{2-} to HS^- reduction
Pd	Formation of metallic Pd^0
Ag	Formation of metallic Ag^0 SO_4^{2-} to HS^- reduction
Sm	Effect of phosphates in water Stability of the solid hydroxo-carbonate
Ho	Effect of phosphates in water Stability of the solid hydroxo-carbonate
Th	Cristallinity of the solid phase Uncertain thermodynamic data for aqueous carbonates
Pa	Lack of thermodynamic data
U	Silicate solid precipitation TDB data on solid stability
Np	Crystallinity of the solid phase
Pu	Effect of phosphates in water Stability of the solid hydroxo-carbonate SO_4^{2-} to HS^- reduction
Am/Cm	Effect of phosphates in water Stability of the solid hydroxo-carbonate

6 Quantification of data and uncertainties

This chapter presents the calculations conducted to select the solubility limiting solid phase for each element under the conditions of interest. It is also included in this chapter a sensitivity analyses showing the impact of different groundwater parameters on the solubility of the different elements under study, as well as a quantification of the impact of the uncertainties identified in Chapter 5 on the solubility of each element.

6.1 Strategy for the selection of solubility limiting solid phases

The detailed strategy followed for the selection of the solubility limiting solid phases is developed and presented here. The strategy is based on expert judgement that, in turn, is based on the knowledge of the composition of the waters of interest, the information regarding kinetics of the formation of the solid phases available and analogies with other similar systems.

Given the relevance of the solubility limits for the evaluations of the performance of a repository, during the expert judgement it is of crucial interest to compare the selected values with additional information gathered from independent laboratory experiments, as well as their comparison with data gathered from natural analogue studies representing the conditions expected to develop in the vicinity of a spent fuel repository.

Thus, in this exercise we have not only conducted systematic solubility calculations, but assessed the validity of the selected values in front of additional experimental and thermodynamic data.

The expert judgement of the selection of limiting solid phases as well as solubility limits has been conducted on the basis of three main sources of information:

- Experimental data from laboratory spent fuel dissolution experiments (Chapter 4.1).
- Experimental data from natural analogue studies (Chapter 4.2).
- Calculated data based on solubility calculations for the studied scenario by taking into consideration all the associated uncertainties as well as calculation limitations (present chapter).

The data from laboratory experiments selected for the discussion are those related with spent fuel leaching experiments and with solubility studies of the phases *a priori* selected to act as potential solubility controllers. Regarding to the data from natural analogue studies, they have been used to give an idea of the concentration limits expected and their affect by the main geochemical parameters.

Different criteria have been followed for the selection, depending on the element and on the variables affecting its behaviour. Of course, the level of accuracy or of certainty varies from element to element. This is due to the variability in the degree of information among different elements both in terms of experimental and of thermodynamic data available to conduct solubility calculations. We have focused our sensitivity calculations on those parameters or issues considered of most interest depending on the radioelement, as for example, the influence of the carbonate content or the crystallinity of the solid.

The approximations followed in the solubility assessment are detailed below:

1. Calculations have been undertaken with the Reference Case. A wider description of the composition of the reference water used as well as the thermodynamic database and the geochemical codes used can be found in Chapter 3.
2. Calculations have been undertaken at the reference temperature of 15°C, which is the average expected in groundwater at the repository depth (see Chapter 3).

3. The redox state of the water contacting the fuel is one of the parameters of major influence on the solubility of some of the radioelements. Thus, the different redox scenarios considered for the Reference case in the present calculations are in agreement with the discussion undertaken in Chapter 3.
4. We have not considered the potential microbiologically mediated reduction of sulphate although it has been discussed the potential effect of this process when considered necessary.
5. The precipitation of both, calcite and gypsum have been allowed during the sensitivity analyses undertaken, in case that an oversaturation occurs in the system, although these solid phases have not been considered to be present in the initial state of the system.

The main identifications needed along the procedure to give solubility values for each element under the different redox conditions evaluated have been:

1. To identify the main geochemical parameters affecting the speciation of the element of interest.
2. To identify the main aqueous species of the element expected in the environment of interest.
3. To identify which are the main solid phases of the element likely to precipitate under the geochemical conditions of the system.

The following tools have been used to follow the former methodology:

1. Predominance diagrams. These diagrams are very useful to identify which are the main aqueous or solid phases that the element under study may form under the conditions of interest.
2. Fractional diagrams, showing how the concentration of a metal is distributed among the several aqueous species as a function of any chemical variable of the system, such as pH, Eh, HCO_3^-, etc.
3. Solubility calculations to see how the solubility of a given solid phase varies with the conditions of the system, for example, with pH and CO_3^{2-} concentration.
4. An expert judgement of the main solubility governing solid phases as well as of the relevant parameters to consideration has been done after the previous detailed procedure and by taking into account both, the relative importance of the different uncertainties associated to each element (see Chapter 5) and the information gathered from lab and natural systems (see Chapter 4).
5. Once the expert judgement and the sensitivity analysis of the parameters affecting the behaviour of the element in question have been evaluated, solubility calculations under the conditions of interest have been performed in order to give a concentration value for each element under the different redox scenarios studied.

6.2 Elements of the groups IA to VIIIA

6.2.1 Carbon

Carbon is an activation product forming impurities in the fuel, and it is also present in the structural elements of the fuel assembly. Its only radioactive isotope is ^{14}C, which represents a minor proportion of carbon in terms of mass. An estimated 5% of carbon is present both in the gap and in the grain boundaries /EUR 1996/.

The solubility of elemental carbon under the chemical conditions of interest, in the absence of carbonate reduction, will be basically determined by calcite saturation. The solubility curve of calcite under the conditions of the reference water is shown in Figure 6-1 as a function of the calcium concentration.

Therefore, we can see that the reference groundwater is nearly in equilibrium with calcite, although slightly undersaturated.

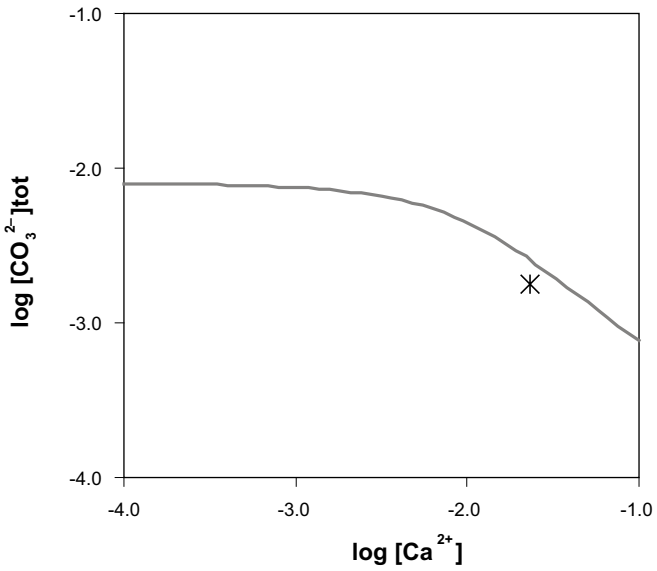

Figure 6-1. *Total carbonate concentration in equilibrium with calcite under the composition of the reference water (except for $[CO_3^{2-}]$ and $[Ca^{2+}]$). The symbol stands for the composition in terms of $[Ca^{2+}]$ and $[CO_3^{2-}]$ of the reference groundwater.*

Methane generation would lead to a very high solubility for total carbon in solution. Nevertheless, the reduction of carbonate to form methane is thermodynamically plausible (see Figure 6-2) although needs of one of the two following conditions:

a) High temperature. A paper dealing with the reduction of metal carbonates to methane /Kudo et al. 1999/ indicates that the yield of methane generation reaches a maximum of 17% at 400°C and does not occur in the absence of biological activity until the temperature exceeds 150°–200°C.

b) Presence of biological activity. This condition depends on the presence of bacteria in the vicinity of the canister, which is not expected to occur.

According to the studied scenario, temperatures are low and the presence of biological activity has been disregarded. Therefore, the reduction of carbonate to methane has not been considered.

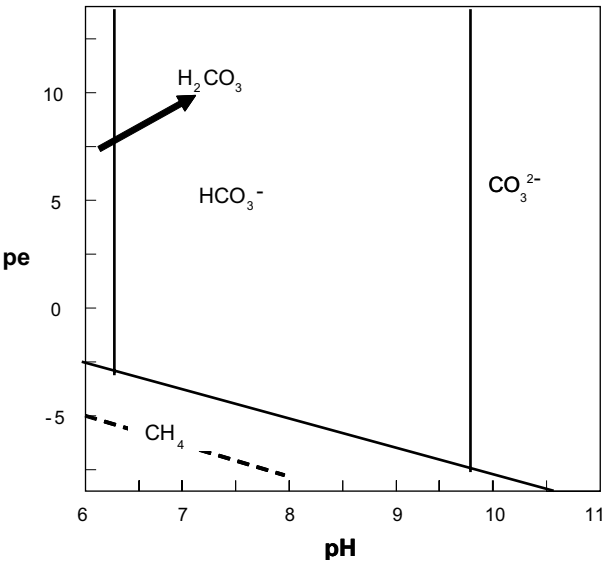

Figure 6-2. *pe/pH diagram for the carbon system. The dashed line stands for the water stability field.*

6.2.2 Caesium

This element is not solubility limited in the range of conditions of interest. The aqueous speciation in solution is dominated by the free cation Cs^+ in most natural groundwaters, with no influence of the main variables of the system, pH and carbonate content, in the range of conditions of interest for this work. Nevertheless, its aqueous speciation changes when varying the concentration of chloride in the water. The fraction of the aqueous species CsCl(aq) increases when increasing the concentration of chloride, as shown in Figure 6-3.

The fraction of CsCl(aq) in the reference groundwater ($[Cl^-] = 0.153M$) is around 6%, and it may increase up to 34% in the saline water (where $[Cl^-] = 1.28M$). Cs is not solubility controlled.

6.2.3 Strontium

The aqueous speciation of strontium under the composition of the reference groundwater is mainly dominated by the free Sr^{2+} cation (more than 90%) with some contributions of aqueous sulphate species within the pH range studied ($6 < pH < 11$). An increase of total sulphate concentrations up to 0.05M would imply an increase in the contribution of $SrSO_4(aq)$ species up to a 30% of the total aqueous Sr concentration (see Figure 6-4).

Two different solid phases appear as likely to control the solubility of Sr: celestite ($SrSO_4(s)$) and strontianite ($SrCO_3(s)$). The predominance of one over the other depends on the sulphate to carbonate ratio as shown in Figure 6-5. Due to the high sulphate content of the reference groundwater, the pure solid phase expected to control the solubility of strontium is celestite (open circle in Figure 6-5). Nevertheless, variations in the groundwater composition by increasing and/or decreasing the carbonate and sulphate concentrations respectively would lead to a change in the solubility controlling phase from celestite to strontianite.

Figure 6-6 shows the solubility curves of strontianite (grey dashed line) and celestite (black solid line) under the conditions of the reference groundwater.

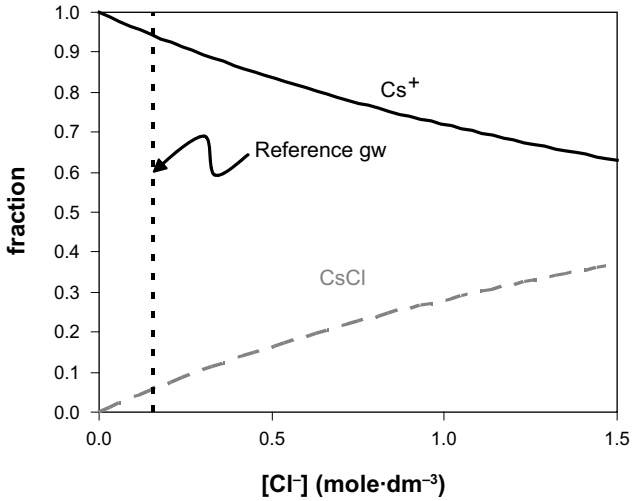

Figure 6-3. *Fractional diagram showing the aqueous speciation of caesium as a function of the chloride concentration, under the conditions of the reference groundwater. Vertical dashed line indicates the $[Cl^-]$ of the reference groundwater.*

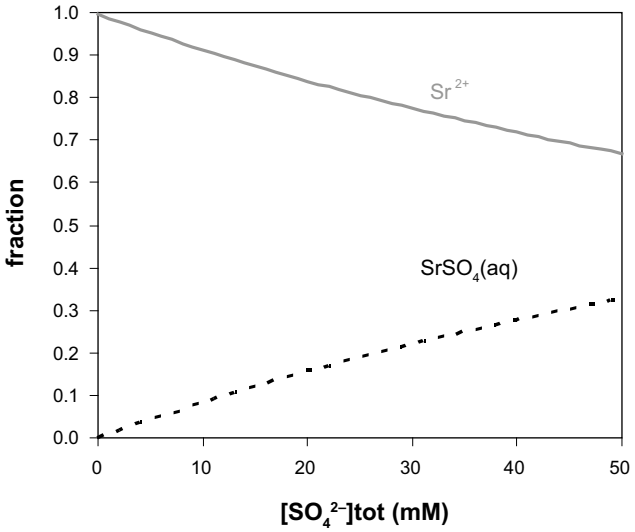

Figure 6-4. *Fractional diagram showing the aqueous speciation of strontium as a function of $[SO_4^{2-}]$tot at pH = 7.*

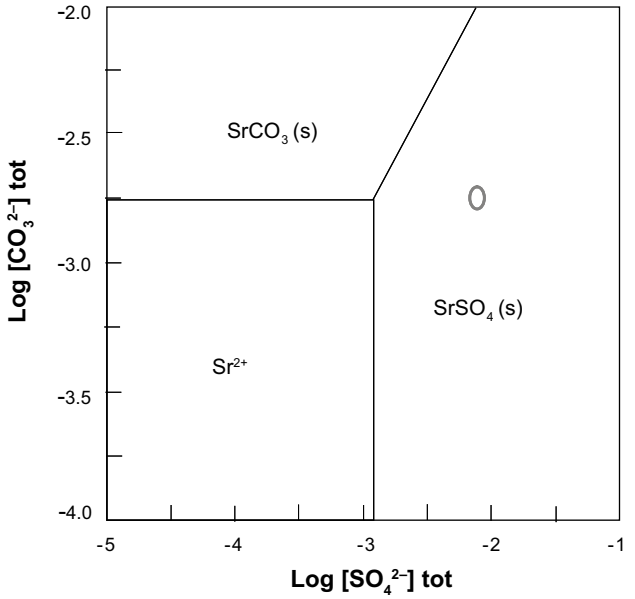

Figure 6-5. *Predominance $[CO_3^{2-}]$-$[SO_4^{2-}]$ diagram showing the speciation of strontium. [Sr]tot = 10^{-3}M. The open circle stands for the reference water composition.*

As discussed in Chapter 5, one of the conceptual uncertainties important to include during the discussion of this element is the reduction of sulphate to sulphide, which has not been considered here due to the very slow kinetics, normally favoured in the presence of sulphate reducing bacteria (SRB). If sulphate were allowed to be reduced to sulphide (black dashed line in Figure 6-6), the solubility of celestite would increase for pH values lower than 6.2, giving rise to a solubility control exerted by strontianite.

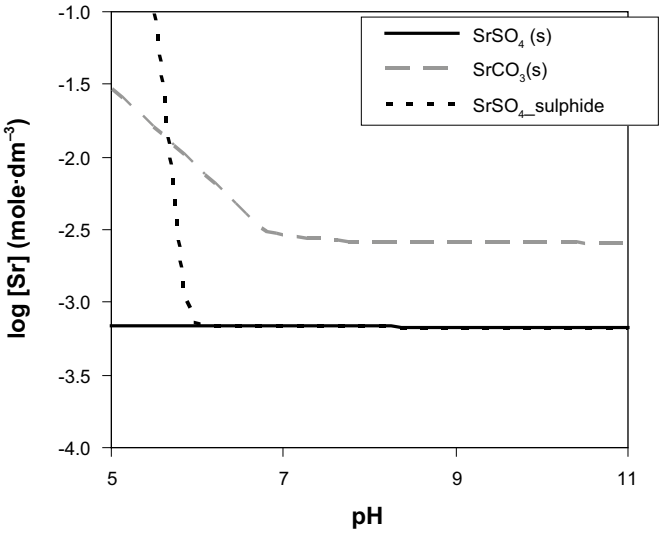

Figure 6-6. *Solubility curves of strontianite and celestite as a function of pH (pe = –2.42) using the reference groundwater composition. The line labelled $SrSO_4$_sulphide stands for a case where the reduction of sulphate to sulphide has been allowed (for explanations see text).*

Only pure solid phases have been considered in this analysis without considering the formation of mixed solid phases. Natural analogue studies have shown that the concentration of Sr in groundwaters may be governed by co-precipitation processes with major elements, leading to smaller strontium concentrations than the ones predicted from the solubilities of solids containing that element as major component. Sr is normally associated with Ca, therefore, the possibility of co-precipitation of strontium with gypsum or calcite should not be disregarded as the controlling process of aqueous concentration of this radionuclide in the studied system.

Calculated strontium concentration limits are given in Table 6-1. Although the effect is not very important, the higher reducing conditions found when $pH_2(g) = 10^{-2}$ atm implies a slightly increase in the solubility as a consequence of the reduction of sulphate to sulphite.

6.2.4 Radium

This radionuclide belongs to the Group II in the periodic table and its chemical behaviour is very similar to the one of strontium. Radium aqueous speciation is dominated by the free cation (Ra^{2+}) in all the pH range studied (Figure 6-7 (a)) under the conditions of the reference groundwater.

This aqueous speciation dominated by Ra^{2+} with small contributions of $RaSO_4(aq)$ in the reference case, might change for groundwaters with a high chloride content like saline groundwaters, where chloride can reach very high concentrations. In that case, the contribution of the species $RaCl^+$ (Figure 6-7 (b)) may affect the Ra solubility.

The larger stability of $RaSO_4(s)$ (black solid line in Figure 6-8) with respect $RaCO_3(s)$ (grey solid line) indicates that this solid will exert the solubility control under the conditions of the Forsmark reference groundwater.

Table 6-1. Sr solubility-controlling phases and concentration values (in mole·dm^{-3}) under different redox conditions.

	T = 15°C pe gw	$pO_2(g)$ = 0.2 atm	$pH_2(g)$ = 10^{-7} atm	$pH_2(g)$ = 10^{2} atm
[Sr] (mole·dm^{-3})	Celestite $6.7 \cdot 10^{-4}$	Celestite $6.7 \cdot 10^{-4}$	Celestite $6.7 \cdot 10^{-4}$	Celestite $6.9 \cdot 10^{-4}$

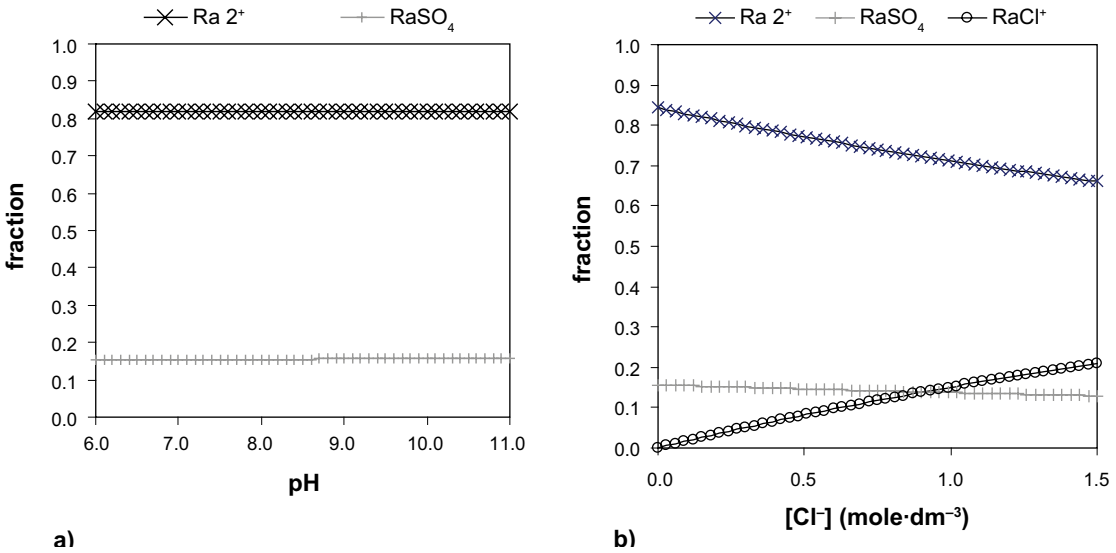

Figure 6-7. *Fractional diagram showing the aqueous speciation of radium (a) as a function of pH and (b) as a function of the chloride concentration (pH = 7), under the conditions of the reference groundwater composition, [Ra^{2+}] = 10^{-5}M.*

As in the case of strontium, one of the conceptual uncertainties to consider is the reduction of sulphate to sulphide. If sulphate were allowed to reduce to sulphide (black dashed line in Figure 6-8), the solubility of $RaSO_4$(s) would considerably increase for pH below 6.

Similarly to the case of strontium, the concentration of Ra in groundwaters may be governed by co-precipitation processes with major elements, leading to smaller radium concentrations than the ones predicted from the solubilities of solids containing that element as major component. Only pure solid phases have been considered in this analysis without considering the formation of mixed solid phases, as discussed in Chapter 3 and, therefore, one uncertainty in the calculation is the possibility of co-precipitation of radium with gypsum or calcite if these solid phases form in our system.

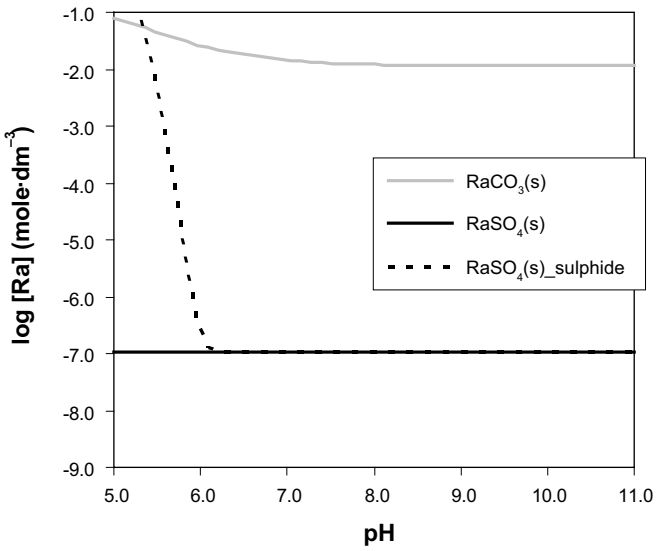

Figure 6-8. *Solubility curves of $RaCO_3$(s) (grey solid line) and $RaSO_4$(s) (black solid line) as a function of pH (pe = –2.42) using the reference groundwater composition. The line labelled $RaSO_4$_sulphide stands for a case where the reduction of sulphate to sulphide has been allowed (for explanations see text).*

Calculated strontium concentration limits are given in Table 6-2. The higher reducing conditions found when Radium $pH_2(g) = 10^{-2}$ atm implies an increase of the solubility of this metal as a consequence of the reduction of sulphate to sulphite.

6.2.5 Tin

The aqueous speciation of tin is dominated by the hydrolysis complexes of Tin(IV). Figure 6-9 shows the aqueous speciation of this element under the reference groundwater composition.

The speciation is dominated by $Sn(OH)_4(aq)$ up to pH 8. In the pH range 8 to 10, the penta-hydroxide dominates and, from pH = 10 upwards, Tin(IV) hexa-hydroxide is the predominant aqueous species.

A sensitivity analysis of the dependence of Tin(IV) solubility of the different tin pure solid phases likely to precipitate as a function of pH is shown in Figure 6-10. Amorphous SnO_2 controls Tin(IV) solubility between pH 6 and 9, while at pH values higher than 9, the mixed calcium and tin hydroxide solid phase reported by /Lothenbach et al. 2000/ may govern Sn concentrations in solution. Then, tin solubility in the reference groundwater (pH = 7) will be most likely controlled by the precipitation of $SnO_2(am)$.

Given that one of the solids most likely to govern the solubility of this element contains calcium, a predominance diagram showing the dependence on the aqueous calcium concentration has been drawn (Figure 6-11). As seen, the uncertainty related to the calcium concentrations

Table 6-2. Summary of Ra solubility-controlling phase and concentration values (in mole dm^{-3}) under the different redox conditions.

	T = 15°C			
	pe gw	$pO_2(g)$ = 0.2 atm	$pH_2(g)$ = 10^{-7} atm	$pH_2(g)$ = 10^{2} atm
[Ra] (mole·dm^{-3})	$RaSO_4$ $9.8\cdot10^{-8}$	$RaSO_4$ $9.8\cdot10^{-8}$	$RaSO_4$ $9.8\cdot10^{-8}$	$RaSO_4$ $1.0\cdot10^{-7}$

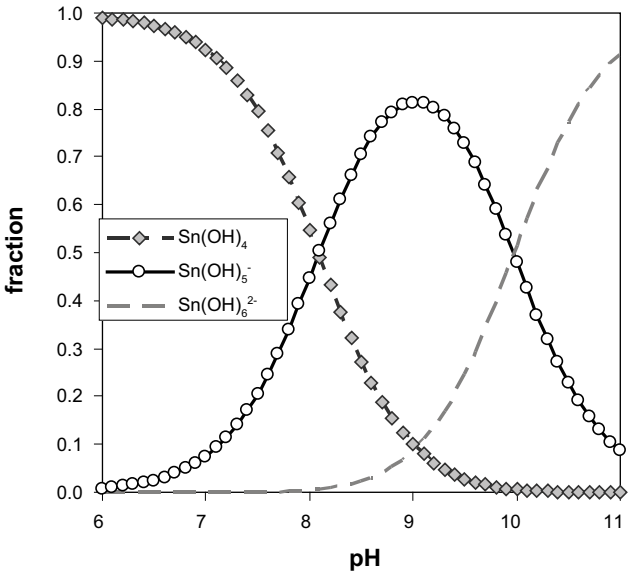

Figure 6-9. *Fractional diagram of Tin(IV) showing the aqueous speciation as a function of pH under the reference groundwater composition. [Sn] = 10^{-5}M.*

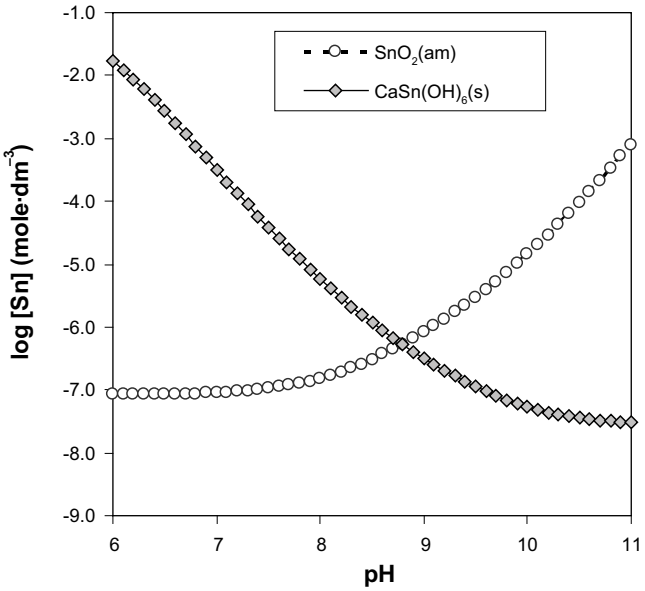

Figure 6-10. *Solubility of tin solid phases as a function of pH (pe = –2.42) under the composition of the reference groundwater.*

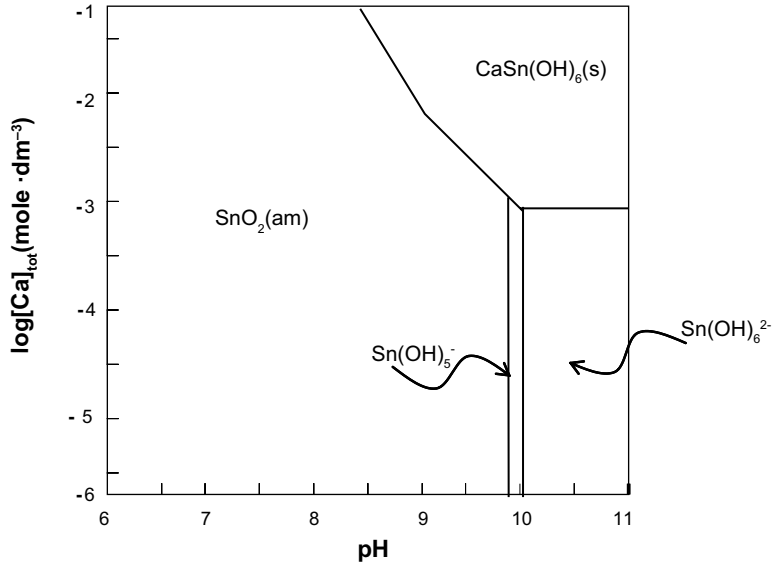

Figure 6-11. *Predominance pH/log [Ca] diagram showing the main solid phases able to govern the solubility of tin.*

in groundwater might be important at relatively high calcium concentrations and pH values. Thereby, the precipitation of the mixed calcium and tin hydroxide solid phase might occur instead of SnO_2(am) from pH = 8.5 to 11 and from log [Ca] = –1 to –3 respectively.

Another uncertainty to take into consideration is the one related with the presence or not in the system of SRB (see Chapter 5). Indeed, if sulphate were reduced to sulphide, sulphide solid phases might exert the solubility control at reducing pe values (see Figure 6-12). At pe < −4 both, SnS(s) and SnS_2(s) would be able to control the solubility of tin producing very low aqueous concentrations. At pe above −4, though, the solubility of these solids increase due to the oxidation of sulphide to sulphate, with the subsequent shift to oxide solid phases as solubility controlling solids.

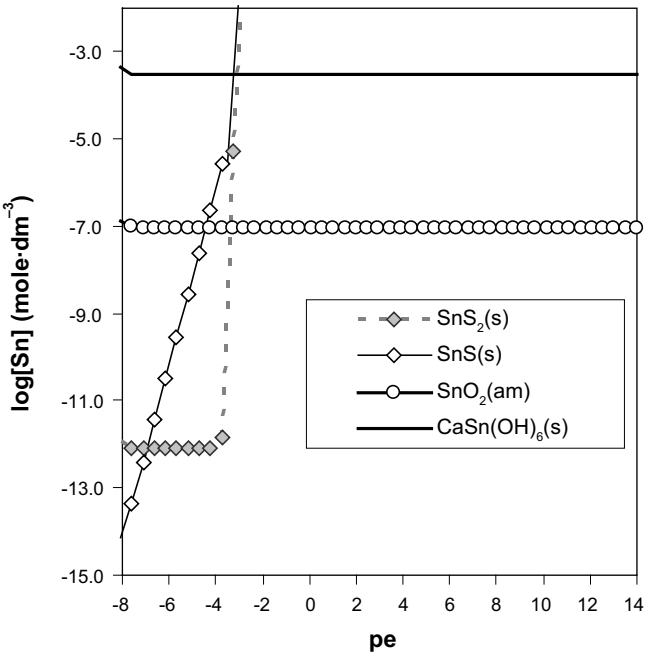

Figure 6-12. *Solubility of several tin solid phases as a function of pe (right) (pH = 7) under the composition of the reference groundwater.*

Calculated tin concentration limits are given in Table 6-3. The effect of more reducing conditions found when $pH_2(g) = 10^2$ atm translates into an increase of the solubility induced by the reduction of Sn(IV) to Sn(II) species.

6.2.6 Selenium

Selenium is mainly found in nuclear spent fuel as selenide located predominantly in the gaps and grain boundaries and forming a volatile compound of composition Cs_2Se /Johnson and Tait 1997/. It will consequently dissolve from the matrix, under anoxic and reducing environments, in the form of Se(-II) species, HSe^- at the pH of the reference groundwater. The presence of Fe(II) in the aqueous solution may cause the precipitation of FeSe(s) which is the solid phase considered as solubility limiting in the present analysis.

Selenium is, though, highly mobile in oxidising environments, forming selenite species under slightly oxidising conditions and selenate under more oxidising conditions. The pe-pH predominance diagram of Se is shown in Figure 6-13.

The stability of FeSe(s) is very dependent on the pH and the redox potential of the system. The redox equilibrium:

$SeO_3^{2-} + 7\ H^+ + 6\ e^- = HSe^- + 3H_2O$,

presents a $\log K^0 = 53.06$.

Table 6-3. Sn solubility-controlling phases and concentration values (in mole dm^{-3}) under the different redox conditions considered.

	T = 15°C pe gw	$pO_2(g)$ = 0.2 atm	$pH_2(g)$ = 10^{-7} atm	$pH_2(g)$ = 10^2 atm
[Sn] (mole·dm^{-3})	SnO_2 $8.6\cdot10^{-8}$	SnO_2 $8.6\cdot10^{-8}$	SnO_2 $8.6\cdot10^{-8}$	SnO_2 $1.2\cdot10^{-7}$

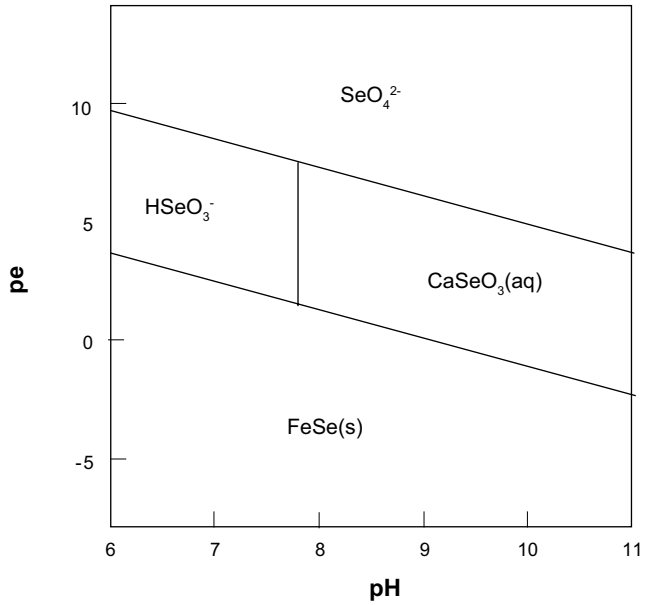

Figure 6-13. *pe/pH diagrams showing the predominant species and solid compounds of selenium under the reference groundwater composition. [Se]tot = 10^{-6}M.*

Therefore, FeSe(s) can be considered as the solubility limiting phase only when the following condition applies

$pe + pH \leq 7.58$

The solubility curve of FeSe(s) under the reference groundwater composition ([Fe]tot = $3.31 \cdot 10^{-5}$ M) as a function of pe is shown in Figure 6-14. According to the previous pe+pH constrain, within the pH range of the analyses (6 to 11) the pe will vary between –3.5 and 1.6. An increase in the solubility is observed for pe values higher than 0.7, due to the oxidation to SeO_3^{2-}.

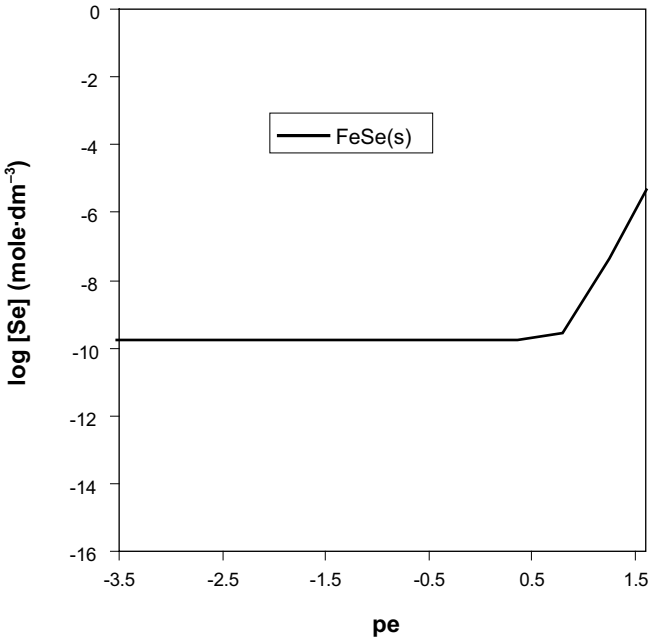

Figure 6-14. *Solubility curve of FeSe(s) as a function of pe calculated by using the reference groundwater composition ([Fe]tot = $3.31 \cdot 10^{-5}$ M). Solubility in mole/dm^3.*

The effect of the concentration of aqueous iron on the solubility of FeSe(s) is shown in Figure 6-15. As expected, a lower iron content in the contacting groundwater implies higher selenium concentrations released to the solution.

In addition to the iron concentration in the aqueous phase, there are other uncertainties deserved to be mentioned. Precipitation of native selenium has not been taken into consideration in the present analysis, since this solid phase may be found in the source term but it does not probably precipitate under the low temperature regime expected in this subsystem.

The reduction of sulphate to sulphide would also directly affect the stability of the governing solid phase (FeSe(s)) under reducing conditions by considerably increasing its solubility due to the stabilisation of the aqueous iron sulphide species.

Calculated solubilities for the reference groundwater composition at the different redox conditions are shown in Table 6-4.

Table 6-4. Se solubility-controlling phase and concentration values (in mole dm^{-3}) under the different redox conditions.

	T = 15°C pe gw	$pO_2(g)$ = 0.2 atm	$pH_2(g)$ = 10^{-7} atm	$pH_2(g)$ = 10^{2} atm
[Se] (mole·dm^{-3})	FeSe $1.4 \cdot 10^{-10}$	n.s.l.	FeSe $1.4 \cdot 10^{-10}$	FeSe $1.4 \cdot 10^{-10}$

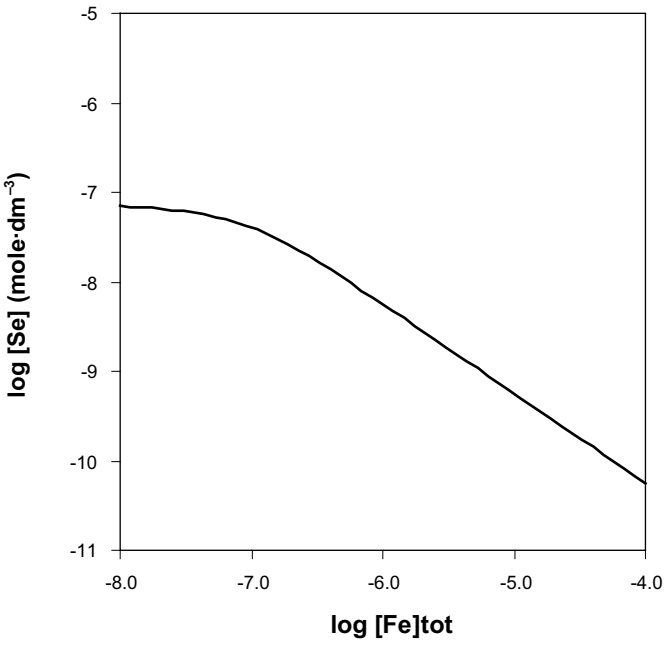

Figure 6-15. *Solubility curve of FeSe(s) as a function of the total iron concentration in groundwater (pe = –2.42, pH = 7). Solubility in mole/dm^3.*

6.3 Transition elements

6.3.1 Zirconium

Zirconium is a transition metal that belongs to group 4 in the periodic table of the elements. It is a non redox sensitive element and it occurs predominantly in the IV valence state.

The aqueous speciation is dominated by $Zr(OH)_4(aq)$ within the pH range studied (see Figure 6-16).

$Zr(OH)_4(s)$ is the solubility controlling phase (Figure 6-17). As expected, there is no pH-dependence of the solubility of $Zr(OH)_4(s)$ in the pH range studied, given that the aqueous speciation is fully dominated by $Zr(OH)_4(aq)$.

According to the previous analyses, the dominant aqueous species of zirconium under the studied conditions is $Zr(OH)_4(aq)$, which is in equilibrium with the solid phase $Zr(OH)_4(s)$ (Table 6-5). Being a non redox sensitive element, no effects are observed due to the change in the redox conditions of the system.

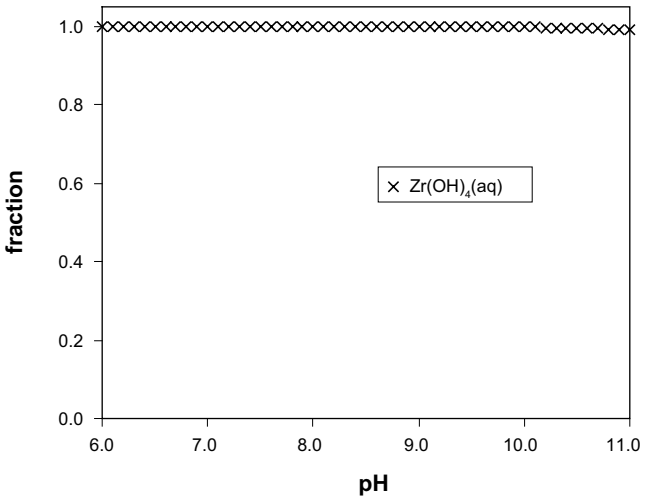

Figure 6-16. *Fractional diagram showing the speciation of zirconium in the aqueous phase as a function of pH under the conditions of the reference groundwater (pe = –2.42) ([Zr] = 10^{-7} mole·dm^{-3}).*

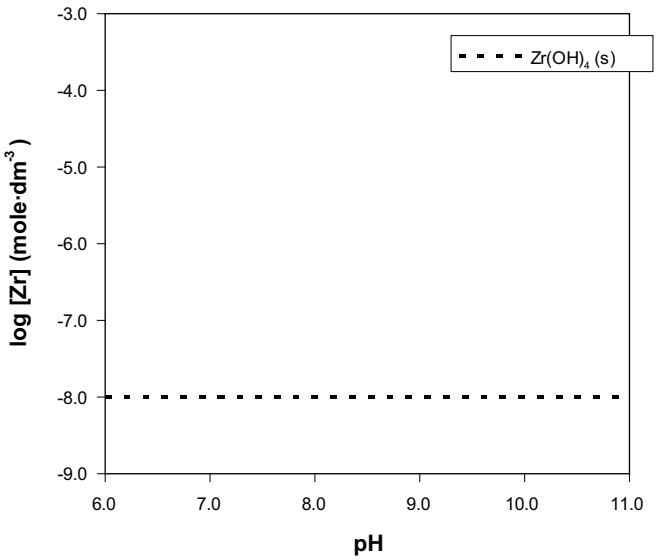

Figure 6-17. *$Zr(OH)_4(s)$ solubility as a function of pH using the reference groundwater composition (pe = –2.42).*

Table 6-5. Zr solubility-controlling phase and concentration values (in mole dm^{-3}) under the different redox conditions.

	T = 15°C pe gw	$pO_2(g)$ = 0.2 atm	$pH_2(g)$ = 10^{-7} atm	$pH_2(g)$ = 10^{2} atm
[Zr] (mole·dm^{-3})	$Zr(OH)_4(s)$ $9.7 \cdot 10^{-9}$	$Zr(OH)_4(s)$ $9.7 \cdot 10^{-9}$	$Zr(OH)_4(s)$ $9.7 \cdot 10^{-9}$	$Zr(OH)_4(s)$ $9.7 \cdot 10^{-9}$

An uncertainty related with this element is that related with the crystallinity of the solid phase formed. As explained in Chapter 5, the formation of the more crystalline solid phases has not been considered in front of amorphous phases, given that many of the processes of crystallization occur through a process of dehydration, which is favoured when increasing temperature, or a process of aging time.

6.3.2 Niobium

Niobium is a transition metal that belongs to group 5 in the periodic table of the elements. In natural waters it is mainly found in the pentavalent oxidation state.

There is a general lack of thermodynamic data in the literature on niobium, what constitutes an important drawback when studying the behaviour of this element. The influence of pH on the solubility of $Nb_2O_5(s)$ and the underlying aqueous speciation is shown in Figure 6-18a and b respectively.

The speciation is governed by $Nb(OH)_5$ and NbO_3^-, being the later more important at higher pHs (Figure 6-18b). The solubility of the solid phase increases with pH due to the formation of the oxoanion NbO_3^-.

Table 6-6 summarizes the niobium concentration values in equilibrium with the selected solubility controlling phase under the different redox conditions studied and calculated with the composition of the reference groundwater.

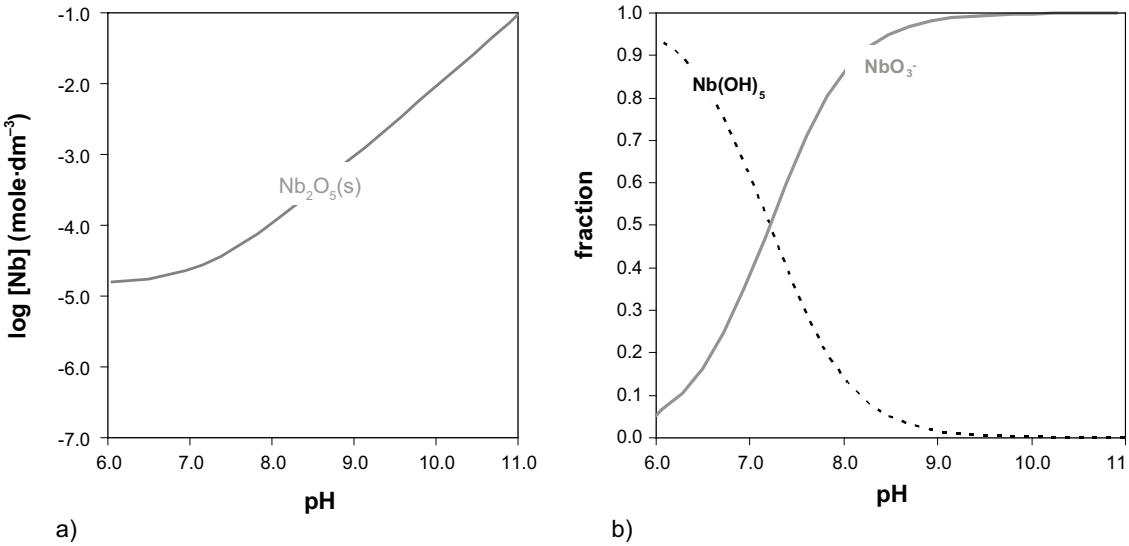

Figure 6-18. *Diagram showing the dependence of $Nb_2O_5(s)$ solubility and the predominant aqueous speciation on (pe = –2.42) the pH. Calculations corresponding to the conditions of the reference groundwater composition.*

Table 6-6. Nb solubility-controlling phase and concentration values (in mole dm^{-3}) under the different redox conditions.

	T = 15°C			
	pe gw	$pO_2(g)$ = 0.2 atm	$pH_2(g)$ = 10^{-7} atm	$pH_2(g)$ = 10^{2} atm
[Nb] (mole·dm^{-3})	Nb_2O_5 $2.4 \cdot 10^{-5}$	Nb_2O_5 $2.4 \cdot 10^{-5}$	Nb_2O_5 $2.4 \cdot 10^{-5}$	Nb_2O_5 $2.4 \cdot 10^{-5}$

6.3.3 Technetium

Technetium is a transition metal of the group 7. The most stable redox states for Tc are IV and VII. This radioelement may be immobilised under reducing conditions due to the high stability of Tc(IV) phases. Under oxidising conditions, though, it is not solubility limited given the large stability of aqueous Tc(VII) complexes, mainly in the form of TcO_4^-.

Figure 6-19 shows the aqueous speciation of Technetium (left) and the solid phases able to precipitate (right).

The aqueous Tc speciation under reducing conditions will be dominated by $TcO(OH)_2(aq)$ in the pH range of interest. When increasing the redox potential of the system, technetium oxidises and the aqueous speciation is dominated by the oxo-anion pertechnate in all the pH range studied (see Figure 6-19a).

The solid phase able to control technetium concentrations in groundwaters is, even under very reducing conditions, technetium dioxide ($TcO_2 \cdot 1.63H_2O(s)$), as shown in Figure 6-19b. Under oxidising conditions, technetium is not solubility limited.

The influence of pH and pe on the solubility of the solid phase is shown in Figure 6-20.

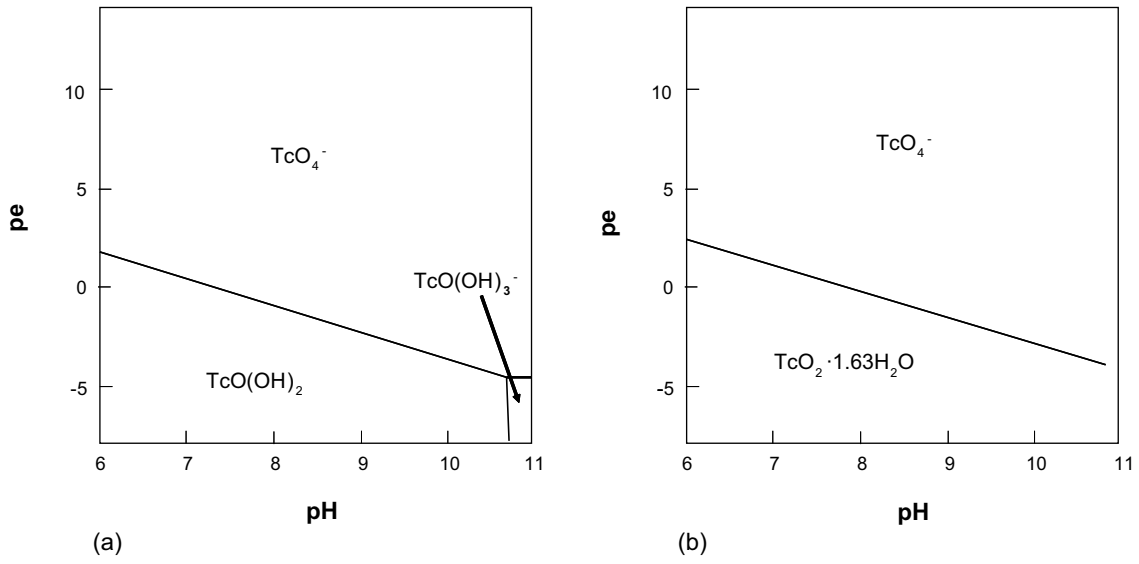

Figure 6-19. *pe/pH diagrams showing technetium species (a) and solid phases (b). [Tc] = 10^{-7}.*

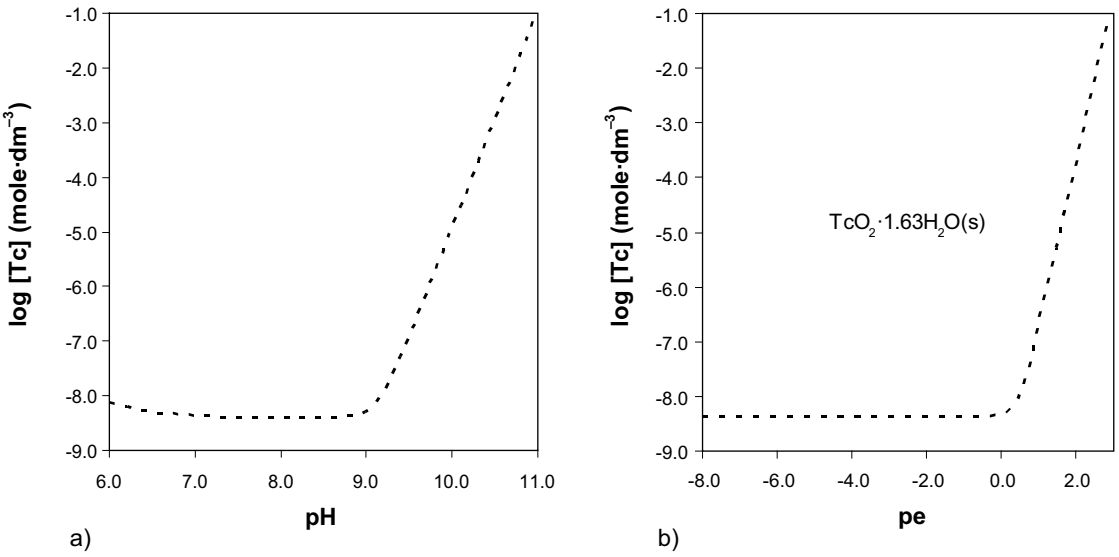

Figure 6-20. *Solubility curve of $TcO_2 \cdot 1.63H_2O(s)$ (a) as a function of pH (fixed pe = –2.42) (b) as a function of pe (fixed pH = 7), calculated by using the reference groundwater composition.*

The higher stability of the aqueous species and the lack of dependence on pH of the solubility of technetium oxide is in agreement with the predominance of the $TcO(OH)_2$ species in the aqueous phase under the reference water (Figure 6-20). The solubility increases in the alkaline range driven by the oxidation of the aqueous species to pertechnate. The slightly increase of the solubility observed in the neutral to acid range is due to the increase of the hydroxo-carbonate aqueous species in detriment of $TcO(OH)_2$.

The precipitation of metallic technetium has not been considered due to the slow kinetics normally associated to the formation of metals from solution. Tc minerals are not found in nature. However, Tc oxides are easily formed in laboratory conditions while Tc(cr) is only obtained by prolonged reductions of previous oxides. Because of that, we have not considered Tc(cr) as a possible solubility controlling phase. Under reducing conditions, the solubility limiting solid phase is the hydrous technetium dioxide (Table 6-7).

6.3.4 Nickel

Nickel is a transition metal of the group number ten. This metal is mainly found in the +2 oxidation state in aqueous and solid states.

As shown in Figure 6-21, the aqueous nickel speciation is dominated by hydrolysis complexes at basic pH range, while free Ni^{2+} with some contributions of chloride species are the most important aqueous complexes from pH 6 to 9, under the conditions of the reference groundwater composition.

Nickel oxide and solid nickel carbonate are the most probably solid phases exerting the solubility control of this element. Figure 6-22 shows the solubility of the different nickel solid phases thermodynamically able to precipitate, as a function of the pH and pe of the system, respectively.

Table 6-7. Tc solubility-controlling phases and concentration values (in mole dm^{-3}) under the different redox conditions.

	T = 15°C pe gw	$pO_2(g)$ = 0.2 atm	$pH_2(g)$ = 10^{-7} atm	$pH_2(g)$ = 10^{2} atm
[Tc] (mole·dm^{-3})	$TcO_2 \cdot 1.6H_2O$ $4.4 \cdot 10^{-9}$	n.s.l.	$TcO_2 \cdot 1.6H_2O$ $4.4 \cdot 10^{-9}$	$TcO_2 \cdot 1.6H_2O$ $4.4 \cdot 10^{-9}$

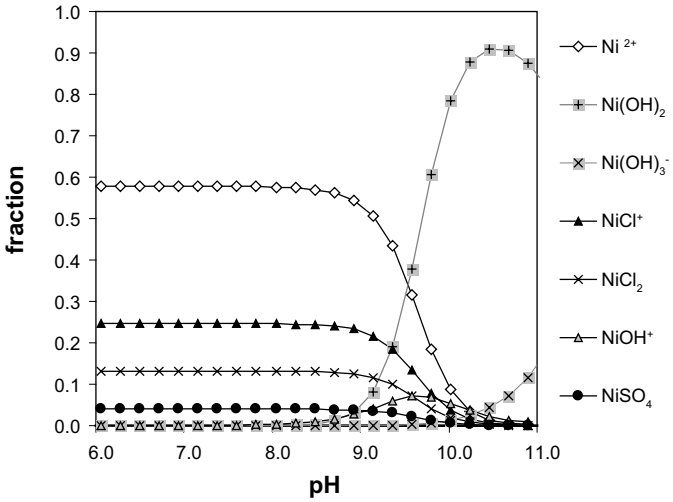

Figure 6-21. *Fractional diagram showing the nickel aqueous species as a function of pH. Calculations conducted by using the reference groundwater composition, (pe = –2.42) [Ni] = 10^{-4} mol·dm^{-3}.*

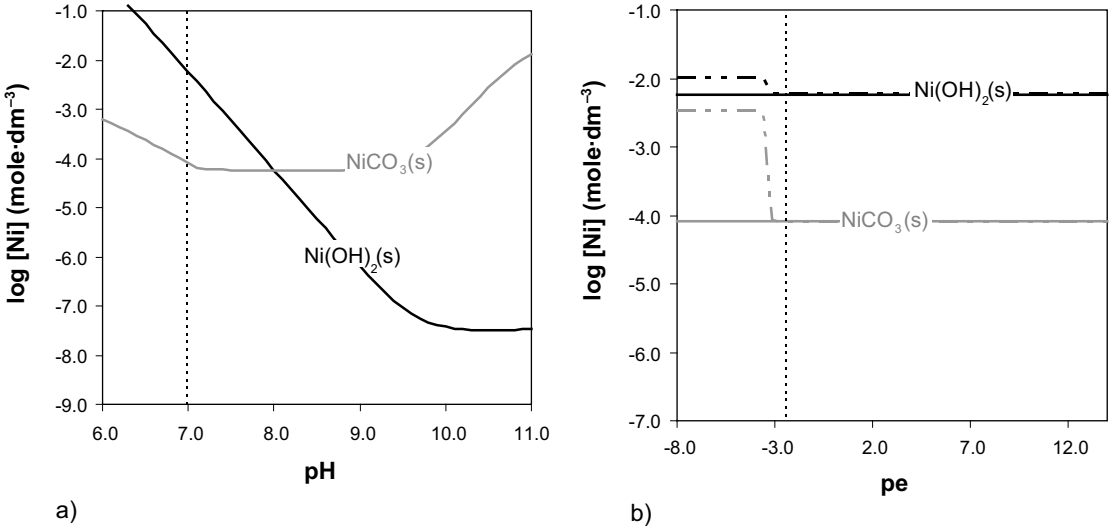

Figure 6-22. *Solubility curves of $Ni(OH)_2(s)$ and $NiCO_3(s)$ solid phases as a function of pH (a) at a fixed pe = –2.42, and as a function of pe (b) at a fixed pH = 7, by using the reference groundwater composition (solid lines). Dashed lines in (b) stand for the solubility of the solid phases by assuming the formation of sulphide species in the system. Vertical solid dotted lines in both plots indicate the pH and pe of the reference groundwater respectively.*

The solubility of Ni can be either controlled by $NiCO_3(s)$ or $Ni(OH)_2(s)$, depending on the pH of the studied system. At pH = 7, which is the pH value of the reference state the solid governing the solubility of this element is $NiCO_3(s)$. Nevertheless, this solubility limiting solid phase might change to the hydroxide solid for pH above 8.

As discussed in Chapter 5, one of the conceptual uncertainties that may affect Ni solubility is the reduction of sulphate to sulphide. If sulphate is allowed to reduce to sulphide in the system, the solubility of both, $Ni(OH)_2(s)$ and $NiCO_3(s)$ would increase for pe values below –3 (dashed line in Figure 6-22b), due to the predominance of nickel sulphide aqueous species (see Figure 6-23).

Table 6-8 summarizes nickel concentrations values in equilibrium with the controlling solid phase under the different redox conditions of interest.

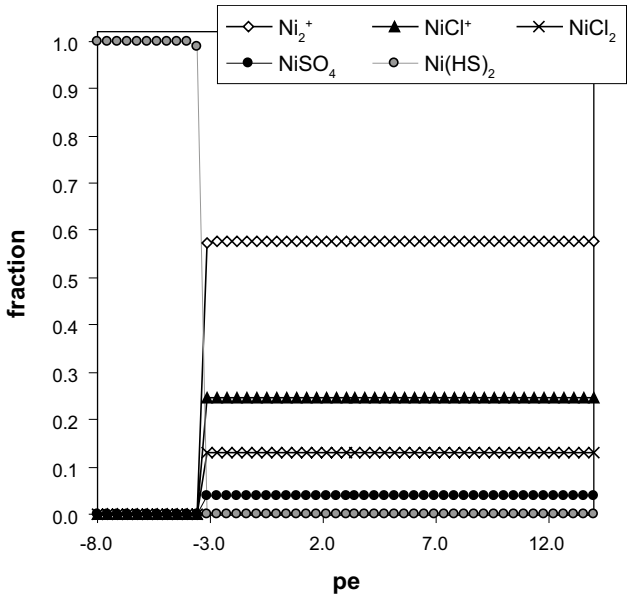

Figure 6-23. *Fractional diagram showing the nickel aqueous species as a function of pe. Calculations conducted by using the reference groundwater composition and allowing the reduction of sulphate to sulphide. [Ni] = 10^{-4} mol·dm^{-3} (for explanations see text).*

Table 6-8. Ni solubility-controlling phases and nickel concentration values (in mole dm^{-3}) under different redox conditions.

	T = 15°C pe gw	$pO_2(g)$ = 0.2 atm	$pH_2(g)$ = 10^{-7} atm	$pH_2(g)$ = 10^{2} atm
[Ni] (mole·dm^{-3})	$NiCO_3$ $5.5\cdot10^{-5}$	$NiCO_3$ $5.5\cdot10^{-5}$	$NiCO_3$ $5.5\cdot10^{-5}$	$NiCO_3$ $5.5\cdot10^{-5}$

6.3.5 Palladium

Palladium is a transition metal that belongs to the platinum group metals (PGM). This element may be found at several valence states, 0, +2 and +4, although the common redox state is +2 in aqueous media.

Figure 6-24 shows the distribution of palladium aqueous species in the pH range studied. The main aqueous species is $Pd(OH)_2(aq)$ at pH > 7 while chloride species are predominant at lower pH.

Given the stability of aqueous palladium chloride species, a sensitivity analysis of the effect of the concentration of this ligand on the Pd speciation has been conducted (see Figure 6-25). At the reference pH of 7, aqueous palladium chloride species become dominant for chloride concentrations over 0.3 M.

The solid phases most likely to precipitate are palladium oxides. Two solid phases are reported in the literature, PdO and $Pd(OH)_2(s)$. According to the Ostwald's rule, the amorphous solid has been selected as exerting the solubility control. Figure 6-26 shows the solubility curve of $Pd(OH)_2(s)$ as a function of the pH of the system. The solubility increases at pH below 7 due to the stabilisation of aqueous chloride species (see Figure 6-24).

Metallic Pd is not considered due to the slow kinetics normally associated to the formation of metals from solution (see Chapter 5).

Table 6-9 summarizes the calculated solubilities for palladium under the different redox conditions studied.

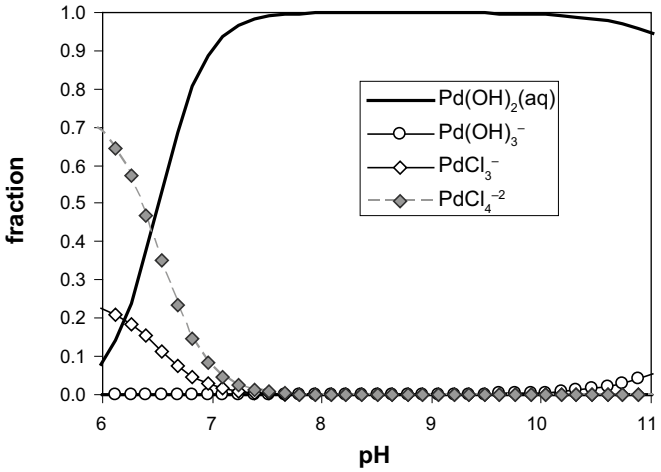

Figure 6-24. *Fractional diagram of the palladium aqueous species, $[Pd]_{tot} = 10^{-5}$ mol·dm^{-3} as a function of pH by using the reference groundwater composition (pe = –2.42).*

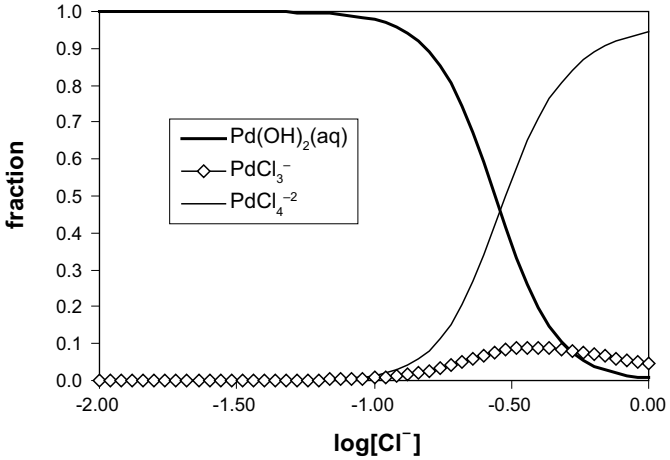

Figure 6-25. *Fractional diagram of palladium aqueous species as a function of the chloride concentration in solution. Calculations correspond to the reference groundwater composition, $[Pd]_{tot} = 10^{-5}$ mol·dm^{-3}.*

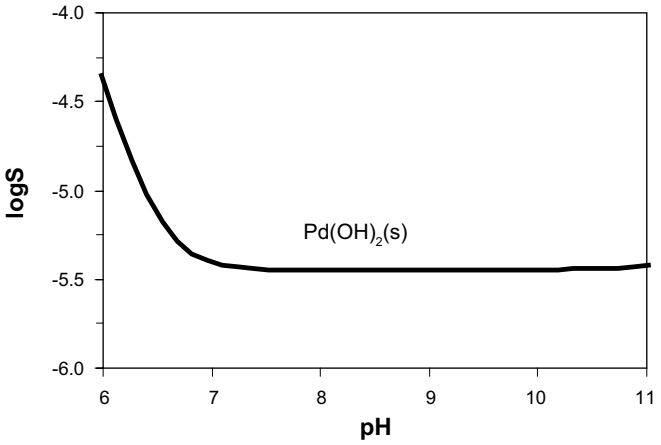

Figure 6-26. *Solubility curve of $Pd(OH)_2(s)$ as a function of pH by using the reference groundwater composition (pe = –2.42).*

Table 6-9. Pd solubility-controlling phases and solubility values (in mole dm^{-3}) under different redox conditions.

	T = 15°C pe gw	$pO_2(g)$ = 0.2 atm	$pH_2(g)$ = 10^{-7} atm	$pH_2(g)$ = 10^{2} atm
[Pd] (mole·dm^{-3})	$Pd(OH)_2$ $2.9 \cdot 10^{-6}$	$Pd(OH)_2$ $2.9 \cdot 10^{-6}$	$Pd(OH)_2$ $2.9 \cdot 10^{-6}$	$Pd(OH)_2$ $2.9 \cdot 10^{-6}$

6.3.6 Silver

Silver is a transition metal of the IB group. This metal is found in nature mainly as native metal and in solution mainly in the +1 oxidation state.

Figure 6-27 shows the aqueous speciation of silver under the reference groundwater composition. The high chloride concentration of the water together with the high stability of silver chloride species is reflected in Figure 6-27, where silver aqueous species dominate the speciation of this element within the pH range studied.

Given the high stability of the aqueous chloride species, it might be expected that for groundwaters with relatively high chloride content, the silver speciation is completely dominated by aqueous chloride species. Figure 6-28 shows the predominance diagram of silver aqueous species as a function of the chloride concentration in groundwater.

It is not surprising, then, that the solid phase exerting the solubility control under the conditions of the reference groundwater is AgCl(s) (see Figure 6-29).

As in the case of palladium, due to the slow kinetics associated to the formation of metallic silver, it has not been considered in the solubility calculations.

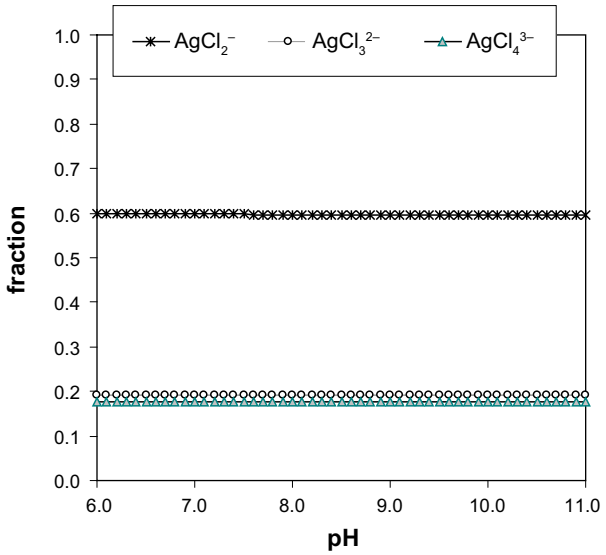

Figure 6-27. *Fractional diagram of silver aqueous species as a function of the pH of the system, under the reference groundwater composition. $[Ag]_{tot} = 10^{-6}$ mol·dm^{-3} (pe = –2.42).*

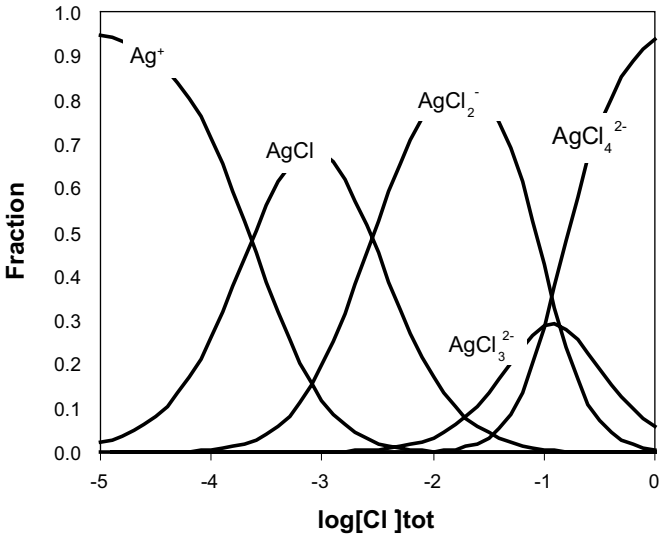

Figure 6-28. *Fractional diagram of silver aqueous complexes as a function of chloride concentration. Plot calculated at pH = 7 and* $[Ag]_{tot} = 10^{-6}$ *mol·dm*$^{-3}$.

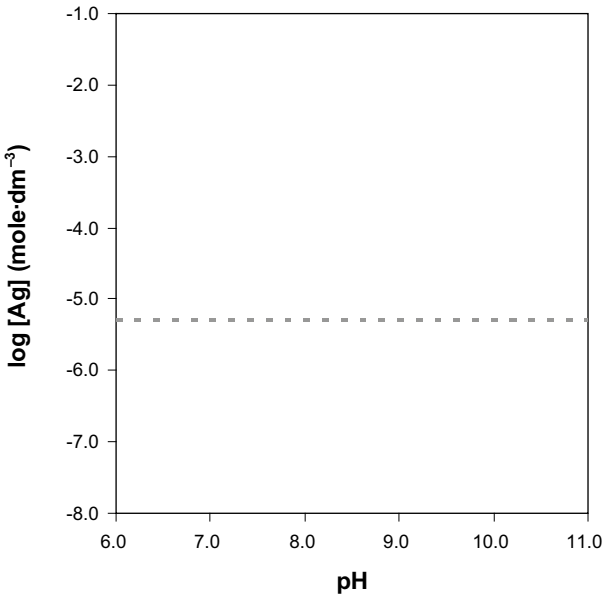

Figure 6-29. *Solubility curve of AgCl(s) as a function of pH, by using the reference groundwater composition (pe = –2.42).*

Table 6-10 summarises the calculated solubilities for Ag under the different redox conditions studied.

In principle, the aqueous speciation of silver is not affected by the redox conditions of the media. Nevertheless, if reduction of sulphate to sulphide occurred due to the presence of SRB (see Chapter 5), the aqueous speciation of this element as well as the solid phase governing its solubility, would change as a function of the pe of the media. The effect of pe on both, the speciation as well as the solubility of silver sulphide species present in the system is shown in Figure 6-30.

Then, the presence of SRB under reducing conditions might increase the solubility of silver as a consequence of the formation of silver sulphide species for pe value below –1.8.

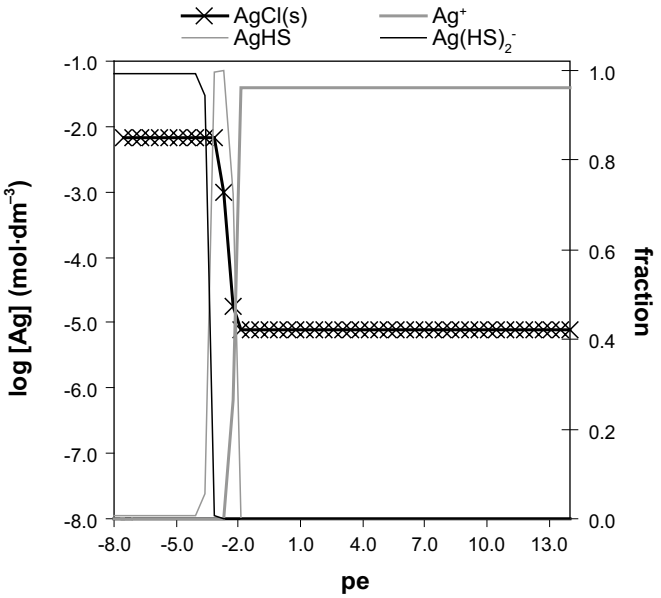

Figure 6-30. *Solubility of AgCl(s) solid phase and underlying aqueous speciation as a function of pe by using the reference water composition, pH = 7 and allowing reduction of sulphate to sulphide (for explanations see text).*

Table 6-10. Ag solubility-controlling phases and solubility values (in mole dm^{-3}) for each one of the studied groundwaters.

	T = 15°C pe gw	$pO_2(g)$ = 0.2 atm	$pH_2(g)$ = 10^{-7} atm	$pH_2(g)$ = 10^{2} atm
[Ag] (mole·dm^{-3})	AgCl $4.4 \cdot 10^{-6}$	AgCl $4.4 \cdot 10^{-6}$	AgCl $4.4 \cdot 10^{-6}$	AgCl $4.4 \cdot 10^{-6}$

6.4 Lanthanides

6.4.1 Samarium

This element is not redox sensitive and its chemical behaviour is basically controlled by the pH and the carbonate content of groundwaters. In the pH range between 6 and 9 under the reference groundwater composition the free cation Sm^{3+} dominates the aqueous speciation, with some contributions of carbonate and sulphate species (Figure 6-31a). The allowance of calcite precipitation in the system (Figure 6-31a compared to Figure 6-31b) leads to a wider predominance range of free Sm^{3+} in detriment of aqueous samarium carbonate species. At pH > 9, hydrolysis species dominate the aqueous speciation of samarium.

The most likely precipitating solid phases are samarium hydroxide, samarium carbonate and the mixed samarium hydroxo-carbonate, whose calculated solubilities are shown in Figure 6-32.

In the acidic pH range, carbonate solid phases might exert the solubility control (either $SmCO_3OH(c)$ or $Sm_2(CO_3)_3(c)$), while the mixed $SmCO_3OH(c)$ solid is the most likely solubility controlling phase between pH 7 and 10. At pH > 10, the solid oxyhydroxide would be the solid phase exerting the solubility control (Figure 6-32).

Table 6-11 summarises the calculated solubilities for Sm under the different redox conditions studied.

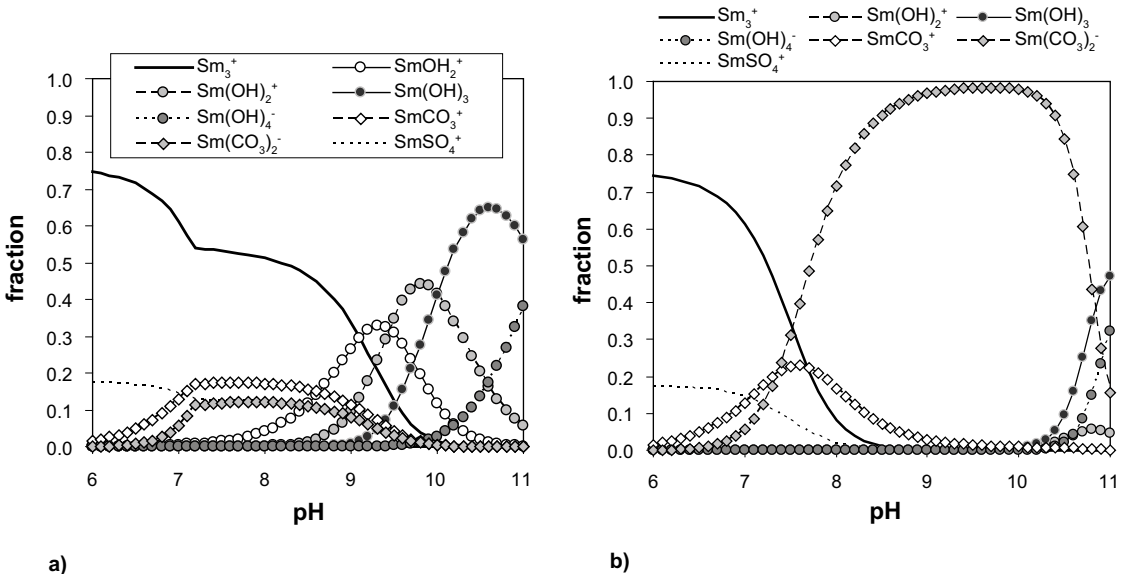

Figure 6-31. *Fractional diagram showing the Sm predominant aqueous species by using the reference groundwater composition, [Sm] = 5·10⁻⁷M. (a) Allowing the precipitation of calcite in the system. The inflexion point in the Sm^{3+} curve at pH 7 indicates the onset of calcite precipitation in the system. (b) Avoiding the precipitation of calcite in the system.*

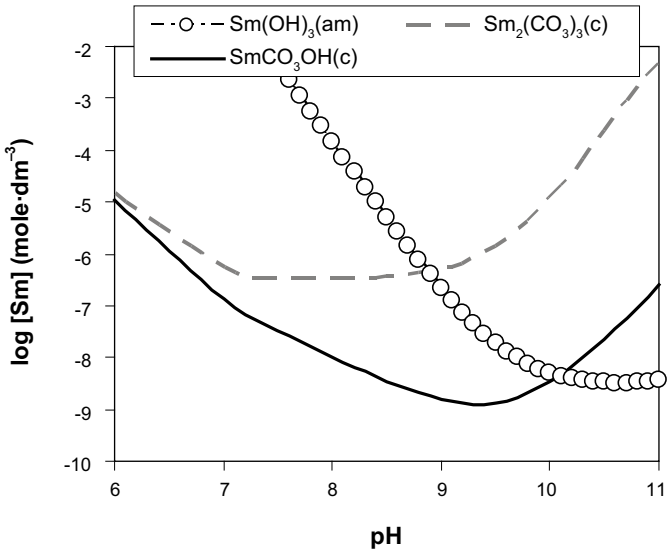

Figure 6-32. *Solubility of the different samarium solid phases as a function of pH under the reference groundwater composition. Solubility expressed in mole/dm³.*

Table 6-11. Sm solubility-controlling phases and solubility values (in mole dm⁻³) under different redox conditions.

	T= 15°C pe gw	$pO_2(g)$ = 0.2 atm	$pH_2(g)$ = 10^{-7} atm	$pH_2(g)$ = 10^{2} atm
[Sm] (mole·dm⁻³)	$SmOHCO_3$ $1.1\cdot10^{-7}$	$SmOHCO_3$ $1.1\cdot10^{-7}$	$SmOHCO_3$ $1.1\cdot10^{-7}$	$SmOHCO_3$ $1.1\cdot10^{-7}$
	$Sm_2(CO_3)_3$ $4.4\cdot10^{-7}$	$Sm_2(CO_3)_3$ $4.4\cdot10^{-7}$	$Sm_2(CO_3)_3$ $4.4\cdot10^{-7}$	$Sm_2(CO_3)_3$ $4.4\cdot10^{-7}$

One of the main uncertainties in the assessment of the behaviour of Sm is the concentration of phosphate in the system (see discussion in Chapter 5). Phosphates have been identified to form both, strong aqueous complexes in solution and stable solid phases with lanthanides, leading to lower lanthanide concentrations in natural waters than those previously calculated. The lack of phosphate measurements in the reference groundwater, thus, poses a limitation in the assessment of a proper solubility limit for this element. Nevertheless, calculations undertaken under the saline groundwater composition where phosphate measurements are available (Figure 6-33), show that solid phosphates may exert the solubility control leading to lower samarium concentrations, more in line with measured samarium concentrations in natural waters (see Chapter 4).

The stability of the mixed carbonate solid phase, which has been assumed to exert the solubility control in the pH range from 7 to 10, might have associated an important uncertainty given that its stability has been estimated on the basis of analogies with other lanthanides /see Duro et al. 2005/.

6.4.2 Holmium

Ho is not redox sensitive and has a chemical behaviour very similar to the one of Sm, controlled by pH and the carbonate content of the waters studied.

In the pH range between 6 and 9 the free cation dominates the aqueous speciation, although with contribution of the carbonate and sulphate species (see Figure 6-34).

At pH above 9, $Ho(OH)_4^-$ dominates until 11 while in the case of Sm, there is a predominance of the different hydrolysis products depending on the pH and the tetra-hydroxide complex does not dominate until pH above 11. As in the case of samarium, the allowance of calcite precipitation in the system leads to a wider predominance range of free Ho^{3+} in detriment of aqueous holmium carbonate species (see plot of samarium Figure 6-31a compared to Figure 6-31b).

Calculated solubilities under the reference groundwater composition are shown in Figure 6-35 as a function of pH.

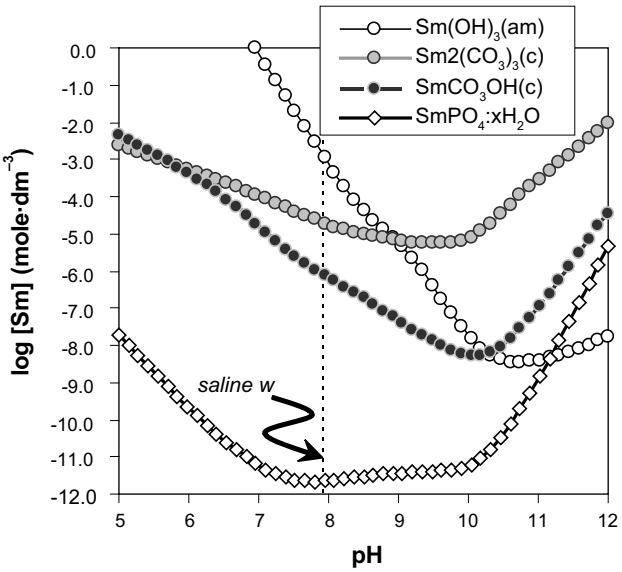

Figure 6-33. *Fractional diagram showing the Sm predominant aqueous species by using the saline groundwater composition, [Sm] = 5·10⁻⁷M.*

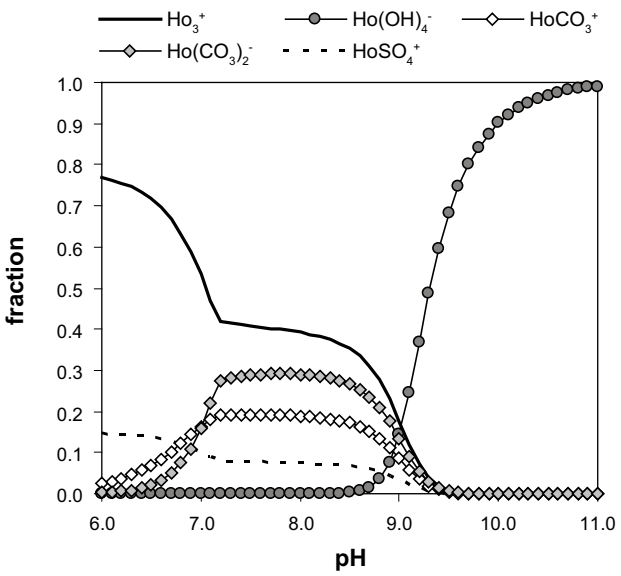

Figure 6-34. *Fractional diagram showing the Ho predominant aqueous species. [Ho] = 5·10⁻⁷M.*

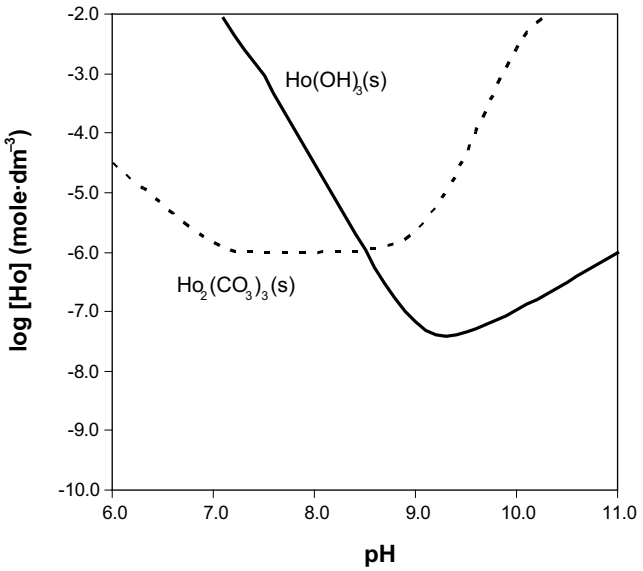

Figure 6-35. *Solubility limits of the different holmium solid phases as a function of pH.*

The solubility curves are similar to those of samarium: in the acidic range, carbonate solid phases exert the solubility control, while in the basic range solid oxyhydroxides dominate and, therefore, the solid hydroxide control the solubility of these elements. In the case of Holmium, though, mixed hydro-carbonate solid phases have not been reported (for explanations see /Spahiu and Bruno 1997/). Thus, the solubility controlling phase under the conditions of the reference groundwater is $Ho_2(CO_3)_3(s)$ (Figure 6-35).

Table 6-12 summarizes the holmium concentrations in equilibrium with the solubility controlling phase under the different redox conditions studied.

Table 6-12. Ho solubility-controlling phases and concentration values (in mole dm^{-3}) under the different redox condition.

	T = 15°C pe gw	$pO_2(g)$ = 0.2 atm	$pH_2(g)$ = 10^{-7} atm	$pH_2(g)$ = 10^{2} atm
[Ho] (mole·dm^{-3})	$Ho_2(CO_3)_3$ $1.2\cdot10^{-6}$	$Ho_2(CO_3)_3$ $1.2\cdot10^{-6}$	$Ho_2(CO_3)_3$ $3.0\cdot10^{-6}$	$Ho_2(CO_3)_3$ $3.1\cdot10^{-6}$

6.5 Actinides

6.5.1 Thorium

This radionuclide is mainly found in the redox state +4 and can be considered a non redox sensitive radioelement. The concentration of thorium in groundwater seems to be limited by the solubility of thorium oxide (ThO_2(am)). The variation of the solubility of the amorphous thorium oxide with pH is shown in Figure 6-36.

The main aqueous species under the conditions of the reference groundwater is the mixed hydroxo-carbonate of stoichiometry $ThCO_3(OH)_3^-$, which is, at the same time, the main underlying aqueous species in equilibrium with the solid phase under the conditions plotted in Figure 6-37.

The influence of carbonate in the solubility of $ThO_2\cdot2H_2O$ at pH of the reference groundwater can be seen in Figure 6-38, with an increase of the solubility when increasing the total carbonate concentration of the system.

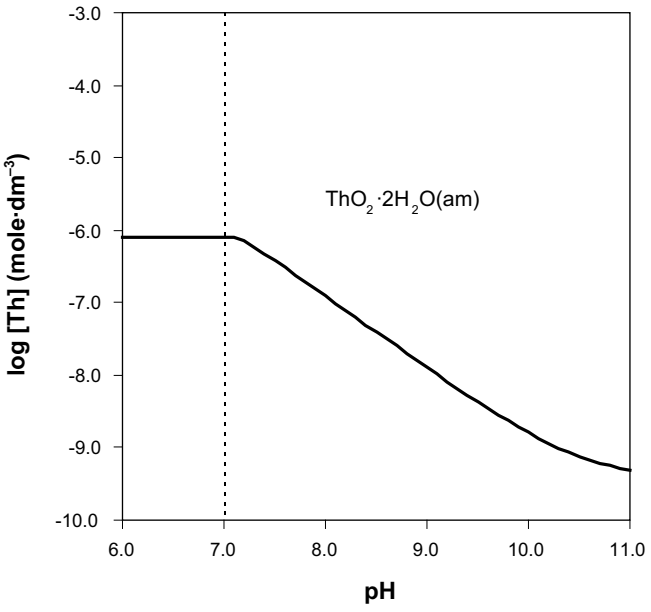

Figure 6-36. *Thorium concentrations in equilibrium with $ThO_2\cdot2H_2O$ (am) as a function of pH under the conditions of the reference groundwater. Vertical dashed line stands for the pH measured in the reference groundwater.*

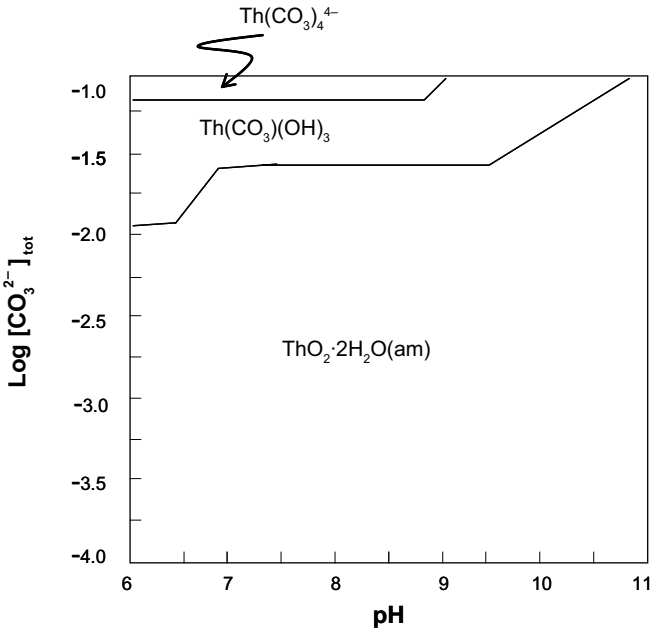

Figure 6-37. *pH/[CO_3^{2-}] predominance diagram of Th(IV). [Th] = 5·10^{-6} M.*

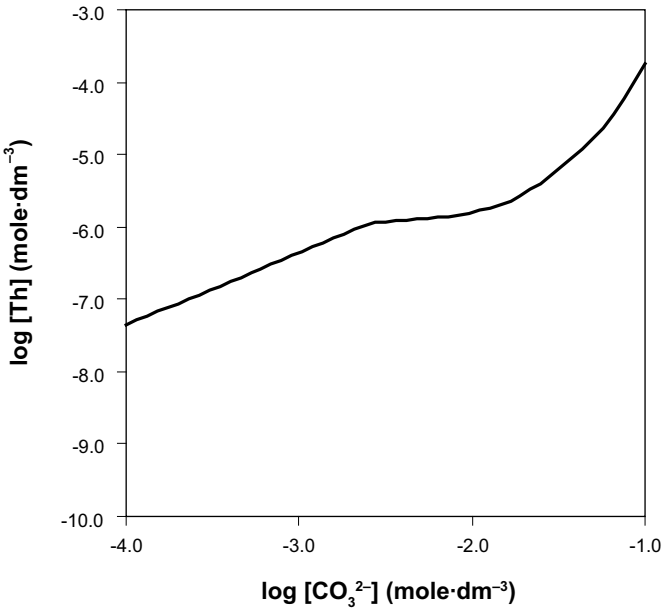

Figure 6-38. *Variation of the solubility of $ThO_2·2H_2O$ (am) with the total carbonate concentration under the conditions of the reference groundwater.*

The most important uncertainty concerning this element is related to the thermodynamic database, specially for the scheme of aqueous carbonate species as well as for the solid crystallinity. Although many efforts have been devoted in the last years to establish both, the existence and the stability of mixed hydroxo-carbonato thorium species and the stability of thorium oxide, it has been an open question until nowadays (see discussion in /Duro et al. 2005/). A recent study of this complex system together with new solubility studies /Altmaier et al. 2005/ propose a different scheme than that here considered. Nevertheless calculated thorium concentrations here are slightly higher than those measured in natural waters.

The calculated [Th] in equilibrium with the solid are summarized in Table 6-13.

Table 6-13. Th solubility-controlling phases and concentration values (in mole dm^{-3}) under the different redox contitions.

	T = 15°C pe gw	$pO_2(g)$ = 0.2 atm	$pH_2(g)$ = 10^{-7} atm	$pH_2(g)$ = 10^{2} atm
[Th] (mole·dm^{-3})	$ThO_2{\cdot}2H_2O$ $7.9{\cdot}10^{-7}$	$ThO_2{\cdot}2H_2O$ $7.9{\cdot}10^{-7}$	$ThO_2{\cdot}2H_2O$ $7.9{\cdot}10^{-7}$	$ThO_2{\cdot}2H_2O$ $7.9{\cdot}10^{-7}$

6.5.2 Protactinium

Pa can occur in the +IV and +V oxidation state. Under the conditions of interest, the aqueous speciation is dominated by $PaO_2OH(aq)$ without dependence on either pH or pe of the system studied. The solid phase that may exert a solubility control is $Pa_2O_5(s)$ and its solubility is also constant with pH and pe within the studied range of variability of these parameters.

The most important uncertainty concerning this element is that thermodynamic data for protactinium available in the literature is rather scarce.

6.5.3 Uranium

Uranium belongs to the actinide group. In the environment, it occurs in the oxidation states +3, +4, +5 and +6, and non-stoichiometric oxides (i.e. U_3O_8 or U_3O_7) are relatively common under certain redox conditions.

Uranium aqueous speciation is very dependent on pe and pH (see Figure 6-39). Under reducing conditions, uranium is predominantly in the tetravalent state. In general terms, the aqueous chemistry of uranium at reducing conditions is mainly dominated by $U(OH)_4(aq)$ in the pH range under study. Under oxidising conditions, and in the pH and carbonate concentrations found in most natural waters, the predominant aqueous species of hexavalent uranium are carbonates.

The solid phases that may form in the system are strongly dependent on the composition of the groundwaters. Under reducing conditions, UO_{2+x} phases can appear. The very stable $UO_{2.0}$ can accept excess oxygen in its cubic fluorite structure up to a non-stoichiometric composition corresponding to x = 0.33, i.e. $UO_{2.33}$ or U_3O_7. Under oxidising conditions, hexavalent uranium solids appear. The precipitation of U(VI) oxyhydroxides is very fast and, thus, not kinetically limited. Under the presence of silicate in the groundwater, as it is the case of interest for this analysis, different silicate solid phases can also form. Uranophane, $(Ca(UO_2)_2(SiO_3OH)_2\ 5H_2O)$ has been found to form as secondary phase in the vicinity of massive uranium ores and, therefore, its formation can be possible under the flow regimes expected in the surroundings of the repository. Soddyite can form at lower pH values depending on the conditions of groundwater. Another solid that has been observed to form in natural formations under oxidising conditions is becquerelite, a mixed U(VI)-Ca(II) oxide ($CaU_6O_{19}{\cdot}11H_2O$) /see Finch et al. 1995/.

Table 6-14. Pa solubility-controlling phases and concentration values (in mole dm^{-3}) under the different redox conditions.

	T = 15°C pe gw	$pO_2(g)$ = 0.2 atm	$pH_2(g)$ = 10^{-7} atm	$pH_2(g)$ = 10^{2} atm
[Pa] (mole·dm^{-3})	Pa_2O_5 $3.0{\cdot}10^{-7}$	Pa_2O_5 $3.0{\cdot}10^{-7}$	Pa_2O_5 $3.0{\cdot}10^{-7}$	Pa_2O_5 $3.0{\cdot}10^{-7}$

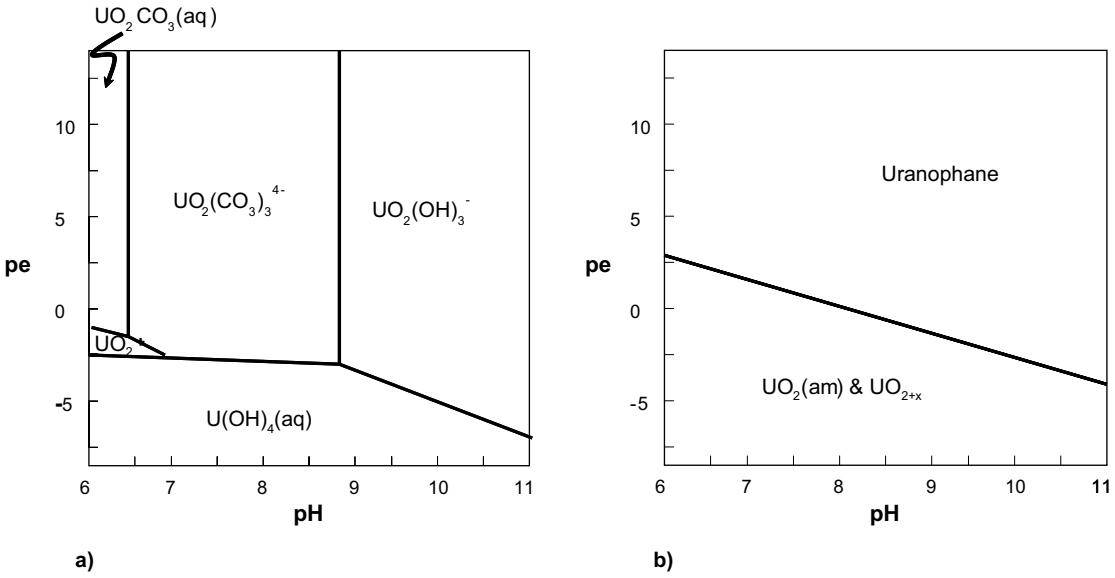

Figure 6-39. *pe/pH diagrams with predominant uranium species under the reference groundwater composition (a) and solid phases (b). Calculations performed with [U]tot = 10^{-5}M [CO_3^{2-}]tot = $1.77 \cdot 10^{-3}$M, [Si] = $1.85 \cdot 10^{-4}$M and [Ca] = $2.33 \cdot 10^{-2}$M.*

A general description of the system, in terms of main aqueous species (Figure 6-39a) and main solid phases likely to form (Figure 6-39b) for the groundwater composition of interest in this study is given in Figure 6-39a and Figure 6-39b respectively.

From the former figures, it seems clear that under reducing conditions, solids of the type UO_{2+x} are the ones able to control the aqueous concentration of uranium. Under oxidising conditions, though, uranophane may form.

From Figure 6-40 it is possible to notice that, in case of an oxidising intrusion affecting the system, the uranium solubility would be limited by the precipitation of becquerelite and/or uranophane, depending on the total silicon in the system. The boundary between these two solids is located at a total silicon concentration of $10^{-4.5}$ mole/dm^3.

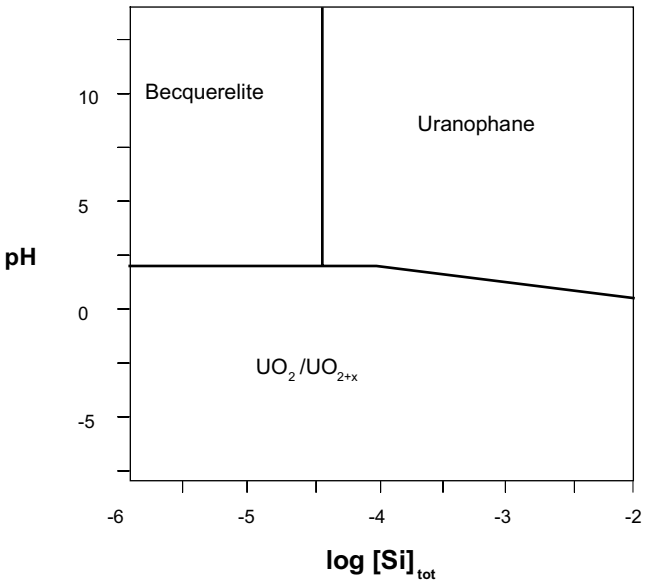

Figure 6-40. *Predominance diagram of uranium solid phases as a function of pe and total concentration of silicon in the system. Composition of the reference groundwater used. [U] = 10^{-5}mole/dm^3.*

One of the main uncertainties arising from the study of this element is related with the precipitation of calcium uranates and coffinite ($USiO_4$, which were omitted in the present calculations due to the few thermodynamic data available. Although both solids have been observed in laboratory experiments and natural systems respectively, the only thermodynamic data available are coming from few experimental data and calorimetric studies performed with crystalline solid phases respectively, which gives unrealistic low uranium concentrations. The lack of thermodynamic data from solubility experiments with less crystalline solid phases leads to disregard these solids for giving uranium concentration limits. Figure 6-41 shows the predominance area of uranium solids if they are taken into consideration.

Therefore, the solubility calculations will be conducted in equilibrium with becquerelite and uranophane under oxidising conditions, and UO_{2+x} under reducing conditions.

Calculated concentrations of uranium in equilibrium with the different selected solid phases are summarized in Table 6-15.

Table 6-15. U solubility-controlling phase and solubility value (in mole dm^{-3}) under different redox conditions.

	T = 15°C pe gw	$pO_2(g)$ = 0.2 atm	$pH_2(g)$ = 10^{-7} atm	$pH_2(g)$ = 10^{2} atm
[U] (mole·dm^{-3})	$UO_2{\cdot}2H_2O$ $9.5{\cdot}10^{-9}$	Uranophane $1.7{\cdot}10^{-6}$	$UO_{2.67}$ $3.4{\cdot}10^{-8}$	$UO_2{\cdot}2H_2O$ $6.8{\cdot}10^{-10}$
	Uranophane $1.9{\cdot}10^{-6}$	Becquerelite $2.5{\cdot}10^{-6}$	$UO_2{\cdot}2H_2O$ $7.9{\cdot}10^{-10}$	$UO_{2.34}$ $1.5{\cdot}10^{-9}$
	Becquerelite $3.0{\cdot}10^{-6}$			$UO_{2.25}$ $3.0{\cdot}10^{-11}$

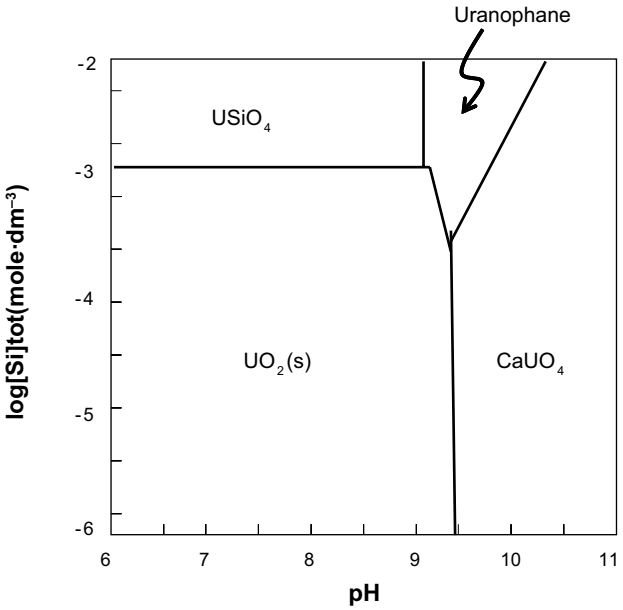

Figure 6-41. *Predominance diagram of uranium solid phases when including the precipitation of calcium uranates and coffinite ($USiO_4$) as a function of pH and [Si] under the composition of the reference groundwater. [U] = 10^{-5}mole/dm^3. pe = –5.*

6.5.4 Neptunium

Neptunium is another radioactive element of the actinoid group. Given its electronic configuration, this radioelement may be found at different oxidation states: +3, +4, +5 and +6 depending on the redox environment.

Neptunium concentrations under the conditions of interest for this work are expected to be controlled by the precipitation of neptunium(IV) dioxide. This solid is stable over a relatively wide pe range, from very reducing (pe = –8) to slightly oxidising conditions (pe = 2). Figure 6-42 shows neptunium concentrations in groundwaters by assuming equilibrium with neptunium dioxide. According to the Ostwald's rule, the amorphous phase will precipitate first, so, this solid has been the one selected for the sensitivity analysis and for the solubility calculations.

Figure 6-43 shows the aqueous speciation of neptunium under the reference groundwater conditions as a function of the pH of the system. $Np(OH)_4(aq)$ is the predominant species in almost all the pH range of interest.

Neptunium concentrations governed by the precipitation of neptunium dioxide might depend on the solution composition in the present environmental conditions studied, specially on the carbonate concentration present in the system, which can have an important effect on the solubility of this solid (see Figure 6-44).

Two solid phases may exert the solubility control depending on the redox environment. The stability of these solids as a function of pe is shown in Figure 6-45 to assess the different redox ranges where these solids would exert the solubility control.

Based on Figure 6-45, neptunium dioxide will exert the solubility control in reducing and slightly oxidising environments. In oxic conditions, Np_2O_5 will be the solid phase controlling neptunium concentrations in groundwater.

The different neptunium aqueous complexes dominating the aqueous speciation as a function of pe are shown in Figure 6-46. Np(IV) species are predominant until pe around 4, where Np(V) species come over basically as the oxocation NpO_2^+.

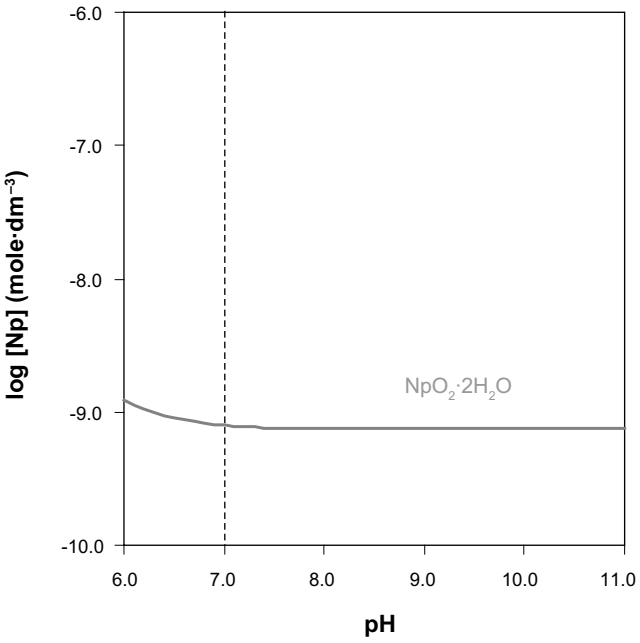

Figure 6-42. *Neptunium concentrations in groundwater in equilibrium with $NpO_2 \cdot 2H_2O$ as a function of pH. Calculations conducted by using the reference groundwater composition. Vertical dashed line indicates the pH of the reference groundwater.*

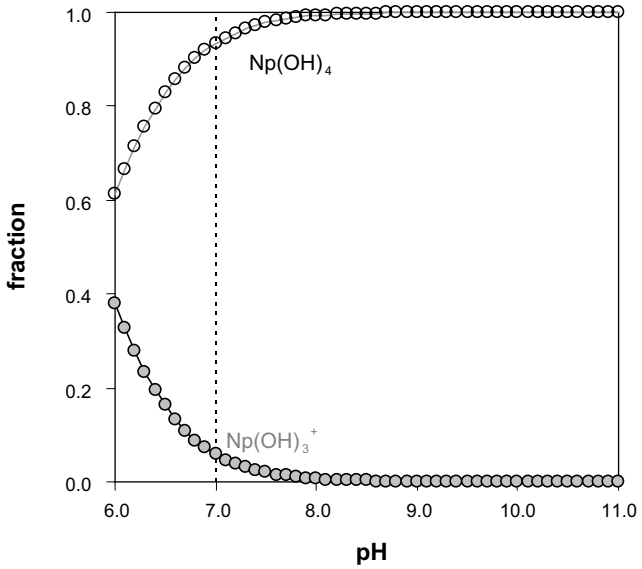

Figure 6-43. *Fractional diagram showing aqueous neptunium species under the reference groundwater composition as a function of pH. [Np] = 10^{-8}M. Dashed vertical line indicates the pH of the reference groundwater.*

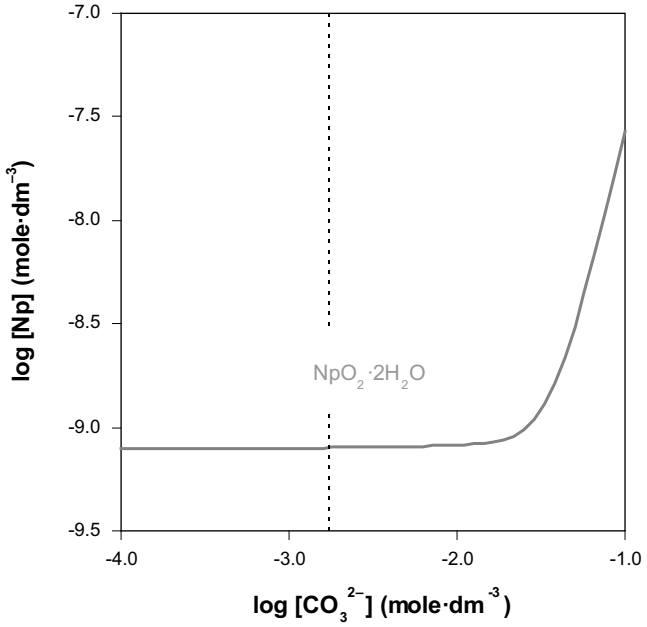

Figure 6-44. *Neptunium concentrations in groundwater in equilibrium with $NpO_2 \cdot 2H_2O$ as a function of $[CO_3^{2-}]$ under the reference groundwater composition. Dashed line indicated the carbonate concentration of the reference groundwater.*

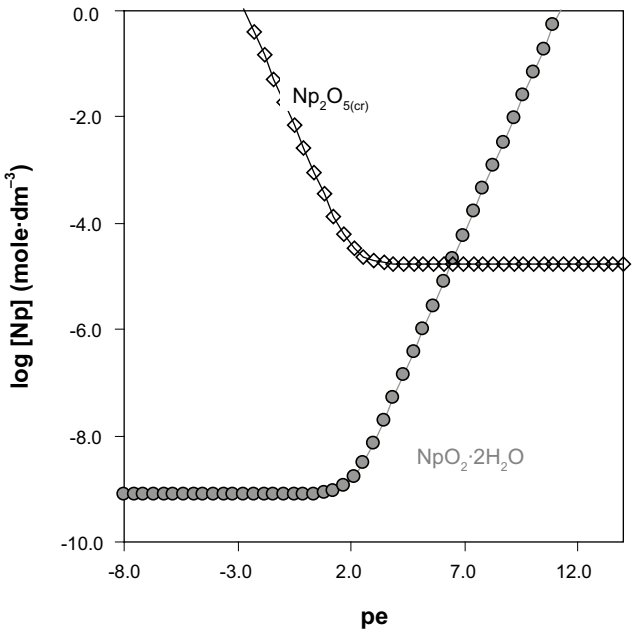

Figure 6-45. *Neptunium concentrations (mol/dm³) in groundwater in equilibrium with $NpO_2 \cdot 2H_2O$ and Np_2O_5 as a function of pe. Calculations conducted under the reference groundwater composition, pH = 7.*

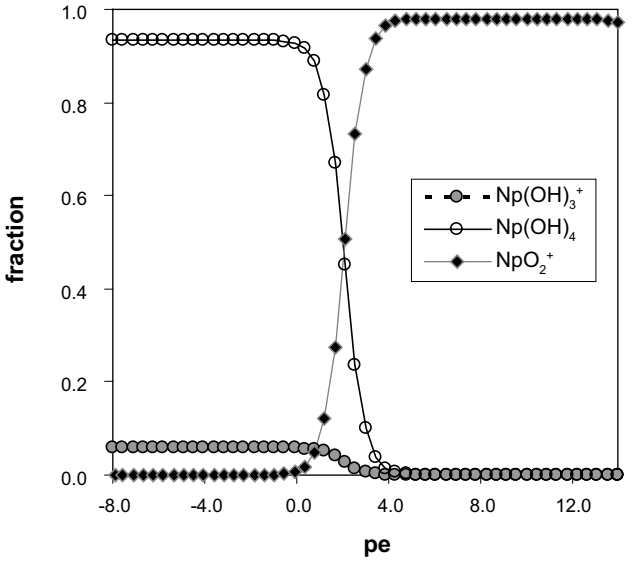

Figure 6-46. *Fractional diagram showing neptunium aqueous species in the reference groundwater composition as a function of pe. [Np] = 10^{-8}M, pH = 7.*

The Np solubility-controlling phase under the conditions of the reference groundwater is the amorphous Np(IV) oxide ($NpO_2 \cdot 2H_2O$(am)) (Table 6-16). Only at oxidising pe (pO_2(g) = 0.2 atm) the solubility limiting phase is changed given that Np(IV) is oxidised to Np(V) and Np(VI). In this case, Np_2O_5(cr) exerts the solubility control and the speciation is dominated by NpO_2^+.

Table 6-16. Np solubility-controlling phases and concentration values (in mole dm^{-3}) under the different redox conditions.

	T = 15°C pe gw	$pO_2(g)$ = 0.2 atm	$pH_2(g)$ = 10^{-7} atm	$pH_2(g)$ = 10^{2} atm
[Np] (mole·dm^{-3})	$NpO_2 \cdot 2H_2O$ $1.0 \cdot 10^{-9}$	Np_2O_5 $1.7 \cdot 10^{-5}$	$NpO_2 \cdot 2H_2O$ $1.0 \cdot 10^{-9}$	$NpO_2 \cdot 2H_2O$ $1.0 \cdot 10^{-9}$

6.5.5 Plutonium

Plutonium is located in the periodic table between Np and Am. The chemical behaviour of this actinide is quite similar to the one of neptunium and this radionuclide may be also found at different oxidation states, +3, +4, +5 and +6 depending on the environmental redox conditions.

The aqueous speciation will mainly depend on the master variables pe and pH, although the groundwater composition i.e. carbonates, sulphates, phosphates will also have an important role on determining the aqueous complexes dominating Pu species in solution. Figure 6-47 shows a pe/pH diagram with the predominant Pu aqueous species as a function of the main variables of the system, under the reference groundwater composition.

Pu speciation will be dominated by hydrolysis species in almost all the stability field studied, with the neutral species of Pu(IV) dominating in a wider pe and pH range. Under the conditions of the reference groundwater, the aqueous speciation is dominated by the free Pu^{3+} ion with contributions of sulphate and carbonate Pu (III) species (see Figure 6-48).

Although a more crystalline form of tetravalent Pu oxide is selected in /Guillaumont et al. 2003/, the experimental data available in the literature fall in between the solubility calculated by equilibrating waters with the PuO_2(am, hyd) selected by /Guillaumont et al. 2003/ and the one obtained with the $Pu(OH)_4$(am) solid selected in /Lemire and Garisto 1989/ (see Figure 6-49 and /Duro et al. 2005/). For the sake of conservatism of the results, the sensitivity analyses and

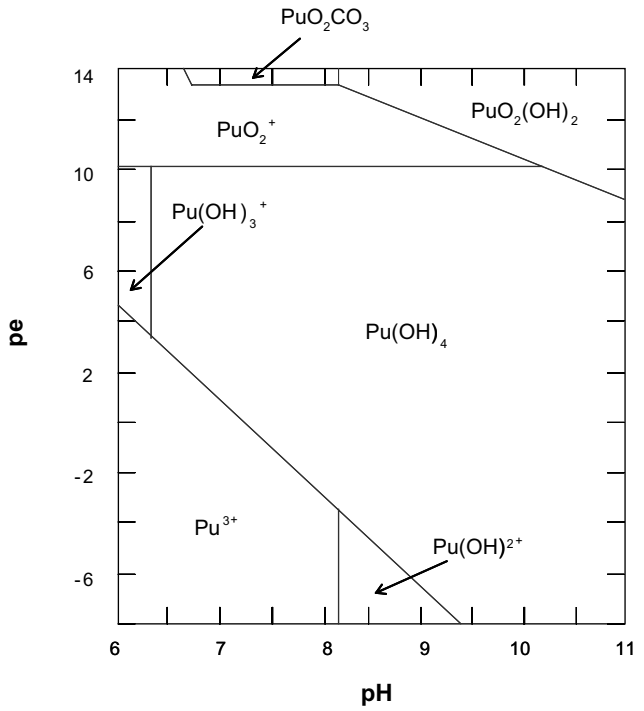

Figure 6-47. *pe/pH diagram with predominant plutonium aqueous species. Calculations performed with [Pu]tot. = 10^{-7}M under the reference groundwater composition.*

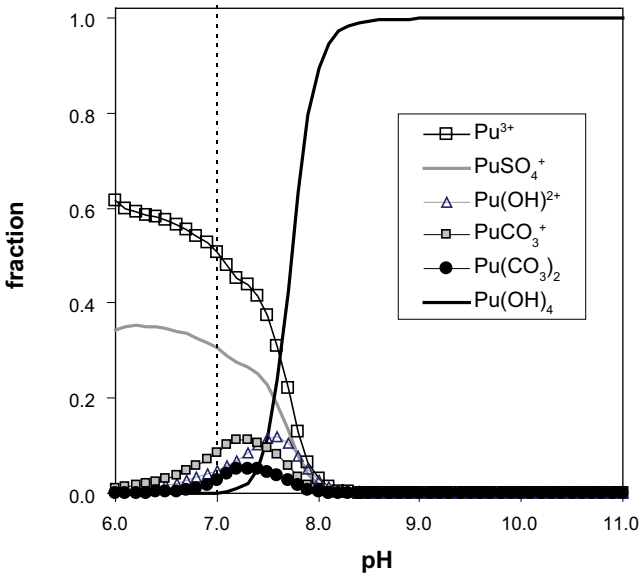

Figure 6-48. *Fractional diagram showing the aqueous plutonium speciation as a function of the pH of the system under the reference groundwater composition, at pe = –2.42. Vertical dashed line shows the pH of the reference groundwater.*

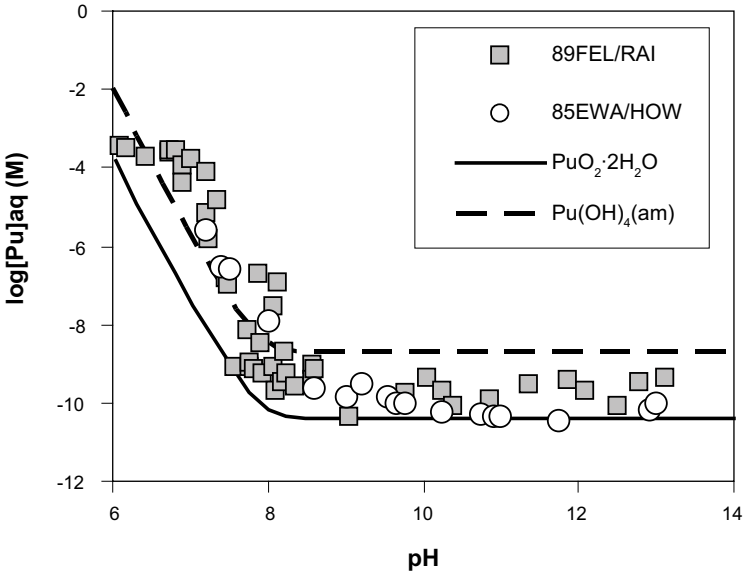

Figure 6-49. *Comparison between experimental data on PuO_2(am) solubility experiments and solubility calculated by using the set of data selected in this work.*

solubility calculations have been conducted with the amorphous form of $Pu(OH)_4$(am), although also the results obtained with PuO_2 (am,hyd) are reported here.

The calculated solubilities of the selected solid phases are shown in Figure 6-50 as a function of pH. In the neutral and alkaline range $Pu(OH)_4$(am) will be the solid phase controlling Pu concentrations in groundwaters. This phase destabilises in the acidic range, where the solid presenting the lower solubility control is the mixed hydroxo-carbonate.

The pe dependence of the solubility of the different plutonium solid phases is shown in Figure 6-51. The plutonium solid phases that may govern plutonium concentrations in waters are mainly plutonium (III) and plutonium (IV) (hydr)oxides under very reducing and slightly reducing or oxidising conditions respectively, including an hydroxo-carbonate of plutonium(III).

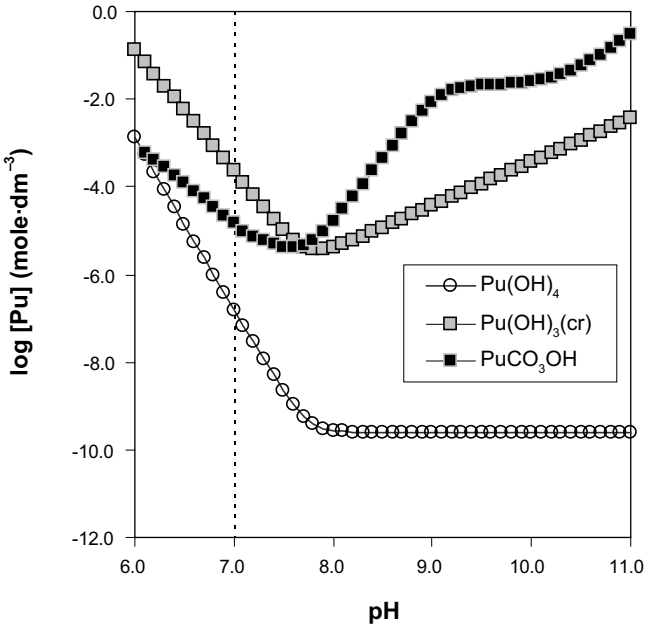

Figure 6-50. *Plutonium concentrations (mol/dm³) in groundwater in equilibrium with different Pu solid phases as a function of pH under the reference groundwater composition. Dashed line stands for the pH of the reference groundwater.*

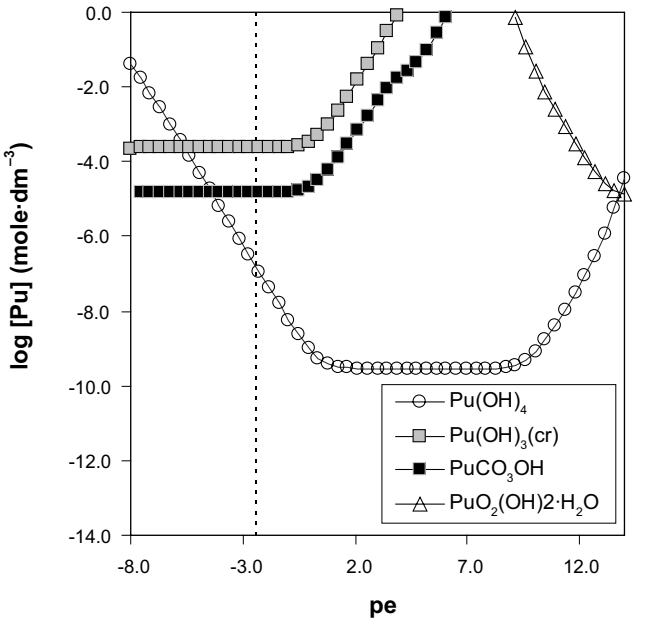

Figure 6-51. *Plutonium concentrations (mol/dm³) in groundwater in equilibrium with different Pu solid phases as a function of pe under the reference groundwater composition.*

Figure 6-51 shows that the tetravalent plutonium oxide will be the solid phase exerting the solubility control under slightly reducing and oxidising conditions in the reference groundwater. This solid will destabilise when moving to more reducing conditions due to the reduction of Pu(IV) to Pu(III) and consequently a different solid phase, such as $Pu(OH)_3(s)$ or $PuOHCO_3(s)$ will control plutonium concentrations under reducing condition.

One of the main uncertainties in the assessment of the behaviour of Pu is the concentration of phosphate in the system (see discussion in Chapter 5). Phosphates have been identified to

form stable Pu(III) solid phases leading to lower Pu concentrations. Therefore, a phosphate of plutonium (III) might be the predominant aqueous species in neutral and reducing waters if phosphates were present. The lack of phosphate measurements in the reference groundwater, thus, might pose a limitation in the assessment of a proper solubility limit for this element.

Then, calculations undertaken under the saline groundwater composition where phosphate measurements have been done (Figure 6-52), show that $PuPO_4$ (s) appears as the solubility controlling solid under reducing conditions.

It is also in the reducing environments where other of the uncertainties associated to the plutonium speciation arises. As discussed in Chapter 5 the reduction of sulphate to sulphide has not been considered here. Nevertheless, Figure 6-48 shows that one of the main plutonium species under the reducing conditions is $PuSO_4^+$. Thus, in case that the reduction of sulphate to sulphide was allowed, Pu sulphate complexes would not be stable implying a change in the aqueous speciation.

Table 6-17 summarizes the Pu solubility-controlling phases as well as the concentration values under the different redox conditions studied in the reference case. Pu is a redox sensitive element and because of this, the solubility-limiting phase varies depending on the pe considered.

Table 6-17. Pu solubility-controlling phases and concentration values calculated (in mole·dm^{-3}) under the different redox conditions.

	T = 15°C pe gw	$pO_2(g)$ = 0.2 atm	$pH_2(g)$ = 10^{-7} atm	$pH_2(g)$ = 10^{2} atm
[Pu] (mole·dm^{-3})	$Pu(OH)_4(s)$ $1.3\cdot10^{-7}$	$PuO_2(OH)_2\cdot H_2O$ $1.3\cdot10^{-5}$	$Pu(OH)_4(s)$ $1.6\cdot10^{-6}$	$PuOHCO_3$ $1.2\cdot10^{-5}$
	$PuOHCO_3$ $1.2\cdot10^{-5}$	PuO_2CO_3 $1.0\cdot10^{-5}$	$PuOHCO_3$ $1.2\cdot10^{-5}$	
	$Pu(OH)_3(cr)$ $1.9\cdot10^{-4}$	$Pu(OH)_4(s)$ $2.2\cdot10^{-4}$		

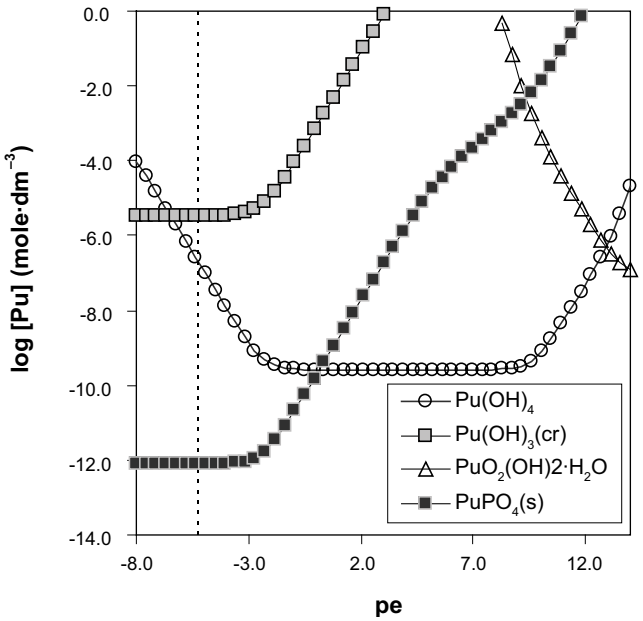

Figure 6-52. *Plutonium concentrations (mol/dm^3) in groundwater in equilibrium with different Pu solid phases as a function of pe under the saline groundwater composition.*

6.5.6 Americium and curium

As it is discussed in /Duro et al. 2005/, given the chemical analogy existing between americium and curium, we present in this section the discussion undertaken for americium, and the same analyses will apply to curium.

Americium is one of the so-called trivalent actinides, given that its most stable oxidation state in waters is +3. Am(IV) solid phases are also reported in the literature although americium species in aqueous solutions have not been identified. Am(V) hydroxides have been investigated, nevertheless they have not been included in the database because they are only relevant at very high redox potentials, which is out of the scope of the present work.

Am aqueous species dominating in reference water are shown in Figure 6-53.

Hydrolysis species dominate in the alkaline range while the free cation is the predominant aqueous species in the neutral and slightly acid pH range. It is important to highlight the contribution of carbonate and some sulphate aqueous complexes in the reference water. As in the case of Samarium and Holmium, allowing calcite precipitation in the system (Figure 6-53a compared to Figure 6-53b) leads to a wider predominance range of free Am^{3+} in detriment of aqueous americium carbonate species.

As shown in figure Figure 6-54, three solid phases may exert the solubility control in the reference groundwater depending on the pH range considered. At pH = 7, the pH of the reference groundwater composition (Table 1), two different solid phases, the mixed hydroxo-carbonate and $Am_2(CO_3)_3(s)$, might exert the solubility control, while the first one is the solubility controlling phase in the pH range from 7 to 9 approximately. At slightly acidic pH, the solubility control might be exerted by both, the americium carbonate as well as the mixed hydroxo-carbonate. In the alkaline range (pH > 9), americium hydroxide might determine americium concentrations in the same groundwaters composition.

One of the uncertainties in the assessment of the behaviour of Am, as in the case of Sm and Ho, is the concentration of phosphate in the system (see discussion in Chapter 5). Phosphates forms stable solid phases with Am, leading to lower concentrations than those previously

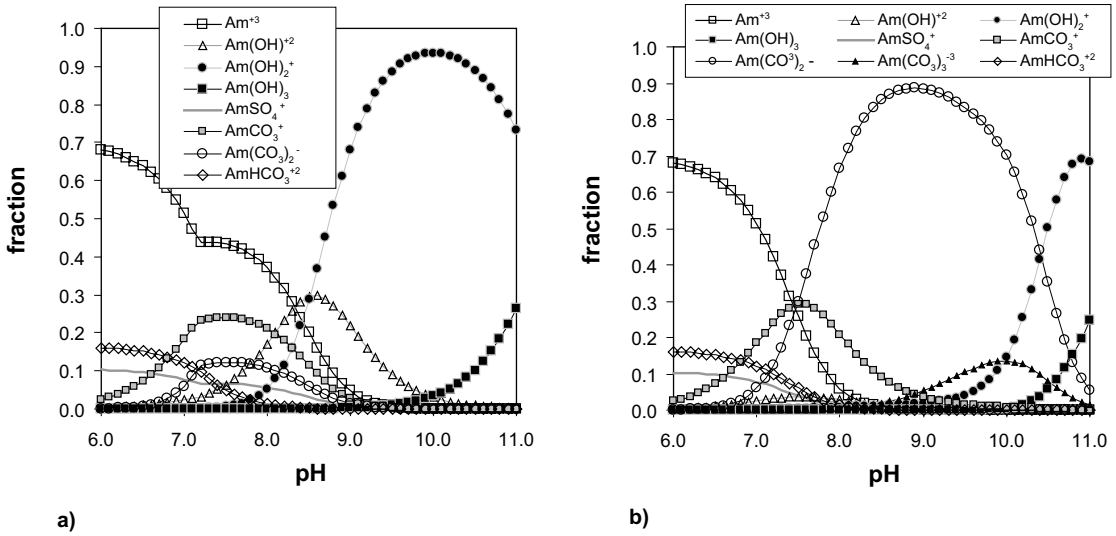

Figure 6-53. *Fractional diagrams with Am aqueous species as a function of pH, under the reference groundwater composition. [Am] = 10^{-6} mole·dm^{-3}. (a) Allowing the precipitation of calcite in the system. The inflexion point in the Am^{3+} curve at pH 7 indicates the onset of calcite precipitation in the system. (b) Avoiding the precipitation of calcite in the system.*

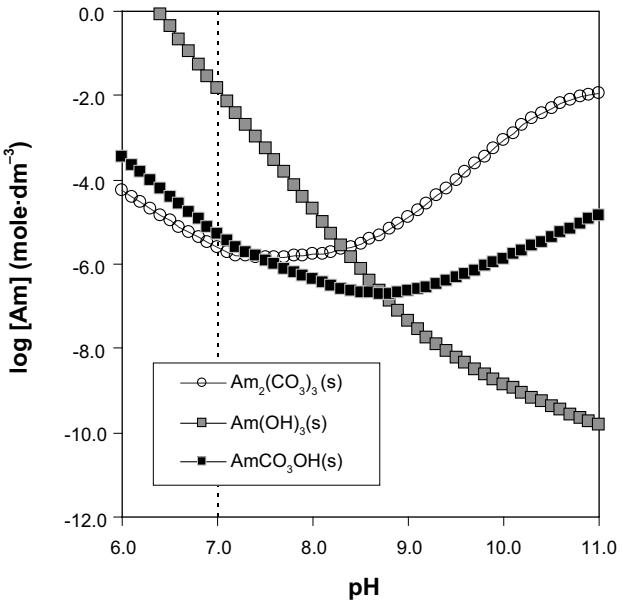

Figure 6-54. *Americium concentrations (mole/dm^3) in groundwater in equilibrium with different Am solid phases as a function of pH under the reference groundwater composition.*

calculated. The lack of phosphate measurements in the reference groundwater, thus, limits the assessment of a proper solubility limit for this element. Calculations undertaken under the saline groundwater composition where phosphate measurements have been done (Figure 6-55), show that solid phosphates may exert the solubility control leading to lower samarium concentrations.

Table 6-18 summarizes the calculated Am concentrations in equilibrium with the different solid phases able to exert the solubility control under the reference groundwater composition.

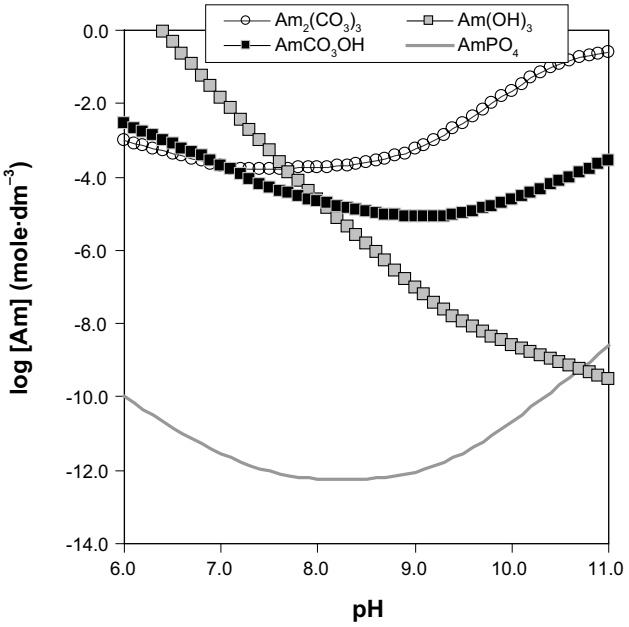

Figure 6-55. *Americium concentrations (mole/dm^3) in groundwater in equilibrium with different Am solid phases as a function of pH under the saline groundwater composition.*

Table 6-18. Am solubility-controlling phases and calculated concentration values (in mole dm^{-3}) under the different redox conditions.

	T = 15°C pe gw	$pO_2(g)$ = 0.2 atm	$pH_2(g)$ = 10^{-7} atm	$pH_2(g)$ = 10^{2} atm
[Am] **(mole·dm^{-3})**	$AmOHCO_3$ $8.7 \cdot 10^{-6}$	$AmOHCO_3$ $8.7 \cdot 10^{-6}$	$AmOHCO_3$ $8.7 \cdot 10^{-6}$	$AmOHCO_3$ $8.7 \cdot 10^{-6}$
	$Am_2(CO_3)_3$ $4.1 \cdot 10^{-6}$	$Am_2(CO_3)_3$ $4.1 \cdot 10^{-6}$	$Am_2(CO_3)_3$ $4.1 \cdot 10^{-6}$	$Am_2(CO_3)_3$ $4.1 \cdot 10^{-6}$

7 Assessment of the solubility of sulphur at the bentonite-granite interphase

As stated in section 5.1 of the main solubility report, one of the uncertainties existing in the system relates to the reversibility of the oxidation-reduction process of sulphur. The relevance of aqueous sulphide in the near field system is itsH potential capacity to enhance the corrosion of the copper canister /King et al. 2001/. Assuming that the sulphate to sulphide reduction can only proceed under the presence of sulphate reducing bacteria (SRB), it is unlikely that this process can occur in the bentonite buffer. Therefore, the source for sulphide that can potentially enter into the near field system should be the groundwater, if SRB were present in the host rock, enhancing the reduction process.

One of the minerals expected to control sulphide concentrations in natural waters is pyrite as this mineral is present in the fracture fillings of the host rock. However, in the near field, according to the Ostwald Step Rule (see section 5.1), the precipitation of a less crystalline phase will be favoured and, therefore, the precipitation of amorphous iron sulphide (FeS) would control the sulphide aqueous concentration once S(-II) species diffuse into the near field from the host rock (Figure 7-1). The thermodynamic data for the two sulphide minerals considered in this study is listed in Table 7-1.

Table 7-1. Sulphide minerals considered in the calculations.

	Reaction	Log K	Reference
Pyrite	$FeS_2 + 2H^+ + 2e^- = Fe^{2+} + 2\ HS^-$	–18.5	/Hummel et al. 2002/
FeS(am)	$FeS + H^+ = Fe^{2+} + HS^-$	–3.92	/Ball and Nordstrom 1991/

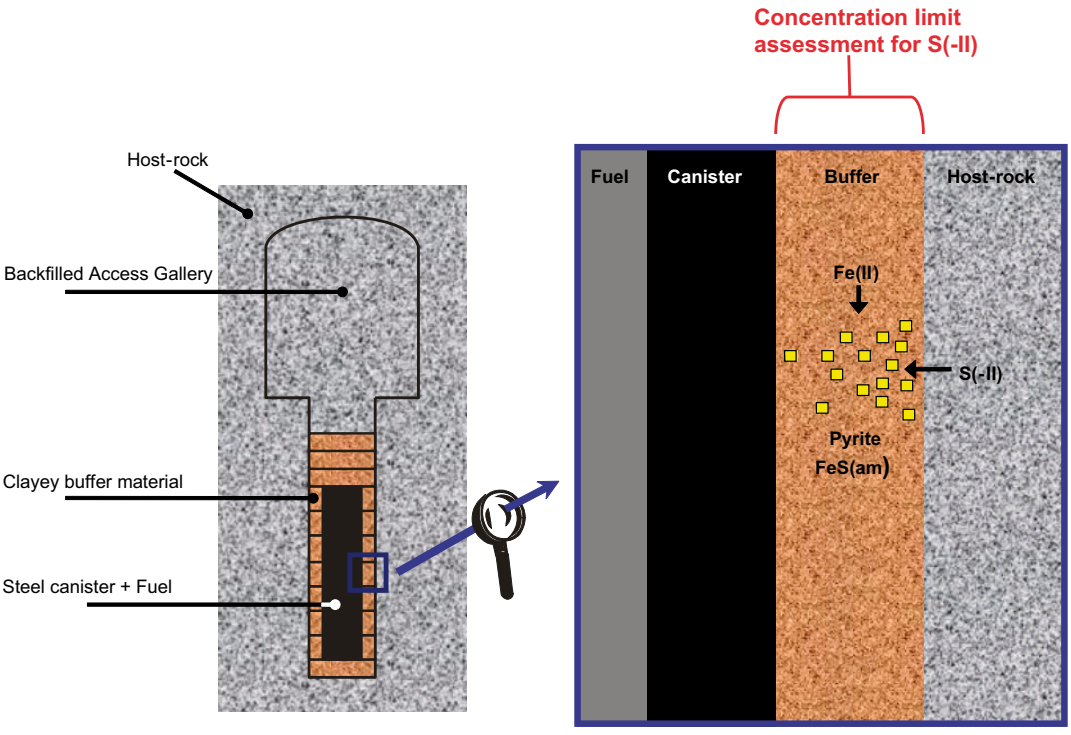

Figure 7-1. Schematic representation of the system under study for the control of S(-II) concentration in the near field.

In this section we asses the effect of considering the sulphate – sulphide equilibrium due to the presence of SRB in the system and calculate the concentration limits with regards to sulphide.

First of all, it is important to assess the sulphide concentration in the different groundwaters considered in the present study (Table 3-1). To do so, we assumed the presence of SRB that can favour the S(VI) to S(-II) reduction. The predominance diagrams for sulphur species for the three groundwater types considered are presented in Figure 7-2. According to these diagrams it is clear that only in the Saline water the predominant sulphur species are S(-II), although in the Forsmark reference groundwater, the proximity to the S(VI)-S(-II) boundary indicates that significant concentrations of S(-II) species could be expected. The ice-melting water is oxidised and, therefore, the concentration of S(-II) species is negligible.

The Forsmark groundwater composition is in equilibrium with pyrite (Table 7-2) and almost in equilibrium with gypsum ($SI_{gypsum} = -0.48$). However, aqueous sulphur is dominated by S(VI) species ($6.80 \cdot 10^{-3}$ moles·dm^{-3}) with minor contribution of S(-II) species ($1.27 \cdot 10^{-11}$ moles·dm^{-3}).

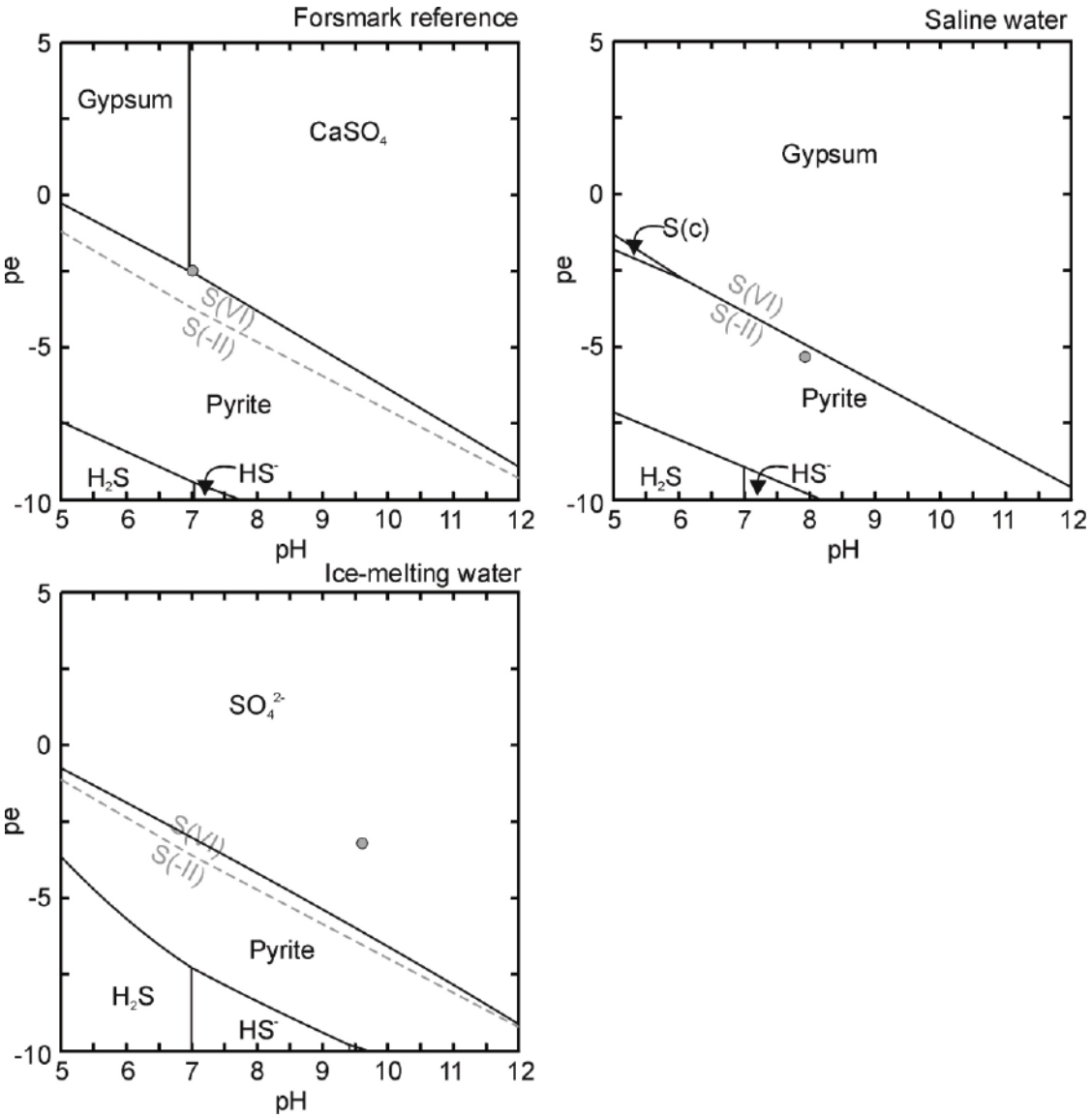

Figure 7-2. *Predominance pH-pe diagrams showing the speciation of sulphur for the different groundwater compositions considered in the present study. The S(VI)-S(-II) boundary has also been plotted to identify the predominant aqueous sulphur redox state species. Grey dots represent the pH-pe conditions of the selected groundwaters. Forsmark Reference Groundwater: $[S]_{tot} = 6.80 \cdot 10^{-3}$ moles·dm^{-3}; Saline water: $[S]_{tot} = 3.56 \cdot 10^{-2}$ moles·dm^{-3} and; Ice-melting water: $[S]_{tot} = 6.10 \cdot 10^{-5}$ moles·dm^{-3}.*

Table 7-2. Calculated concentrations of S(-II), S(VI), and Fe_{tot} and saturation indices of amorphous FeS, pyrite and calcite for the selected groundwaters and for the same groundwaters equilibrated with pyrite, and pyrite and calcite.

	(moles·dm^{-3})			Saturation indices		
	[S(–II)]	[S(VI)]	$[Fe]_{tot}$	FeS(am)	Pyrite	Calcite
Forsmark	$1.27\cdot10^{-11}$	$6.80\cdot10^{-3}$	$3.31\cdot10^{-5}$	–5.44	–0.01	–0.15
Equil. pyrite	$1.30\cdot10^{-11}$	$6.80\cdot10^{-3}$	$3.31\cdot10^{-5}$	–5.43	0.00	–0.15
Equil. pyrite + calcite	$1.20\cdot10^{-11}$	$6.80\cdot10^{-3}$	$3.31\cdot10^{-5}$	–5.29	0.00	0.00
Saline water	$3.56\cdot10^{-2}$	$1.01\cdot10^{-7}$	$7.66\cdot10^{-6}$	4.23	14.36	0.20
Equil. pyrite	$3.56\cdot10^{-2}$	$9.55\cdot10^{-8}$	$3.40\cdot10^{-20}$	–10.13	0.00	0.18
Equil. pyrite + calcite	$3.56\cdot10^{-2}$	$6.33\cdot10^{-8}$	$3.76\cdot10^{-20}$	–10.09	0.00	0.00
Ice-melting water [1)]	$3.72\cdot10^{-29}$	$6.10\cdot10^{-5}$	$2.74\cdot10^{-9}$	–24.04	–35.06	0.18
Equil. pyrite	$2.94\cdot10^{-9}$	$6.10\cdot10^{-5}$	$4.70\cdot10^{-9}$	–3.90	0.00	0.18
Equil. pyrite + calcite	$2.72\cdot10^{-9}$	$6.10\cdot10^{-5}$	$4.58\cdot10^{-9}$	–3.97	0.00	0.00

[1)] In this case the concentration of S(IV) species is higher than the S(-II) species [S(IV)] = $1.03\cdot10^{-20}$ moles·dm^{-3}.

The case of saline water is very different (Table 7-2) as the concentration of sulphur is dominated by S(-II) species ($3.56\cdot10^{-2}$ moles·dm^{-3}), with minor contribution of S(VI) species ($1.01\cdot10^{-7}$ moles·dm^{-3}). In this case it seems that the redox of the system is controlled by the C(IV)/C(-IV) pair, as the pH-pe conditions of this water plot on this boundary (Figure 7-3). This water composition is oversaturated with respect to the two sulphide minerals considered (pyrite and amorphous FeS with saturation indices of 14.36 and 4.23, respectively). However, the proximity of the pH-pe conditions of this water to the pyrite-gypsum boundary could indicate that this water is in equilibrium with these minerals. Therefore, assuming the equilibrium with pyrite does not modify significantly the concentration of both S(-II) and S(VI) aqueous species (Table 7-2), but an important decrease in Fe concentration is predicted.

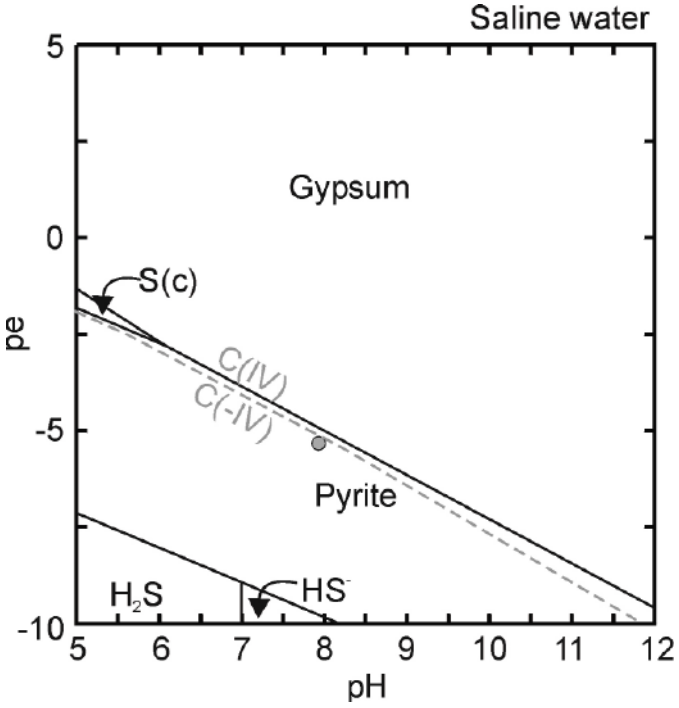

Figure 7-3. *Predominance pH-pe diagram showing the speciation of sulphur for the saline water composition. The C(IV)-C(-IV) boundary has also been plotted to identify the predominant aqueous carbon redox state species. Grey dot represents the pH-pe conditions of the saline water.*

Finally, the ice-melting water composition is far from the equilibrium with sulphide minerals, being aqueous sulphur dominated by S(VI) species (Table 7-2). However, by forcing the equilibration with pyrite, although S(VI) species still predominate over the S(-II) species, an increase the concentration S(-II) species is predicted ($2.94 \cdot 10^{-9}$ moles·dm^{-3}), which is accompanied by a decrease in the redox potential of the system to pe = –5.9.

According to Table 7-2, the maximum S(-II) concentration corresponds to the case of considering saline water, where S(-II) are the predominant aqueous sulphur species ($3.56 \cdot 10^{-2}$ moles·dm^{-3}), whereas for the other cases the S(-II) concentration is always below $2.7 \cdot 10^{-9}$ moles·dm^{-3}. Therefore, assuming that these S(-II) concentrations can enter in the bentonite buffer, we can assess the maximum concentration of aqueous sulphide that can contact the canister by assuming the possible equilibrium with amorphous FeS or even pyrite in the absence of SRB in the near field (i.e. decoupling the sulphate-sulphide reaction).

To perform these calculations we use the near field pore water from Table 3-1 and add the sulphide concentration from Table 7-2, but preventing the transformation of sulphate to sulphide and sulphide to sulphate, as bacterial activity is not expected in the near field. The results from the calculations are listed in Table 7-3. The resulting concentration when pore water with added sulphide from groundwater is equilibrated with pyrite is maintained at very low values (Figure 7-4). According to this figure, the precipitation of pyrite will result in a S(-II) concentration of $1.17 \cdot 10^{-11}$ moles·dm^{-3} (considering a total iron concentration of $3.31 \cdot 10^{-5}$ moles·dm^{-3}). The aqueous sulphide concentration increases as total iron concentration decreases, leading to a concentration of $3.84 \cdot 10^{-9}$ moles·dm^{-3} when total iron concentration is 10^{-10} moles·dm^{-3}. The pore water with added sulphide is subsaturated with respect to amorphous FeS and, therefore a very high concentration of total iron is needed to achieve saturation in this solid (> 1 mole·dm^{-3}).

The behaviour of aqueous sulphide from ice-melting groundwater previously equilibrated with pyrite follows a similar pattern. When assuming equilibration with pyrite, the concentration of aqueous S(-II) slightly decreases to $1.21 \cdot 10^{-10}$ moles·dm^{-3}, due to the predicted precipitation of small amounts of pyrite. The near field pore water after adding the sulphide from groundwater is always subsaturated in amorphous FeS, and therefore a large amount of iron is needed to force precipitation of this solid.

Table 7-3. Calculated concentrations of S(-II), Fe_{tot} and pe values assuming equilibrium of near field pore water (with added sulphide concentrations from Table 7-2) with pyrite or amorphous FeS.

	(moles·dm^{-3})		
	[S(-II)]	$[Fe]_{tot}$	pe
Forsmark			
Equil. pyrite	$1.17 \cdot 10^{-11}$	$3.31 \cdot 10^{-5}$	–2.46
Equil. FeS(am)	Subsaturated with respect to FeS(am)		
Saline water			
Equil. pyrite	$3.55 \cdot 10^{-2}$	$4.90 \cdot 10^{-21}$	–4.03
Equil. FeS(am)	$3.56 \cdot 10^{-2}$	$2.97 \cdot 10^{-9}$	1.64
Ice-melting water [1)]			
Equil. pyrite	$1.21 \cdot 10^{-10}$	$3.31 \cdot 10^{-5}$	–3.48
Equil. FeS(am)	Subsaturated with respect to FeS(am)		

[1)] In this case the added S(-II) concentration to the near field pore water is that from previous equilibration of ice-melting water with pyrite.

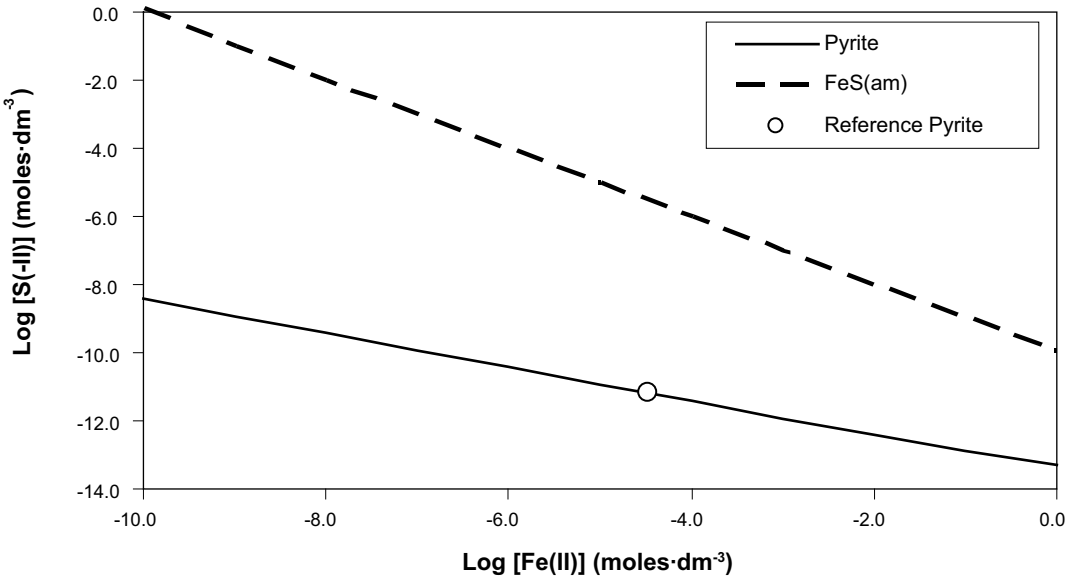

Figure 7-4. *Aqueous sulphide concentration in equilibrium with pyrite and amorphous FeS as a function of total iron concentration. The open circle represents the calculated sulphide concentration for the near field pore water in equilibrium with pyrite considering a total iron concentration of* $3.31 \cdot 10^{-5}$ *moles·dm*$^{-3}$.

Finally, the case where sulphide from saline water is added to the near field pore water results in no significant depletion of the added sulphide content, due to the high initial concentration of sulphide. Anyhow, the precipitation of either pyrite or FeS(am) lead to substantial changes in the redox state of the system and a decrease of the initial iron content. These results indicate that this is the worse case for the stability of the copper canister, as very large amounts of sulphide can reach the canister surface.

8 Recommended concentration limits

The concentration limits recommended in this chapter are based on the following assumptions:

I) The selection of the solubility limiting phases presented in the preceding sections.

II) The reference scenario is that corresponding to the intrusion of reference Forsmark groundwater in the system.

III) Radionuclides will precipitate forming individual solid phases.

IV) The rate of dissolution of radionuclides from spent fuel is fast enough as to ensure that equilibrium with individual solid phases is achieved for times shorter than the residence time of water in the system.

V) Radionuclides are released from the spent fuel independently from one each other or, at least, none of the radionuclides interferes in the geochemical behaviour of the other.

In Table 8-1, the solubility of the radionuclides calculated under the different scenarios defined in section 3.2, as well as the selected solubility controlling solid phases and the recommended concentration limits under the reference scenario are given. In some cases, the results obtained from the equilibration of the groundwater with different solid phases are presented, for the sake of completeness of the analyses.

In Appendix C, a review of the concentration limits recommended by waste management agencies in other countries is given.

In Appendix D, plots comparing the recommended concentration limits with those calculated during the SR 97 exercise and with the ranges of concentration of radionuclides measured from spent fuel dissolution experiments and in natural waters are presented.

Table 8-1. Results of the solubility calculations obtained in the present work. The first 4 columns of results in the table refer to the composition of the reference groundwater under different redox events. Columns 5 to 7 of the results indicate the concentrations calculated under the different groundwater compositions presented in section 3.2. The last column in the table presents the recommended concentration limits (RCL). For the sake of clarity, the solid phases producing the reported concentrations are indicated in each case.

[RN] ($mole \cdot dm^{-3}$)	Reference Forsmark groundwater				Variation scenarios			RCL
	pe gw	$pO_2(g)$ = 0.2 atm	$pH_2(g)$ = 10^{-7} atm	$pH_2(g)$ = 10^{2} atm	Saline	Bentonite	Ice melting	
C	$CaCO_3$	$CaCO_3$	$CaCO_3$	$CaCO_3$	$CaCO_3$	$CaCO_3$	$CaCO_3$	**$CaCO_3$**
	$7.1 \cdot 10^{-3}$	$7.1 \cdot 10^{-3}$	$7.1 \cdot 10^{-3}$	$7.1 \cdot 10^{-3}$	$1.03 \cdot 10^{-4}$	$3.99 \cdot 10^{-3}$	$3.13 \cdot 10^{-4}$	**$7.1 \cdot 10^{-3}$**
Cs	n.s.l.	n.s.l.	n.s.l.	n.s.l.	n.s.l.	n.s.l.	n.s.l.	
Sr	Celestite	Celestite	Celestite	Celestite	Celestite	Celestite	Strontianite	**Celestite**
	$6.7 \cdot 10^{-4}$	$6.7 \cdot 10^{-4}$	$6.7 \cdot 10^{-4}$	$6.9 \cdot 10^{-4}$	$2.2 \cdot 10^{-4}$	$2.3 \cdot 10^{-4}$	$1.4 \cdot 10^{-5}$	**$6.7 \cdot 10^{-4}$**
Ra	$RaSO_4$	$RaSO_4$	$RaSO_4$	$RaSO_4$	$RaSO_4$	$RaSO_4$	$RaSO_4$	**$RaSO_4$**
	$9.8 \cdot 10^{-8}$	$9.8 \cdot 10^{-8}$	$9.8 \cdot 10^{-8}$	$1.0 \cdot 10^{-7}$	$4.9 \cdot 10^{-8}$	$4.0 \cdot 10^{-8}$	$8.6 \cdot 10^{-7}$	**$9.8 \cdot 10^{-8}$**
Sn	SnO_2	SnO_2	SnO_2	SnO_2	SnO_2	SnO_2	SnO_2	**SnO_2**
	$8.6 \cdot 10^{-8}$	$8.6 \cdot 10^{-8}$	$8.6 \cdot 10^{-8}$	$1.2 \cdot 10^{-7}$	$9.0 \cdot 10^{-8}$	$8.7 \cdot 10^{-8}$	$2.7 \cdot 10^{-6}$	**$8.6 \cdot 10^{-8}$**
Se	FeSe	n.s.l.	FeSe	FeSe	FeSe	FeSe	FeSe	**FeSe**
	$1.4 \cdot 10^{-10}$		$1.4 \cdot 10^{-10}$	$1.4 \cdot 10^{-10}$	$8.8 \cdot 10^{-11}$	$1.3 \cdot 10^{-10}$	$1.2 \cdot 10^{-9}$	**$1.4 \cdot 10^{-10}$**
Zr	$Zr(OH)_4(s)$	$Zr(OH)_4(s)$	$Zr(OH)_4(s)$	$Zr(OH)_4(s)$	$Zr(OH)_4(s)$	$Zr(OH)_4(s)$	$Zr(OH)_4(s)$	**$Zr(OH)_4(s)$**
	$9.7 \cdot 10^{-9}$	$9.7 \cdot 10^{-9}$	$9.7 \cdot 10^{-9}$	$9.7 \cdot 10^{-9}$	$6.6 \cdot 10^{-9}$	$9.6 \cdot 10^{-9}$	$1.0 \cdot 10^{-8}$	**$9.7 \cdot 10^{-9}$**

[RN] (mole·dm^{-3})	Reference Forsmark groundwater				Variation scenarios			RCL
	pe gw	**$pO_2(g)$ = 0.2 atm**	**$pH_2(g)$ = 10^{-7} atm**	**$pH_2(g)$ = 10^{2} atm**	**Saline**	**Bentonite**	**Ice melting**	
Nb	Nb_2O_5	Nb_2O_5	Nb_2O_5	Nb_2O_5	Nb_2O_5	Nb_2O_5	Nb_2O_5	**Nb_2O_5**
	$2.4\cdot10^{-5}$	$2.4\cdot10^{-5}$	$2.4\cdot10^{-5}$	$2.4\ 10^{-5}$	$1.1\cdot10^{-4}$	$2.6\cdot10^{-5}$	$2.9\cdot10^{-3}$	**$2.4\cdot10^{-5}$**
Tc	$TcO_2\cdot1.6H_2O$	n.s.l.	$TcO_2\cdot1.6H_2O$	$TcO_2\cdot1.6H_2O$	$TcO_2\cdot1.6H_2O$	$TcO_2\cdot1.6H_2O$	$TcO_2\cdot1.6H_2O$	**$TcO_2\cdot1.6H_2O$**
	$4.4\cdot10^{-9}$		$4.4\cdot10^{-9}$	$4.4\cdot10^{-9}$	$4.1\cdot10^{-9}$	$4.4\cdot10^{-9}$	$4.5\cdot10^{-9}$	**$4.4\cdot10^{-9}$**
Ni	$NiCO_3$	$NiCO_3$	$NiCO_3$	$NiCO_3$	$NiCO_3$	$NiCO_3$	$NiCO_3$	**$NiCO_3$**
	$5.5\cdot10^{-5}$	$5.5\cdot10^{-5}$	$5.5\cdot10^{-5}$	$5.5\cdot10^{-5}$	$5.0\cdot10^{-4}$	$3.8\cdot10^{-5}$	$6.1\cdot10^{-7}$	**$5.5\cdot10^{-5}$**
					$Ni(OH)_2$	$Ni(OH)_2$	$Ni(OH)_2$	
					$2.1\cdot10^{-4}$	$3.4\cdot10^{-3}$	$4.4\cdot10^{-8}$	
Pd	$Pd(OH)_2$	$Pd(OH)_2$	$Pd(OH)_2$	$Pd(OH)_2$	$Pd(OH)_2$	$Pd(OH)_2$	$Pd(OH)_2$	**$Pd(OH)_2$**
	$2.9\cdot10^{-6}$	$2.9\cdot10^{-6}$	$2.9\cdot10^{-6}$	$2.9\cdot10^{-6}$	$5.7\cdot10^{-6}$	$2.8\cdot10^{-6}$	$2.7\cdot10^{-6}$	**$2.9\cdot10^{-6}$**
Ag	AgCl	AgCl	AgCl	AgCl	AgCl	AgCl	AgCl	**AgCl**
	$4.4\cdot10^{-6}$	$4.4\cdot10^{-6}$	$4.4\cdot10^{-6}$	$4.4\cdot10^{-6}$	$5.1\cdot10^{-5}$	$4.5\ 10^{-6}$	$6.9\cdot10^{-7}$	**$4.4\cdot10^{-6}$**
Sm	$SmOHCO_3$	$SmOHCO_3$	$SmOHCO_3$	$SmOHCO_3$	$SmOHCO_3$	$SmOHCO_3$	$SmOHCO_3$	**$Sm_2(CO_3)_3$**
	$1.1\cdot10^{-7}$	$1.1\cdot10^{-7}$	$1.1\cdot10^{-7}$	$1.1\ 10^{-7}$	$7.2\cdot10^{-8}$	$9.0\cdot10^{-8}$	$2.2\cdot10^{-9}$	**$4.4\cdot10^{-7}$**
	$Sm_2(CO_3)_3$	$Sm_2(CO_3)_3$	$Sm_2(CO_3)_3$	$Sm_2(CO_3)_3$	$Sm_2(CO_3)_3$	$Sm_2(CO_3)_3$	$Sm_2(CO_3)_3$	
	$4.4\cdot10^{-7}$	$4.4\cdot10^{-7}$	$4.4\cdot10^{-7}$	$4.4\cdot10^{-7}$	$4.1\cdot10^{-6}$	$3.6\cdot10^{-7}$	$3.0\cdot10^{-7}$	
Ho	$Ho_2(CO_3)_3$	$Ho_2(CO_3)_3$	$Ho_2(CO_3)_3$	$Ho_2(CO_3)_3$	$Ho_2(CO_3)_3$	$Ho_2(CO_3)_3$	$Ho_2(CO_3)_3$	**$Ho_2(CO_3)_3$**
	$1.2\cdot10^{-6}$	$1.2\cdot10^{-6}$	$3.0\cdot10^{-6}$	$3.1\cdot10^{-6}$	$2.6\cdot10^{-5}$	$9.9\cdot10^{-7}$	$2.2\cdot10^{-6}$	**$1.2\cdot10^{-6}$**
Th	$ThO_2\cdot2H_2O$	$ThO_2\cdot2H_2O$	$ThO_2\cdot2H_2O$	$ThO_2\cdot2H_2O$	$ThO_2\cdot2H_2O$	$ThO_2\cdot2H_2O$	$ThO_2\cdot2H_2O$	**$ThO_2\cdot2H_2O$**
	$7.9\cdot10^{-7}$	$7.9\cdot10^{-7}$	$7.9\cdot10^{-7}$	$7.9\cdot10^{-7}$	$2.3\cdot10^{-8}$	$1.0\cdot10^{-6}$	$2.1\cdot10^{-7}$	**$7.9\cdot10^{-7}$**
Pa	Pa_2O_5	Pa_2O_5	Pa_2O_5	Pa_2O_5	Pa_2O_5	Pa_2O_5	Pa_2O_5	**Pa_2O_5**
	$3.0\cdot10^{-7}$	$3.0\cdot10^{-7}$	$3.0\cdot10^{-7}$	$3.0\cdot10^{-7}$	$2.0\cdot10^{-7}$	$3.0\cdot10^{-7}$	$3.2\cdot10^{-7}$	**$3.0\cdot10^{-7}$**
U	$UO_2\cdot2H_2O$	Uranophane	$UO_{2.67}$	$UO_2\cdot2H_2O$	$UO_2\cdot2H_2O$	$UO_2\cdot2H_2O$	$UO_2\cdot2H_2O$	**$UO_2\cdot2H_2O$**
	$9.5\cdot10^{-9}$	$1.7\cdot10^{-6}$	$3.4\cdot10^{-8}$	$6.8\cdot10^{-10}$	$4.5\cdot10^{-10}$	$1.0\cdot10^{-7}$	$5.3\cdot10^{-6}$	**$9.5\cdot10^{-9}$**
	Uranophane	Becquerelite (nat)	$UO_2\cdot2H_2O$	$UO_{2.34}$	Uranophane	Uranophane	Uranophane	
	$1.9\cdot10^{-6}$	$2.5\cdot10^{-6}$	$7.9\cdot10^{-10}$	$1.5\cdot10^{-9}$	$2.1\cdot10^{-5}$	$1.4\cdot10^{-5}$	$1.2\cdot10^{-8}$	
	Becquerelite (nat)			$UO_{2.25}$	Becquerelite (nat)	Becquerelite (nat)	Becquerelite (nat)	
	$3.0\cdot10^{-6}$			$3.0\cdot10^{-11}$	$4.6\cdot10^{-4}$	$7.7\cdot10^{-6}$	$2.4\cdot10^{-7}$	
Np	$NpO_2\cdot2H_2O$	Np_2O_5	$NpO_2\cdot2H_2O$	$NpO_2\cdot2H_2O$	$NpO_2\cdot2H_2O$	$NpO_2\cdot2H_2O$	$NpO_2\cdot2H_2O$	**$NpO_2\cdot2H_2O$**
	$1.0\cdot10^{-9}$	$1.7\cdot10^{-5}$	$1.0\cdot10^{-9}$	$1.0\cdot10^{-9}$	$5.1\cdot10^{-10}$	$1.1\cdot10^{-9}$	$8.3\cdot10^{-10}$	**$1.0\cdot10^{-9}$**
Pu	$Pu(OH)_4$(s)	$PuO_2(OH)^{2}\cdot H_2O$	$Pu(OH)_4$(s)	$PuOHCO_3$	$Pu(OH)_4$ (s)	$Pu(OH)_4$ (s)	$Pu(OH)_4$ (s)	**$Pu(OH)_4$(s)**
	$1.3\cdot10^{-7}$	$1.3\cdot10^{-5}$	$1.6\cdot10^{-6}$	$1.2\cdot10^{-5}$	$2.7\cdot10^{-8}$	$7.4\cdot10^{-8}$	$1.3\cdot10^{-10}$	**$1.3\cdot10^{-7}$**
	$PuOHCO_3$	PuO_2CO_3	$PuOHCO_3$		$PuOHCO_3$	$PuOHCO_3$	$PuOHCO_3$	
	$1.2\cdot10^{-5}$	$1.0\cdot10^{-5}$	$1.2\cdot10^{-5}$		$4.7\cdot10^{-6}$	$1.3\cdot10^{-5}$	$5.9\cdot10^{-4}$	
	$Pu(OH)_3$(cr)	$Pu(OH)_4$(s)			$Pu(OH)_3$ (cr)		$Pu(OH)_3$ (cr)	
	$1.9\cdot10^{-4}$	$2.2\cdot10^{-4}$			$3.8\cdot10^{-7}$		$8.2\cdot10^{-6}$	
Am/Cm	$AmOHCO_3$	$AmOHCO_3$	$AmOHCO_3$	$AmOHCO_3$	$AmOHCO_3$	$AmOHCO_3$	$AmOHCO_3$	**$AmOHCO_3$**
	$8.7\cdot10^{-6}$	$8.7\cdot10^{-6}$	$8.7\cdot10^{-6}$	$8.7\cdot10^{-6}$	$9.1\cdot10^{-6}$	$4.1\cdot10^{-6}$	$1.1\cdot10^{-7}$	**$8.7\cdot10^{-6}$**
	$Am_2(CO_3)_3$	$Am_2(CO_3)_3$	$Am_2(CO_3)_3$	$Am_2(CO_3)_3$	$Am_2(CO_3)_3$	$Am_2(CO_3)_3$	$Am_2(CO_3)_3$	
	$4.1\cdot10^{-6}$	$4.1\cdot10^{-6}$	$4.1\cdot10^{-6}$	$4.1\cdot10^{-6}$	$3.7\cdot10^{-5}$	$1.9\cdot10^{-6}$	$1.7\cdot10^{-6}$	
					$Am(CO_3)_2Na\cdot5H_2O$	$Am(CO_3)_2Na\cdot5H_2O$	$Am(CO_3)_2Na\cdot5H_2O$	
					$2.7\cdot10^{-5}$	$1.0\cdot10^{-6}$	$1.7\cdot10^{-5}$	

9 References

Aksoyoglu S, Bajo C, Mantovani M, 1990. Grimsel Test Site: Batch sorption experiments with iodine, bromine, strontium, sodium and caesium on Grimsel mylonite. Nagra Technical report NTB 91-06, Nagra, Wettingen, Switzerland.

Alaux-Negrel G, Beaucaire C, Michard G, Toulhoat P, Ouzounian G, 1993. Trace metal behaviour in natural granitic waters. Journal of Contaminant Hydrology 13, 309–325.

Altmaier M, Neck V, Müller R, Fanghänel Th, 2005. Solubility of $ThO_2 \cdot xH_2O$ in carbonate solution and the formation of ternary Th(IV) hydroxide-carbonate complexes, Radiochimica Acta, 93, 83–92.

Anton M P, Gasco C, Sanchezcabeza J A, Pujol L, 1994. Geochemical association of plutonium in marine sediments from Palomares (Spain). Radiochimica Acta 66:7, 443–446.

Arcos D, Domènech C, Grandia F, 2005. Reactive transport models for deep radioactive waste disposal. Geochim. Cosmochim. Acta, 69-10 supplement 1, Toxic and Radioactive Waste Disposal. Goldschmidt Conference Abstracts 2005. p. A416.

Arcos D, Grandia F, Domènech C, 2006. Geochemical evolution of the near field of a KBS-3 repository. SKB TR-06-16, Svensk Kärnbränslehantering AB.

Baes C F, Mesmer R E, 1976. The Hydrolysis of Cations. New York. John Wiley and Sons.

Bajo C, Hoehn E, Keil R, Bayens B, 1989. Chemical characterisation of the groundwater from fault zone AU 96m. In Grimsel Test Site-Laboratory Investigations in support of the migration experiment; in Bradbury ed.; Nagra Technical Report NTB 88–23; Nagra, Wettingen, Switzerland.

Ball J W, Nordstrom D K, 1991. User's manual for WATEQ4F, with revised thermodynamic data base and test cases for calculating speciation of major, trace, and redox elements in natural waters. U.S. Geological Survey Open-File Report 91-183, Denver, Colorado.

Berner U, 2002. Project Opalinus Clay: radionuclide concentration limits in the near-field of a repository for spent fuel and vitrified high-level waste. NAGRA-TR-02-10.

Bethke C M, 2000. The Geochemist's Workbench 3.1: A User's Guide to Rxn, Act2, Tact, React, and Gtplot. University of Illinois.

Bockris J O M, Ed. 1977. Environmental Chemistry. New York, Plenum Press.

Bond K A, Heath T G, Tweed C J, 1997. HATCHES: A Referenced Thermodynamic Database for Chemical Equilibrium Studies. Nirex Report NSS/R379.

Brookins D G, 1988. Eh-pH Diagrams for geochemists. New York. Springer-Verlag Pubs.

Brookins D G, 1989. Aqueous Geochemistry of Rare Earth Elements. in Geochemistry and Mineralogy of Rare Earth Elements (B R Lipin and G A McKay, Eds.). Blacksburg. Mineralogical Society of America. Reviews in Mineralogy. Vol. 21.

Brown P L, Haworth A, Sharlan S M, Tweed C J, 1991. HARPHRQ: A geochemical speciation program based on PHREEQE. Nirex Safety Studies Report NSS R.188.

Bruno J, Forsyth R S, Werme LO, 1985. Spent UO_2-fuel dissolution. Tentative modelling of experimental apparent solubilities. Mater. Res. Soc. Symp. Proceedings MRS Vol. 44, 413–420.

Bruno J, Cross J E, Eikenberg J, McKinley I G, Read D, Sandino A, Sellin P, 1992. Testing models of trace element geochemistry at Poços de Caldas. Journal of Geochemical Exploration 45, 451–470.

Bruno J, Casas I, 1994. Spent fuel dissolution modelling. In Final Report of SKB/AECL Cigar Lake Analog Study (J J Cramer and J A T Smellie, Eds.). SKB-(AECL) TR-94-04, Svensk Kärnbränslehantering AB. (10851).

Bruno J, Duro L, 1996. Extending the RDC model to the minor components of the spent fuel matrix. Modelling of apparent Pu solubilities from Studsvik leaching experiments. QuantiSci Internal Report.

Bruno J, Cera E, de Pablo J, Duro L, Jordana S, Savage D, 1997. Determination of radionuclide solubility limits to be used in SR 97. Uncertainties associated to calculated solubilities. SKB TR-97-33, Svensk Kärnbränslehantering AB.

Bruno J, Arcos D, Duro L, 1999. Processes and features affecting the near fiel hydrochemistry Groundwater-bentonite interaction QuantiSci Internal Report. SKB TR-99-29, Svensk Kärnbränslehantering AB.

Bruno J, Cera E, Eklund U-B, Eriksen T E, Grivé M, 1999a. Experimental determination and chemical modelling of radiolytic processes at the spent fuel/water interface. SKB TR-99-26, Svensk Kärnbränslehantering AB.

Bruno J, Cera E, Duro L, Grivé M, Sellin P, 2000. Determination and uncertainties of solubility limits to be used by SKB in the SR 97 performance assessment. Radiochimica Acta 88, 823–828.

Bruno J, Duro L, Grivé M, 2002. The applicability and limitations of thermodynamic geochemical models to simulate trace element behaviour in natural waters. Lessons learned from natural analogue studies. Chem. Geol. 190, 371–393.

Bruno J, Cera E, Grivé M, Duro L, Eriksen T E, 2003a. Experimental determination and chemical modelling of radiolytic processes at the spent fuel/water interface. Experiments carried out in carbonate solutions in absence and presence of chloride. SKB TR-03-03, Svensk Kärnbränslehantering AB.

Byrd J T, Andreae M O, 1986. Geochemistry of tin in rivers and estuaries. Geochimica et Cosmochimica Acta 50: 835–845.

Caballero E, Reyes E, Huertas F, Yáñez J, Linares J, 1986. Elementos traza en las bentonitas de Almeria. Boletin Sociedad Española de Mineralogía 9, 63–70.

Choppin G R, Stout B E, 1989. Actinide behaviour in natural waters. The Science of the Total Environment 83, 203–216.

Copenhaver S A, Krishnaswami S L, Turekian K K, Epler N, Cochran J K, 1993. Retardation of ^{238}U and ^{232}Th decay chain radionuclides in Long Island and Connecticut aquifers. Geochimica et Cosmochimica Acta 57, 597–603.

Cramer J, Vilks P, Miller H, Bachinski D, 1994. Hydrogeochemistry: Water sampling and analysis. in Final Report of SKB/AECL Cigar Lake Analog Study (J.J. Cramer and J.A.T. Smellie, Eds.). SKB-(AECL) TR 94-04, Svensk Kärnbränslehantering AB. (10851).

Curti E, Wersin P, 2002. Assessment of porewater chemistry in the bentonite backfill for the Swiss SF/HLW repository. NAGRA-TR-02-09.

Cutter G A, 1989. Freshwater systems. in Occurrence and Distribution of Selenium (M. Ihnat, Ed.). CRC Press, Boca Raton, 99, 243–262.

Decarreau B L, 1985. Partitioning of divalent transition elements between octahedral sheets of trioctahedral smectites and water. Geochimica et Cosmochimica Acta 49, 1537–1544

Dickson B L, 1985. Radium isotopes in saline seepages, southwestern Yilgarn, Western Australia. Geochimica et Cosmochimica Acta 49, 349–360.

Doerner H A, Hoskins W M, 1925. Co-precipitation of radium and barium sulphates. Journal of the American Chemical Society 47, 662–675.

Doyle G A, Lyons W B, Miller G C, Donaldson S G, 1995. Oxyanion Concentrations in Eastern Sierra Nevada Rivers. 1. Selenium. Applied Geochemistry 10:5, 553–564.

Duro L, Grivé M, Cera E, Domènech C, Bruno J, 2005. Update of a thermodynamic database for radionuclides to assist solubility limits calculation for PA. Enviros Report, 2005.

Edmunds W M, Cook R L F, Miles D L, Cook J M, 1987. The origin of saline groundwaters in the Carnmenellis granite (U.K.): further evidence from minor and trace elements. in Saline Water and Gases in Crystalline Rocks (P. Fritz and S.K. Frape, Eds.). Geological Association of Canada Special Paper 33, pp 127–143.

Edmunds W M, Cook J M, Kinniburg D G, Miles D G, Trafford J M, 1989. Trace-element occurrence in British groundwaters. British Geological Survey. Research Report SD/89/3. Nottingham.

Eikenberg J, Bayens B, Bradbury M H, 1991. The Grimsel Migration Experiment: A Hydrogeochemical Equilibration Test. Nagra Technical Report NTB 90-39. Nagra, Wettingen, Switzerland.

Elderfield H, Greaves M J, 1989. The rare earth elements in seawater. Nature 296:5854, 214–219.

Elderfield H, Upstill-Goddard R, Sholkovitz E R, 1990. The rare earth elements in rivers, estuaries, and coastal seas and their significance to the composition of ocean waters. Geochimica et Cosmochimica Acta 54, 971–991.

Elkin E M, 1982. Selenium and selenium compounds. In Encyclopaedia of Chemical Technology Volume 20, John Wiley & Sons, New York.

ENRESA, 1997. Evaluación del comportamiento y de la seguridad de un almacenamiento geológico profundo en granito. Publicación Técnica 06/97.

ENRESA, 1999. Evaluación del comportamiento y de la seguridad de un almacenamiento profundo en arcilla. Publicación Técnica 03/99.

EUR, 1996. First performance assessment of the disposal of spent fuel in a clay layer. European Comission. EUR 16752.

Fabryka-Martin J, Curtis D B, Dixon P, Rokop D, Roensch F, Aguilar R, Attrep M, 1994. Nuclear reaction product geochemistry: Natural nuclear products in the Cigar Lake deposit. in Final Report of SKB/AECL Cigar Lake Analog Study (J J Cramer and J A T Smellie, Eds.). SKB-(AECL) TR 94-04, Svensk Kärnbränslehantering AB. (10851).

Falck W E, Read D, Thomas J B, 1996. Chemval 2: Thermodynamic database. EUR 16897 EN.

Felmy A R, Rai D, Schramke J A, Ryan J L, 1989. The solubility of plutoniumhydroxide in dilute solution and in high-ionic-strength chloride brines. Radiochimica Acta, 48, 29–35.

Finch R J, Suksi J, Rasilainen K, Ewing R C, 1995. The long-term stability of becquerelite. Mater. Res. Soc. Symp. Proceed. Vol. 353 Part1,647–652.

Forsyth R, 1997. The SKB spent fuel corrosion programme. An evaluation of results from the experimental programme performed in the Studsvik Hot Cell Laboratory, Stockholm, Sweden. SKB TR-97-25, Svensk Kärnbränslehantering AB.

Friese J I, Buck E C, McNamara B K, Hanson B D, Marschman S C, 2003. Exixting Evidence for the Fate of Neptunium in the Yucca Mountain Repository. Pacific Northwest National Laboratory report, PNNL-14307, June 2003.

Fukai R, Yokoyama Y, 1982. Natural Radionuclides in the Environment. in The Hanbook of Environmental Chemistry. The Natural Environment and the Biogeo-chemical Cycles (O. Hutzinger, Ed.). Springer-Verlag Berlin Heidelberg. Vol. 1.

Gascoyne M, 1988. Reference groundwater composition for a depth of 500 m in the Whiteshell Research Area – comparison with synthetic groundwater WN-1. Atomic Energy of Canada Limited Technical record, TR-463.

Gauthier-Lafaye F, 1995. Oklo, Analogues naturels. Rapport final: Volume 2: Les Réacteurs de Fission et les Systèmes Géochimiques. 2ème partie: Géologie des réacteurs, études des épontes et des transferts anciens. Institut de Protection et de Sureté Nucléaire. Oklo-Rapport final 2-2. Strasbourg.

Giffaut E, Bourbon X, Michau N, Schumacher S, 2000. Barrières Ouvragées argileuses et cimentaires. Représentations phénoménologiques associées au comportement des radioéléments. Fournitures des données de base en vue des calculs de sûreté. C NT AMAT 00.070.

Gimeno M J, 1999. Estudios del comportamiento geoquímico de las tierras raras en un sistema natural de aguas ácidas (Arroyo del Val-Bádenas). Tesis. Universidad de Zaragoza.

Golightly J P, 1981. Nickeliferous laterite deposits. Economic Geology 75th Anniversary Volume. 710–735.

Gómez P, Turrero M J, Martínez B, Melón A, Gimeno M J, Peña J, Mingarro M, Rodríguez V, Gordienko F, Hernández A, Crespo M T, Ivanovich M, Reyes E, Caballero E, Plata A, Fernández J M, 1995. Hydrogeochemical study of El Berrocal site. CIEMAT. Task Group Report 4 EB-CIEMAT (95) 35. Madrid.

Gosselin D C, Smith M R, Lepel E A, Laul J C, 1992. Rare earth elements in chloride-rich groundwater, Palo Duro Basin, Texas, USA. Geochimica et Cosmochimica Acta 56, 1495–1505.

Grambow B, Loida A, Dressler P, Geckeis H, Gago J, Casas I, de Pablo J, Giménez J, Torrero M E, 1996. Long Term Safety of Radioactive Waste Disposal: Chemical Reaction of Fabricated and High Burnup Spent UO_2 Fuel with Saline Brines. Final Report FZK 5702 pp 174.

Grambow B, Loida A, Martínez-Esparza A, Díaz-Arocas P, de Pablo J, Paul J-L, Marx G, Glatz J-P, Lemmens K, Ollila K, Christensen H, 2000. Source term for performance assessment of spent fuel as a waste form. Final report, EUR 19140.

Grauch R I, 1989. Rare Earth Elements in Metamorphic Rocks. in Geochemistry and Mineralogy of Rare Earth Elements (B R. Lipin and G A. McKay, Eds.). Blacksburg. Mineralogical Society of America. Reviews in Mineralogy. Vol. 21.

Gray W J, 1988. Salt Repository Project. Effect of surface oxidation α-radiolysis and salt brine composition on the spent fuel and UO_2 leaching performance. PNL/SRP-6689UC-70.

Grenthe I, 1991. Thermodynamics in migration chemistry. Radiochim. Acta, 52/53, pp. 425–432

Grenthe I, Fuger J, Konings, R J M, Lemire R J, Muller A B, Nguyen-Trung C, Wanner H, 1992. Chemical Thermodynamics 1; Chemical Thermodynamics of Uranium (Wanner H. and Forest I. eds.). NEA OECD, Elsevier.

Guillaumont R, Fanghänel J, Neck V, Fuger J, Palmer D A, Grenthe I, Rand M H, 2003. Chemical Thermodynamics 5. Update on the Chemical Thermodynamics of Uranium, Neptunium, Plutonium, Americium and Technetium. NEA OECD, Elsevier.

Guillaumont R, Fanghänel T, Neck V, Fuger J, Palmer D A, Grenthe I, Rand M H, 2003. Update on chemical thermodynamics of Uranium, Neptunium, Plutonium, Americium and Technetium. Chemical Thermodynamics 5. ISBN: 0-444-51401-5. 919 p.

Heath T G, Pilkington C J, Tweed C J, Williams S J, 1998. Radionuclide solubility at high pH. AEA Technology plc, Harwell, Didcot, Oxon, OX11 ORA, UK. NIREX SCIENCE REPORT S/98/008.

Helgeson H C, Kirkham D H, Flowers G C, 1981. Amer. Jour. Sci. 281 1249–1516.

Howard J H, 1977. Geochemistry of selenium: formation of ferroselite and selenium behaviour in the vicinity of oxidising sulphide and uranium deposits. Geochimica et Cosmochimica Acta 41, 1665–1678.

Hummel W, Berner U, Curti E, Pearson F J, Thoenen T, 2002. Nagra/PSI Chemical Thermodynamic Data Base 01/01. ISBN: 1-58112-620-4. 565 p.

Humphris S E, Thompson G, 1978. Trace element mobility during hydrothermal alteration of oceanic basalts. Geochimica et Cosmochimica Acta 42, 127–136.

Hunt G J, Bailly du Bois P, Kershaw P J, Masson M, 2002. Has 99Tc from Shellafield entered the English Channel? In: Proceedings from the International Conference on radioactivity in the environment. 1–5 September 2002 in Monaco.

Ikeda N, 1955. Determination of minute quantities of tin in hot spring waters. Nippon Kagaku Zassi 76, 1011.

JNC, 2000. Second Progress Report on Research and Development for the Geological Disposal of HLW in Japan. H12: Project to Establish the Scientific and Technical Basis for HLW Disposal in Japan. JNC TN1410 2000-001 (plus three Supporting Reports). Available also in the Internet: http://www.jnc.go.jp/kaihatu/tisou/zh12/h12/index.html.

Johnson L H, LeNeveu D M, Shoesmith D W, Oscarson D W, Gray M N, Lemire R J, Garisto N C, 1994. The disposal of Canada's Nuclear Fuel Waste: The vault model fro Postclosure Assesment. AECL-10714, COG-93-4.

Johnson L H, Tait J C, 1997. Release of segregated nuclides from spent fuel. SKB TR-97-18, Svensk Kärnbränslehantering AB.

King F, Ahonen L, Taxén C, Vuorinen U, Werme L, 2001. Copper corrosion under expected conditions in a deep geologic repository. SKB TR-01-23, Svensk Kärnbränslehantering AB.

Kraemer T F, Reid D F, 1984. The occurrence and behaviour of radium in saline formation water of the U.S. Gulf Coast region. Isotope Geoscience 2, 153–174.

Kraemer T F, Kharaka Y K, 1986. Uranium geochemistry in geopressures-geothermal aquifers of the U.S. Gulf Coast. Geochimica et Cosmochimica Acta 50, 1,233–1,238.

Krauskopf K B, 1967. Introduction to Geochemistry. McGraw-Hill, New York.

Krishnaswami S, Graustein W C, Turekian K K, 1982. Radium, thorium and radioactive lead isotopes in groundwaters: applications to the in situ determination of absorption-desorption rate constants and retardation factors. Water Resources Research 18, 1633–1675.

Kudo K, Komatsu K, 1999. Reduction of alkali metal carbonate to methane with water in the presence of Raney alloy. Journal of Molecular Catalysis A: chemical, 145, 159–167.

Laaksoharju M, Gustafson G, Pedersen K, Rhén I, Skårman C, Tullborg E-L, Wallin B, Wikberg, P, 1995. Sulphate reduction in the Äspö HRL tunnel, SKB TR-95-25, Svensk Kärnbränslehantering AB.

Langmuir D, Herman J S, 1980. The mobility of thorium in natural waters at low temperatures. Geochimica et Cosmochimica Acta 44, 1753–1766.

Langmuir D, Melchior D, 1985. The geochemistry of Ca, Sr, Ba and Ra sulfates in some deep brines from the Palo Duro Basin, Texas. Geochimica et Cosmochimica Acta 49, 2423–2432.

Langmuir D, Riese A C, 1985. The thermodynamic properties of radium. Geochimica et Cosmochimica Acta 49, 673–680.

Laul J C, Smith M R, Hubbard N, 1985. Behaviour of natural uranium, thorium and radium isotopes in the Wolfcamp brine aquifers, Palo Duro Basin, Texas. Mater. Res. Soc. Symp. Proceedings MRS Vol. 44, 475–482.

Lemire R J, 1984. An assessment of the thermodynamic behaviour of Neptunium in water and model groundwaters from 25 to 150°C. Atomic Energy of Canada Limited, AECL-7817

Lemire R J, Garisto F, 1989. The solubility of U, Np, Pu, Th and Tc in a geological disposal vault for used nuclear fuel. AECL-10009.

Lemire R J, Fuger J, Nitsche H, Potter P, Rand M H, Rydberg J, Spahiu K, Sullivan J C, Ullman W J, Vitorge P, Wanner H, 2001. Chemical Thermodynamics 4. Chemical thermodynamics of neptunium and plutonium. NEA OECD, Elsevier.

Leonard K S, McCubbin D, Brown J, Bonfeld R, Brooks T, 1997. Distribution of technetium-99 in UK Coastal Waters. Mar. Poll. Bull. 34, 8, pp. 628–636.

Lin S, Popp R K, 1984. Solubility and complexing of Ni in the system NiO-H_2O-HCl. Geochimica et Cosmochimica Acta 48, 2713–2722.

Linklater CM, Albinsson Y, Alexander W R, Casas I, McKinley I G, Sellin P, 1994. A Natural Analogue of High pH Cement Pore Waters from the Maqarin Area of Northern Jordan. Comparison of Predicted and Observed Trace Element Chemistry of Uranium and Selenium. Fourt International Conference on the Chemistry and Migration Behaviour of Actinides and Fission Products in the Geosphere, Charleston, SC USA; December 12–17, 1993, p. 639–644. Oldenbourg Verlag, München 1994.

Lloyd J W, Heathcote J A, 1985. Natural inorganic hydrochemistry in relation to groundwater. An Introduction. Oxford. Oxford University Press.

Loida A, Grambow B, Geckeis H, 1996. Anoxic corrosion of various high burnup spent fuel samples. Journal of Nuclear Materials, 238, 11–22.

Lothenbach B, Ochs M, Hager D, 2000. Thermodynamic data for the solubility of tin (IV) aqueous cementitious environments. Radiochim. Actam 88, 521–526.

MacKenzie A B, Scott R D, Linsalata P, Miekeley N, Osmond J K, Curtis D B, 1991. Natural radionuclide and stable element studies of rock samples from the Osamu Utsumi mine and Morro do Ferro analogue study sizes, Poços de Caldas, Brazil. SKB. Poços de Caldas Report 7.

Mazor E, 1962. Radon and radium content of some Israeli water sources and a hypothesis on underground reservoirs of brines, oils and gases in the Rift valley. Geochimica et Cosmochimica Acta 26, 706–786.

McKelvey B A, Orians K J, 1993. Dissolved zirconium in the North Pacific Ocean. Geochimica et Cosmochimica Acta 57, 3801–3805.

McKibben M A, Williams A E, Hall G E M, 1990. Solubility and transport of platinum-group elements and Au in saline hydrothermal fluids: constraints from geothermal brine data. Economic Geology 85, 1926–1934.

McKinley I G, Bath A H, Berner U, Cave M, Neil C, 1988. Results of the Oman analogue study. Radiochimica Acta 44/45, 311–316.

McLennan S M, 1989. Rare Earth Elements in Sedimentary Rocks: Influence of Provenance and Sedimentary Processes. in Geochemistry and Mineralogy of Rare Earth Elements (B R. Lipin and G A. McKay, Eds.). Blacksburg. Mineralogical Society of America. Reviews in Mineralogy. Vol. 21.

Michard A, Beaucaire C, Michard G, 1987. Uranium and rare-earth elements in CO_2-rich waters from Vals-les-Bains (France). Geochimica et Cosmochimica Acta 51, 901–909.

Michard A, 1989. Rare earth element systematics in hydrothermal fluids. Geochimica et Cosmochimica Acta 53, 745–750.

Michel J, Moore W S, 1980. ^{228}Ra and ^{226}Ra content of groundwater in Fall Line aquifers. Health Physics 38, 663–671.

Miekeley N, Coutinho de Jesus C, Porto da Silveira C L, Linsalata P, Morse R, Osmond J K, 1991. Natural series radionuclide and rare-earth element geochemistry of waters from the Osamu Utsumi mine and Morro do Ferro analogue study sizes, Poços de Caldas, Brazil. SKB. Poços de Caldas Report 8.

Miller W M, Smith G M, Towler P A, Savage D, 1994. Natural elemental mass movement in the vicinity of the Äspö Hard Rock Laboratory. Intera Information Technologies IG3427-2. Melton.

Möller P, Dulski P, Szacki W, Malow G, Riedel E, 1988. Substitution of tin in cassiterite by tantalum, niobium, tungsten, iron and manganese. Geochimica et Cosmochimica Acta 52, 1497–1503.

Nordstrom D K, Smellie J A T, Wolf M, 1991. Chemical and isotopic composition of groundwaters and their seasonal variability at the Osamu Utsumi and Morro do Ferro analogue study sizes, Poços de Caldas, Brazil. SKB. Poços de Caldas Report 6.

Oelkers E H, Helgeson H C, 1990. Geochim.Cosmochim.Acta, 54 727–738.

Oudin E, Cocherie A, 1988. Fish debris record the hydrothermal activity in the Atlantis Ii deep sediments (Red Sea). Geochimica et Cosmochimica Acta 52, 177–184.

Paige C R, Kornicker W A, Hileman O E, Snodgrass W J, 1993. Study of the dynamic equilibrium in the $BaSO_4$ and $PbSO_4$/aqueous solution systems using $133Ba^{2+}$ and $210Pb^{2+}$ as radiotracers. Geochimica et Cosmochimica Acta 57, 4435–4444.

Parkhurst D L, Appelo C A J, 2001. User's guide to PHREEQC (Version 2.4.6). A computer program for speciation, batch reaction, one dimensional transport and inverse geochemical calculations. U.S. Department of the Interior. U.S. Geological Survey. Water-Resources Investigations.

Pearson F J Jr, Berner U, 1991. Nagra Thermochemical Data Base I. Core Data. Technical Report 91-17.

Pearson F J Jr, Berner U, Hummel W, 1992. Nagra Thermochemical Data Base II. Supplemental Data 05/92. Technical Report 91-18.

Pentcheva E, 1965. The distribution of rare and dispersed elements in Bulgarian saline underground waters. Compt. Rend. Acad. Bulgare Sci. 18, 149.

Pérez del Villar L, De la Cruz B, Pardillo J, Cózar J S, Pelayo M, Marín C, Rivas P, 1995. Lithogeochemical characterization and evolutive model of the El Berrocal site: Analogies with a HLRWR. CIEMAT. Topical Report 2. Madrid.

Puigdomènech I, 2001. Hydrochemical stability of groundwaters surrounding a spent nuclear fuel repository in a 100,000 year perspective. SKB TR-01-28, Svensk Kärnbränslehantering AB.

Puigdomènech I, 2002. MEDUSA (Make Equilibrium Diagrams Using Sophisticated Algorithms) Windows interface to the MS-DOS versions of INPUT, SED and PREDOM (FORTRAN programs drawing chemical equilibrium diagrams) Vers. 31 July. 2002. Royal Institute of Technology, Stockholm, Sweden.

Rittenhouse G, Fulton R B, Grabowski R J, Bernard J L, 1969. Minor elements in oilfield waters. Chemical Geology 4, 189.

Salvi S, Williams-Jones A E, 1990. The role of hydrothermal processes in the granite-hosted Zr, Y, REE deposit at Strange Lake, Quebec/Labrador: evidence from fluid inclusions. Geochimica et Cosmochimica Acta 54, 2403–2418.

Santschi P H, Bajo C, Mantovani M, Orciuolo D, Cranston R E. Bruno J, 1988. Uranium in pore waters from North Atlantic (GME and Southern Nares Abyssal Plain) sediments. Nature Vol. 331, (6152) 155–157.

Sebesta F, Sedlacek J, John J, Sandrik R, 1981. Behaviour of radium and barium in a system including uranium mine waste waters and adjacent surface waters. Environmental Science and Technology 15, 71–75.

Seyfried W E, Dibble W E, 1980. Seawater-peridotite interaction at 300°C and 500 bars: implications for the origin of oceanic serpentinites. Geochimica et Cosmochimica Acta 44, 309–321.

Seyfried W E, Bischoff J L, 1981. Experimental seawater-basalt interaction at 300°C and 500 bars: chemical exchange, secondary mineral formation and implications for the transport of heavy metals. Geochimica et Cosmochimica Acta 45, 135–147.

Shanbhag P M, Morse J W, 1982. Americium Interaction with Calcite and Aragonite Surfaces in Seawater. Geochimica et Cosmochimica Acta 46, 241–246.

Short S A, Lowson R T, 1988. $^{234}U/^{238}U$ and $^{230}Th/^{234}U$ activity ratios in the colloidal phases of aquifers in lateritic weathered zones. Geochimica et Cosmochimica Acta 52, 2555–2563.

Silva R J, Bidoglio G, Rand M H, Robouch P B, Wanner H, Puigdomenech I, 1995. Chemical Thermodynamics 2; Chemical Thermodynamics of Americium . NEA OECD, Elsevier.

Siu K W M, Berman S S, 1989. The marine environment. in Occurrence and Distribution of Selenium (M. Ihnat, Ed.). CRC Press, Boca Raton, pp 263–293.

SKI, 2000. Opinions on SKB's safety assessments SR97 and SFL 3-5. A review by SKI consultants. SKI Report 00:47.

Smedley P L, 1991. The geochemistry or rare earth elements in groundwater from the Carnmenellis area, southwest England. Geochimica et Cosmochimica Acta 55, 2767–2779.

Smellie J, Cramer J, MacKenzie A, 1994. Mineralogy and Lithogeochemistry: Geochemical and isotopic features of the host sandstones and clay halo. in Final Report of SKB/AECL Cigar Lake Analog Study (J J. Cramer and J A T. Smellie, Eds.). SKB-(AECL) TR-94-04, Svensk Kärnbränslehantering AB. (10851).

Spahiu K, Bruno J, 1995. A selected thermodynamic database for REE to be used in HLNW performance assessment exercises. SKB TR 95-35, Svensk Kärnbränslehantering AB.

Spalding R F, Druliner A D, Whitside L S, Struempler A W, 1984. Uranium geochemistry in groundwater from Tertiary sediments. Geochimica et Cosmochimica Acta 48, 2679–2692.

Stroes-Gascoyne S, 1992. Trends in the short-term release of fission products and actinides to aqueous solution from used CANDU fuels at elevated temperatures. Journal of Nuclear Materials 190, 87.

Stumm W, Morgan J J, 1996. Aquatic chemistry: chemical equilibria and rates in natural waters. New York. John Wiley & Sons, 3rd Edition.

Sturchio N C, Bohlke J K, Markun F J, 1993. Radium isotope geochemistry of thermal waters, Yellowstone National park, USA. Geochimica et Cosmochimica Acta 57, 1203–1214.

Tait J C, Stroes-Gascoyne S, Hocking W H, Duclos A M, Porth R J, Wilkin D L, 1991. Dissolution Behavior of used CANDU fuel under disposal conditions. Scientific Basis for Nuclear Waste Management XIV, 212, 189.

Turner D R, Whitfield M, Dickson A G, 1981. The equilibrium speciation of dissolved components in freshwater and seawater at 25°C and 1 atm pressure. Geochim. et Cosmochim. Acta 45, 855–881.

Velde B, 1988. Experimental pseudomorphism of talc and serpentine in (Ni, Mg)Cl2 aqueous solutions. Geochimica et Cosmochimica Acta 52, 415–424.

Vuorinen U, Kulmala S, Hakanen M, Ahonen L, Carlsson T, 1998. Solubility database for TILA-99. POSIVA 98-14.

Wang L, Dierckx A, De Cannière P, 2000. Speciation and solubility of radionuclides in Boom Clay. R-3508. Waste and disposal SCK-CEN, Mol, Belgium.

Wanner H, Wersin P, Sierro N, 1992. Thermodynamic modelling of bentonite-groundwater interaction and implications for near field chemistry in a repository for spent fuel. SKB 92-37, Svensk Kärnbränslehantering AB.

Weast R C, ed. 1975. Handbook of Geochemistry and Physics. Cleveland, CRC-Press Inc.

Wedepohl K H, 1978. Handbook of Geochemistry II-3. Springer-Verlag, Berlin.

Westall J C, Zachary J L, Morel F M M, 1976. MINEQL, A computer program for the calculation of chemical equilibrium composition of aqueous systems. Massachussets Institut of Technology, Cambridge, Massachussets, Technical Note Nr.18.

Whitfield M, Turner D R, 1987. The role of particles in regulating the composition of seawater. in Aquatic Surface Chemistry: Chemical Processes at the Particle-Water Interface (W. Stumm, ed.). New York. J. Wiley and sons. Environmental Science and Technology.

Wilson C N, Shaw H F, 1987. Experimental study of the dissolution of spent fuel at 85°C in natural groundwater. Mater. Res. Soc. Symp. Proceedings MRS Vol. , 84, 123.

Wilson C N, 1990a. Results from NNWSI series 2 bare fuel dissolution tests. Pacific Northwest Laboratory, Report PNL-7169, UC-802.

Wilson C N, 1990b. Results from NNWSI series 3 spent fuel dissolution tests. Pacific Northwest Laboratory, Report PNL-7170, UC-802.

Wolery T J, 1992a. EQ3NR, A computer program for geochemical aqueous speciation-solubility calculations: Theoretical Manual, User's Guide and related documentation (Version 7.0) September 14, 1992. Livermore, CA, USA: Lawrence Livermore National Laboratory. UCRL-MA-110662 PT III, p. 246.

Wolery T J, 1992b. EQ3NR, A software package for geochemical modelling of aqueous system (Version 7.0). Livermore, CA, USA: Lawrence Livermore National Laboratory. UCRL-MA-110662 PT I-IV.

Wollenberg H A, 1975. Radioactivity of geothermal systems. In Second U.N. Symposium on the Development and Use of Geothermal Resources, San Francisco, Lawrence Berkeley Laboratory, University of California, 1283–1292.

Yui M J, Azuma J, Shibata M, 1999. JNC Thermodynamic database for performance assessment of High-Level Radioactive Waste Disposal system. JNC TN8400 99-070.

Zukin J G, Hammond D E, Ku T-L, Elders W A, 1987. Uranium-thorium series radionuclides in brines and reservoir rocks from two deep geothermal boreholes in the Salton Sea geothermal field, southeastern California. Geochimica et Cosmochimica Acta 51, 2719–2731.

Appendix A

Range of concentrations measured from spent fuel dissolution experiments conducted in groundwater and under reducing and anoxic conditions.

T	solution	log[RN] (mole·dm^{-3})									
		U	Np	Pu	Am	Cm	Mo	Tc	Cs	Sr	Ba
25ºC	granitic gw	-6.15 ↓ -3.80	-9.41 ↓ -6.21	-9.17 ↓ -4.77	-7.71 ↓ -7.44		-5.82 ↓ -4.93	-7.76 ↓ -5.76	-7.11 ↓ -4.75	-7.44 ↓ -5.73	-6.36 ↓ -5.90
	clayey water	-6.45 ↓ -6.53		-6.45 ↓ -6.53	-8.26 ↓ -7.79				-4.39 ↓ -4.32	-4.96 ↓ -4.85	
25ºC	granitic gw	-7.38 ↓ -4.99		-10.64 ↓ -8.74				-8.79 ↓ -7.45	-6.69 ↓ -5.74	-7.97 ↓ -6.51	
85ºC	granitic gw	-8.36 ↓ -7.10		-11.12 ↓ -10.52		-14.14 ↓ -13.01	-6.70 ↓ -5.59	-8.22	-8.08 ↓ -6.22	-9.14 ↓ -7.40	
	clayey water	-8.21 ↓ -7.48		-11.12 ↓ -10.20		-13.89 ↓ -13.07	-5.77 ↓ -5.37		-8.09 ↓ -7.35	-9.07 ↓ -8.64	

T	solution	log[RN](mole·dm^{-3})					
		Zr	Y	La	Nd	Sm	Eu
25ºC	granitic gw	-7.45 ↓ -7.11	-8.34 ↓ -7.41	-7.62 ↓ -7.29	-8.05 ↓ -6.91	-8.85 ↓ -8.04	-8.76 ↓ -7.30
	clayey water						-7.42 ↓ -7.99

Appendix B

Range of concentration of the trace elements of interest measured in rocks, minerals and natural waters (seawater, fresh water and groundwater)

The following explanations and abbreviations are useful for the interpretation of the table below.

Crystalline media:

EB (El Berrocal): granitic Hercinian massif intercepted by a quartz vein with associated primary U mineralisations.

Palm (Palmottu): U deposit located within Precambrian metamorphosed supreacrustal and sedimentary rocks.

Äspö: porphyritic granite-granodiorite with fine lenses of metabasalts, metavolcanites and pegmatites.

Sanstone-clay media:

Oklo: fossil natural nuclear reactor systems located in a Precambrian sedimentary basin.

CL (Cigar Lake): water saturated sandstone at the unconformity contact with high-grade metamorphic rocks.

UK: chalk, limestone and sandstone of several aquifers.

Alkaline volcanic media:

PdC(Poços de Caldas): subvolcanic phonolite strongly altered by hydrothermal and supergene processes.

Hyperalkaline media:

Maqarin: spontaneous combustion of bituminous-rich marl has produced natural cements, which, through interaction with normal pH groundwater, has produced hyperalkaline waters.

Oman: system of hyperalkaline springs generated by low temperature serpentinisation reactions.

Stab.	isot.	Rocks contents (ppm)	Minerals	Ocean contents (M)	Resid. time (years)	Fresh w. contents (M)	Ground water contents (M)
Cs		Soils: 5, Earth Crust: 1, Sed. and Ign. rocks: 10 Äspö: 3 CL: <1.3 PdC: 0.5–5.0	Polucite	$2.3–3.7 \cdot 10^{-9}$	$6 \cdot 10^{5}$		Äspö: $1.9 \cdot 10^{-8}$ CL: $<5.2 \cdot 10^{-7}$
Sr		Soils: 300, Earth Crust: 385, Sediments: 450, Igneous Rocks: 350 EB: <6.85 CL: 1,680 PdC: 100–350	Celestine, strontianite	$8.9–9.0 \cdot 10^{-5}$	$4 \cdot 10^{6}$		EB, Palm: 10^{-6} CL: $10^{-7}–10^{-6}$, UK: $0.22–80 \cdot 10^{-6}$ PdC: $10^{-8}–10^{-5}$
Ra	226		Barite, celestine, anglesite	$1.6–7.0 \cdot 10^{-16}$		$<10^{-12}$	CL: $0.1–5.0 \cdot 10^{-13}$ Maqarin $<10^{-10}$ Other : $<5 \cdot 10^{-12}$
Sn		Soils: 10, Earth Crust: 40, Sediments: 16, Igneous Rocks: 32 EB: <30 PdC: 5–20	Cassiterite (pyroxenes, micas, amphiboles, sulphides)	$5–20 \cdot 10^{-12}$		$2 \cdot 10^{-11}$	UK: $2.5–8.4 \cdot 10^{-9}$ Maqarin: 10^{-9}, Oman$<2 \cdot 10^{-9}$
Se	79	Shales: 0.6 PdC: 0–120	Clausthalite (PbSe), galena (pyrite, sphalerite, ...)	$0.2–2.4 \cdot 10^{-9}$	$3 \cdot 10^{4}$	$0.2–9.0 \cdot 10^{-9}$	CL: $<3.8 \cdot 10^{-7}$ Maqarin: $10^{-6}–10^{-5}$, Oman $<3 \cdot 10^{-9}$
I	129	CL ore: $1.4 \cdot 10^{-6}$	Iodate solids, fluorapatite	$2–5 \cdot 10^{-7}$	$3 \cdot 10^{5}$		UK: $1.6–26 \cdot 10^{-8}$, CL $<7.8 \cdot 10^{-8}$
Zr		Soils: 300, Earth Crust: 190, Sediments: 200, Igneous Rocks: 170 EB: 50–65 CL: <2,740 PdC: 100–2,500	Zircon, baddeleyite (ilmenite, rutile, perovskite)	$1.2–30 \cdot 10^{-11}$			UK $<8 \cdot 10^{-9}$ Maqarin$< 10^{-7}$
Nb	93	Soils: 115, Earth Crust, granite, basalt and shale: 20, Peridotites: 1.5, Syenites 100 CL: 50 PdC: 30–320	Niobite (pyroxene, amphiboles, micas, cassiterite)	10^{-10}			
Tc	99	CL ore: $8.5 \cdot 10^{-7}$					CL calc $<10^{-9}$
Ni		Ultramaphic-maphic: 200-2,000, Granite-shale 0.5–95, Sandstones: <20 PdC: 10–60	Olivine, pyroxene, amphibole, spinel (clay minerals)	$2–10 \cdot 10^{-9}$	$8 \cdot 10^{4}$	$3 \cdot 10^{-9}$	Palmottu: 10^{-8} Oklo, EB: $\sim 10^{-6}$ CL,PdC, Maqarin: 10^{-7}

Stab. isot.		Rocks contents (ppm)	Minerals	Ocean contents (M)	Resid. time (years)	Fresh w. contents (M)	Ground water contents (M)
Pd		PdC: 0.4–26	Olivine, bronzite, diopside, serpentine, zircon	$1.8–6.6 \cdot 10^{-13}$	$5 \cdot 10^{4}$		Brines: $0.2–20 \cdot 10^{-9}$ Oman: $3–7 \cdot 10^{-9}$
Ag		Soils: 1, Earth Crust: 0.06, Sediments: 0.5, Igneous Rocks: 0.2 Oklo: 6–40 PdC: 0.2–10	Sulphides: pyrite, galena (40 ppm)	$1–23 \cdot 10^{-12}$	$5 \cdot 10^{3}$		UK: $<10^{-9}$ PdC: $5 \cdot 10^{-7}$
Sm		Granites: 9.4 EB: 2 Oklo: 1.7-24 CL: <48.2 PdC: 3–10	Monazite, bastnasite, cerite	$2.7–6.8 \cdot 10^{-12}$	200	$5 \cdot 10^{-14}–8 \cdot 10^{-10}$	Geothermal: 10^{-7}, Brines: $4 \cdot 10^{-8}$ Oklo: 10^{-12} PdC: $6.6 \cdot 10^{-9}$ Maqarin: $<6.6 \cdot 10^{-12}$ Other: $10^{-11}–10^{-7}$
Eu		EB: 0.06 Oklo: 0.5-41 CL: 3 PdC: 2.5	Monazite, bastnasite, cerite, plagioclase	$0.6–1.8 \cdot 10^{-12}$	500	$10^{-14}–2 \cdot 10^{-10}$	Oklo: $10^{-13}–10^{-10}$ PdC: $<2 \cdot 10^{-9}$ Maqarin: $<7 \cdot 10^{-12}$ Others: $0.16–40 \cdot 10^{-9}$
Ho		EB: 0.3 PdC: 2	Monazite, gadolinite	$1–3.6 \cdot 10^{-12}$		$8.7 \cdot 10^{-15}$	Oklo: $10^{-13}–10^{-10}$ PdC: $<3.7 \cdot 10^{-9}$ Others: $<8.5 \cdot 10^{-9}$
Th	232	Granite: 17, Basalt: 2.2, shale: 11, feldspars, biotites and amphiboles: 0.5-50 CL: <141 EB: 7	Thorianite, thorite (uraninite, zircon, monazite)	$0.5–15 \cdot 10^{-13}$	50	$4 \cdot 10^{-11}–4 \cdot 10^{-9}$	EB: $>1.75 \cdot 10^{-11}$ Oklo: 10^{-9}, CL: $10^{-10}–10^{-9}$ PdC: $0.06–0.14 \cdot 10^{-9}$ Maqarin: 10^{-11}, Oman: $<0.2 \cdot 10^{-9}$
Pa	231	Marine sediments: 10^{-5}, Earth Crust: 10^{-6}	Pitchblende (0.1 ppm)	$10^{-17}–10^{-14}$			
U		Apatite:10–100, Biotite: 1–60, Feldspar: 0.1–10, Granite: 4.8 EB: 16.5 CL: 220	Uraninite, pitchblende, allanite, apatite	$1.4 \cdot 10^{-8}$	$3 \cdot 10^{5}$		EB, Palm: $10^{-6}–10^{-9}$ Oklo: $10^{-5}–10^{-10}$, CL: 10^{-7}, UK: $<10^{-7}$ PdC: 10^{-9} Oman: $4 \cdot 10^{-11}$ Other: $10^{-9}–4 \cdot 10^{-7}$
Np							CL calc: $<10^{-10}$
Pu	239	CL ore: $1.2 \cdot 10^{-6}$		$2.9 \cdot 10^{-17}$		$2 \cdot 10^{-18}–2 \cdot 10^{-14}$	CL calc: $<10^{-9}$
Am	243						$10^{-13}–10^{-10}$
Cm	247						$10^{-13}–10^{-10}$

Appendix C

Concentration limits recommended in other PA exercises.

In this appendix we present reported solubility limits proposed by 8 different nuclear waste management agencies corresponding to the following countries in their respective performance assessment exercises:

- Belgium, Mol Site exercise.
- Canada, AECL 1994 exercise.
- Finland, TILA-99 exercise.
- France, ANDRA 2001 exercise.
- Japan, H12 project.
- Spain, ENRESA PA 1999 for clay media and ENRESA PA 2000 for granite media.
- Switzerland, Opalinus Clay Project.
- United Kingdom, NIREX PA 2000.

The former PA exercises refer to two different host-rock concepts: granite and clay. Belgium, Canada, France and Spain report solubility assessment exercises in clayey media, while Finland, Japan, Switzerland, United Kingdom and also Spain have conducted performance assessment exercises in granite host rocks.

Although the groundwater conditions used in the solubility assessment vary among different countries, there is a general coincidence concerning the geochemical conditions used for this assessment. The groundwater conditions, in terms of pH and redox potential, agree with the ones of interest for SKB, that is, pH > 7.0 and reducing conditions. Solubility assessments reported for different conditions are indicated in the text when applicable.

The elements selected for solubility assessment may also differ among the various countries. In this work, we only include those elements selected for this study and listed in Table 3-3. In addition, in the case of reporting calculated solubilities, the thermodynamic database and the geochemical code used in the assessment can also vary, giving rise to some differences in the recommended values. Some of the agencies rely not only on solubility calculations but also on evidences from laboratory experiments and natural analogue studies to select concentration limits for the radionuclides of interest. This can lead to important apparent discrepancies between the values recommended by different countries.

Two solubility values are reported in this work: proposed and conservative. The criteria followed to report both values are specified below:

Proposed values correspond to:

i) either best estimates in the original documents when available, or to

ii) range of solubility values when best estimates not given in the original documents.

Conservative values correspond to:

i) either conservative values when reported in the original documents, or to

ii) the upper limit of the proposed solubility range given in the original documents when not conservative values available.

Concentration limits in this section are analysed in two ways:

- By countries, to provide a deeper understanding of the approaches and models followed in each PA exercise that led to the selected concentration limit for each radioelement.
- By elements, to summarise and identify coincidences or discrepancies among approaches and models for the same element.

Country-based analysis

Belgium

All the concentration limits reported in this section correspond to the Belgian PA exercise and are published in /Wang et al. 2000/.

The Belgian PA selected a clayey groundwater with fixed pH = 8.2 and reducing redox potential (–275 mV). The input water composition used is derived from the reported EG/BS water analyses collected from the Experimental Gallery Bottom Shaft piezometer located at the basis of the first access shaft of the HADES underground research laboratory and has been adapted for in situ Boom Clay conditions.

/Wang et al. 2000/ proposed concentration limits for the following radionuclides: Ac, Ag, Am, C, Ca, Cl, Cm, Cs, I, Mo, Nb, Ni, Np, Pa, Pd, Pu, Ra, Rb, Se, Sm, Sn, Sr, Tc, Th, U and Zr. Only those selected in the present work are summarised in Table C-1.

The solubility calculations assumed equilibrium between the selected groundwater and the most likely solubility limiting solid phases, which have been selected based on their saturation states in a supersaturated solution presenting arbitrary high concentration of the radioelement of interest.

No co-precipitation is considered assuming that the selection of pure solid phases is a conservative approach.

The calculations have been performed by means of the geochemical code The Geochemist's Workbench ® 3.1 /Bethke 2000/.

The thermodynamic database "thermo.com.V8.R6+.dat" derived from the Lawrence Livermore National Laboratory (LLNL) thermodynamic database for EQ3/6 code, version 8, release 6 has been used for most of the elements.

For U, Am and Tc the NEA databases have been selected. For Np and Pu, the LLNL database was updated with data in /Lemire et al. 2001/. For Nb, data in "thermo_com.R7beta" have been considered. Data for Pa and Cm are discussed in terms of chemical analogies due to the lack of selected thermodynamic data for these elements.

All calculations refer to 25°C.

Neither data gathered from natural analogues, nor from laboratory experiments, have been compared with the results of the calculations.

The Belgian solubility limits for the elements selected in this study and reported in /Wang et al. 2000/ are shown in Table C-1.

Proposed values correspond to the reported solubilities for all the solubility limiting solid phases.

Conservative values are assumed to be the upper limit of the proposed solubility range, that is, the most soluble solid phase.

Table C-1. Radionuclide solubility limits selected in Belgium. Clayey and reducing conditions, pH = 8.2, Eh = –275 mV, $pCO_2(g) = 10^{-2.31}$ atm. Solubilities in mol/dm³.

Element	Solid	Proposed	Conservative
Cs	No solubility limited		
Sr	$SrSO_4$	high	High
	$SrCO_3$	$4.5 \cdot 10^{-7}$	
	Clinoptilolite-Sr	$1.6 \cdot 10^{-7}$	
Ra	$RaSO_4$	$4.9 \cdot 10^{-5}$	$4.9 \cdot 10^{-5}$
Sn	$SnSO_4$ / SnS_2 / Sn_2S_3	high	High
	SnO_2	$2.7 \cdot 10^{-8}$	
Se	Se(s)	$2.9 \cdot 10^{-7}$	$2.9 \cdot 10^{-7}$
	$FeSe_2$	$1.9 \cdot 10^{-9}$	
Zr	ZrO_2	$6.7 \cdot 10^{-10}$	$6.7 \cdot 10^{-10}$
	$ZrSiO_4$	$1.3 \cdot 10^{-13}$	
	$CaZrO_3$	insoluble	
Nb	Nb_2O_5	10^{-4}	10^{-4}
Tc	$TcO_2 \cdot 1.6H_2O$	$4.5 \cdot 10^{-9}$	$4.5 \cdot 10^{-9}$
	Tc(s)	$1.4 \cdot 10^{-11}$	
	TcO_2(c)	$4.5 \cdot 10^{-13}$	
Ni	$NiCO_3$	$3.1 \cdot 10^{-3}$	$3.1 \cdot 10^{-3}$
	$Ni(OH)_2$	$3.6 \cdot 10^{-4}$	
	NiO	$1.9 \cdot 10^{-4}$	
	$Ni_3(PO_4)_2$	$6 \cdot 10^{-5}$	
	Ni_2SiO_4	$7.4 \cdot 10^{-8}$	
Pd	PdO(c)	$7.5 \cdot 10^{-3}$	$7.5 \cdot 10^{-3}$
	Pd(s)	insoluble	
Ag	Ag_3PO_4	high	high
	AgCl	$7.1 \cdot 10^{-7}$	
	Ag_2S / Ag(m)	insoluble	
Sm	$Sm(OH)_3$(s)	$5 \cdot 10^{-4}$	$5 \cdot 10^{-4}$
	$Sm_2(CO_3)_3$(s)	$4.4 \cdot 10^{-7}$	
	$SmPO_4{:}10H_2O$	$2.1 \cdot 10^{-11}$	
Th	$Th(OH)_4$	$4.2 \cdot 10^{-7}$	$4.2 \cdot 10^{-7}$
	ThO_2	$6.8 \cdot 10^{-15}$	
Pa	Pa_2O_5	10^{-7}	10^{-7}
	PaO_2	10^{-11}	
U	$UO_{2.67}$	$3.8 \cdot 10^{-3}$	$3.8 \cdot 10^{-3}$
	U_3O_8(c)	$3.7 \cdot 10^{-3}$	
	UO_2(am)	$3.6 \cdot 10^{-5}$	
	$UO_{2.33}$	$3.5 \cdot 10^{-7}$	
	$UO_{2.25}$	$5 \cdot 10^{-8}$	
	$USiO_4$	$1.4 \cdot 10^{-9}$	
	UO_2(c)	$4 \cdot 10^{-10}$	
Np	$Np(OH)_4$	$1.6 \cdot 10^{-9}$	$1.6 \cdot 10^{-9}$
	NpO_2(c)	$4.0 \cdot 10^{-18}$	
Pu	$Pu(OH)_4$	$2 \cdot 10^{-9}$	$2 \cdot 10^{-9}$
	PuO_2(c)	$1.5 \cdot 10^{-17}$	
Am	$Am(OH)_3$(am)	$7.1 \cdot 10^{-4}$	$7.1 \cdot 10^{-4}$
	$Am(OH)_3$(c)	$1.1 \cdot 10^{-5}$	
	$Am_2(CO_3)_3$	$6.7 \cdot 10^{-7}$	
	$AmOHCO_3$	$1.2 \cdot 10^{-7}$	
Cm	By analogy to Am	By analogy to Am	By analogy to Am

Canada

All data referred to Canadian solubilities are reported in /Lemire and Garisto 1989/ and /Johnson et al. 1994/.

The reported solubilities are used for the so-called vault model of the Canadian concept, that comprises used CANDU fuel bundles in Grade-2 titanium containers, surrounded by a compacted buffer material (mixture of sand and bentonite) and emplaced in a plutonic rock.

The granitic groundwater used in this assessment contents primarily $CaCl_2$, NaCl and Na_2SO_4. /Lemire and Garisto 1989/ reported ranges for the composition of the contacting water resulting from the interaction between groundwater and the buffer material. In that exercise a log-uniform distribution was selected to describe the concentration of $CaCl_2$, Na_2SO_4, NaCl, inorganic carbon, inorganic fluoride and total inorganic phosphorous. A triangular and a uniform distribution function was used to describe hydrogen ion concentration and redox potential respectively.

The solubilities for the 5 selected radionuclides (U, Th, Tc, Np and Pu) have been calculated in the redox potential range, Eh, between 0 and 0.5 V and for pH values from 5 to 10. The bases for selecting these ranges are detailed in /Lemire and Garisto 1989/. The choice of Eh reflects the range of conditions compatible with the solubility-limited dissolution model: slightly reducing conditions expected in deep groundwaters and oxidising conditions caused by radiolysis effects.

The lower limit of the selected range, responding to the lower limit for the stability field of water, is comparable to the reference value of Eh for WRA-500 water /Gascoyne 1988/, which is –30 mV at pH 7.8.

The pH range selection includes measured pH in groundwaters from the WRA, in solutions resulting from contacting distilled water with Avonlea clays, and calculated values for solutions resulting from contacting WN-1M model groundwater with clay.

The authors consider that most of the remainig radionuclides will have high solubilities, with an upper level set at 2 $mol \cdot dm^{-3}$.

The solubility model used to calculate the concentrations for the selected radionuclides by the Canadian agency is described in detail in /Lemire and Garisto 1989/. They derive mathematical expressions for the solubility calculation in a systematic fashion based on thermodynamic principles, that is, they express the solubility as a sum of terms:

$$C(solid) = \Sigma q_i \times [M_i] \qquad \text{eq. 10}$$

where M_i represents the metal species in equilibrium with the solid under the given water contact conditions. These species are then expressed in terms of their equilibrium constants, leading to expressions of the solubilities of the different solids of interest as a function of the environmental conditions.

Lemire and Garisto assumed that the solids more likely to control the solubility of the selected radionuclides are the hydrated forms of the MO_2 oxides. Given that U_4O_9 can form by oxidation of UO_2 without disrupting the crystal structure, this solid was also considered.

For Tc, the selected solid is metallic technetium.

/Lemire and Garisto 1989/ used a probabilistic distribution model to propose concentration limits. Their calculations were based on 40,000 sampled contact waters and sets of equilibrium constants /Lemire and Garisto 1989/. Radionuclide concentrations were plotted versus the number of cases studied.

Given that the purpose of this chapter is to report a solubility range and/or the best solubility value given by each agency we have decided to give as *proposed* values a range of concentrations

including a representative sampling of the results obtained and as *conservative* values the upper limits of the calculated concentrations. Only calculated solubilities at 25°C are reported in this work.

The selection of solubility values is detailed below and summarised in Table C-2.

Uranium. More than 85% of the cases resulted in total uranium concentrations lower than 10^{-8} mol·dm^{-3}, with solubilities ranging between this limit and $10^{-10.5}$ mol·dm^{-3}. Around a 5% of the cases resulted in total uranium concentrations higher than 10^{-6} mol·dm^{-3}, value that has been considered as the lower limit of the conservative range. The highest uranium solubility represents oxidative dissolution of U_4O_9.

Neptunium. More than 85% of the neptunium solubilities range between 10^{-9} and 10^{-7} mol·dm^{-3}. As for uranium, approximately 5% of the cases studied produced neptunium solubilities above 10^{-6} mol·dm^{-3}, which is the value proposed as the lower limit of the conservative range.

Plutonium. Around 70% of the cases studied have plutonium solubilities ranging between 10^{-11} and 10^{-6} mol·dm^{-3}. Conservative values consider the highest plutonium solubilities calculated, by taking as lowest limit 10^{-5} mol·dm^{-3}, this range includes around a 23% of the cases studied.

Thorium. Solubilities of thorium range between $10^{-10.5}$ and more than 10^{-2} mol·dm^{-3}. An 80% of the cases studied fall within the $10^{-10.5}$ to 10^{-8} mol·dm^{-3} range. As conservative value we take those solubilities higher than 10^{-6}, what integrates around 8% of the calculated cases.

Technetium. The range of calculated solubility spans over 12 orders of magnitude, from 10^{-14} to 10^{-2} mol·dm^{-3}, which is a consequence of the different stability of the solid phases considered, in combination with the wide range of redox conditions tested. This range encloses around a 64% of the calculations. As the authors indicate, concentrations lower than 10^{-12} are unrealistically low and they argue that this is the result of the lack of adequate thermodynamic data in the database of solution species with oxidation states lower than (III). The conservative value is estimated with a lowest limit at 10^{-2} mol/dm^3 and includes approximately 3% of the cases studied.

Table C-2. Range of radionuclide solubility limits selected in Canada. Clayey and oxidising conditions (see text). Solubilities in mol/dm^3.

Element	Solid	Proposed	Conservative
U	UO_2(am) and U_4O_9	$10^{-10.5}$–10^{-8}	> 10^{-6}
Np	NpO_2(am)	10^{-9}–10^{-7}	> 10^{-6}
Pu	PuO_2(am)	10^{-11}–10^{-6}	> 10^{-5}
Th	ThO_2(am)	$10^{-10.5}$–10^{-8}	> 10^{-6}
Tc	TcO_2(am) and Tc(s)	10^{-14}–10^{-2}	> 10^{-2}

Finland

Solubility limits for the Finnish PA included in this section are reported in /Vuorinen et al. 1998/.

The Finnish concept for final spent fuel disposal considers granite host-rock. Concentration limits are proposed both for near and far field conditions. In this work we will report only those limits proposed for the near field.

Four different near-field groundwater compositions differing in their redox conditions (oxidising and reducing) and ionic strength (fresh and saline) are considered in the work of /Vuorinen et al. 1998/.

For the sake of comparison we have selected two of the reported groundwater conditions, corresponding to fresh and saline waters under reducing conditions (see Table C-3) in agreement with the groundwaters selected by SKB.

Table C-3. Near-field groundwater compositions used in the Finnish PA for assessment of concentration limits.

	Fresh groundwaters	Saline groundwaters
Eh (in mV)	From –413 to –254	From –373 and –254 mV
pH	From 7 to 10	From 7 to 9
$[CO_3^{2-}]$tot (in mol·dm^{-3})	From $7.4 \cdot 10^{-3}$ to $2.8 \cdot 10^{-3}$	From $1.4 \cdot 10^{-3}$ to $1.3 \cdot 10^{-5}$
Comments	Calcite saturation and equilibrium magnetite/hematite	

The Finnish PA reports concentration limits for the following radionuclides: Am, C, Cl, Cm, Cs, Cu, Fe, Ho, I, Nb, Ni, Np, Pa, Pd, Pu, Ra, Se, Sm, Sn, Sr, Tc, Th and Zr. The selection is based on both, a literature data evaluation (experimental results from spent fuel dissolution experiments and natural systems) and thermodynamic calculations.

Literature data review is focused on spent fuel dissolution experiments conducted mainly in the frame of the Swedish programme of corrosion studies on spent nuclear fuel /Forsyth 1997/, USA in the frame of the Yucca Mountain Project /Wilson 1990/ and Germany with some results obtained within the experimental programme implemented by FZK-INE /Loida et al. 1996/. Measured concentrations in several natural groundwaters have been also reviewed and reported for comparison.

Radionuclide concentrations were calculated by using the EQ3NR code /Wolery 1992a/ in the geochemical software package EQ3/6 /Wolery 1992b/. The DATA0.COM thermodynamic database /Wolery, 1992b/ and the SR 97-TDB /Bruno et al. 1997/ are used. All solubility calculations have been conducted at 25°C. No indications are given regarding the procedure for selecting the limiting solid phases. Co-precipitation processes are considered for example in the discussion on the Ra solubility assessment, although for the sake of conservatism, recommended values rely on the solubility of the pure solid phase.

Figures shown in this document as *proposed* values (see Table C-4) correspond to the ones reported as recommended values in /Vuorinen et al. 1998/. *Conservative* values are not reported by those authors although they state that solubilities proposed for TILA-99 are assumed to be more conservative than realistic. Therefore we do not select conservative values, in agreement with the original source.

France

ANDRA provides solubility limits calculated under clay and cement conditions but only those obtained under clay conditions have been included in this report. All the solubility values reported in this section are taken from /Giffaut et al. 2000/.

The French reference groundwater has a pH in the range 7.0 to 8.5 and a redox potential below –200 mV, the partial pressure of CO_2 ranges between 10^{-2} and 10^{-4} atm. Solubility limits are proposed for Am, C, Cl, Cm, Cs, Ho, I, Mo, Nb, Ni, Np, Pa, Pb, Pd, Pu, Ra, Se, Sm, Sn, Sr, Tc, Th, U and Zr.

All values reported are supported by thermodynamic calculations. No information about the geochemical code used is given in /Giffaut et al. 2000/. The authors used the ANDRA thermodynamic database (ANDRA TDB Version 1997) for all the elements except for actinides, for which they modified the database according to the results obtained within the project "Actinides" carried out by Andra. All solubility calculations refer to 25°C and calcite saturation was kept in all cases.

A reference value (Csat) and a conservative value (Ccons) are recommended in /Giffaut et al. 2000/ for each element. Csat values correspond to solubility calculated under the conditions of the reference groundwater and are taken in the present work as *proposed* values, while Ccons stand for the maximum solubility obtained in the range of geochemical conditions of interest and they are presented here as *conservative* values. The French solubility limits proposed in /Giffaut et al. 2000/ for the elements of interest of this work are shown in Table C-5.

Table C-4. Radionuclide solubility limits selected in Finland for the elements selected in the present study. Two groundwaters selected: fresh and saline groundwaters. Solubilities in mol/dm³.

Element	Solid	Proposed (fresh)	Proposed (saline)
Cs	Not solubility limited		
Sr	$SrSO_4$	$8 \cdot 10^{-6}$	$8 \cdot 10^{-5}$
Ra	$RaSO_4$	$2 \cdot 10^{-9}$	$7 \cdot 10^{-9}$
Se	based on published data, no solid selection	10^{-7}	10^{-7}
Zr	ZrO_2	10^{-8}	10^{-8}
Nb	Nb_2O_5	10^{-3}	10^{-4}
Tc	$TcO_2 \cdot 2H_2O$	10^{-8}	10^{-8}
Ni	based on published data, no solid selection	10^{-5}	10^{-5}
Pd	PdO	$6 \cdot 10^{-9}$	$6 \cdot 10^{-9}$
Sn	SnO_2	10^{-6}	10^{-6}
Ho	$Ho_2(CO_3)_3$	$5 \cdot 10^{-6}$	$2 \cdot 10^{-6}$
Sm	$Sm_2(CO_3)_3$	$7 \cdot 10^{-7}$	$5 \cdot 10^{-7}$
Th	$Th(OH)_4$	$4 \cdot 10^{-8}$	$4 \cdot 10^{-8}$
Pa	PaO_2	$2 \cdot 10^{-9}$	$2 \cdot 10^{-9}$
Np	$Np(OH)_4$	$2 \cdot 10^{-9}$	$2 \cdot 10^{-9}$
Pu	$Pu(OH)_3$	$5 \cdot 10^{-9}$	$2 \cdot 10^{-8}$
Am	$AmOHCO_3$	10^{-7}	$2 \cdot 10^{-7}$
Cm	$CmOHCO_3$	$3 \cdot 10^{-9}$	$3 \cdot 10^{-8}$

Table C-5. Radionuclide solubility limits selected in France. Clayey and reducing conditions, pH = 7–8.5, Eh < –200 mV, $pCO_2(g) = 10^{-4}$–10^{-2} atm. Solubilities in mol/dm³.

Element	Solid	Proposed	Conservative
Cs	No solubility limited		
Sr	$SrCO_3$	10^{-5}	10^{-5}
Ra	$RaSO_4$	10^{-6}	10^{-5}
Sn	SnO_2	10^{-8}	$5 \cdot 10^{-7}$
Se	FeSe	$5 \cdot 10^{-10}$	10^{-8}
Zr	$Zr(OH)_4$	10^{-9}	$5 \cdot 10^{-5}$
Nb	Nb_2O_5	10^{-7}	$3 \cdot 10^{-6}$
Tc	TcO_2(am)	10^{-8}	$3 \cdot 10^{-7}$
Ni	NiO / $Ni_2SiO_4 \cdot xH_2O$	$3 \cdot 10^{-6}$	10^{-5}
Pd	Pd(s)	10^{-10}	$5 \cdot 10^{-7}$
Sm	$Sm(OH)_3$ / $SmOHCO_3$	$7 \cdot 10^{-8}$	10^{-7}
Ho	$Ho(OH)_3$ / $HoOHCO_3$	$7 \cdot 10^{-8}$	$5 \cdot 10^{-7}$
Th	ThO_2	$2 \cdot 10^{-10}$	$5 \cdot 10^{-7}$
Pa	$Pa_2O_5 \cdot H_2O$	10^{-6}	10^{-6}
U	UO_2(am)	$2 \cdot 10^{-9}$	$5 \cdot 10^{-8}$
Np	$Np(OH)_4$	10^{-9}	$3 \cdot 10^{-8}$
Pu	$Pu(OH)_4$	$4 \cdot 10^{-9}$	10^{-7}
Am	$Am(OH)_3$ / $AmOHCO_3$	$7 \cdot 10^{-8}$	10^{-6}
Cm	$Cm(OH)_3$ / $CmOHCO_3$	$7 \cdot 10^{-8}$	10^{-6}

Japan

All the solubility values included in this section are reported in /JNC 2000/.

The chemical composition of the buffer porewater used in the assessment was calculated by means of a geochemical model, assuming key reactions like cation exchange, dissolution and precipitation of accessory minerals, redox reactions and equilibrium with a fresh type model groundwater.

The water compositions are specified in /JNC 2000/. The main variables of interest for the solubility calculations are: pH = 8.4; Eh = –276 mV and $[CO_3^{2-}]tot = 1.6 \cdot 10^{-2}$ mol·dm^{-3}. The following radionuclides are studied: Ac, Am, Cm, Cs, Nb, Np, Pa, Pb, Pd, Pu, Ra, Se, Sm, Sn, Tc, Th, U and Zr.

Radionuclide concentrations have been calculated by using the geochemical code PHREEQE /Parkhurst and Appelo 2001/ after selection of the solubility controlling phase.

The JNC Thermodynamic database /Yui et al. 1999/ is used in this assessment and all calculations refer to 25°C.

Effects of co-precipitation were considered for Ra. Measured concentrations from solubility experiments were also reviewed and, in those cases were measured concentrations were larger than calculated solubilities, the measured ones were proposed, that is the case of Zr, Nb, Sn and Pd. There is no indication on whether reported concentrations are considered as realistic, recommended, proposed or conservative, therefore, we report these data as *proposed* values. The Japanese solubility limits reported in /JNC 2000/ for the elements selected in this work are shown in Table C-6.

Table C-6. Radionuclide solubility limits selected in Japan. Granitic environment, pH = 8.4, Eh = –276 mV, [C]tot = $1.6 \cdot 10^{-2}$ mol·dm^{-3}. Solubilities in mol/dm^3.

Element	Solid	Proposed
Cs	Not solubility limited	
Ra	Ra-Ca-CO_3 (co-precipitation)	10^{-12}
Sn	SnO_2(am)	$5 \cdot 10^{-6}$
Se	$FeSe_2$(cr)	$3 \cdot 10^{-9}$
Zr	ZrO_2(am)	10^{-6}
Nb	Nb_2O_5(am)	10^{-4}
Tc	TcO_2(am)	$4 \cdot 10^{-8}$
Pd	Pd(s)	10^{-9}
Sm	$SmOHCO_3$(cr)	$2 \cdot 10^{-7}$
Th	ThO_2(am)	$5 \cdot 10^{-6}$
Pa	Pa_2O_5(s)	$2 \cdot 10^{-8}$
U	UO_2(am)	$8 \cdot 10^{-9}$
Np	$Np(OH)_4$	$2 \cdot 10^{-8}$
Pu	$Pu(OH)_4$	$3 \cdot 10^{-8}$
Am	$AmOHCO_3$(cr)	$2 \cdot 10^{-7}$
Cm	$CmOHCO_3$(cr)	$2 \cdot 10^{-7}$

Spain

Two performance and safety assessment exercises have been published by the Spanish agency (ENRESA) responding to two different geological formations for hosting a potential deep geological disposal for nuclear wastes: granitic and clay host rocks. The first assessment in a granitic environment /ENRESA 1997/ was conducted with the aim to establish the methodological bases for a safety assessment study. The second assessment in clay formation /ENRESA 1999/ was intended to analyse the clay concept and to consolidate the existing safety assessment methodology and tools.

In this report we report the solubility assessments presented in both exercises, which are detailed below.

Granitic host-rock

All the solubility values reported in this work are included in /ENRESA 1997/.

The solubility calculations have been conducted by using the geochemical code PHREEQC /Parkhurst and Appelo 2001/ and the CHEMVAL thermodynamic database version 6.T /Falk et al. 1996/.

Concentration limits were proposed for the following radionuclides: Ac, Am, C, Cl, Cm, Cs, I, Nb, Ni, Np, Pa, Pb, Pu, Ra, Sm, Sr, Tc, Th, U and Zr at 75°C.

Solubility limits were calculated by taking into account the variability given by the main environmental conditions, redox conditions ($-400 < Eh < -260$ mV) and pH ($5.0 < pH < 12$). In this report, we consider those values reported for $pH > 7.0$.

Based on the results obtained by the thermodynamic calculations and taking into account solubilities assessed in other performance assessment exercises, ranges of solubilities are proposed for the selected radionuclides. These ranges are shown in Table C-7 as *proposed* values, and upper limit of these ranges is given as the *conservative* value.

Table C-7. Radionuclide solubility limits for the elements of interest selected in Spain for granitic formations. –400 < Eh < –260 mV, 7 < pH < 11, T = 75°C. Solubilities in mol/dm³.

Element	Solid	Proposed	Conservative
Cs	No solubility limited		
Sr	$SrCO_3$ / $Sr(OH)_2$	10^{-4}–10^{-1}	10^{-1}
Ra	$RaSO_4$	10^{-6}–10^{-3}	10^{-3}
Nb	No solubility limited		
Tc	Tc_3O_4 / $Tc(OH)_3$	10^{-15}–high	high
Ni	No solubility limited		
Sm	$Sm_2(CO_3)_3$ / $Sm(OH)_3$	10^{-14}–10^{-6}	10^{-6}
Th	ThO_2	10^{-15}–10^{-7}	10^{-7}
Pa	Pa_2O_5	10^{-7}–10^{-6}	10^{-6}
U	UO_2	10^{-9}–10^{-4}	10^{-4}
Np	$Np(OH)_4$	10^{-12}–10^{-8}	10^{-8}
Pu	$Pu(OH)_4$	10^{-10}–10^{-3}	10^{-3}
Am	$Am_2(CO_3)_3$ / $Am(OH)_3$ / AmO_2	10^{-14}–10^{-7}	10^{-7}
Cm	$CmOHCO_3$ / $Cm(OH)_3$	10^{-10}–10^{-4}	10^{-4}

Clay formation

All solubility values here reported in this work are included in /ENRESA 1999/.

Thermodynamic calculations were performed with the geochemical code EQ3/6 /Wolery 1992ab/.

The thermodynamic database used for the calculations was the PSI database /Pearson and Berner 1991/, updated for some specific radionuclides with data reported in other sources, mainly /Pearson et al. 1992, Grenthe et al. 1992/ and /Silva et al. 1995/.

Solubility limits for the selected radionuclides (Ac, Am, Cm, Nb, Ni, Np, Pa, Pb, Pd, Pu, Ra, Se, Sm, Sn, Tc, Th, U and Zr) were calculated by equilibrating the porewater with the solubility controlling solid phase under the geochemical conditions after selection of these solid phases.

Solubility calculations were performed under the chemical composition of different bentonite porewaters (FEBEX, S-2, MX-80, MCA-C) and synthetic waters used in laboratory experiments. Also calculations referring to the physicochemical conditions established for the reference case were reported, that is reducing conditions (Eh = –260 mV) and alkaline media ($7.0 < pH < 12.5$), T = 25°C.

A parametric study of these variables by varying pH from 5 to 11 and Eh from –230 to –430 mV was conducted.

Solubility ranges were proposed based on the thermodynamic calculations but also considering the assessment of solubilities of the previous exercise in a granitic media adapted to clay medium. The results obtained were in agreement with the previous ones.

The calculations were also compared with the concentrations proposed in other performance assessment exercises, especially the one performed by SCK-CEN in Belgium, given the resemblances between the Boom clay and the clayey conditions selected by ENRESA.

For the final concentration assessment also experimental results were considered. This process finished with the establishment of the solubility limits giving a range of solubilities as well as a single value for each radionuclide as a best estimate.

The assessed solubilities are detailed in Table C-8. In this table we report as *proposed* values the best estimates, while as *conservative* values we select the upper limits of the proposed ranges.

Table C-8. Radionuclide solubility limits for the elements of interest selected in Spain for clay formations. Eh = –260 mV, 7 < pH < 9, T = 25°C. Solubilities in mol/dm³.

Element	Solid	Proposed	Conservative
Cs	Not solubility limited		
Ra	$RaSO_4$	$5 \cdot 10^{-9}$	10^{-6}
Sn	SnO_2	10^{-6}	10^{-5}
Se	$FeSe_2$	10^{-8}	10^{-7}
Zr	ZrO_2	10^{-7}	10^{-6}
Nb	Nb_2O_5	10^{-5}	10^{-3}
Tc	TcO_2(am)	10^{-8}	10^{-7}
Ni	Not solubility limited		
Pd	PdO	$2 \cdot 10^{-8}$	10^{-6}
Sm	$Sm_2(CO_3)_3$ / $SmOHCO_3$	10^{-8}	10^{-6}
Th	ThO_2(am)	10^{-7}	10^{-6}
Pa	Pa_2O_5	$3 \cdot 10^{-7}$	10^{-6}
U	UO_2	$7 \cdot 10^{-7}$	10^{-4}
Np	$Np(OH)_4$	10^{-9}	10^{-5}
Pu	$Pu(OH)_4$	10^{-8}	10^{-6}
Am	$AmOHCO_3$	10^{-6}	10^{-5}
Cm	$CmOHCO_3$	10^{-6}	10^{-5}

Switzerland

All the solubilities included in this sub-section are those reported in /Berner 2002/.

The solubility calculations have been conducted with the geochemical code MINEQL/PSI /Westall et al. 1976/ by using the updated NAGRA/PSI Chemical Thermodynamic Data Base 01/01 /Hummel et al. 2002/.

Thermodynamic data for elements not included in the NAGRA/PSI Data Base 01/01 were taken from older compilations. The assessment of solubilities reported in /Berner 2002/ relies solely on geochemical calculations.

The Swiss base case considers clay waters, reducing conditions (Eh = –193.6 mV) and neutral pH (pH = 7.25), with a pCO_2 ranging between $10^{-3.6}$ and $10^{-1.4}$ atm with a reference value of $10^{-2.2}$ atm.

The reference bentonite pore water used for calculating solubility and speciation is described in detail in /Curti and Wersin 2002/. The effect of temperature has not been considered due to the lack of information on reaction enthalpies in the thermodynamic database used, therefore, calculations have been done at the reference temperature of 25°C. Co-precipitation processes have been considered in some cases.

Solubility limits were obtained by increasing the amount of every radionuclide in one liter of the reference solution until saturation with the most stable solid included in the database occurs.

The radionuclides included in this analyses are Ac, Ag, Am, Be, C, Ca, Cd, Cl, Cm, Co, Cs, Eu, Fe, H, Hf, Ho, I, Mo, Nb, Ni, Np, Pa, Pb, Pd, Pm, Po, Pu, Ra, Ru, Sb, Se, Sn, Sr, Tc, Th, U and Zr.

A range of solubilities conforming the lower limits and the maximum concentrations given in /Berner 2002/ are reported for each element of interest in Table C-9 as *proposed* values, while the upper limits are shown in the same table as *conservative* values.

Table C-9. Radionuclide solubility limits selected in Switzerland in clay formations. Eh = –193.6 mV, pH = 7.25, $pCO_2 = 10^{-2.2}$, T = 25°C. Solubilities in mol/dm³.

Element	Solid	Proposed	Conservative
Sr	$SrSO_4$	$1.9 \cdot 10^{-5}$	$1.2 \cdot 10^{-4}$
Ra	$BaRaSO_4$, solid solution	$4 \cdot 10^{-12}$–$2 \cdot 10^{-11}$	10^{-10}
Sn	SnO_2	$5 \cdot 10^{-9}$–10^{-8}	10^{-7}
Se	Se(s)	$2.1 \cdot 10^{-11}$–$5 \cdot 10^{-9}$	10^{-5}
Zr	ZrO_2	$3 \cdot 10^{-11}$–$2 \cdot 10^{-9}$	$2 \cdot 10^{-9}$
Nb	Nb_2O_5	$3 \cdot 10^{-5}$	
Tc	TcO_2(am)	10^{-9}–$4 \cdot 10^{-9}$	10^{-8}
Ni	$NiCO_3$	10^{-5}–$3 \cdot 10^{-5}$	$8 \cdot 10^{-5}$
Pd	$Pd(OH)_2$	$5 \cdot 10^{-8}$	$2 \cdot 10^{-7}$
Ag	AgCl / Ag		$3 \cdot 10^{-6}$
Ho	In analogy to Eu	$3 \cdot 10^{-7}$–$5 \cdot 10^{-7}$	$9 \cdot 10^{-7}$
Th	ThO_2(am)	$2 \cdot 10^{-7}$–$7 \cdot 10^{-7}$	$3 \cdot 10^{-6}$
Pa	Pa_2O_5	~10^{-8}	
U	UO_2	$3 \cdot 10^{-10}$–$3 \cdot 10^{-9}$	$5 \cdot 10^{-7}$
Np	$Np(OH)_4$	$3 \cdot 10^{-9}$–$5 \cdot 10^{-9}$	10^{-8}
Pu	$Pu(OH)_4$	$3 \cdot 10^{-9}$–$5 \cdot 10^{-8}$	10^{-6}
Am	$AmOHCO_3$	$5 \cdot 10^{-8}$–10^{-6}	$3 \cdot 10^{-5}$
Cm	In analogy to Am	$5 \cdot 10^{-8}$–10^{-6}	$3 \cdot 10^{-5}$

United Kingdom

All the solubility values presented in this sub-section are taken from /Heath et al. 1998/.

NIREX carried out an extensive research programme including experimental measurements and thermodynamic modelling calculations to determine the solubilities, under repository conditions, of those radioelements of relevance.

Thermodynamic modelling was used to complement experimental solubility measurements, mainly to provide an interpretation of the experimental data and estimates of solubility for related chemical conditions for which direct experimental data were not available.

Solubility studies were conducted under reducing alkaline conditions, in agreement with the NIREX disposal concept, dominated by the presence of cement. These conditions cause that aqueous speciation is mostly dominated by hydroxyl-complexes and that solubility controlling solid phases are likely to be oxides or hydroxides.

Solubility calculations were performed with the code HARPHRQ /Brown et al. 1991/. The HATCHES thermodynamic database /Bond et al. 1997/ was used in the calculations. Predicted solubilities at 25°C are proposed for 6 radionuclides: Ni, Np, Pu, Tc, Th and U.

Two groundwater compositions were used in the calculations, pH = 9.8 and Eh = –300 mV and pH = 12.3 and Eh = –450 mV.

The solubility measurements were performed by using two different approaches, oversaturation and undersaturation. Cement-equilibrated waters were used in these studies, the pH was controlled by the solubility of calcium hydroxide, with the carbonate level restricted by solubility with calcite. Experiments were carried out either under nitrogen atmosphere or by adding a reducing agent to keep low Eh values.

For NIREX, the experimental data provide the main source of information on radionuclide solubility in a cementitious environment. Nevertheless, given that data were not produced for the full range of repository conditions, they must complement the assessment by the solubility predictions obtained by conducting geochemical calculations.

Solubility limits proposed in Table C-10 reflect both experimental measurements as well as thermodynamic calculations.

Conservative values correspond to the maximum values either determined from solubility experiments or calculated. The selection of solubility limits is specified below.

Uranium. Concentrations of uranium measured from experiments and calculated solubilities range between $3 \cdot 10^{-8}$ and $5 \cdot 10^{-7}$ mol·dm^{-3} for U(IV) solid phases limiting the aqueous U concentration. The conservative value stands for the concentration of uranium in equilibrium with an hexavalent uranium oxide ($UO_3 \cdot 2H_2O$).

Table C-10. Radionuclide solubility limits proposed by Nirex, measured and calculated data, T = 25°C. Solubilities in mol/dm³.

Element	Solid	Proposed	Conservative
Tc	TcO_2(am)	$4 \cdot 10^{-8}$–10^{-6}	10^{-6}
Ni	$Ni(OH)_2$	$4 \cdot 10^{-8}$–$4 \cdot 10^{-7}$	$7 \cdot 10^{-5}$
Th	ThO_2(am)	$4 \cdot 10^{-9}$–$8 \cdot 10^{-9}$	$8 \cdot 10^{-9}$
U	UO_2(am)	$3 \cdot 10^{-8}$–$5 \cdot 10^{-7}$	$2 \cdot 10^{-6}$
Np	$Np(OH)_4$	$5 \cdot 10^{-9}$–$8 \cdot 10^{-9}$	$8 \cdot 10^{-9}$
Pu	$Pu(OH)_4$	$7 \cdot 10^{-11}$–$4 \cdot 10^{-10}$	$4 \cdot 10^{-10}$

Plutonium. Measured plutonium concentrations range between 10^{-10} and $4{\cdot}10^{-10}$ mol·dm^{-3}. Predicted plutonium concentrations are slightly lower, $7{\cdot}10^{-11}$ mol·dm^{-3}, corresponding to the solubility of $Pu(OH)_4(s)$. Therefore, we report a range that spans over this variability.

Neptunium. Using concrete-equilibrated water, the solubility of neptunium was found to be $8{\cdot}10^{-9}$ mol·dm^{-3} independently on pH within the studied range (10^{-13}). The calculated solubility is very close to the measured value, $5{\cdot}10^{-9}$ mol·dm^{-3}, when considering $Np(OH)_4$ the solubility limiting phase.

Thorium. Solubilities measured from oversaturation experiments ranged between $4{\cdot}10^{-9}$ and $8{\cdot}10^{-9}$ mol·dm^{-3} in the pH interval 8 to 13. Calculated solubilities in both groundwaters were $5{\cdot}10^{-9}$ mol·dm^{-3} with ThO_2 selected as the solid phase limiting the Th aqueous concentration.

Nickel. The experimental measurements indicated nickel aqueous concentrations between $7{\cdot}10^{-5}$ mol·dm^{-3} at pH 8 and $3{\cdot}10^{-8}$ mol·dm^{-3} at pH 12. Calculated solubilities in equilibrium with $Ni(OH)_2$ ranged from $4{\cdot}10^{-8}$ to $4{\cdot}10^{-7}$ at pH 12.3 and 9.8 respectively.

Technetium. Solubility measurements indicated concentrations on the order of 10^{-7} mol·dm^{-3} and independent on pH within pH 7 and 13. $TcO_2(s)$ calculated solubilities showed pH dependence, indicating a concentration of Tc on the order of 10^{-6} mol·dm^{-3} at pH 12.3 and of $4{\cdot}10^{-8}$ mol·dm^{-3} at pH 9.8

Element-based analysis

In this section we compare the different concentration limits proposed by the agencies for a given element. The values recommended under saline and/or not reducing conditions are out of the scope of this comparison.

Caesium

Given the lack of stable Cs solid phases, all agencies classify this element as no-solubility limited.

Strontium

Sr solubility limits have been calculated by the Belgian, the Swiss and the French agencies under clayey conditions and in the Spanish and Finnish PA under granitic groundwaters. Significant differences exist among the different proposed values.

The Belgian agency calculates Sr concentrations controlled by solubility of 4 different solid phases, NAGRA takes into account $SrSO_4$ and ANDRA considers $SrCO_3$. Spain and Finland also consider different limiting solid phases, strontianite and celestite respectively.

The values proposed by these agencies are shown in Table C-11.

Table C-11. Solubility proposed by SCK-CEN, NAGRA and ANDRA for Sr in clayey media and by ENRESA and POSIVA in granitic media, under reducing conditions. Values in mol/dm^3.

Solid	Belgium pH = 8.2	Switzerland pH = 7.25	France 7.0 < pH < 8.5	Finland (fresh) 7 < pH < 10	Spain (granite) 7 < pH < 11
Clinoptilolite-Sr	$1.6{\cdot}10^{-7}$	***	***		
$SrCO_3$ (strontianite)	$4.5{\cdot}10^{-7}$	***	10^{-5}		> 10^{-4}
$SrSO_4$ (celestite)	High	$1.2{\cdot}10^{-4}$	***	$8{\cdot}10^{-6}$	

The solubility of strontianite differs in more than one order of magnitude between SCK-CEN and ANDRA. This difference is mainly attributed to the different carbonate content of the waters used in the calculations. The carbonate content used by SCK-CEN (Belgium) is more than two orders of magnitude larger (10^{-2} mol·dm^{-3}) than the carbonate content used by ANDRA (France), ($5 \cdot 10^{-5}$ mol·dm^{-3}). This parameter is related to the solubility of calcite and, therefore, it reflects the differences in calcium concentration and pH.

The different concentrations of strontium proposed in the Spanish case (between 10^{-1} and 10^{-4} mol·dm^{-3}) are basically attributed to the fact that two solid phases ($SrCO_3$ and $Sr(OH)_2$) were considered as likely to limit the concentration of this element in solution (see Table C-7).

The selection of celestite instead of strontianite as solubility limiting solid phase depends basically on the concentration ratio of the counter ions. In the case of Switzerland the ratio $[CO_3]/[SO_4] = 0.009–0.05$, while in Belgium this ratio is 6,000. On the other hand the different stability constants considered for this solid phase also play a key role for selecting one solid phase instead of another.

$Sr^{2+} + CO_3^{2-} \leftrightarrow SrCO_3(s)$ $\quad \log K^0_{SCK\text{-}CEN} = 10.02$ (LLNL.dat)
$\log K^0_{ANDRA} = 9.27$ /Giffaut et al. 2000/

$Sr^{2+} + SO_4^{2-} \leftrightarrow SrSO_4(s)$ $\quad \log K_{SCK\text{-}CEN} = 5.68$ (LLNL.dat)
$\log K_{NAGRA} = 6.63$ /Hummel et al. 2002/

Radium

All the agencies have selected $RaSO_4(s)$ as Ra solubility limiting phase. Switzerland and Japan also consider co-precipitation of Ra with Ca. The different concentration limits proposed for Ra by the different agencies are shown in Figure C-1.

The most relevant parameter affecting the solubilitiy of Ra under the assumption of equilibrium with $RaSO_4(s)$ is the concentration of sulphate which, in turn, depends on the concentration of other metals forming stable species with sulphate, e.g. Sr, Ca, Ba.

Reported Ra concentrations range between 10^{-9} and 10^{-3} mol·dm^{-3}. The upper limit is produced by the ENRESA calculations, and is a consequence of the high temperature used in the Spanish assessment (75°C), given that the reaction of $RaSO_4(s)$ dissolution is endothermic and, therefore, its solubility increases with temperature.

No important differences in calculated solubilities can be attributed to diverging thermodynamic databases.

Calculated aqueous Ra concentrations were lower when assuming co-precipitation processes, in better agreement with measured Ra levels in natural systems. Nevertheless, for the sake of conservatism most agencies prefer to consider only pure solid phases in the analyses.

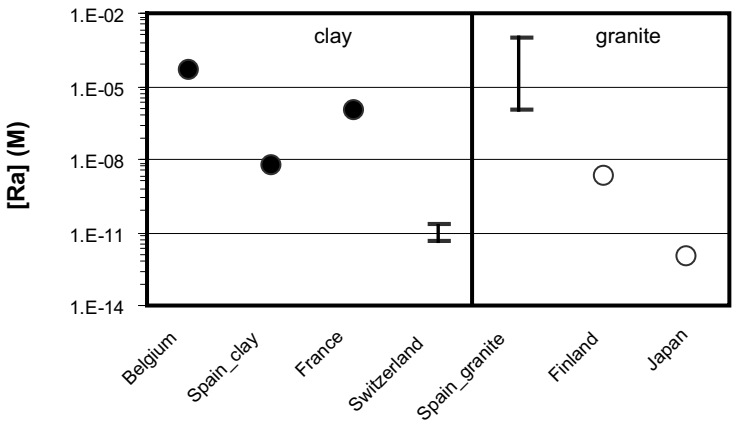

Figure C-1. *Ra concentration limits proposed by the different agencies.*

Tin

The solubility limiting phase selected by all agencies is the oxide $SnO_2(s)$. Solubilities reported by all the agencies range from $5{\cdot}10^{-9}$ to $5{\cdot}10^{-6}$ mol/dm^3. The Sn concentrations proposed by these agencies are shown in Figure C-2.

Belgium, France and Switzerland agencies propose tin concentrations ranging in the lower limits (10^{-8} mol·dm^{-3}), whereas Spain, Finland and Japan calculate solubility limits around 10^{-6} mole·dm^{-3}.

Although theses differences might be a priori attributed to the different crystallinity of the solid phase used in the calculations, a closer review to the thermodynamic databases shows that this is not the case (see below):

$SnO_2(s) + 2H_2O \leftrightarrow Sn(OH)_4(aq)$

$\log K_{SCK\text{-}CEN} = -7.57$ (LLNL.dat)
$\log K_{NAGRA} = -7.30$ /Hummel et al. 2002/
$\log K_{ANDRA} = -7.91$ /Giffaut et al. 2000/
$\log K_{ENRESA} = -7.61$ /Pearson et al. 1992/

The main reasons for the three orders of magnitude over which the values span are: i) The different aqueous speciation and ii) the variability in the groundwater composition used by the different agencies, what leads to the selection in many cases of the upper solubility limit calculated, which results in strong overestimations of the values.

Selenium

Different solids have been assumed to control the concentration of Se in clayey media, iron selenides and metallic Se(s), see Table C-12.

Solubilities reported for iron selenides depend on the aqueous iron concentration considered. The difference in more than two orders of magnitude of selenium concentrations in the aqueous phase when equilibrating with metallic selenium is due to the different redox potential, given that an increase of 100 mV in the redox potential produces, approximately, two orders of magnitude increase of the solubility.

Only JNC and Posiva report concentration limits for Se under granitic conditions. Japan considers the solubility control exerted by iron selenides, $FeSe_2$, and obtains a Se aqueous concentration very similar to the one reported by the Belgian agency under clayey conditions by assuming solubility control exerted by the same solid phase. The finish agency bases its selection on published experimental data, and proposes a conservative value of 10^{-7} mol·dm^{-3}.

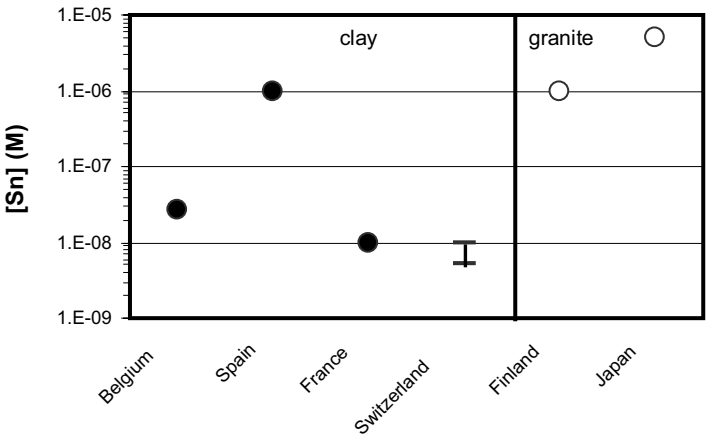

Figure C-2. *Sn concentrations considered by the different agencies for the assessment of solubilities.*

Table C-12. Solubility limits and solid phases selected by the different agencies for selenium. Values in mol/dm³.

	Se(s)	FeSe	$FeSe_2$	No selection
Belgium pH = 8.2	$2.9 \cdot 10^{-7}$	***	$1.9 \cdot 10^{-9}$	***
Switzerland pH = 7.25	$2.1 \cdot 10^{-11}$–$5 \cdot 10^{-9}$	***	***	***
France 7.0 < pH < 8.5	***	$5 \cdot 10^{-10}$	***	***
Spain (clay) 7 < pH < 9	***	***	10^{-8}	***
Finland (fresh) 7 < pH < 10	***	***	***	10^{-7}
Japan pH = 8.4	***	***	$3 \cdot 10^{-9}$	***

Zirconium

ZrO_2 has been selected as the solubility limiting phase for Zr under both, clay and granite environments.

SCK-CEN, the Belgian agency, has also calculated Zr concentrations by assuming equilibrium with $ZrSiO_4$ leading to lower solubilities (10^{-13} mol·dm^{-3}).

Proposed solubilities range in general between 10^{-9} and 10^{-6} mol·dm^{-3}. The differences are mainly attributed to the different degree of crystallinity of the solid phase exerting the solubility control.

The solubility constants selected by the agencies for ZrO_2(s) to form the most stable aqueous species under the conditions of interest ($Zr(OH)_4$(aq)) are given below:

$ZrO_2(s) + 2H_2O \leftrightarrow Zr(OH)_4$

$\log K_{NAGRA} = -11.60$ /Hummel et al. 2002/
$\log K_{SCK\text{-}CEN} = -9.17$ (LLNL.dat)
$\log K_{POSIVA} = -9.17$ (Data0.com)
$\log K_{ENRESA} = -8.60$ (HATCHES v.7.)
$\log K_{JNC} = -8.00$ /Yui et al. 1999/

The values proposed by the different agencies for this radionuclide are shown in Figure C-3.

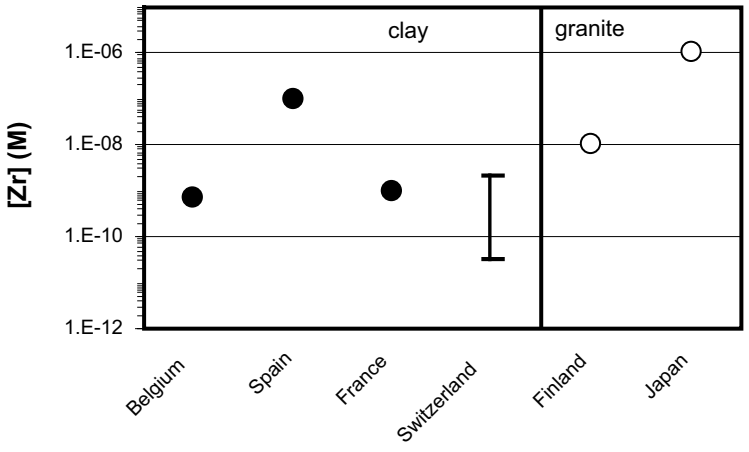

Figure C-3. *Zr concentration limits proposed by the different agencies.*

Niobium

Nb_2O_5 has been considered by all the agencies, both in clay and granite media, as the solid phase controlling the aqueous Nb concentration.

The values reported are similar, and the existing differences can be attributed to the different solubility constants included in the thermodynamic databases for this solid phase, which are shown below:

$Nb_2O_5 + 7H_2O \leftrightarrow 2Nb(OH)_6^- + 2H^+$

$\log K_{NAGRA} = -24.34$ /Hummel et al. 2002/
$\log K_{SCK\text{-}CEN} = -24.40$ (LLNL.dat)
$\log K_{ANDRA} = -20.88$ /Giffaut et al. 2000/

Proposed concentration limits are shown in Figure C-4.

Technetium

TcO_2(am) is the solid phase selected in most of the performance assessment exercises here reviewed for assessing Tc solubilities. Technetium concentrations in equilibrium with TcO_2(am) range between $4 \cdot 10^{-9}$ and $4 \cdot 10^{-8}$ mol·dm^{-3}.

The Belgian agency considers other technetium solid phases, Tc(s) and the crystalline TcO_2 phase, what leads to lower solubility limits.

The Spanish agency considered other technetium oxides, Tc_3O_4 and $Tc(OH)_3$ for their solubility assessment in granite, and obtained a wide range of solubilities, which spanned from 10^{-15} mol·dm^{-3} to concentrations over 1 M.

Concentration limits are shown in Figure C-5.

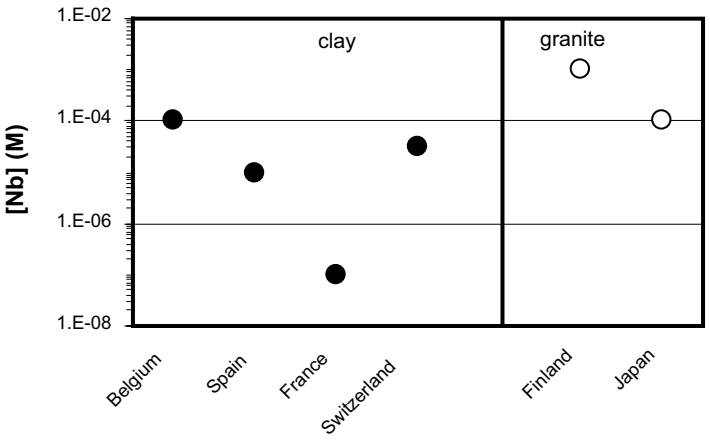

Figure C-4. *Nb concentration limits proposed by the different agencies.*

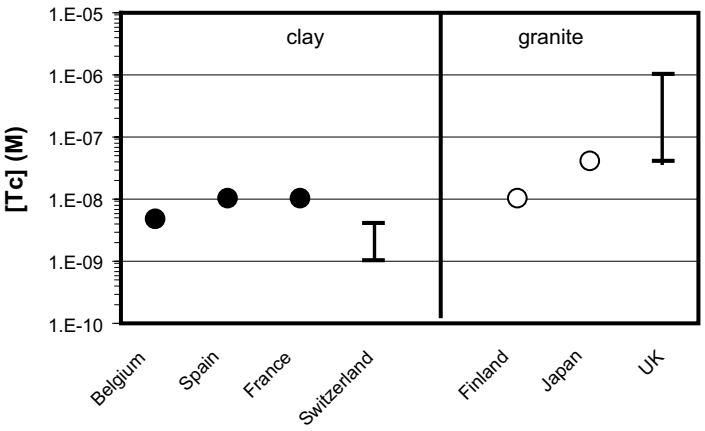

Figure C-5. *Tc concentration limits proposed by the different agencies.*

Nickel

The assessment of the Ni concentration limits is rather conflictive. Not only the reported solubilities are different, but also the solid phases selected to exert the solubility control differ among agencies (see Table C-13).

These discrepancies arise, in many cases, from an attempt to explain the Ni concentrations measured in natural systems, which do not seem to respond to the solubility of any of the solid phases included in the most common thermodynamic databases.

ENRESA assumes that this element is not solubility limited while POSIVA selects a value based on published experimental data, without attributing the concentration control to the precipitation of any solid phase.

In the case of selecting $NiCO_3$ as solubility controlling phase, the differences between the figures proposed by SCK-CEN and NAGRA arise from the different carbonate concentration in solution and from the discrepant solubility constants used for this solid, as shown below:

$NiCO_3(s) \leftrightarrow Ni^{2+} + CO_3^{2-}$ $\quad \log K_{NAGRA} = -11.20$ /Hummel et al. 2002/
$\quad \log K_{SCK\text{-}CEN} = -6.82$ (LLNL.dat)

The differences when selecting Ni_2SiO_4 as solubility controlling solid are due to the different degree of crystallinity of the solid, while the Belgian agency calculates the Ni concentration in equilibrium with a dehydrated Nickel silicate, the French agency equilibrates a hydrated Ni_2SiO_4 with its reference groundwater.

The different pH of the reference water used by NIREX, in combination with the different Ni thermodynamic database used by NIREX and SCK-CEN produces that the calculation of Ni in equilibrium with $Ni(OH)_2(s)$ reported by the British agency is down to 4 orders of magnitude lower than the one obtained by SCK-CEN.

In Figure C-6 the influence of pH on the solubility of $Ni(OH)_2(s)$ is calculated by using both thermodynamic databases. The results shown in the plot highlight the causes for the different solubilities.

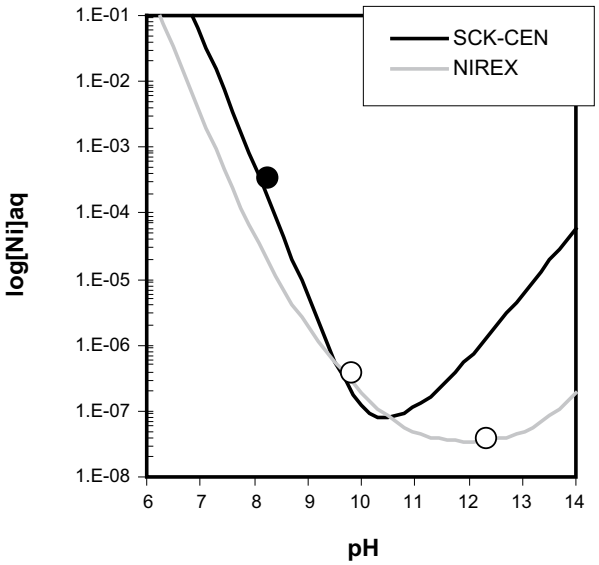

Figure C-6. *$Ni(OH)_2$ solubility as a function of pH calculated by using SCK-CEN and NIREX thermodynamic databases. Open and solid circles stand for proposed values by Nirex and SCK-CEN respectively. $[CO_3^{2-}] = 0$.*

Table C-13. Nickel limiting solid phases and solubility limits reported by the different agencies in clayey and granitic environments and under reducing conditions. Solubilities in mol/dm³.

Solid	SCK-CEN	ANDRA	NAGRA	NIREX	POSIVA
$NiCO_3$	$3.1 \cdot 10^{-3}$	***	10^{-5}–$3 \cdot 10^{-5}$	***	***
$Ni(OH)_2$	$3.6 \cdot 10^{-4}$	***	***	$4 \cdot 10^{-8}$–$4 \cdot 10^{-7}$	***
Ni_2SiO_4	$7.4 \cdot 10^{-8}$	$3 \cdot 10^{-6}$	***	***	***
No selection	***	***	***	***	10^{-5}

Palladium

Two solid phases have been selected by the different agencies as likely to control the solubility of Pd: i) palladium oxide and ii) metallic palladium.

Proposed concentration limits range between 10^{-9} and $5 \cdot 10^{-8}$ mol·dm^{-3} (see Figure C-7) with the exception of the value proposed by SCK-CEN.

These slight differences are due to the different pH of the reference groundwaters of each country.

The value reported by SCK-CEN when assuming solubility control exerted by PdO falls out of the aforementioned range. This value is unrealistically high if compared with the values reported by the other agencies for the same solid phase and it is the result of the different solubility constant used by this agency, differing in more than four orders of magnitude from the others.

$PdO(s) + 2H^+ \leftrightarrow Pd^{2+} + H_2O$ $\quad \log K_{Posiva} = -4.40$ /Bruno et al. 1997/
$\log K_{SCK\text{-}CEN} = 0.06$ (LLNL.dat)

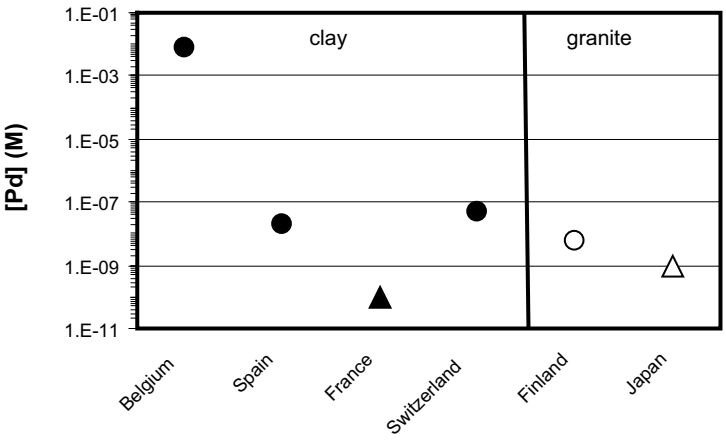

Figure C-7. *Pd concentrations proposed by the different agencies for the assessment of solubilities. Triangles and circles stand for Pd(s) and PdO(s) as limiting solid phases respectively.*

Silver

Silver concentration limits have been only reported by SCK-CEN and NAGRA, i.e. under clayey conditions.

SCK-CEN calculates Ag concentrations of $7.1 \cdot 10^{-7}$ mol·dm^{-3} by assuming equilibrium with AgCl(s) (SCK-CEN), and report a very low concentration when assuming solubility control exerted by Ag(m).

NAGRA proposes a conservative value of $3 \cdot 10^{-6}$ mol·dm^{-3}.

Samarium

The Sm concentration limits reported by the different agencies are based on the solubility of three different solid phases: $Sm(OH)_3$, $SmOHCO_3$ and $Sm_2(CO_3)_3$ (Table C-14).

The selection of one solid or another depends on the thermodynamic databases and on the reference groundwater composition, which is out of the scope of this chapter.

According to the values shown in Table C-14 the Sm solubility ranges from 10^{-8} to 10^{-6} mol·dm^{-3} with only one exception: the high solubility limit calculated by SCK-CEN when assuming equilibrium with $Sm(OH)_3$, which is probably due to the different crystallinity of the solid phase considered.

The wide range of concentrations reported by ENRESA in the granite exercise covers calculated concentrations in a wide range of environmental conditions, as well as the solubility limits of the two phases considered in the exercise.

Holmium

This lanthanide has been included in the assessment exercises conducted by Finland, France and Switzerland.

The concentration limits and limiting solid phases proposed by the French and the Swiss agencies were taken by analogy to samarium and europium respectively, while the finish agency carried out independent solubility calculations, considering $Ho_2(CO_3)_3$ as the phase exerting the solubility control. Solid phases and solubility limits are given in Table C-15.

Table C-14. Solubility limits and solid phases selected by the different agencies for samarium. Solubilities in mol/dm³.

	$Sm(OH)_3$	$SmOHCO_3$	$Sm_2(CO_3)_3$
Belgium pH = 8.2	$5 \cdot 10^{-4}$	***	$4.4 \cdot 10^{-7}$
France 7.0 < pH < 8.5	$7 \cdot 10^{-8}$		***
Spain (clay) 7 < pH < 9	***	10^{-8}	
Finland (fresh) 7 < pH < 10	***	***	$7 \cdot 10^{-7}$
Japan pH = 8.4	***	$2 \cdot 10^{-7}$	***
Spain (granite) 7 < pH < 11	10^{-14}–10^{-6}		10^{-14}–10^{-6}

Table C-15. Solubility limits and solid phases selected by the different agencies for holmium. Solubilities in mol/dm³.

	$Ho(OH)_3$	$HoOHCO_3$	$Ho_2(CO_3)_3$
France 7.0 < pH < 8.5	$7 \cdot 10^{-8}$		***
Switzerland pH = 7.25	***	$3 \cdot 10^{-7}$–$5 \cdot 10^{-7}$	***
Finland (fresh) 7 < pH < 10	***	***	$5 \cdot 10^{-6}$

Thorium

ThO_2(am) is considered by the agencies as the solid phase exerting the Th solubility control.

Resulting concentrations range mostly between $4 \cdot 10^{-9}$ and $5 \cdot 10^{-6}$ mol·dm^{-3}. The differences are probably due to the various groundwater compositions, together with the different stability constants included in the thermodynamic databases to conduct the equilibrium calculations. No systematic variations as a function of the concept host-rock are observed (see Figure C-8).

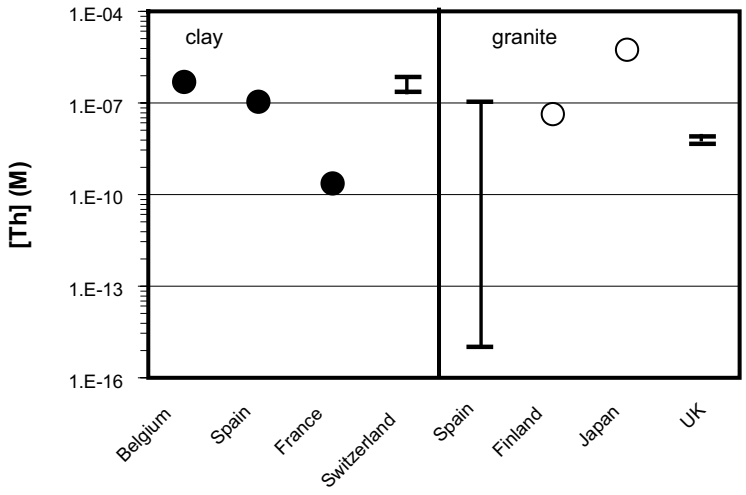

Figure C-8. *Th concentrations proposed by the different agencies for the assessment of solubilities.*

Protactinium

Three different solid phases have been proposed as likely to control the Pa solubility: PaO_2, Pa_2O_5 and $Pa_2O_5{\cdot}H_2O$. Reported solubilities are shown in Table C-16.

Data reported by assuming equilibrium with hydrated or de-hydrated Pa_2O_5 range from 10^{-8} to 10^{-6} mol·dm^{-3}, while those in equilibrium with PaO_2, range from 10^{-11} to $2{\cdot}10^{-9}$ mol·dm^{-3}.

Table C-16. Protactinium limiting solid phases and solubility limits reported by all the agencies in clayey and granitic environments and reducing conditions. Solubilities in mol/dm^3.

Solid	SCK-CEN	ENRESA (clay)	ANDRA	NAGRA	POSIVA	JNC	ENRESA (granite)
PaO_2	10^{-11}	***	***	***	$2{\cdot}10^{-9}$	***	***
Pa_2O_5	10^{-7}	$3{\cdot}10^{-7}$	***	~ 10^{-8}	***	$2{\cdot}10^{-8}$	10^{-7}–10^{-6}
$Pa_2O_5{\cdot}H_2O$	***	***	10^{-6}	***	***	***	***

Uranium

The amorphous U(IV) oxide, UO_2(s), is the solid proposed as exerting the U solubility in all the performance assessment exercises here reviewed.

SCK-CEN has also calculated U concentrations by considering a solubility control exerted by other solid phases: UO_2(c), $USiO_4$, $UO_{2.25}$, $UO_{2.33}$, U_3O_8 and $UO_{2.67}$.

Solubility limits calculated by the different agencies are given in Figure C-9.

Proposed concentration limits range from $3{\cdot}10^{-10}$ to 10^{-4} mol·dm^{-3}. In agreement with this wide range of solubilities, conservative values selected by the agencies differ in more than four orders of magnitude (see values in Table C-1 and Table C-9 for comparison).

A comparison of the solubility constant reported in the different thermodynamic databases for this solid phase as well as the stability constants of the two main hydrolysis products under the conditions of interest is presented in Table C-17.

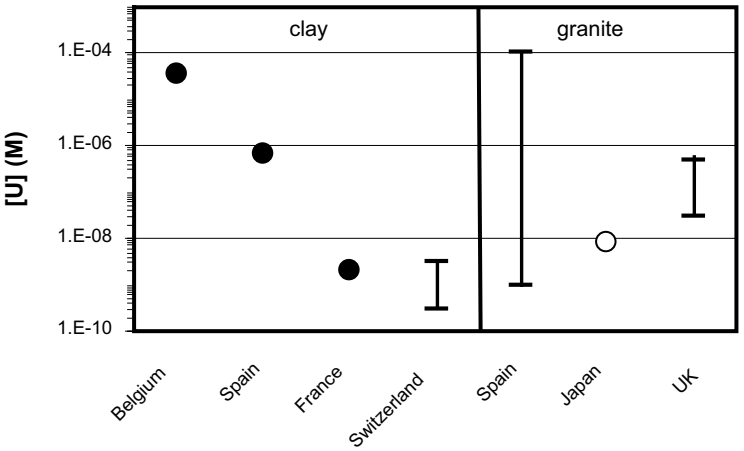

Figure C-9. *U concentrations proposed by the different agencies for the assessment of U solubilities.*

Table C-17. Solubility and hydrolysis constants reported in the different databases and used for solubility calculations by the different countries.

A	B	C	D	E
Country	**Database**	**UO_2 +4H^+ = U^{4+} + 2H_2O**	**U^{4+} + 4H_2O = $U(OH)_4$ + 4H^+**	**U^{4+} + 5H_2O = $U(OH)_5^-$ + 5H^+**
		logKs	**logK_{14}**	**logK_{15}**
Belgium	LLNL	0.11	–4.5	Not included
Spain (clay)	NEA-TDB	–1.60*	–4.5	–16.5
France	AndraTDB	–4.85	–4.5	–22.5
Switzerland	Nagra-PSI (2002)	0.00	–9.0	Not included
Spain (granite)	Nagra-PSI (1992)	0.10	–4.5	–16.54
Japan	JNC	2.59	< –11.6	Not included
UK	Hatches	0.93	–14.3	–22.7

*logKs selected from /Bruno et al. 1985/

In most cases, the predominant aqueous species under the conditions of interest is $U(OH)_4(aq)$ and, therefore, from the combination of values in column C and D in Table C-17 the solubility proposed by each agency can be obtained, corresponding to the following equilibrium reaction:

$$UO_2(s) + 2\ H_2O = U(OH)_4(aq) \qquad \text{eq. 11}$$

The resulting logK values for eq. 11 are shown:

Country	logK(1.1)
Belgium	–4.39
Spain (clay)	–6.10
France	–9.35
Switzerland	–9.00
Spain (granite)	–4.40
Japan	–9.01

Neptunium

The amorphous Np(IV) oxide has been selected by all the agencies as solubility limiting phase for Np. The proposed Np concentrations range from 10^{-8} to 10^{-9} mol/dm^3 (see Figure C-10).

The wide range reported by the Spanish agency in granitic media responds to the different groundwater compositions accounted for in the calculations.

Plutonium

All the solubility assessment exercises considered here have selected the amorphous Pu(IV) oxide as solubility limiting phase except POSIVA.

The Finnish agency reports the concentration of Pu in equilibrium with $Pu(OH)_3(s)$. In spite of this difference, the reported solubilities are very similar, ranging from $2{\cdot}10^{-9}$ to $5{\cdot}10^{-8}$ mol/dm^3 (Figure C-11).

The UK agency, NIREX, gives slightly lower solubilities for this radionuclide, $7{\cdot}10^{-11} < Pu < 4{\cdot}10^{-10}$ mol·dm^{-3}. The upper limit of this range comes from experimental results. Although the

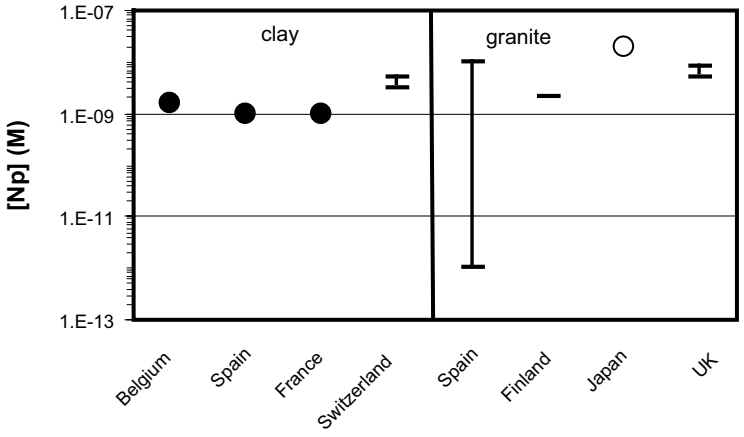

Figure C-10. *Np concentrations proposed by the different agencies for the assessment of solubilities.*

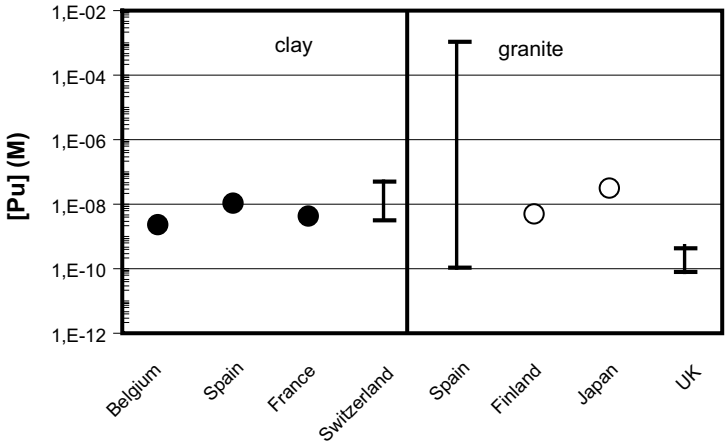

Figure C-11. *Pu concentrations proposed by the different agencies for the assessment of solubilities.*

same authors /Heath et al. 1998/ point out that the reported concentrations are lower than the ones obtained in similar studies, e.g. /Felmy et al. 1989/, they conclude that both sets of data are not inconsistent.

The wide range reported by the Spanish agency in granitic media responds to the different groundwater compositions considered in the calculations, and no selection of a best estimate for the solubility of this actinide is given.

Americium

Most of the agencies assume that $AmOHCO_3$ exerts the Am solubility control.

The French agency proposes a solubility limit of $7 \cdot 10^{-8}$ mol·dm^{-3} based on groundwater equilibrium either with $Am(OH)_3$ or $AmOHCO_3$. This value is lower (four orders of magnitude) than the one calculated by SCK-CEN for the solubility of $Am(OH)_3$ ($7.1 \cdot 10^{-4}$ mol·dm^{-3}).

Two solubility constants responding to two degrees of crystallinity are given in the databases used by these agencies. Belgium uses the amorphous phase for their calculations but France does not indicate which phase was included. On the other hand, France considered a range of $pCO_2 = 10^{-4}$ to 10^{-2} atm, while Belgium carried out their calculations at a fixed CO_2 pressure of $10^{-2.31}$. Figure C-12 shows solubility variations for both, the crystalline and the amorphous phases, as a function of the partial pressure of carbon dioxide considered.

In the pH range of interest, from 7 to 8.5 we can see that the differences may, in some cases, be larger than four orders of magnitude.

The Spanish agency in granite media proposes different solid phases, $Am_2(CO_3)_3(s)$, $Am(OH)_3(s)$ and $AmO_2(s)$, leading to a wide solubility range, which is accentuated by the large variations in the groundwater composition considered.

As shown in Figure C-13, solubility limits proposed for this actinide range between $5 \cdot 10^{-8}$ and 10^{-6} mol·dm^{-3}.

Curium

Belgium, France, Japan and Switzerland propose solubility limits of Cm based on chemical analogies with americium, reporting concentrations in the range from $5 \cdot 10^{-8}$ to 10^{-6} mol·dm^{-3}.

Spain proposes the same solubility in clays for Cm than for Am.

Finland reports a concentration limit for Cm = $3 \cdot 10^{-9}$ mol·dm^{-3}, obtained by assuming equilibrium with $CmOHCO_3$. This value is around two orders of magnitude lower than the one proposed for americium. The difference is due to the different solubility constant of $CmOHCO_3$ (logK = –8.50, Hatches v.7) with respect to the one of $AmOHCO_3$ (logK = –7.20, Data0.com).

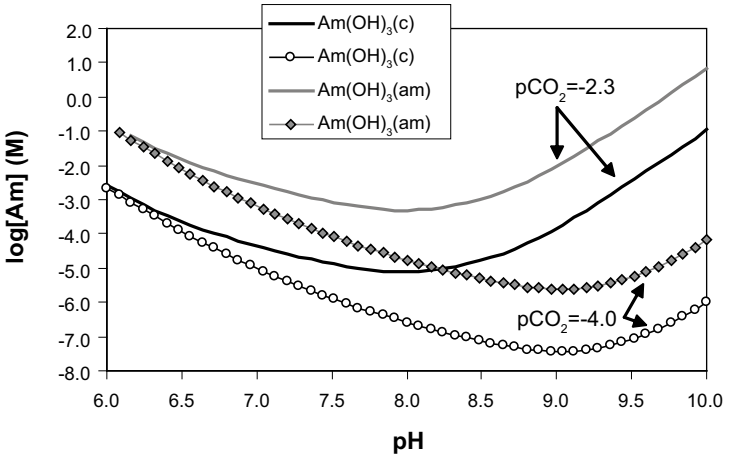

Figure C-12. *$Am(OH)_3$ solubility curves as a function of pH. The database used for aqueous species does not necessarily coincides with the ones used by the French and the Belgium agencies. The results have only illustrative purposes.*

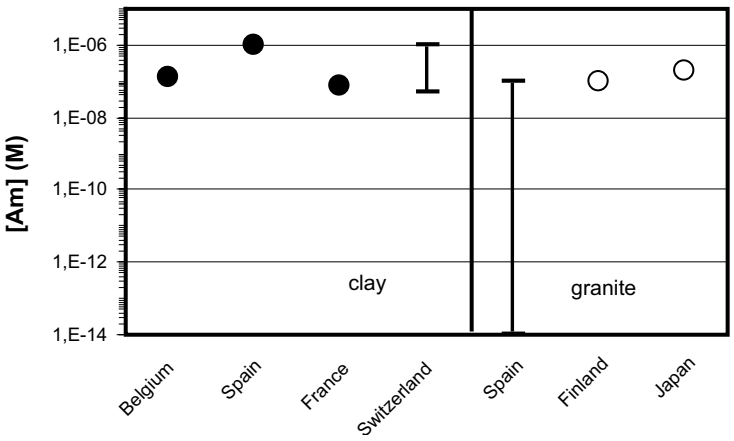

Figure C-13. *Am concentrations proposed by the different agencies for the solubility assessment.*

Appendix D

Plots comparing the recommended concentration limits (*Refgw* in the legend) with those recommended during the SR 97 exercise, the concentrations measured from spent fuel dissolution experiments shown in Appendix B (*Exp.* in the legend) and concentrations determined in natural waters shown in Appendix B (*NGW* in the legend).

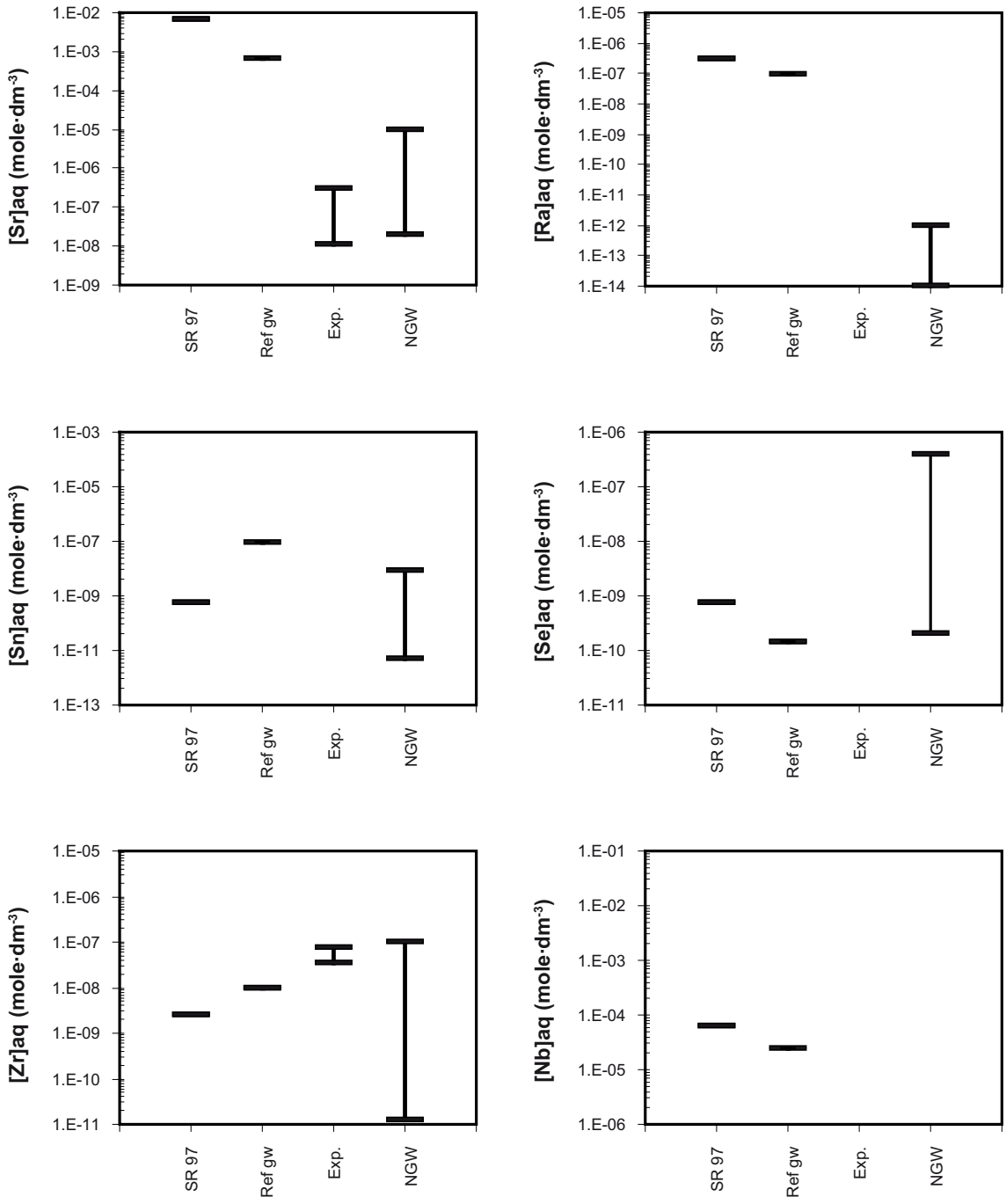

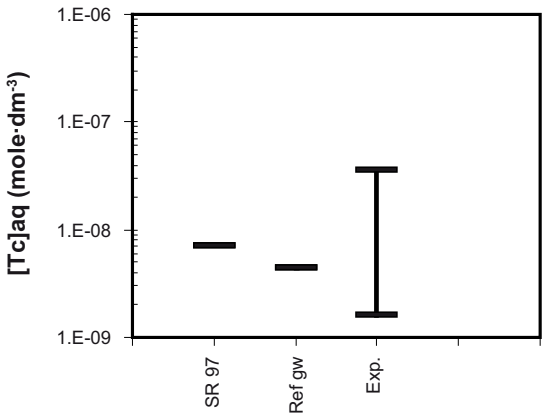
[Tc]aq (mole·dm-3)
1.E-06
1.E-07
1.E-08
1.E-09
SR 97
Ref gw
Exp.

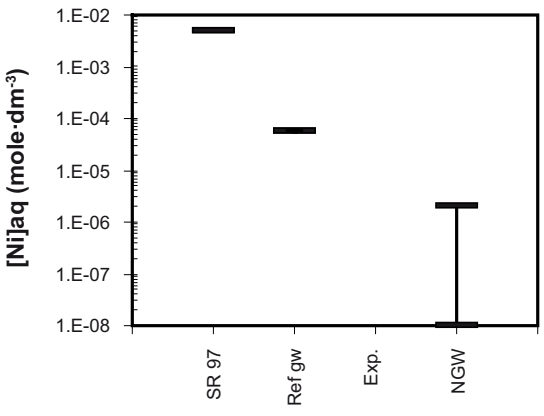
[Ni]aq (mole·dm-3)
1.E-02
1.E-03
1.E-04
1.E-05
1.E-06
1.E-07
1.E-08
SR 97
Ref gw
Exp.
NGW

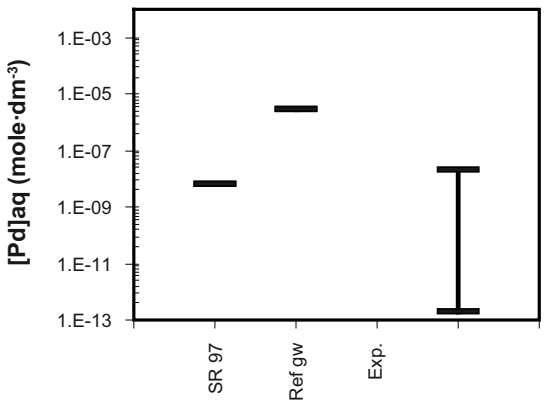
[Pd]aq (mole·dm-3)
1.E-03
1.E-05
1.E-07
1.E-09
1.E-11
1.E-13
SR 97
Ref gw
Exp.

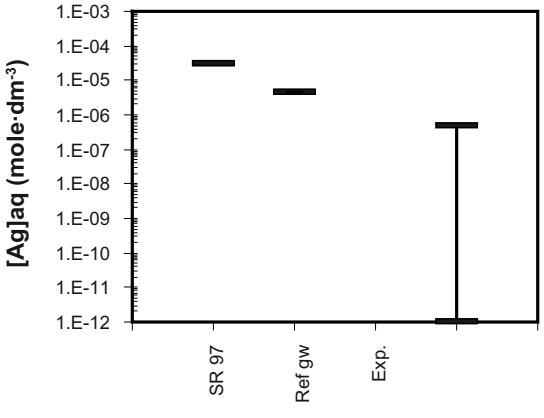
[Ag]aq (mole·dm-3)
1.E-03
1.E-04
1.E-05
1.E-06
1.E-07
1.E-08
1.E-09
1.E-10
1.E-11
1.E-12
SR 97
Ref gw
Exp.

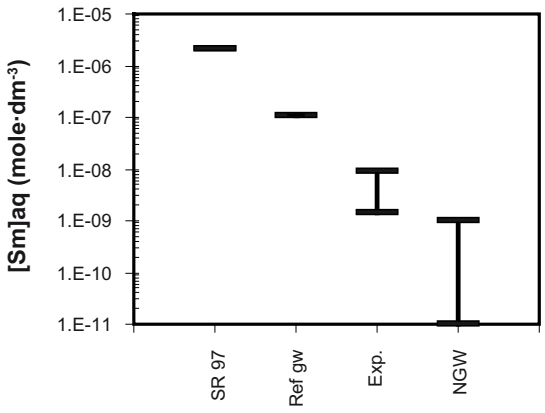
[Sm]aq (mole·dm-3)
1.E-05
1.E-06
1.E-07
1.E-08
1.E-09
1.E-10
1.E-11
SR 97
Ref gw
Exp.
NGW

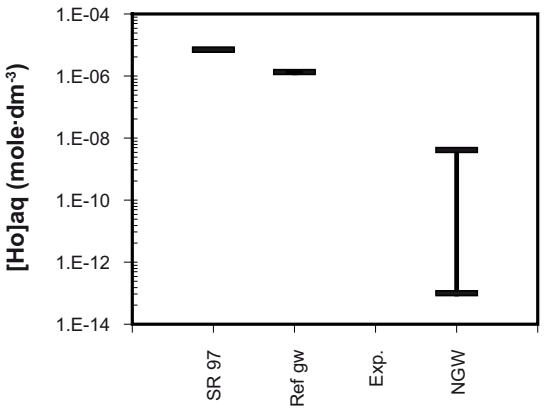
[Ho]aq (mole·dm-3)
1.E-04
1.E-06
1.E-08
1.E-10
1.E-12
1.E-14
SR 97
Ref gw
Exp.
NGW

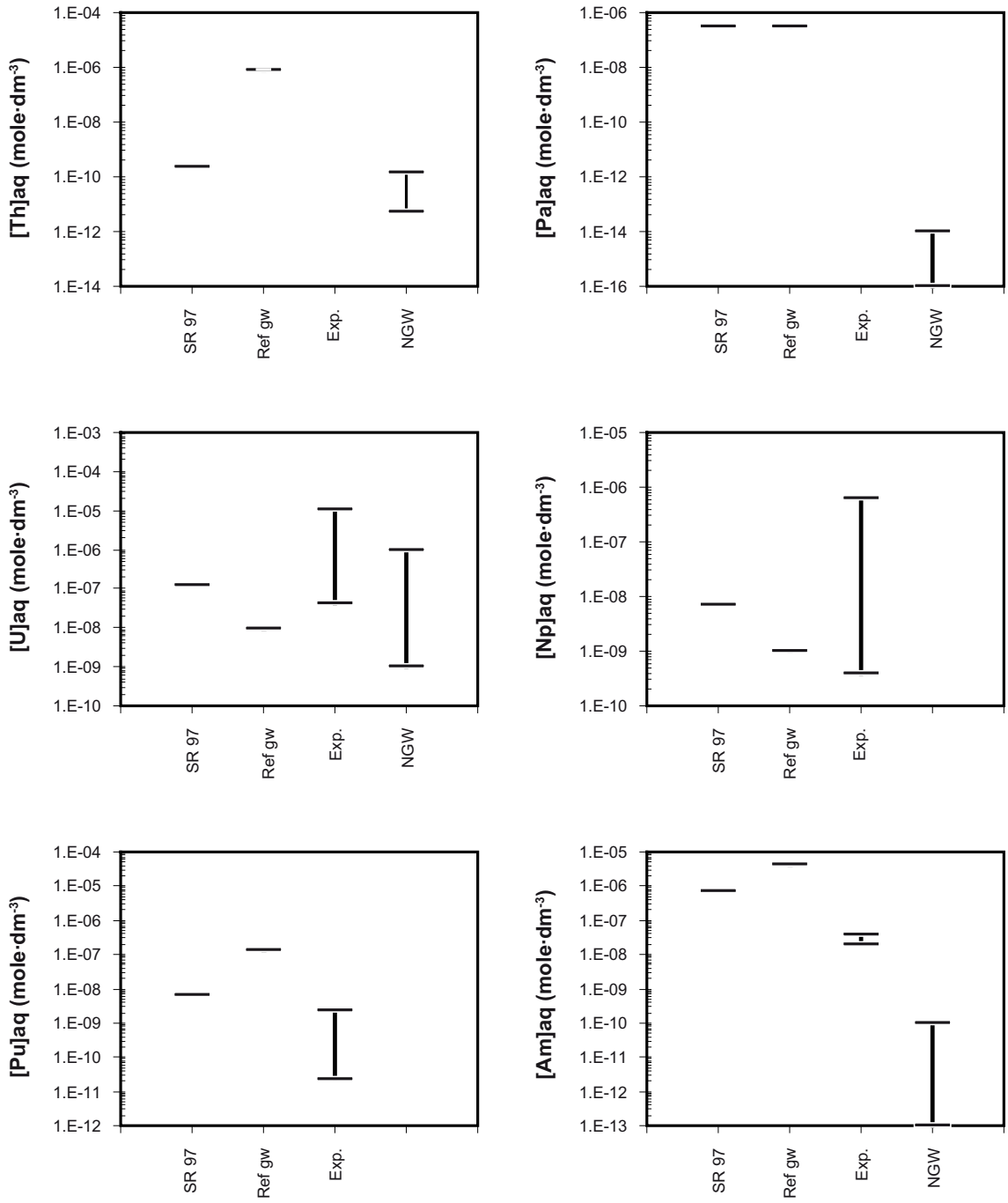
[Th]aq (mole·dm-3)
1.E-04
1.E-06
1.E-08
1.E-10
1.E-12
1.E-14
SR 97
Ref gw
Exp.
NGW
[Pa]aq (mole·dm-3)
1.E-06
1.E-08
1.E-10
1.E-12
1.E-14
1.E-16
SR 97
Ref gw
Exp.
NGW
[U]aq (mole·dm-3)
1.E-03
1.E-04
1.E-05
1.E-06
1.E-07
1.E-08
1.E-09
1.E-10
SR 97
Ref gw
Exp.
NGW
[Np]aq (mole·dm-3)
1.E-05
1.E-06
1.E-07
1.E-08
1.E-09
1.E-10
SR 97
Ref gw
Exp.
[Pu]aq (mole·dm-3)
1.E-04
1.E-05
1.E-06
1.E-07
1.E-08
1.E-09
1.E-10
1.E-11
1.E-12
SR 97
Ref gw
Exp.
[Am]aq (mole·dm-3)
1.E-05
1.E-06
1.E-07
1.E-08
1.E-09
1.E-10
1.E-11
1.E-12
1.E-13
SR 97
Ref gw
Exp.
NGW